

**PROCESS INTENSIFICATION IN
CONCENTRATION OF FRUIT JUICE BY
ROTATING PACKED BED**

**Thesis submitted by
Moumita Sharma**

**Doctor of Philosophy
(Engineering)**

**Department of Chemical Engineering
Faculty Council of Engineering and Technology
Jadavpur University
Kolkata - 700032
2022**

**PROCESS INTENSIFICATION IN
CONCENTRATION OF FRUIT JUICE BY
ROTATING PACKED BED**

**Thesis submitted for
Doctor of Philosophy (Engineering)
of
Jadavpur University
by
Moumita Sharma**

**Under the guidance
of
Dr. Avijit Bhowal
Professor
Chemical Engineering Department
Jadavpur University
Kolkata - 700032
&
Dr. Siddhartha Datta
Ex-Professor
Chemical Engineering Department
Jadavpur University
Kolkata - 700032**

JADAVPUR UNIVERSITY
KOLKATA – 700032, INDIA

INDEX NO: 69/16/E

1. Title of the Thesis: Process Intensification in concentration of fruit juice by Rotating packed bed

2. Name, Designation and Institution of Supervisors:

Dr. Avijit Bhowal

Professor,

Chemical Engineering Department,

Jadavpur University, Kolkata – 700032, India.

&

Dr. Siddhartha Datta

Ex-Professor,

Chemical Engineering Department,

Jadavpur University, Kolkata – 700032, India.

3. List of Publications in Referred Journals:

1. Sharma, Moumita, Bhowal, Avijit, Datta, Siddhartha, & Das, Papita, “Performance evaluation of a baffled rotating contactor for the concentration of fruit juice by air stripping”, Chemical Engineering Research and Design, vol. 176, pp. 14-22, 2021.

4. List of Patents: Nil

5. List of Conference Presentations & Publications:

1. Sharma, Moumita, Goswami, Nilutpal & Bhowal, Avijit, “Thermal Performance of cross-flow Rotating Spray bed”, IOP Conference Series Materials Science and Engineering 894(1):012013, July 2020 (conference paper).

2. Sharma, Moumita, Goswami, Nilutpal & Bhowal, Avijit, Datta, Siddhartha, “Process intensification in a cross-flow rotating packed bed for evaporative cooling of water”, *Materials Today: Proceedings*, 2022, <https://doi.org/10.1016/j.matpr.2022.12.177> (conference paper).
3. Sharma, Moumita, Bhowal, Avijit, & Datta, Sidhartha, “Effective concentration of sucrose solution by Air stripping”, in Chemcon- 2017 held at HIT, Haldia during December 27-30, 2017.
4. Sharma, Moumita, Goswami, Nilutpal, & Bhowal, Avijit, “Thermal Performance of a cross-flow Rotating Spray bed”, 6th International conference on Chemical and Material Engineering (ICCME 2019) Singapore, held at NTU Singapore on October 19-21, 2019.
5. Sharma, Moumita, Bhowal, Avijit, & Datta, Sidhartha, “Concentration of solution by air stripping”, 2nd International conference on advances in Bioprocess Engineering and Technology (ICABET 2020) organized by Heritage Institute of Technology during January 20-22, 2020.
6. Sharma, Moumita, Goswami, Nilutpal, & Bhowal, Avijit, “Evaporative cooling in a cross-flow rotating spray bed”, International conference on Energy and Sustainable Development (IECSD 2020) held at Jadavpur University during February 14-15, 2020.
7. Sharma, Moumita, Bhowal, Avijit, & Datta, Sidhartha, “Concentration of sucrose solution by Air stripping in Rotating packed bed”, in 10th International conference on Sustainable waste management towards circular economy (IconSWM-CE 2020), held at Jadavpur University during December 2-7, 2020.
8. Sharma, Moumita, Bhowal, Avijit, & Datta, Sidhartha, “Process Intensification in Concentration of fruit juice by Air Stripping in Packed bed under centrifugal field”, 11th International Conference on Sustainable Waste Management & Circular Economy 2021 (11th IconSWM-CE) & IPLA Global Forum 2021, held at IconSWM-

ISWMAW Secretariat, Jadavpur University, Kolkata, India (Virtual Mode);
December 01-04, 2021.

9. Sharma, Moumita, Goswami, Nilutpal, Bhowal, Avijit, & Datta, Sidhartha, “ Process Intensification in a cross-flow rotating packed bed for evaporative cooling of water”, International conference on Advances in chemical and Material sciences (ACMS 2022) held at Heritage Institute of Technology, Kolkata during April 14-16, 2022.
10. Sharma, Moumita, Goswami, Nilutpal, Bhowal, Avijit, & Datta, Sidhartha, “Sustainable remedy to prevent thermal pollution of water by evaporative cooling in high gravity equipment”, in International Conference on Sustainable Resilient Remediation (ICSRR’2023) organized by CES, Anna University, Chennai during Feb 2nd and 3rd, 2023.
11. Sharma, Moumita, Bhowal, Avijit, & Datta, Sidhartha, “Process Intensification in Concentration of watermelon juice by Air Stripping under high gravity”, in International Conference on Chemical Engineering Innovations and Sustainability (ICEIS - 2023) held at Jadavpur University during Feb 26-27, 2023.

PROFORMA – 1
“Statement of Originality”

I Moumita Sharma registered on 28th December, 2016 do hereby declare that this thesis entitled **“Process Intensification in concentration of fruit juice by Rotating Packed bed”** contains literature survey and original research work done by the undersigned candidate as part of Doctoral studies.

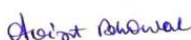
All information in this thesis have been obtained and presented in accordance with existing academic rules and ethical conduct. I declare that, as required by these rules and conduct, I have fully cited and referred all materials and results that are not original to this work.

I also declare that I have checked this thesis as per the “Policy on Anti Plagiarism, Jadavpur University, 2019”, and the level of similarity as checked by iThenticate software is 8%.

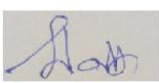
Moumita Sharma

Moumita Sharma
Date: 29/09/2023

Certified by Supervisor(s):


Professor
CHEMICAL ENGINEERING DEPARTMENT
JADAVPUR UNIVERSITY
Kolkata-700 032

1. Dr. Avijit Bhowal
Professor,
Chemical Engineering Department,
Jadavpur University, Kolkata – 700032, India

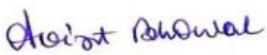

Ex-Professor
CHEMICAL ENGINEERING DEPARTMENT
JADAVPUR UNIVERSITY
Kolkata-700 032

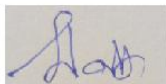
2. Dr. Siddhartha Datta
Ex-Professor,
Chemical Engineering Department,
Jadavpur University, Kolkata – 700032, India.

PROFORMA – 2

CERTIFICATE FROM THE SUPERVISORS

This is to certify that the thesis entitled “**PROCESS INTENSIFICATION IN CONCENTRATION OF FRUIT JUICE BY ROTATING PACKED BED**” submitted by Moumita Sharma, who got her name registered on 28.12.2016 (Index. No. 69/16/E and Registration No. D-7/E/1005/16) for the award of Ph.D. (Engineering) degree of Jadavpur University is absolutely based upon her own work under the supervision of Dr. Avijit Bhowal and Dr. Siddhartha Datta and that neither her thesis nor any part of the thesis has been submitted for any degree/diploma or any academic award anywhere before.


Professor
CHEMICAL ENGINEERING DEPARTMENT
JADAVPUR UNIVERSITY
Kolkata-700 032


Ex-Professor
CHEMICAL ENGINEERING DEPARTMENT
JADAVPUR UNIVERSITY
Kolkata-700 032

Dr. Avijit Bhowal

Professor,

Chemical Engineering Department,

Jadavpur University,

Kolkata – 700032.

Dr. Siddhartha Datta

Ex-Professor,

Chemical Engineering Department,

Jadavpur University,

Kolkata – 700032.

A Thesis

To the memory of

My Late Father

And Dedicated to my Beloved

Mother, Uncle and Aunt

Acknowledgement

I am sincerely grateful to my supervisors Dr. Avijit Bhowal and Dr. Siddhartha Datta at the Department of Chemical Engineering, Jadavpur University for guiding me in every steps of my PhD journey. I was able to complete this dissertation with the help of their persistence and patience. They provided me the freedom to explore on my own and at the same time the guidance to recover when my steps faltered in crisis situations, and I have been really blessed to have them as mentors. They enriched my critical thinking skills, verbal communication skills, and data analysis skills necessary for experimentations and publishing. I am also grateful to Dr. Papita Das for her help, guidance and encouragement in time of need. I appreciate the Department Head Dr. Rajat Chakraborty for his prompt assistance with administrative requirements. I would also like to express my gratitude to the department's supporting staff for maintaining all the equipment in the central analysis laboratory.

Through these challenging years, Sudhanya Karmakar, my lab partner, friend, and senior, has been a huge support. I am appreciative of her assistance positively during the experimentation, and compilation of the thesis. My sincere gratitude goes out to my seniors, Dr. Jayant Modak, Mr. Nilutpal Goswami, and Dr. Abhijit Mondal for their kind counsel. My sincere gratitude goes out to Mr. Nilay Ghosh and Mr. Malay Ghosh for their unwavering support during the PhD research experimentations. A special thanks goes out to Mr. Anup Pardey, Mr. Sandipan Bhowmick, and Mr. Mridul Dey, who were my lab mates at the Heat and Mass Transfer Research Laboratory. They helped me out with the experiments and also supported me with counsel and kind cooperation.

I owe a debt of deep gratitude to my late father Amal Chandra Sarma, who unfortunately didn't stay in this world long enough to see his daughter become a doctorate fellow. Most importantly, none of this would have been possible without the love, care, support and patience of my mother Shila Sarma, my uncle Ratan Sarma and aunt Sukla Sarma throughout these research journey.

Finally, I appreciate the financial assistance by UGC (Delhi) and West Bengal State Government fellowship scheme of Jadavpur University.

Moumita Sharma

Moumita Sharma
Department of Chemical Engineering
Jadavpur University
Kolkata-700032

CONTENTS

	Page Number	
Chapter 1	Introduction	1-16
1.1	Nutritional value of fruits and their products	1
1.2	Concentration of juice	3
1.3	Production of fruit juice concentrates	4
1.4	Methodologies for juice concentration	5
1.4.1	Evaporation	6
1.4.2	Freeze concentration	6
1.4.3	Membrane techniques	6
1.4.3.1	Reverse Osmosis	7
1.4.3.2	Filtration techniques	8
1.4.3.3	Electro dialysis	9
1.4.3.4	Membrane Distillation	10
1.4.4	Spray drying	11
1.4.4	Ohmic Heating	11
1.4.5	Hydrate Separation Technology	11
Chapter 2	Literature Review	17-56
2.1	Evaporation	17
2.1.1	Natural Circulation evaporators	18
2.1.1.1	Horizontal tube evaporator	18
2.1.1.2	Short tube vertical evaporator	19
2.1.1.3	Long tube vertical evaporator	20
2.1.2	Forced circulation evaporators	21
2.1.3	Film-type evaporators	22
2.1.3.1	Falling Film evaporator	22
2.1.3.2	Wiped Film evaporator	25
2.1.4	Multiple-effect evaporators	27
2.2	Spray drying	29
2.3	Freeze concentration	30
2.4	Membrane concentration	32
2.4.1	Micro filtration	33

2.4.2	Ultra filtration	33
2.4.3	Nano filtration	34
2.4.4	Reverse Osmosis	34
2.4.5	Electrodialysis	34
2.4.6	Pervaporation	35
2.4.7	Membrane/osmotic distillation	35
2.4.8	Concentration polarization and Membrane fouling	37
2.5	Direct Contact Evaporation	39
2.6	Air Stripping in High gravity contactors	41
Chapter 3	Aims and Objectives	57-71
Chapter 4	Materials and methods	73-91
4.1	Rotating Contactors	73
4.1.1	RC-1 (Rotating baffled contactor)	74
4.1.2	RC-2 (Rotating Packed bed)	75
4.2	Experimental setup for humidification using Air –Water	76
4.3	Experimental setup for fruit juice	77
4.3.1	Preparation of fruit juice	77
4.3.2	Experimental procedure	78
4.4	Conventional evaporator	79
4.5	Physiochemical Analysis of fruit juices	81
4.5.1	Materials	81
4.5.2	Analysis methodology	82
Chapter 5	Simultaneous heat and mass transfer studies in rotating contactors	93-109
5.1	Introduction	93
5.2	Mathematical modelling	93
5.3	Results and Discussions	94
5.3.1	Effect on Evaporation rate	94
5.3.1.1	Effect of rotational speed	94
5.3.1.2	Effect of air flow rate	96
5.3.1.3	Effect of water flow rate	97

	5.3.1.4 Effect of temperature	98
	5.3.2 Effect on volumetric mass transfer Coefficient (K_Va)	99
	5.3.3 Comparison with other processes	104
5.4	Conclusion	107
Chapter 6	Concentration of citrus fruit juice in rotating contactors	111-132
6.1	Introduction	111
6.2	Materials and Methods	111
	6.2.1 Preparation of juice	111
	6.2.2 Experimental Procedure	112
6.3	Statistical Analysis	112
6.4	Physicochemical Analytical methods	112
6.5	Result and Discussion	113
	6.5.1 Influence of rotor speed	113
	6.5.2 Influence of juice flow rate	115
	6.5.3 Influence of air flow rate	116
	6.5.4 Effect of temperature	117
	6.5.5 Optimization using Response surface methodology (RSM)	117
	6.5.6 Model fitting and ANOVA analysis	119
	6.5.7 Interaction among variables	122
	6.5.8 Physiochemical Analysis results	127
6.6	Conclusion	129
Chapter 7	7a. Concentration of Lycopene containing red fruit juices	133-148
7a.1	Introduction	133
7a.2	Preparation of juice	133
7a.3	Result and Discussion	133
	7a.3.1 Effect of rotor speed	134
	7a.3.2 Effect of air flow rate	135
	7a.3.3 Effect of juice flow rate	136
	7a.3.4 Effect of temperature	137

7a.3.5	Comparative study of red fruit juices	138
7a.3.6	Optimization using Response surface methodology (RSM)	139
7a.3.7	Model fitting and ANOVA analysis	139
7a.3.8	Interaction among variables	143
7.3.9	Physiochemical Analysis results	146
7.4	Conclusion	147

7b. Concentration of high level

antioxidant-rich fruit juices 149-165

7b.1	Introduction	149
7b.2	Preparation of juice	149
7b.3	Result and Discussion	149
7b.3.1	Effect of rotor speed	150
7b.3.2	Effect of air flow rate	151
7b.3.3	Effect of juice flow rate	153
7b.3.4	Effect of temperature	154
7b.3.5	Comparative study of antioxidant-rich fruit juices	156
7b.3.6	Statistical analysis	157
7b.3.7	Interactive variables	161
7b.3.8	Physiochemical Analysis results	163
7b.4	Conclusion	164

7c. Concentration of sugar

containing fruit juices 166-180

7c.1	Introduction	166
7c.2	Preparation of juice	166
7c.3	Result and Discussion	166
7c.3.1	Effect of rotor speed	167
7c.3.2	Effect of air flow rate	168
7c.3.3	Effect of juice flow rate	169
7c.3.4	Effect of temperature	169
7c.3.5	Comparative study of antioxidant-rich fruit juices	170

7c.3.6	Response surface method	171
7c.3.7	Interactive effect of the variables	175
7c.3.8	Physiochemical Analysis results	177
7c.4	Conclusion	178
Chapter 8	Overall Conclusion and Future scope	181-184
8.1	Overall Conclusion	181
8.2	Future scope	183
List of Figures		185-191
List of Tables		193-194

Chapter 1

Introduction

Fruits are astounding sources of nutrients like vitamins, minerals, carbohydrates, and various phytochemicals having traditional therapeutic as well as preventive effects. Wide varieties of fruits are grown in temperate, tropical, subtropical, and arid regions all over the world. People are fascinated by natural food products due to the growing health awareness among them and to minimize the potential health risks owing to synthetic food additives.

1.1 Nutritional value of fruits and their products

A human diet must include certain nutrients, such as minerals, amino acids, metals, fatty acids, and vitamins. Fruits and vegetables are considered to be the richest source of micro and macronutrients including calcium, iron, magnesium, potassium, sodium, phosphorous, chlorine, and sulfur. Many fruits possess reasonable amounts of fat and water-soluble vitamins including A, B-complex, C, D, E, and K. The World Health Organization has recommended the daily intake of Vitamin C for adult males, adult females, pregnant women, and lactating women to be 90, 75, 85, and 120 mg/day respectively [1.1]. The biological activities and medicinal functions of citrus fruits like lemon, lime, orange, etc. have been attributed to the presence of bioactive compounds like hydrocinnamic acid, ferulic acid, cyaniding glucoside, flavonoids, hesperidin, and vitamin C. Various nutrients present in different types of fruits daily required intake in the body, and their function is tabulated in Table 1.1 [1.2-1.4].

Based on nutrients present in them fruits are categorized into the following - citrus fruit (orange), Lycopene containing red fruit (tomato and watermelon), antioxidant-rich fruits (pomegranate and black grapes), and sugar-rich fruits (grapes and sugarcane).

Table 1.1: Daily recommendation of various nutrients and their fruit sources

Nutrients	Function	Recommended daily allowance in the body	Source (Fruits)
Carbohydrates	Supplies energy to the body	225-325g	All fruits
Proteins	Helps in the growth, maintenance, and repair of the body, present in all body fluids, hormones, and enzymes.	65 g	guava, kiwis, banana, jackfruit, apricots
Iron	Present in Hemoglobin	18 mg	pomegranate, prunes, apricots, peaches, and strawberries
Calcium	Promotes the growth of muscles, teeth, and bones, is also required to prevent blood clotting, and protects the nervous system and heart.	1000 mg	Orange, blackcurrant, and blackberries
Phosphorus	Helps in the growth of bones and teeth, and plays a vital role in the body system involving enzymes, salts, fats, carbohydrates, etc.	700-1250 mg	grapes, passionfruits, kiwis, avocado, peaches, and figs
Iodine	Helps in the proper functioning of thyroid glands	150 µg	strawberries
vitamin A (carotenoids)	Improves growth, helps to retain vision, essential for the health of the skin, mouth, throat, nose, and digestive system	350-500 µg	orange, black grapes, watermelon, Dried apricots, and peaches
vitamin B ₁ (Thiamin)	Helps in the proper functioning of the nervous system and heart	1.5 mg	avocados, oranges, mandarin
vitamin B ₂ (Riboflavin)	Helps in digestion	1.7 mg	tomato, peaches, and avocados
vitamin B ₃ (Niacin)	Essential for the skin, nervous system, and digestive system.	20 mg	peaches and apricots
vitamin B ₆	Vital for the nervous system, blood vessels, and healthy gums	2 mg	Avocados, watermelon, and bananas
Folic Acid	Prevents anemia and keeps intestinal tracts healthy	0.4 mg	blackberries, dates, and avocados
vitamin C	Vital for cell division, and essential for healthy teeth, bones, and gums.	60 mg	oranges, black currants, strawberries, lime, guava
Vitamin E (tocopherols)	protects essential fatty acids, slows down aging, supports the functioning of red blood cells	30 IU	Mangoes, kiwi, olives, pomegranate

Orange is rich in vitamins C and B along with minerals like magnesium, potassium, and phosphorus. Lycopene is a bright red-colored carotenoid hydrocarbon present in watermelons and tomatoes. They have anti-cancerous and anti-aging properties. Pomegranate and black grapes are rich in antioxidants that support the cardiovascular system and prevent inflammatory diseases. Grapes are loaded with glucose and fructose, whereas sugarcane is rich in sucrose. Hence, they are categorized as sugar-rich fruits.

1.2 Concentration of Juice

Many fruits have their respective flowering and production seasons. Also, they are inherent to certain specific agro-climate zones. The availability of fruits is also restricted on account of their perishable and seasonal nature and fixed harvesting period [1.5]. For example, mango, pineapple, apple, guava, watermelon, pomegranate, and citrus fruits like oranges, sweet lime, and different berries are grown mainly in selective temperature zones [1.6]. The peak season for the cultivation of oranges, tangerines, clementine, lemons, and grapefruits is winter. Fall harvest festivals frequently feature fruits like apples, grapes, cranberries, pears, pomegranates, and others that are at their height of production in the autumn. During these warm summer months, the best and widest selection of fruits and vegetables including watermelon, mango, plums, peaches, tomatoes, and blueberries are found. Fruits grown specifically in the spring are pineapple, strawberries, sour cherries, raspberries, and apricots among others.

Owing to limited shelf life, fruits should be consumed either fresh or processed within a certain period to savor their perishable flavor. However, it is not possible to consume the entire production directly. Sometimes fruits are shipped to regions that are geographically far apart. To avoid spoilage, fruits are processed into items such as dried fruits, fruit juice

concentrates, jam, canned fruit, frozen fruit, jelly, and alcoholic beverages. These are then consumed during the off-season or transported to locations distant from the production zones [1.7]. Natural single-strength juices are available in such a large volume that their packaging, storage, or transportation are practically impossible economically. To overcome these challenges and supply nutritionally rich juice products worldwide, the volume of juice is often reduced by concentrating them. A large portion of the naturally present water content in the fruit juice is physically removed during concentration [1.8, 1.9]. The objectives of the concentration of the juice are:

- a. Reduction of expenditure in packaging, transportation, and storage by reducing the mass and volume of the product.
- b. Reduction of the water activity of the fruit juices thus obtaining a stable concentrated juice. In high concentrations of soluble solids, microbial growth and enzyme activity are effectively inhibited. Concentrated juices are therefore less likely to undergo microbial spoilage than single-strength ones [1.9].

1.3 Production of fruit juice concentrates

The production of the fruit juice concentrate varies according to the nature of the fruits used. Each of these steps involved in the selection and manufacturing of the juice product affects the final quality of the fruit juice. Usually, the fruits that cannot be sold as table grade are used for making juice and concentrates. Due to the high standards of the fresh fruit market, odd-shaped or small-sized fruits that are not infected and free of blemishes, cuts, and diseases can be turned into juice. The process briefly involves the selection of fruits followed by washing and sorting according to various set criteria [1.10]. After the final inspection juice is extracted and treated with enzymes followed by concentration to

the desired level. The concentrated fruit juice is further processed in two ways. One involves aseptic processing, packaging, and storage at 10 °C and the other way includes chilling, packaging, blast freezing, and then frozen storage at -18 °C. A tabular chart showing the entire process layout is given in Figure 1.1.

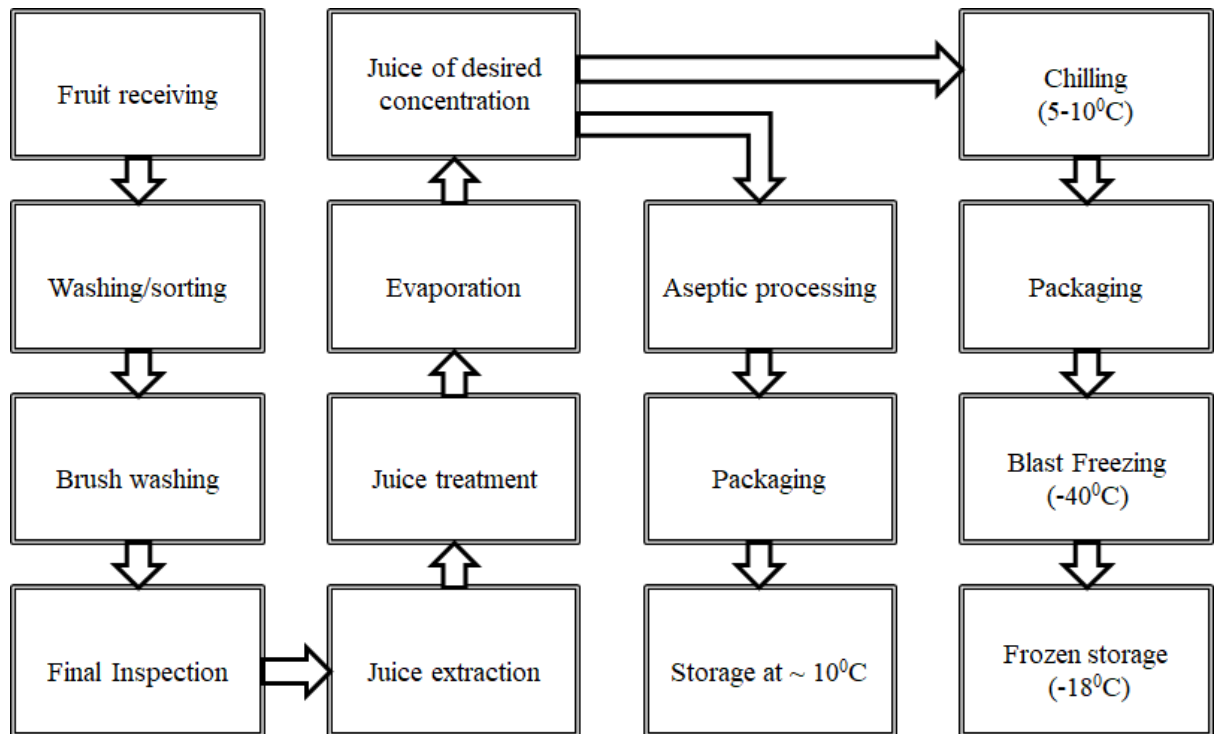


Fig 1.1: Process layout for production of fruit juice concentrate

1.4 Methodologies for juice concentration

Poorly chosen concentration process conditions may negatively impact the product's sensory and nutritional profile, as well as raise production costs. The methods that are widely investigated for the concentration of fruit juices are evaporation, freeze concentration, membrane techniques, and ohmic heating, among others. These processes are briefly described below.

1.4.1 Evaporation

Evaporation is a heat-driven separation technique that produces a more concentrated solution by removing a portion of the solvent from the solution by vaporization. Nearly, 99% of the water (solvent) can be removed by this method, making evaporation the dominant industrial concentration process [1.11]. The heat transfer from the heating medium to the solution takes place indirectly through a metallic wall. The most fundamental method for reducing a liquid's boiling point is to operate it under reduced pressure or vacuum [1.12]. The pressure is reduced by condensing the vapors using heat pumps, vacuum pumps, steam ejectors, etc. [1.7, 1.13, 1.14].

1.4.2 Freeze concentration

A non-thermal process used for the concentration of fruit juice is freeze concentration or cryoconcentration. The process involves freezing the feed juice and then separating the pure ice crystals from the concentrated liquid. The flavor and taste remain intact since there is no involvement of thermal energy [1.15, 1.16]. The process comprises two main steps - crystallization of the water into ice (freezing) and separation. The first step is again divided into nucleation and crystal growth. The second step involves the separation of the non-frozen and frozen constituents and also the recovery of the concentrate that adheres to the surface of the ice crystals.

1.4.3 Membrane techniques

Membrane separation technology is one of the modern techniques applied for the concentration of juices. In the presence of proper driving force, a semi-permeable membrane allows one or more components to pass through. Two types of membranes are employed - organic membranes and inorganic membranes. The most common

materials used to make organic membranes are Cellulose Acetate (CA), Polyethylene (PE), Polypropylene (PP), Polytetrafluoroethylene (PTFE), Polyacrylonitrile (PAN), Polysulfone (PS), Polyimide (PI), and Polyethersulfone (PES). The two main components of inorganic membranes are zirconium oxide (ZrO_2) and aluminum oxide (Al_2O_3). The membrane separation techniques are classified based on their driving force, membrane pore size, and membrane materials into - electrodialysis, microfiltration, reverse osmosis, ultrafiltration, nanofiltration, and osmotic evaporation [1.17-1.22].

The major advantages of the membrane technique are its high selectivity, simple and easy operating techniques, and low energy requirements as phase changes are not required. Different membrane techniques, their mechanism, material, and application are given in Table 1.2 [1.23, 1.24].

1.4.3.1 Reverse Osmosis

Reverse osmosis is a pressure-driven membrane process wherein the solvent in a concentrated solution passes through a semi-permeable membrane in a direction opposite to that of the natural osmosis process due to external pressure (which is higher than the osmotic pressure). All dissolved particles remain in the feed stream and the permeate is composed of a pure solvent. Separation using Reverse Osmosis is accomplished by two methods - through size exclusion and diffusive mechanism [1.25]. Due to the narrow pore size in the Reverse osmosis membranes and the need for overcoming osmotic pressure, the process requires higher pressure than other filtration techniques.

Table 1.2: Different Membrane separation techniques and their applications

Membrane techniques	Pore Size	Membrane material	Membrane type	Mechanism	Driving force	Application
Reverse Osmosis	< 5nm	Thin-film composite, cellulose acetate, aromatic polyamide	Asymmetric, skin type	Solubilization / diffusion	Applied Pressure	Preconcentrate juice, to recover valuable compounds.
Ultra filtration	5-100 nm	Poly sulfone, Polypropylene, nylon 6, acrylic copolymer	Asymmetric, microporous	Convection	Pressure gradient (1-10 bar)	Concentrate skimmed milk, fractionate milk into cheese
Nano filtration	1-5 nm	Polyethylene terephthalate (PTA)	Thin film	Diffusion/ convection	Pressure gradient (10-40 bar)	Concentrate bacteria, protein, divalent salt, lycopene, lactose syrup
Micro filtration	50 nm- 5µm	Cellulose nitrate/acetate, polyamides, polysulfone, metal oxides, etc.	Symmetric, microporous	Convection	Pressure gradient (< 2bar)	Clarification of fat, protein, soluble solids,
Electro dialysis	< 5nm	Sulfonated crosslinked polystyrene	Cationic and anionic exchange membrane	Ion exchange	Pressure gradient (10-100 bar)	De-acidify juice, de-mineralize milk, and whey

1.4.3.2 Filtration techniques

Ultra Filtration (UF) is a membrane technique used for separating macro-solutes based on the differences in molecular shape and size. The principle of this membrane process is hydrodynamic sieving - a mechanism that uses hydrodynamic forces to reject large particles, macromolecules, and colloids from suspending low molecular weight fluids. The UF membranes retain species larger than a specific molecular weight cut-off (MWCO) and allow free passage of solvent and solutes with molecular weights less than a few hundred Daltons. While tiny solutes, such as vitamins, salts, and sugars, pass across the membrane along with water as permeates, they can retain significant components such as microorganisms, proteins, lipids, and colloids.

Micro Filtration membrane techniques use finely porous membranes with nominal pore sizes ranging between 0.025 and 10 μm . Microfiltration is a simple extension of the conventional filtration technique used for separating solids from liquid. A homogeneous porous membrane is used as a depth filter that traps particles on its surface as well as inside the tortuous pores. The membranes used are either isotropic (uniformly porous throughout their thicknesses) or asymmetric (having a graded porosity structure) of pore size 50 nm to 5 μm .

A nanofiltration (NF) membrane is a pressure-driven membrane technology that falls between reverse osmosis (RO) and ultrafiltration (UF). The pore size ranges from 0.2 to 2 nm, while the molecular weight cut-off (MWCO) ranges from 200 to 1000 Daltons. The nanofiltration technique employs “loose Reverse Osmosis” membranes having good rejection toward color substances and organic compounds. The membrane surface is normally charged to improve dissolved ion separation efficiency. As a result, the removal mechanism is not purely filtration but also osmotic. This makes them a true hybrid in nature, bridging reverse osmosis and ultrafiltration membranes. NF membranes can retain particles of low molecular weight like sugar, organic molecules, and also large monovalent and polyvalent ions [1.25]. This technique is generally used in aqueous separations where low operating costs and high productivity are needed.

1.4.3.3 Electrodialysis

Electrodialysis is a membrane technique in which electrically charged membranes are utilized to separate ions from solutions under the driving force of electrical potential difference. The technique utilizes an electrodialysis stack that is built on the filter press principle. The stack contains 200–400 alternate cationic and anionic membranes placed

between two electrodes. The feed solution flows through the stack between each pair of membranes. The positively charged cations in the feed move toward the cathode when an electrical potential difference is provided between the two electrodes. These ions easily pass through the negatively charged (cation exchange) membranes but are retained by the positively charged (anion exchange) membranes. Similarly, negatively charged anions move towards the anode, percolate through the anion exchange membrane, and are restricted by the cation exchange membrane. Thus, ions that are removed from the aqueous feed solution are concentrated in two separate streams.

1.4.3.4 Membrane Distillation

Membrane distillation involves the use of a micro-porous membrane (size ranging between 10 nm – 1 μ m) that is liquid-repellent but vapor permeable in nature. The process partially evaporates a solution through the membrane and separates a heated feed solution from a cooler product solution. As the vapor pressure of the solvent in the feed is higher than the product, the solvent vapor passes through the air-filled pores of the micro-porous membrane and condenses on the product side. Good product quality and high fluxes are obtained over a wide feed concentration range in this technique. The advantages of Membrane Distillation over other conventional separation processes are the low working temperature and pressure. Hence the process requires less stringent mechanical properties and low energy costs. Scaling and fouling problems are also less acute compared to that in reverse osmosis. Recently the Membrane distillation technique is widely used in food concentration and ultra-pure water production. MD is used for the concentration of non-volatile components, like acids, ions, macro-molecules, and colloids from aqueous flows, for removing traces of volatile organic compounds VOCs like

chloroform, benzene, and tri-chloroethylene from water, and for the extraction of organic components like alcohols among others [1.24].

1.4.4 Spray drying

Spray drying was initially developed for the production of fruit powders but is now used to make concentrated fruit juice products as well. The solvent is pumped through a nozzle at the top (atomizer) and sprayed as droplets in a co-current or countercurrent flow of hot gases. The droplets of the solvent are dried in flight before it falls to the bottom of the vessel in a drying chamber.

1.4.5 Ohmic Heating

This technique is also known as electric resistance heating, joule heating, and electro-conductive heating among others. In this technique, alternative current (AC) is passed through the food material. Juices contain a high level of salts and water that can easily conduct electricity through the electrolytic conduction method. Inside the electric fields, there is a movement of ions towards the electrodes having the opposite charge. The rapid movement of ions results in higher kinetic energy and heating of the product. The process provides rapid heating and uniform temperature distribution in various kinds of liquid products resulting in less thermal damage to the volatiles. Ohmic heating has been used in sterilization, pasteurization, evaporation, blanching, fermentation, distillation, cooking, and thawing, among others [1.26-1.31]. Owing to the higher energy efficiency along with very less heating time, ohmic heating can be used as an alternate heating method.

1.4.6 Hydrate Separation Technology

This process was discovered while converting carbon dioxide into its hydrate form. The gas mixes with the liquid to form solid clathrate hydrates which can be easily separated.

This method has also been used for fruit juice concentration. In a feed juice reactor, ethylene gas was inserted by a pressure-regulated cylinder. Nearly 80% of the water content can be removed by this technique. Some of the investigations reported the concentration of fruit juices by hydrates using carbon dioxide hydrate [1.32] and $\text{CCl}_3\text{F}/\text{CH}_3\text{Br}$ hydrates [1.33].

References

- 1.1 Allen, L.H., De Benoist, B., Dary, O., Hurrell, R., “WHO Guidelines on Food Fortification with Micronutrients” WHO, 2006.
- 1.2 World Health Organization & Food and Agricultural Organization of the United Nations, “Vitamin and Mineral Requirements in Human Nutrition”, 2005.
- 1.3 Doets, E.L., de Wit, L.S., Dhonukshe-Rutten, R.A., Cavelaars, A.E., Raats, M.M., Timotijevic, L., et al., “Current micronutrient recommendations in Europe: towards understanding their differences and similarities”, *European Journal of Nutrition*, vol. 47(1), pp. 17-40, 2008.
- 1.4 Bean, H., Schuler, C., Leggett, R.E., Levin, R.M., “Antioxidant levels of common fruits, vegetables, and juices versus protective activity against in vitro ischemia/reperfusion”, *International Urology and Nephrology*, vol. 42(2), pp. 409-415, 2010, doi: 10.1007/s11255-009-9639-5.
- 1.5 Sabanci, S., and Icier, F., “Applicability of ohmic heating assisted vacuum evaporation for concentration of sour cherry juice,” *Journal of Food Engineering*, vol. 212, pp. 262-270, Nov. 2017, doi: 10.1016/j.jfoodeng.2017.06.004.
- 1.6 Yabsley, C., Cross, A., “Miracle Juices: 60 Juices for a Healthy Life”, Creative Publishing International, Beverly, MA, USA, 2001.
- 1.7 Berk, Z., “Production of citrus juice concentrates. Citrus Fruit Processing”, Academic Press, San Diego, CA, pp. 187-217, 2016.
- 1.8 Jeong, S.M., Kim, S.Y., Kim, D.R., Jo, S.C., Nam, K., Ahn, D.U., Lee, S.C., “Effect of heat treatment on the antioxidant activity of extracts from citrus

- peels”, *Journal of Agricultural and Food Chemistry*, vol. 52 (11), pp. 3389–3393, 2004.
- 1.9 Berk, Z., “Food Process Engineering and Technology”, Elsevier, London, 2013.
 - 1.10 Adnan, A., Mushtaq, M., and Ul Islam, T., “Fruit Juice Concentrates,” in *Fruit Juices: Extraction, Composition, Quality and Analysis*, Elsevier Inc., pp. 217–240, 2018, doi: 10.1016/B978-0-12-802230-6.00012-6.
 - 1.11 Standiford, F. C., “Evaporation is a unit operation”, *Chemical Engineering*, vol. 70 (25), pp. 158-159, 1963.
 - 1.12 Prost, J.S., González, M.T., and Urbicain, M.J., “Determination and correlation of heat transfer coefficients in a falling film evaporator,” *Journal of Food Engineering*, vol. 73, no. 4, pp. 320–326, Apr. 2006, doi: 10.1016/j.jfoodeng.2005.01.032.
 - 1.13 Aktaş, M., Khanlari, A., Aktekeli, B., Amini, A., “Analysis of a new drying chamber for heat pump mint leaves dryer”, *International Journal of Hydrogen Energy*, vol. 42 (28), pp. 18034–18044, 2017.
 - 1.14 Ceylan, İ., Gürel, A.E., “Solar-assisted fluidized bed dryer integrated with a heat pump for mint leaves”, *Applied Thermal Engineering*, vol. 106, pp. 899–905, 2016.
 - 1.15 Sánchez, J., Ruiz, Y., Auleda, J.M., Hernández, E., Raventós, M., “Review. Freeze concentration in the fruit juices industry”, *Food Science and Technology International*, vol. 15, pp. 303–315, 2009.
 - 1.16 Pruthi, J.S., “Quick Freezing Preservation of Foods”, Allied Publishers Limited, New Delhi, 1999.
 - 1.17 De Oliveira, R.C., Doce, R.C., & de Barros, S.T.D., “Clarification of passion fruit juice by microfiltration: Analyses of operating parameters, study of membrane fouling and juice quality”, *Journal of Food Engineering*, vol. 111(2), pp. 432–439, 2012.
 - 1.18 Brans, G., Schroën, C.G.P.H., van der Sman, R.G.M., & Boom, R.M., “Membrane fractionation of milk: State of the art and challenges”, *Journal of Membrane Science*, vol. 243, pp. 263–272, 2004.

- 1.19 Arriola, N.A., Dos-Santos, G.D., Prudencio, E.S., Vitali, L., Petrus, J.C.C., & Amboni, R.D.M.C., “Potential of nanofiltration for the concentration of bioactive compounds from watermelon juice”, *International Journal of Food Science and Technology*, vol. 49(9), pp. 2052–2060, 2014.
- 1.20 Kotsanopoulos, K.V., & Arvanitoyannis, I.S., “Membrane processing technology in the food industry: Food processing, wastewater treatment, and effects on physical, microbiological, organoleptic, and nutritional properties of foods”, *Critical Reviews in Food Science and Nutrition*, vol. 55, pp. 1147–1175, 2015.
- 1.21 Gurak, P.D., Cabral, L.M., Rocha-Leao, M.H., Matta, V.M., & Freitas, S.P., “Quality evaluation of grape juice concentrated by reverse osmosis”, *Journal of Food Process Engineering*, vol. 96(3), pp. 421–426, 2010.
- 1.22 Vera, E., Ruales, J., Dornier, M., Sandeaux, J., Persin, F., Pourcelly, G., Valliant, F., Reynes, M., “Comparison of different methods for deacidification of clarified passion fruit juice”, *Journal of Food Engineering*, vol. 59, pp. 361–367, 2003 (a).
- 1.23 Nqombolo, A., Mpupa, A., Moutloali, R.M., Nomngongo, P.N., “Wastewater treatment using membrane technology”, *Wastewater Water Quality*, vol. 29, 2018.
- 1.24 Bhattacharjee, C., Saxena, V.K., Dutta, S., “Fruit juice processing using membrane technology: A review”, *Innovative Food Science and Emerging Technologies*, vol. 43, pp. 136–153, 2017.
- 1.25 Eykamp, W., “Membrane separations in downstream processing”, *Handbook of Downstream Processing*, pp. 90-139, 1997.
- 1.26 Yildiz, H., Bozkurt, H., Icier, F., “Ohmic and conventional heating of pomegranate juice: effects on rheology, color, and total phenolics”, *Food Science and Technology International*, vol. 15, pp. 503e512, 2010.
- 1.27 Cho, W.I., Chung, M.S., “Pasteurization of fermented red Pepper Paste by ohmic heating”, *Innovative Food Science and Emerging Technology*, vol. 34, pp. 180e186, 2016, <http://dx.doi.org/10.1016/j.ifset.2016.01.015>.

- 1.28 Darvishi, H., Hosainpour, A., Nargesi, F., Fadavi, A., “Exergy and energy analyses of liquid food in an Ohmic heating process: a case study of tomato production”, *Innovative Food Science and Emerging Technology*, vol. 31, pp. 73e82, 2015.
- 1.29 Icier, F., Cokgezme, O.F., Sabanci, S., “Alternative thawing methods for the blanched/non-blanched potato cubes: microwave, ohmic, and carbon fiber plate assisted cabin thawing”, *Journal of Food Process Engineering*, vol. 40, pp. e12403, 2017, <http://dx.doi.org/10.1111/jfpe.12403>.
- 1.30 Zell, M., Lyng, J.G., Morgan, D.J., Cronin, D.A., “Minimising heat losses during batch ohmic heating of solid food”, *Food and Bioproducts Processing*, vol. 89, pp. 128e134, 2011, [http:// dx.doi.org/10.1016/j.fbp.2010.04.003](http://dx.doi.org/10.1016/j.fbp.2010.04.003).
- 1.31 Gavahian, M., Farahnaky, A., Sastry, S., “Ohmic-assisted hydrodistillation: a novel method for ethanol distillation”, *Food and Bioproducts Processing*, vol. 98, pp. 44e49, 2016, [http:// dx.doi.org/10.1016/j.fbp.2015.11.003](http://dx.doi.org/10.1016/j.fbp.2015.11.003).
- 1.32 Li, S., Qi, F., Du, K., Shen, Y., Liu, D., Fan, L., “An energy-efficient juice concentration technology by ethylene hydrate formation”, *Separation and Purification Technology*, vol. 173, pp. 80-85, 2017, doi: 10.1016/j.seppur.2016.09.021.
- 1.33 Huang, C.P., Fennema, O., Powrie, W.D., “Gas hydrates in aqueous-organic systems”, *Cryobiology*, vol. 2 (5), pp. 240-245, doi: 10.1016/S0011-2240(66)80129-3.

Chapter 2

Literature survey

Some of the methods for concentrating fruit juice have been outlined in the previous chapter. In this chapter, the results obtained by investigators on the application of these processes and equipment used are elaborately discussed.

2.1. Evaporation

The most common technique used for concentration of the fruit juice industrially is evaporation. Evaporation involves the removal of water content from a solution by boiling off a certain portion of the solvent. Evaporators are used in many different applications [2.1], including:

- minimizing the volume of products like salt, sugar, caustic soda, orange juice, and milk to economize on packing, transportation, and storage expenses.
- recovering distilled water from contaminated streams, including brackish and saltwater.
- converting waste into a useful good, such as by concentrating spent distillery slop after alcohol recovery to create animal feed
- concentrating wastes for quicker disposal, such as waste from nuclear reactors, effluents from dye factories, and blowdown streams from cooling towers
- acquiring a commodity in its most usable state, such as salt from brine or sugar from cane juice.

The three main components of the evaporator design, according to Minton [2.2], are heat transfer, vapor-liquid separation, and efficient energy use. Various types of evaporators used are Natural circulation, Forced circulation, and Film type evaporators.

2.1.1 Natural circulation evaporators

Natural circulation evaporators were the first commercially developed evaporator and are used to evaporate temperature-sensitive and clean products [2.3]. The most common types of natural circulation evaporators are short vertical tube evaporators, long vertical tube evaporators, and horizontal tube evaporators. The schematic diagrams of the three types are shown in Figures 2.1 – 2.3.

2.1.1.1 Horizontal tube evaporator

In a horizontal tube evaporator, steam flows inside the tubes that are positioned horizontally.

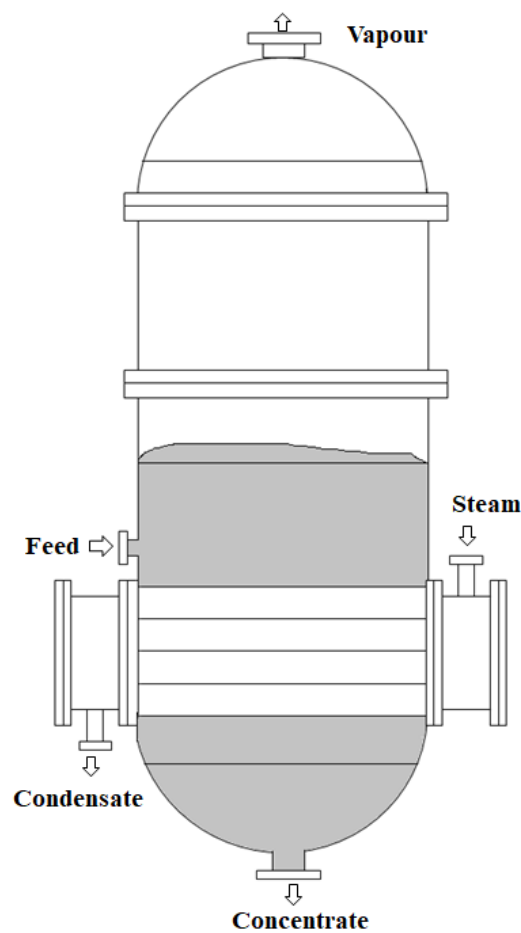


Fig 2.1: Schematic diagram of a horizontal tube evaporator

The solution outside of the tubes gets heated up and the solvent evaporates and exits at the top. Thus the feed gets concentrated and is released at the bottom of the evaporator. The main benefit of a horizontal tube evaporator is the small amount of headroom they require. It is ideal for operations where the final output is a liquid rather than a solid, such as sugar syrups.

2.1.1.2 Short tube vertical evaporator

Short-tube vertical evaporators are made up of a bundle of short tubes that are enclosed in a cylindrical shell and range in length from 4 to 10 feet.

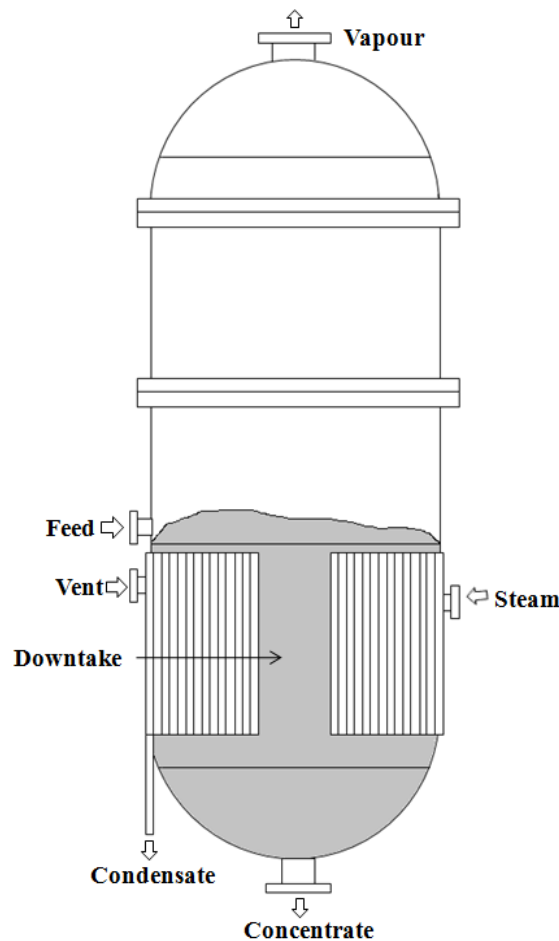


Fig 2.2: Schematic diagram of a short-tube calandria evaporator

It is known as Calandria and the evaporators are also known as Calandria vertical evaporators. The feed is introduced above the upper tube sheet through an opening as shown in Figure 2.2.

The tubes are rolled in between two tube sheets. The liquid flows inside the tube whereas the steam flows outside the tubes. As the liquid gets heated and starts boiling it rises in the tube and returns through the centre downtake. The vapor escapes from the top as the solvents dissipate. The concentrated fluid is collected at the bottom of the evaporator.

Heat transfer is highly dependent on viscosity and temperature, making it unsuitable for temperature-sensitive fluids (milk, fruit juices) and crystalline product manufacture in absence of agitation.

2.1.1.3 Long tube vertical evaporator

The long tube vertical or rising film evaporator is a shell-and-tube heat exchanger where the heating medium is on the shell side. The dilute feed enters at the bottom of the tube sheet and it flows towards the upward direction through the tubes (shown in Figure 2.3). At a certain height above the tubes, boiling commences, and bubbles form increasing the linear velocity and rate of convective heat transfer. The foam thus formed is broken with a vapor-liquid separator provided at the top of the vessel.

Long tube evaporators are used to concentrate cane sugar syrups, black liquor in paper mills, nitrates, and electrolytic tinning liquors, among other things. But higher pressure drops may arise in this equipment and hydrostatic head pressure at the bottom of the tube may increase the temperature causing temperature sensitivity issues in fruit juices.

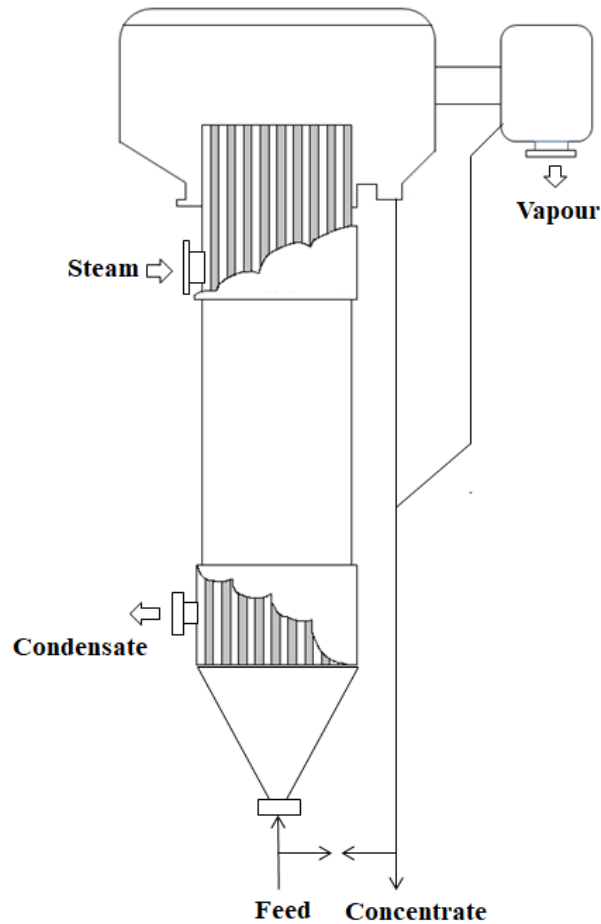


Fig 2.3: Schematic diagram of a long-tube rising film evaporator

2.1.2 Forced circulation evaporators

The forced circulation evaporator (shown in Figure 2.4) consists of a separator (flash chamber), a circulation pump, and a shell and tube heat exchanger. The pump keeps the liquid moving through tubes at a high velocity. The solution is heated inside the heat exchanger without boiling. The flash chamber reduces the pressure and the superheated solution partially evaporates.

The manufacturing of sodium sulfate, sodium chloride, urea, citric acid, magnesium chloride, ammonium sulfate, and caustic potash are all examples of applications where forced circulation is used.

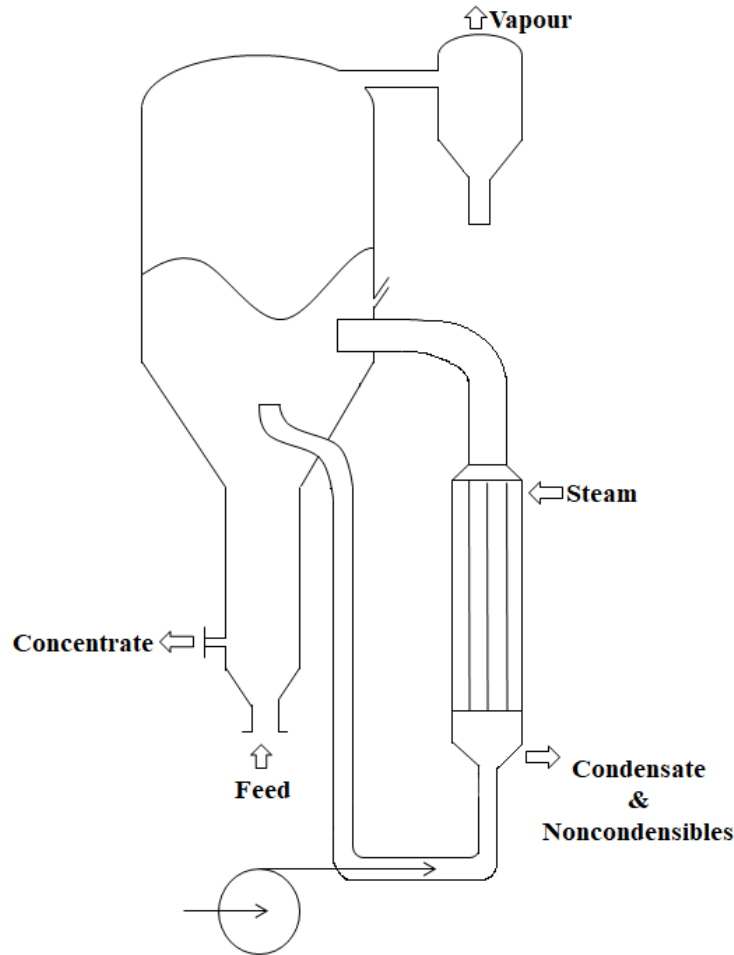


Fig 2.4: Schematic diagram of a forced circulation evaporator

2.1.3 Film-type evaporators

2.1.3.1 Falling Film evaporator

In this evaporator, the feed enters the evaporator at the top, where it is evenly distributed by specially constructed distributors onto the inner surface of the equipment. The action of gravity which pulls the film downward through the heating zone results in a thinner, faster-moving film on the inner surface with a shorter residence period and high heat transfer coefficient. The falling film evaporator is particularly useful when the temperature driving force between the heating medium and the liquid is relatively minimal (less than $9-10^{\circ}\text{C}$) [2.3]. It is ideal for temperature-sensitive products because of

its ability to perform at minimal temperature differences and short residence duration. Good heat transfer performance, especially at low temperatures and minor temperature differences, low initial cost, little floor space needed, and strong vapor-liquid separation characteristics are the main benefits of the falling-film evaporator.

Fouling of the heating surface would occur as a result of the degraded product. Saravacos et al. [2.4] noted that liquid foods such as apple juice and soymilk among others cannot be concentrated at temperatures above 65 °C as precipitates from the liquid foods result in fouling of the tube. This solid layer also acts as a barrier to heat transfer and reduces the evaporation rate.

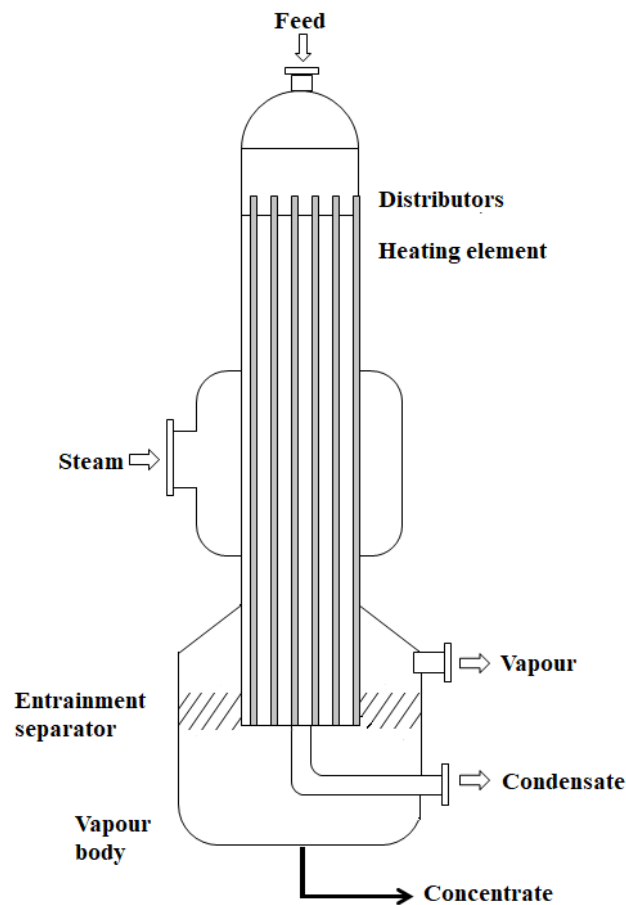


Fig 2.5: Schematic diagram of a falling film evaporator

The main application includes the concentration of fruit juices and producing fresh water from saline waters. The concentration of dairy products (milk protein, whey, skim milk, etc.), black liquor, urea, phosphoric acid, and sugar solutions are some of the other applications of the falling film evaporator.

Although falling film evaporators have been in operation for at least 50 years, they continue to be the focus of several investigations [2.5-2.8]. Angeletti and Moresi [2.9] proposed that there are two mechanisms responsible for vapor evaporation from a falling film. One is direct evaporation occurring at the liquid-vapor interface and the other is bubble formation taking place at the heating tube wall. When the entire temperature difference is below 10^0C , direct liquid-vapor interface evaporation is the dominant mechanism [2.9]. Chun & Sebnun [2.10] and Chen & Jebson [2.11] studied the factors affecting the heat transfer inside a falling film evaporator using water and sucrose solutions. The evaporative heat transfer coefficient was calculated in the range of 2000-4000 $\text{W}/\text{m}^2\text{K}$. Adib et al. [2.12] developed a model for the concentration of sucrose solution in a falling film evaporator. He studied the effect of process parameters (mass flow rate, heat flux, temperature difference, dry matter concentration, etc.) on the boiling heat transfer coefficient. The predicted heat transfer coefficient in his study ranged between 1000-7000 $\text{W}/\text{m}^2\text{.}^0\text{C}$. Karlsson et al. [2.13] studied the heat transfer in falling film evaporation of black liquor. He reported that heat transfer increased with a higher specific mass flow rate. In a high Prandtl region, viscosity is the most dominant parameter for heat transfer in the study. The heat transfer coefficient ranged between 600 and 2500 $\text{W}/\text{m}^2\text{K}$.

2.1.3.2 Wiped film evaporator

Falling film evaporators have worked well with a wide range of materials, but they are not suitable for heat-sensitive, viscous, fouling, or very high boiling liquids. The wiped film evaporator also known as an agitated thin film evaporator (ATFE) solves the problem [2.14-2.16]. Wiped film evaporators use a mechanical wiping device to distribute a thin coating or film of liquid on one side of a metallic wall. Vapors leave the chamber by the vapor discharge nozzle and travel to an external condenser. Nonvolatile compounds are discharged at the evaporator's bottom end.

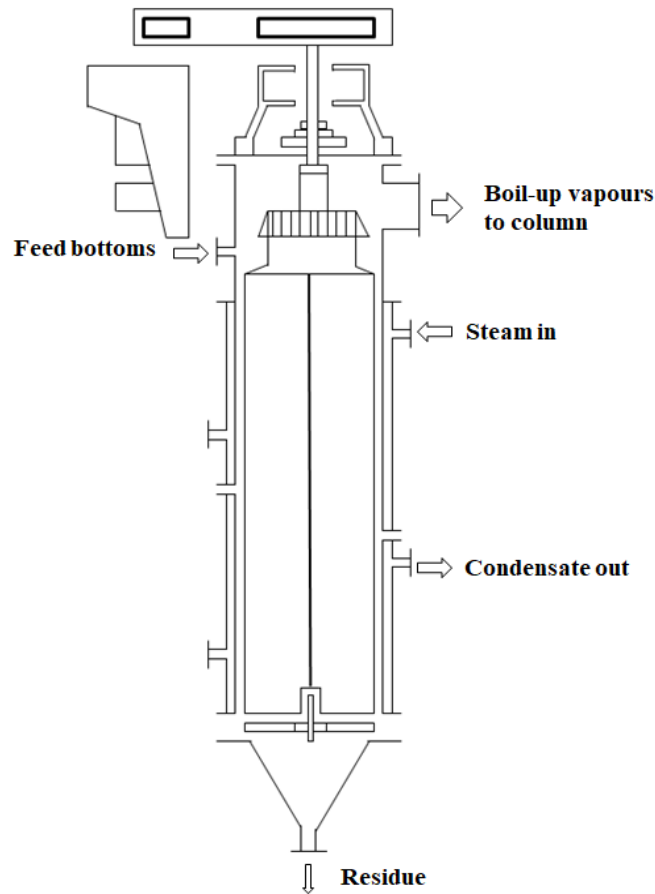


Fig 2.6: Schematic diagram of a wiped film evaporator

Advantages of the wiped film evaporator include:

- Large heat transfer due to rotor turbulence
- short residence time in the heating zone [2.17]
- capacity to handle high solid concentrations and viscous materials (up to 10^5 poise) [2.18]
- and low product degradation resulting in high yields
- plug flow with the least amount of back mixing
- liquid flow rates that are too low to keep the heating surface of a falling-film evaporator consistently moist [2.19].

Food and pharmaceutical concentrations, such as fruits and vegetable purees, biological solutions, gelatinous products, plant and vegetable extracts, lecithin, fermentation broths, and enzymes, are commonly concentrated using agitated thin film evaporators [2.20]. Purification of organic compounds such as herbicides, isocyanates, fatty acids, insecticides, and mineral oils, is performed using this evaporator [2.21, 2.22]. Separation of valuable resources from waste streams, such as motor oils, solvents from paints, volume reduction of inorganic salt streams, glycerin from a crude stream, and water desalination is also carried out using wiped film evaporators [2.23, 2.24].

Parker [2.25] reported the variation in the value of the overall heat transfer coefficient between $1134\text{-}1985 \text{ W/m}^2\cdot^{\circ}\text{C}$ for a thin film scraped surface evaporator (TFSSE). He also reported that length-to-diameter ratio, rotor speed, and feed rate influence the residence time of the liquid in the evaporator. Sangrame et al. [2.16] studied the efficacy of a wiped evaporator for tomato pulp concentration. The overall heat transfer coefficient and evaporation rate for water varied between $476.9\text{-}939 \text{ W/m}^2\cdot^{\circ}\text{C}$ and $14.7\text{-}30.7 \text{ kg/h}$

respectively. The evaporation rate and overall heat transfer coefficient for tomato pulp varied from 13.22-33.72 kg/h and 625.6-910.9 W/m².°C respectively. The evaporation rate and heat transfer coefficient were correlated to the operating parameters using response surface methodology. Zeboudj et al. [2.26] investigated the concentration of sweet orange essential oil in a wiped film evaporator with a heat transfer surface of 0.043 m². When the feed flow rate (65°C) was increased from 0.05 kg/h to 0.65 kg/h, the evaporation rate varied from 0.012 to 0.1 kg/h. Mathematically modeling of thin film evaporators has been reported by Chawankul et al. [2.27] and Pawara et al [2.28]. The thermophysical properties of the orange juice were experimentally determined and modeled as functions of solid content and temperature. Heat transfer was measured with experimental results and predicted using correlations [2.27].

2.1.4 Multiple-effect evaporators

Multiple-effect evaporation is a method of evaporation in which the vapor produced in one step is used as the heating medium in the next. As a result, the first stage serves as a steam generator for the second stage, and so on.

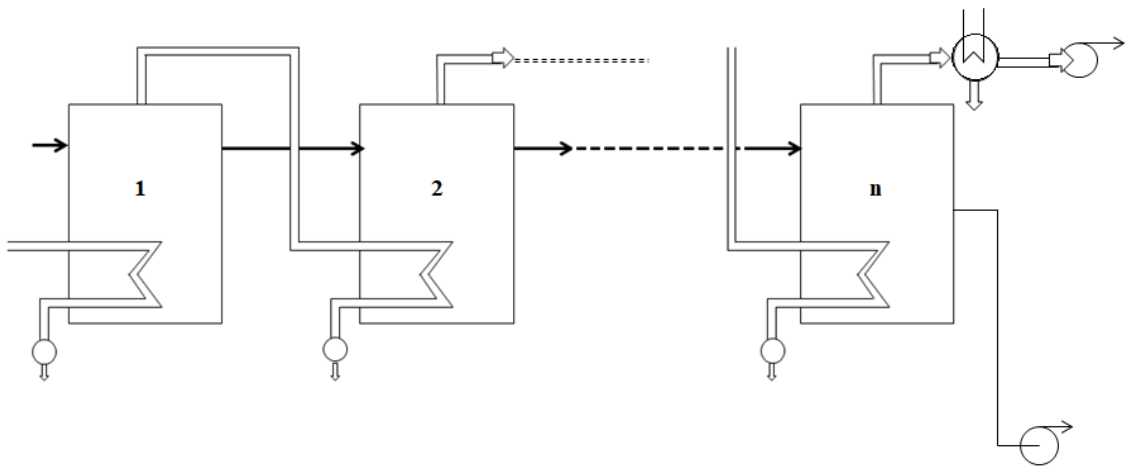


Fig 2.7: Schematic diagram of a multiple-effect evaporator

Ruan et al. [2.29] concluded that the capital cost of a multi-effect evaporator is nearly proportional to the number of effects. The overall cost of evaporation reaches a minimum value for a specific number of impacts. Shell-tube and plate multi-effect evaporators are the two most common varieties of evaporators [2.30]. Plate-type evaporators are less expensive to manufacture, have a lower mass, and take up less area, but they are more problematic during operation due to biological clogging of the heat exchangers. Despite the greater initial investment requirements, tube-type heat exchangers are still a good and popular alternative for fruit juice concentration.

There are numerous studies on the configuration, modeling, and transfer rates of multiple-effect evaporators in the literature [2.31-2.34]. Cyklis et al. [2.35] studied the concentration of apple juice in a multiple-effect falling film evaporator. He reported that energy consumption is influenced by the number of effects. A six-effect evaporator needs to be cleaned after 48 hours of operation otherwise there is a decrease in evaporator capacity due to fouling. The apple juice was concentrated from 10 to 34.9 °Brix and the highest heat transfer coefficient reported was $\sim 2200 \text{ W/m}^2\text{K}$. Ruan et al. [2.29] studied the concentration of fruit juice by the mathematical modeling of a multiple-effect evaporator. Optimum design, modeling, and simulation at different operating conditions in a multi-effect evaporator for the concentration of tomato paste were done by Miranda et al. [2.36] and Simpson et al. [2.37]. The heat transfer coefficient and temperature reported by Miranda et al. [2.36] of the five effects of the evaporator ranged between $175\text{-}1000 \text{ W/m}^2\text{.}^\circ\text{C}$ and $96\text{-}52 \text{ }^\circ\text{C}$.

2.2 Spray drying

The attention of investigators has recently been drawn to the manufacturing of fruit and vegetable-based powders as a more viable solution for cost-effective and secure transportation and storage. Figure 2.8 depicts the operation of a typical spray-drying evaporator. The spray-drying process uses atomization of the particles which results in a large surface area.

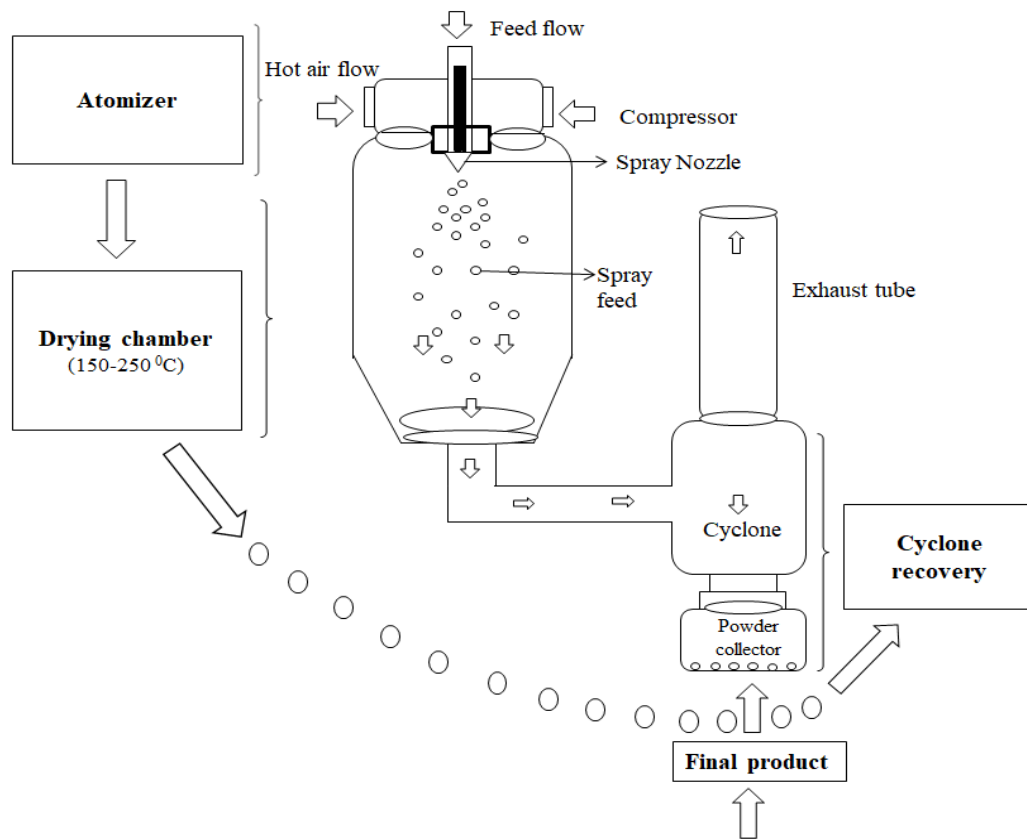


Fig 2.8: Schematic diagram of a spray dryer unit.

Goula et al. [2.38] studied the impact of feed concentration on spray drying tomato pulp pre-concentrated to 78, 82, and 86% wet basis. The experiments were carried out in two spray dryers - one conventional and another with modifications [a pilot-size spray dryer (Buchi, B-191) and an absorption air dryer (Ultracpac 2000)]. The temperature of the inlet

and the dry air flow rate reported in the study ranged between 110-140 °C and 17.5 – 22.75 m³/h respectively. A comprehensive critical review of the recent advances in spray drying in dairy industries was done by Schuck et al. [2.39]. Bhandari et al. [2.40] were the first to use maltodextrins as drying agents to turn concentrated juices of black currant, apricot, and raspberry into powders using spray drying. Goula and Adamopoulos [2.41] developed a new method for producing fruit juice concentrate using dehumidified air as the drying medium and maltodextrin as the binding agent (drying agent). The proposed process was tested on pilot-scale production of orange juice concentrate by varying temperature and drying agent concentration.

Fruit juices containing thermo-sensitive elements including vitamin C, lycopene, β -carotene, anthocyanins, and other essential vitamins cannot be dried with this approach. Furthermore, without a carrier agent, fruit juices with high sugar content and low glass transition temperatures are difficult to dry. Spray drying units require high costs for construction as well as maintenance. Nozzles are often prone to clogging, and atomizers get corroded over time. They also have low thermal efficacy. They lack control over droplet size and the powder produced is of low quality and consistency.

2.3 Freeze concentration

The removal of pure water in the form of ice crystals at sub-zero temperatures used in this method is particularly useful for the concentration or separation of thermo-sensitive biological compounds such as vitamins, anthocyanins, proteins, and other polyphenols, lycopene, and aromatics [2.42-2.44].

Figure 2.9 depicts the freeze concentration process in its most basic form. A crystallizer and a washing column make up this single-stage concentration machine. The crystallizer is essentially a huge vessel with scraped surface heat exchangers that are frequently

encased in cooling coils or flowing refrigerant. A circulating refrigerant cools the outer walls, causing ice to form and crystal development to occur inside the crystallizer. The concentrated liquid is efficiently separated from the ice crystals in the washing column. To remove all traces of concentrated liquid, the compressed ice crystal bed is washed with deliquesce ice. Freeze concentration guarantees that the concentrate retains all of the original product properties. Cryoconcentration, unlike heat evaporation, has minimal impact on the flavor, color, aroma, or nutrients of juice products.

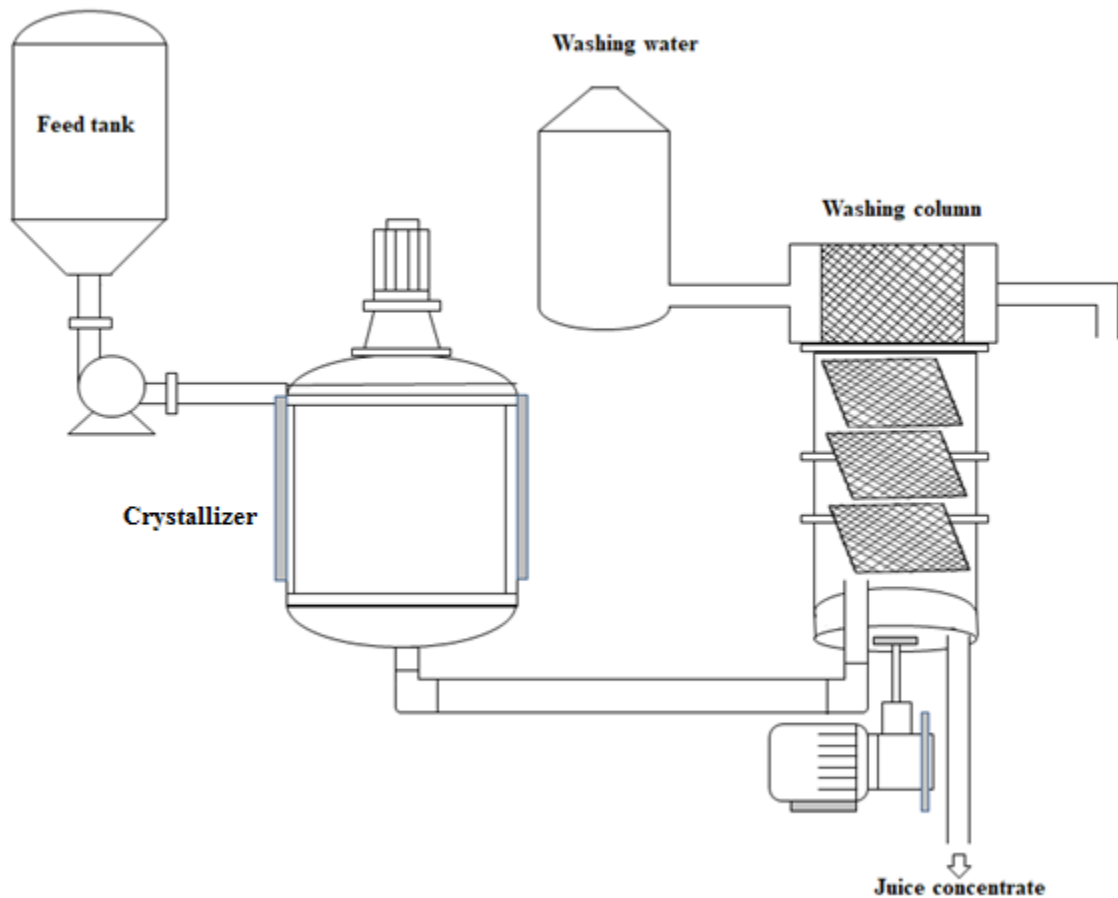


Fig 2.9: Schematic diagram of a freeze concentration unit.

Freezing achieves a concentration level that is higher than reverse osmosis but lower than boiling under the vacuum. Freeze concentration has been widely used in the

concentration of various fruit juices like kiwi, berry, apple, pear, citrus fruits, etc. [2.45-2.51]. It is also applied in winery and distilling, sugar solution concentration, brewing, must production, and making dairy products [2.52-2.56]. It is mainly utilized for the separation of thermosensitive substances like aromatics, lycopene, polyphenols, vitamins, proteins, and anthocyanins among others. The progressive freeze concentration of orange juice was investigated by Sanchez et al. [2.57]. It was noted that after 5 hours of operation the solids concentration in the juice increased linearly over time from an initial 11.1 °Brix to a final concentration of 28.8 °Brix. In a pilot plant falling film cryoconcentrator, Hernández et al. [2.56] examined the freeze concentration of must. After around 10 hours of operation, a final concentration of 29.5 °Brix was reached from the feed concentration of 16.4 °Brix.

The demerits of this technique are long duration time and high equipment and operational cost [2.58]. High operating expenses are primarily due to the juice loss that occurs when ice crystals develop and the difficulty of removing ice crystals without losing food solid contents. Additionally, the degree of concentration achieved is lower than that from evaporation.

2.4 Membrane concentration

The current global energy crisis has prompted industrialists and food scientists to replace drying technologies that use more energy with a new technology called membrane filtration technology [2.59]. Membrane treatments of fruits and vegetables result in a lower loss of nutritional components like vitamins and phytonutrients and provide higher retention of polyphenol oxidase and pectin methylesterase [2.60]. Membrane technology has emerged as a viable alternative to traditional juice clarifying and concentration

methods since they require less labor, and operate at a lower temperature. The organoleptic property of the juice is preserved in these methods due to low-temperature requirements. The advantages of membrane procedures over conventional methods are no thermal damage to the product, aroma retention, low energy usage, and low equipment expense.

Different membrane methods typically employed in the food processing sector are described below, along with their applications in fruit juice processing.

2.4.1 Microfiltration

Microfiltration (MF) is a pressure-driven separation method for purifying, concentrating, or separating macromolecules, colloids, and suspended particles from a solution. The average pore diameters of MF membranes typically vary from 0.1–1.0 μm . The primary goal of MF in the fruit juice processing industry is to remove suspended particles (SS), fat, and high molecular weight (HMW) proteins. MF is commonly used in the fruit juice processing sector for juice clarifying [2.61-2.66]. Pore plugging is one of the major issues in this filtration technique.

2.4.2 Ultrafiltration

Ultrafiltration (UF) is a membrane separation technology based on particle capture or size exclusion. This process is used in the fruit juice industry for clarifying and concentration of the juices [2.67-2.75] by eliminating polluting elements such as yeast, microscopic organisms, moulds, and colloids, as well as proteins, tannins, polysaccharides, etc. which help to maintain product's stability [2.76]. The transport properties of the Ultra filtration membranes are highly affected by fouling, concentration polarization, and interactions between the membrane and the feed stream.

2.4.3 Nanofiltration

Nanofiltration technique is extensively used in hardness reduction during the purification of water, whey demineralization in dairy processing, and removing organic matter in wastewater treatment. The membranes are used in the juice processing industry to concentrate valuable bioactive chemicals from fruit juices, such as lycopene in watermelon juice among others [2.77]. It is also used in juice processing as a clarifying step [2.78, 2.79]

2.4.4 Reverse Osmosis

In Reverse Osmosis, the water content of single-strength juice travels in the opposite direction through the semipermeable membrane when the pressure applied to it greatly exceeds the osmotic pressure. When water is removed from the juice, the juice becomes more concentrated. In the food processing industry, RO is primarily used to concentrate, filter, and recover useful components. Other membrane separation methods, including MF and UF, can be utilized in conjunction with RO. Fruit juices can also be preconcentrated using RO [2.80-2.89]. The product's quality degradation due to heat exposure is considerably decreased, and the process becomes more cost-effective [2.90]. Reverse osmosis is one of the promising membrane-based technologies however it can't handle concentrations higher than 25-30⁰Brix [2.59].

2.4.5 Electrodialysis

In electrodialysis techniques, solutes are removed from a feed solution by using an electric current (DC). Here transportation of ions takes place across anion-exchange and cation-exchange membrane pairs. Streams become enriched and depleted of electrolytes by restricting the migration of ions to only adjacent solution compartments. De-

acidification of fruit juices like mandarin, grape, orange, pineapple, and passion fruit among others [2.91-2.96], demineralization of milk and whey [2.97], and de-ash sugar solutions are some of the applications of electrodialysis in the food business [2.98]. One of the major concerns in electrodialysis is membrane fouling which occurs after relatively short periods of operation since scale-forming ions move uni-directionally on the membrane surface. This results in a gradual increase in electrical resistance and a reduction in efficiency.

2.4.6 Pervaporation

Pervaporation is a separation technique that involves partial vaporization of a liquid feed combination across a non-porous permselective membrane. The following applications have been investigated for the food industry:

- Recovery of aroma in Fruit juices, beer, herbal and flowery compounds [2.99-2.107]
- Wine alcohol elimination [2.108]
- Aroma component restoration during fermentation [2.109]

Despite its potential and successful application, pervaporation has not yet gained recognition among membrane techniques in food industries.

2.4.7 Membrane/osmotic distillation

Membrane distillation (MD) is a temperature-driven process in which two liquid solutions are separated by a microporous hydrophobic membrane at various temperatures. One of the phases is immobilized in the pores of the membranes. An interface between the two phases can thus be formed at the mouth of each pore by carefully controlling the pressure differential between the two phases [2.110]. One of the most significant

advantages of MD is that it may be operated at atmospheric pressure and temperatures well below the boiling point of the solutions. As a result, MD is considered suitable for concentrating fruit juices that are sensitive to high temperatures. Under atmospheric pressure and at room temperature, osmotic evaporation has been effectively used to concentrate milk, juice, instant coffee, and tea products. Soft drink carbonation [2.111], alcohol removal by osmotic distillation [2.112], and fruit juice concentrates are some of their applications in the food business [2.113]. A huge number of fruits like apples, oranges, blackcurrant, pears, etc. were processed by membrane distillation method [2.114-2.119]. But the cost of the membrane and expenses associated with capturing and transferring waste heat supplies in MD technique is extremely high.

A table of different types of juices processed in various membrane techniques along with literature is provided in Table 2.1.

New membrane technologies, such as membrane and osmotic distillation, as well as the integration of various techniques, may help to enhance quality and make fruit juice processing more economically feasible on a large scale [2.120, 2.121]. In the food industries, a wide range of membrane modules, including tubular, hollow fiber, and spiral-wrapped, have been used based on their benefits. The employment of innovative membrane techniques and integrated membrane systems for the production of fruit juice concentrates high in selected elements such as lycopene, vitamin C, colorants, and antioxidants has generated a lot of interest [2.122].

Table 2.1: Literature of various juices concentrated in different membrane techniques

Fruit juice	Membrane technique used	Concentration achieved	Time required	References
Apple	Reverse Osmosis (RO) and Osmotic Evaporation (OE)	25 – 35 °Brix from initial 8.7 °Brix (RO) and 65 °Brix (OE)	100 minutes (RO) and 1800 minutes (OE)	[2.59]
Chokeberry, Redcurrant, and cherry	Ultrafiltration and Membrane Distillation	Chokeberry: 63.9 °Brix from initial 9.4 °Brix. Redcurrant: 62.4 °Brix from initial 9.6 °Brix. Cherry: 65 °Brix from initial 8.7 °Brix.	Chokeberry: 20 hours Redcurrant: 19 hours Cherry: 22 hours	[2.123]
Grapes juice	Reverse Osmosis	28.2 °Brix from initial 13.5 °Brix.	135 minutes	[2.82]
Orange juice	Reverse Osmosis	36 °Brix from initial 8.2 °Brix.	120 minutes	[2.80]
Tomato juice	Microfiltration and Reverse osmosis	14.18 °Brix from initial 4 °Brix.	210 minutes	[2.124]
Peach, Pear, apple, and Mandarin juice	Ultrafiltration and Reverse osmosis	Peach: 30.5 °Brix from initial 12.1 °Brix. Pear: 28.9 °Brix from initial 11.8 °Brix. Apple: 26 °Brix from initial 12.2 °Brix. Mandarin: 22.5 °Brix from initial 10.5 °Brix.	2 hours	[2.125]
Orange juice	Ultrafiltration and Membrane Distillation	65 °Brix from initial 9.5 °Brix	~90 hours	[2.126]
Acerola juice	Microfiltration and Reverse osmosis	29.2 °Brix from initial 7.1 °Brix	~280 minutes	[2.86]
Black currant juice	Reverse osmosis	24.8 °Brix from the initial 17.6 °Brix	1.4 hours	[2.127]
Grapes juice	Membrane and Osmotic distillation	60 °Brix from initial 17 °Brix	12 hours	[2.128]
Passionfruit juice	Osmotic evaporation	60 °Brix from initial 14 °Brix	30 hours	[2.63]
Camu-Camu juice	Reverse osmosis and osmotic evaporation	Total soluble solid changed from 66-634 g/kg	~ 9 hours	[2.87]

2.4.8 Concentration polarization and membrane fouling

Membrane fouling and concentration polarisation are two major issues when utilizing membranes to clarify or concentrate fruit juices. These cause a reduction in membrane

permeability and decrease of permeate flux over time besides changing the physicochemical characteristics of the filtrate.

Concentration polarization refers to a reversible build-up of non-permeated and rejected solute in the external phase adjacent to the membrane-solution interface. This phenomenon is shown in a pictorial form (Figure 2.10) where a mass transfer boundary layer is formed that provides resistance to the back diffusion of retained solute to the properly mixed bulk. A gel layer is developed on the membrane as solutes accumulate and continuously block pores.

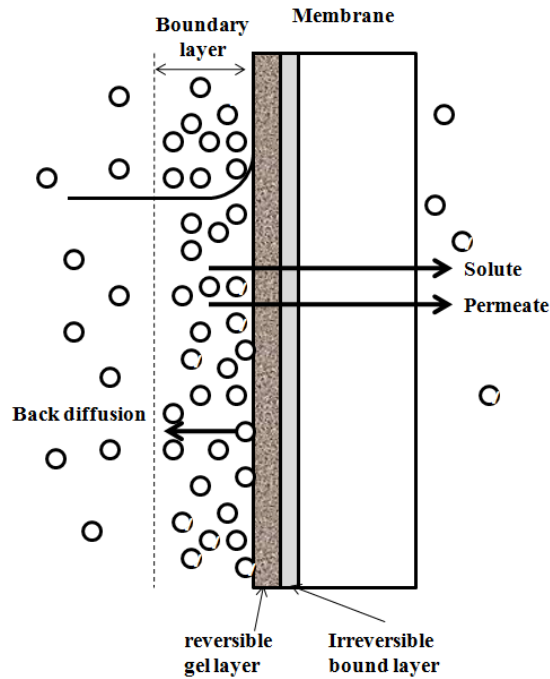


Fig. 2.10: Pictorial representation of concentration polarization

Membrane fouling is a complex phenomenon caused by the presence of numerous colloidal particles in the juice that form a cake layer on the membrane surface or clog the membrane pores. Cell wall polysaccharides and macromolecules, such as pectins (polyuronic acids predominantly generated from -galacturonic acid, primarily abundant in

apple and citrus fruits), lignin, cellulose, and hemicelluloses, make up the fouling components in fruit juice. The degree of membrane fouling impacts the frequency of cleaning, the membrane's lifetime, the membrane area required, and, as a result, membrane plant costs, design, and operation. Fouling caused by concentration polarization is reversible, whereas pore blockage is often irreversible.

2.5 Direct Contact Evaporation

The heat transfer to the solution in the evaporators discussed in section 2.1 occurs through a barrier (tube walls). In direct contact evaporators, the temperature of the liquid is raised by contact with hot gas. The equipment consists of a liquid column through which a superheated gas is bubbled through a sparger located at the base (shown in Figure 2.11). Perforated plates or a set of perforated pipes are generally utilized as spargers. The feed is introduced at the top and comes in contact with the gas directly without any intervening walls. The solution becomes concentrated as water evaporates into the rising gas bubbles due to the difference in partial pressure between the solution and the unsaturated gaseous stream. Direct contact evaporation is used mainly in concentrating chemicals like sulphuric acid, phosphoric acid, ferric chloride, calcium chloride, magnesium chloride, and caustic soda among others [2.129]. They are also used in producing potable water from brackish water and concentration of citrus fruit peel liquor.

The direct contactor evaporators can be efficiently used for concentrating scale-forming liquids as the absence of a fixed heating surface minimizes the effect of fouling. The direct contact between the gas bubbles and the solution also eliminates the heat transfer resistance of the tube wall in falling film evaporators. Due to the reduced resistance

owing to bubbling-driven mixing, the heat transfer efficiency also ranges above 95% [2.129].

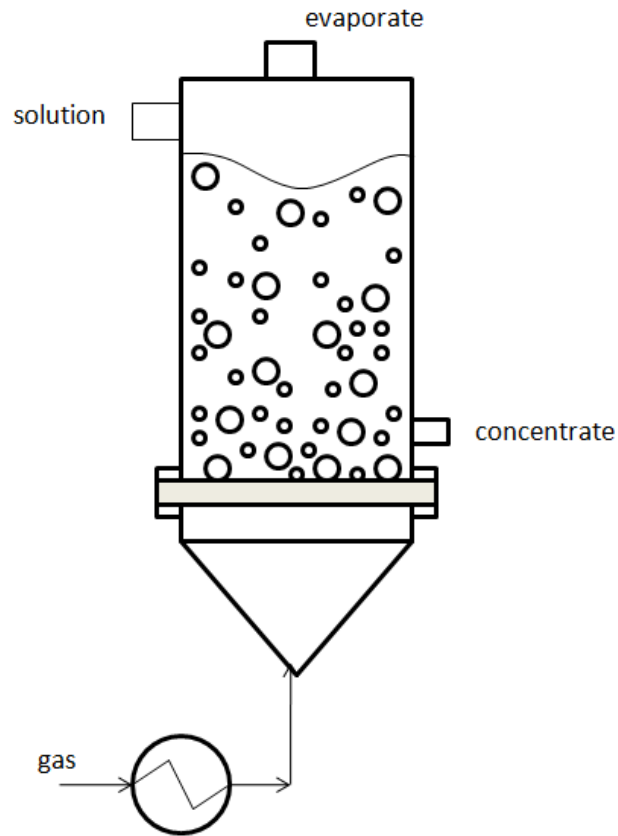


Fig. 2.11: Schematic diagram of a direct contact evaporator unit

Ribeiro et al [2.130] studied the concentration of a model fruit juice (mixture of sucrose and ethyl acetate) by sparging heated bubbles through the solution. They also developed a dynamic model containing mass and energy conservation equations for simultaneous heat and multicomponent mass transfer in superheated bubbles. The evaporation rates of ~15% sucrose solution reported by Ribeiro et al. [2.130] were approximately 0.7 g/min and 1.0 g/min at superficial air velocities of 3.5 cm/s and 6.5 cm/s when the temperature in the bubble column reaches 50 °C.

But bubbling may lead to excessive foaming which makes the process impractical [2.129]. Foam causes loss and possible contamination.

2.6 Air stripping in High Gravity contactors

Goswami et al. [2.131] proposed the use of contactors operating under high gravity for concentration of the solution. Ramshaw and Mallison, [2.132] first proposed the use of rotating packed beds (RPB) with claims of improvements in mass transfer and throughput rates up to 1-2 orders of magnitude and a corresponding drastic reduction in the column size (and consequently the capital and operating cost) for the same production goal. Here the acceleration due to gravity (g) is replaced by centrifugal acceleration (100-1000 times g) and the method was suitably called HiGee (high gravity). The rotor is a doughnut-shaped packing element. For uniform distribution of liquid inside the rotating bed, a liquid distributor is placed near the rotor's eye. On the inner edge of the packing element, the liquid is dispersed as jets or droplets. Centrifugal force causes the droplets to cling to the packing and flow erratically outward as drops, rivulets, and thin films. The gas phase is fed through the casing at the outer periphery of the packed bed for the mass transfer between the liquid and gas phases. Under pressure, the gas phase advances radially inward and moves countercurrent to the liquid's flow. Due to high centrifugal acceleration rapid regeneration takes place in the interface of gas and liquid. As a result, the mass transfer rate increases drastically with consequent improvement in efficiency.

Several advantages of rotating a packed bed are as follows [2.133, 2.134]:

- In contrast to a conventional fixed bed, the rotating packed bed has less of a tendency to flood. This contributes to increased hydraulic capacity and smaller equipment.

- Under the high shear stress produced by centrifugal force in a rotating packed bed, the apparent viscosity of a shear-thinning fluid can be lowered. Therefore, both viscous Newtonian fluids and non-Newtonian fluids can be used inside this apparatus.
- The rotor's ability to self-clean helps treat fouling and solid-containing systems by preventing plugging.
- Moderate alterations in the equipment's orientation have little to no impact.
- Due to minimal equipment holdup, a steady state was reached quickly.
- start-up and shutdown procedures that are short and simple.
- Installation, troubleshooting, and maintenance are made simpler by smaller equipment.
- Better micromixing, higher volumetric gas and liquid side mass transfer coefficients, and higher allowable throughput may all contribute to higher process efficiency in equipment operating under high gravity.

Goswami et al [2.131] studied the concentration of a sub-cooled potassium chloride solution inside a cross-flow rotating packed bed (RPB) with wire mesh packing. The evaporation rate increased from 0.028 kg/min to 0.041 kg/min as the inlet water temperature was varied from 50 °C to 65 °C, and decreased from 0.039 kg/min to 0.031 kg/min with the increase of salt concentration from 10 g/L to 20 g/L. Response surface methodology was utilized to establish the optimum conditions (liquid flow rate, rotational speed of bed, and air flow rate). A theoretical comparison of the evaporation rate of water with a vertical thin film evaporator suggested the

feasibility of getting a higher evaporation rate per unit contactor volume by carrying out the operation in RPB.

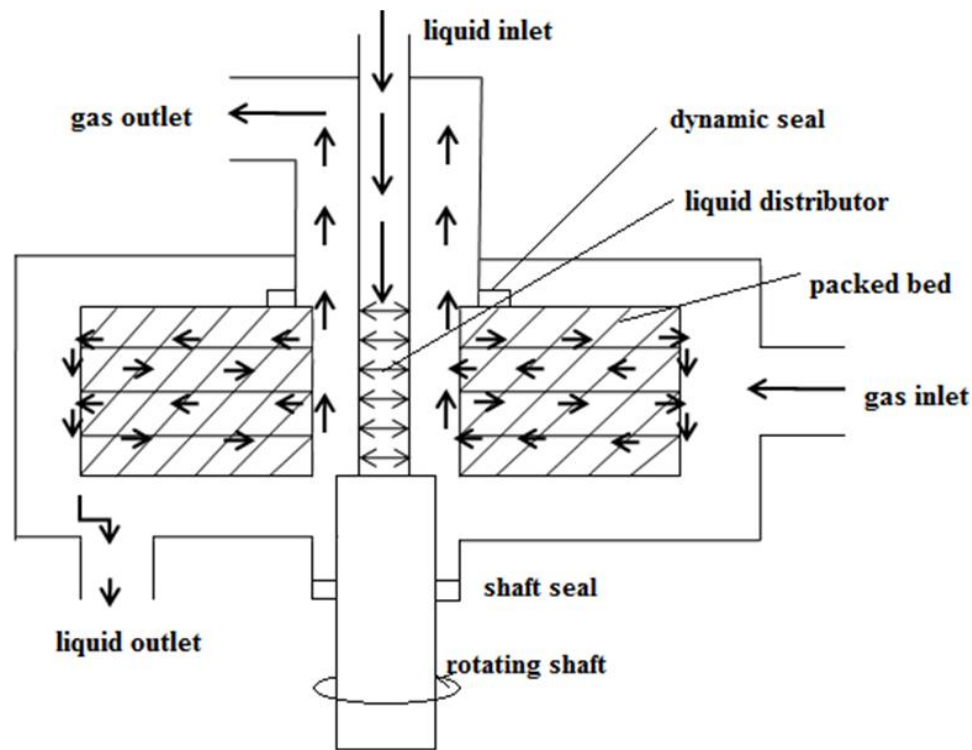


Fig 2.12: Schematic diagram of Rotating Packed bed

References

- 2.1 Standiford, F.C., "Elastomers, Synthetic-Expert Systems", *Kirk-Othmer Encyclopedia of Chemical Technology*, New York: John Wiley & Sons, Inc., 4th edition, vol. 9, pp. 472–493, 2005.
- 2.2 Minton, P.E., "Handbook of Evaporator technology", Noyes publications, New York, NY, pp. 70-100, 1986.
- 2.3 Glover, W.B., "Selecting Evaporators for Process Applications", *Chemical Engineering Progress*, vol. 100(12), pp. 26–33, December 2004.
- 2.4 Saravacos, G., Moyer, J., and Wooster, G., "Concentration of liquid foods in a pilot-scale falling film evaporator," *New York State Agricultural Experiment Station*, Sep. 1970, <https://ecommons.cornell.edu/handle/1813/4031>
- 2.5 Schausberger, P., Nowak, J., Medek, O., "Heat Transfer in Horizontal Falling Film Evaporators", *IDA World Congress*, pp. 1-9, 2009.

- 2.6 Jorge, L.M., Righetto, A.R., Polli, P.A., Santos, O.A., Maciel Filho, R., “Simulation and analysis of a sugarcane juice evaporation system”, *Journal of Food Engineering*, vol. 99, pp. 351–359, 2010.
- 2.7 Lewis, A.E., Khodabocus, F., Dhokun, V., Khalife, M., “Thermodynamic simulation and evaluation of sugar refinery evaporators using a steady state modeling approach”, *Applied Thermal Engineering*, vol. 30, pp. 2180–2186, 2010.
- 2.8 Bu, X., Ma, W., Huang, Y., “Numerical study of heat and mass transfer of ammonia-water in falling film evaporator”, *Heat Mass Transfer*, vol. 48, pp. 725–734, 2012.
- 2.9 Angeletti, S., and Moresi, M., “Modelling of multiple-effect falling film evaporators”, *Journal of Food Technology*, vol. 18, pp. 539-563, 1983.
- 2.10 Chun, K.R., and Seban, R.A., “Heat transfer to evaporating liquid films, *Journal of Heat Transfer, Trans ASME*, vol. 93 (4), pp. 391-396, 1971.
- 2.11 Chen, H., Jebson, R.S., “Factors affecting heat transfer in falling film evaporators”, *Institution of Chemical Engineers*, vol. 75, pp. 111–116, 1997.
- 2.12 Adib, T.A., Heyd, B., and Vasseur, J., “Experimental results and modeling of boiling heat transfer coefficients in falling film evaporator usable for evaporator design,” *Chemical Engineering Processing Process Intensification*, vol. 48, no. 4, pp. 961–968, Apr. 2009, doi: 10.1016/j.cep.2009.01.004.
- 2.13 Karlsson, E., Gordon, M., Olausson, L., Vamling, L., “Heat transfer for falling film evaporation of black liquor up to very high Prandtl numbers”, *International Journal of Heat and Mass Transfer*, vol. 65, pp. 907–918, 2013.
- 2.14 Bott, T.R., & Romero, J.J.B., “Heat transfer across a scraped surface”, *Canadian Journal of Chemical Engineering*, vol. 41 (5), pp. 213-219, 1963.
- 2.15 Saravacos, G.D., “Rheological aspects of fruit juice evaporation. In Spicer A(ed) *Advances in pre-concentration and dehydration of foods*”, *Applied Science Publication Ltd*, London, pp 101-107, 1974.
- 2.16 Sangrame, G., Bhagavathi, D., Thakare, H., Ali, S., and Das, H., “Performance Evaluation of a Thin Film Scraped Surface Evaporator for Concentration of

- Tomato Pulp”, *Journal of Food Engineering*, vol. 43(4), pp. 205–211, 2000, doi:10.1016/S0260-8774(99)00150-8.
- 2.17 Leenaerts, R., “Technique industrielle de la couche mince”, *Techniques del’ingénieur Journal*, vol. 2360, pp. 1–22, 1988.
- 2.18 McKenna, T.F., “Design Model of a Wiped Film Evaporator. Applications to the Devolatilisation of Polymer Melts”, *Chemical Engineering Science*, vol. 50(3), pp. 453–467, 1995, doi:10.1016/0009-2509(94)00257-R.
- 2.19 Mutzenburg, A.B., “Agitated Thin-Film Evaporators. Part 1. Thin-Film Technology”, *Chemical Engineering (New York)*, vol. 72 (19), pp. 175–178, September 13, 1965.
- 2.20 McCabe, W.L., Smith, J.C., & Harriot, P., “Unit operations of chemical engineering”, New York: McGraw Hill, 1993.
- 2.21 Hyde, W.L., Glover, W.B., “Evaporation of Difficult Product,” *Chemical Processing*, vol. 60 (2), pp. 59–61, Feb. 1997.
- 2.22 Zeboudj, S., Belhaneche-Bensemra, N., Belabbes, R., “Use of surface response methodology for the optimization of the concentration of the sweet orange essential oil of Algeria by wiped film evaporator”, *Journal of Food Engineering*, vol. 67, pp. 507–512, 2005.
- 2.23 Mutzenberg, A.B., Giger, A., “Chemical reactions in thin film equipment”, *Transactions of the Institution of Chemical Engineers*, vol. 46, pp. 187–189, 1968.
- 2.24 Bourouni, K., Martin, R., Tadrict, L., Tadrict, H., “Modeling of heat and mass transfer in a horizontal-tube falling-film evaporator for water desalination”, *Desalination*, vol. 114, pp. 111–128, 1997.
- 2.25 Parker, N., “Agitated thin film evaporator - equipments and economics”, *Chemical Engineering*, pp.179-185, 1965.
- 2.26 Zeboudj, S., Belhaneche-Bensemra, N., Belabbes, R., Bourseau, P., “Modelling of flow in a wiped film evaporator”, *Chemical Engineering Science*, vol. 61, pp. 1293 – 1299, 2006.
- 2.27 Chawankul, N., Chuaprasert, S., Douglas, P., and Luewisutthichat, W., “Simulation of an Agitated Thin Film Evaporator for Concentrating Orange

- Juice using AspenPlus”, *Journal of Food Engineering*, vol. 47(4), pp. 247-253, 2001,doi:10.1016/S0260-8774(00)00122-9.
- 2.28 Pawara, S.B., Mujumdar, A.S., Thorat, B.N., “CFD analysis of flow pattern in the agitated thin film evaporator”, *Chemical Engineering Research and Design*, vol. 90, pp. 757–765, 2012.
- 2.29 Ruan, Q., Jiang, H., Nian, M., and Yan, Z., “Mathematical modeling and simulation of countercurrent multiple effect evaporation for fruit juice concentration,” *Journal of Food Engineering*, vol. 146, pp. 243–251, Feb. 2015.
- 2.30 Rao, D.G., “Fundamentals of Food Engineering”, PHI Learning Private Ltd, NewDelhi, 2010.
- 2.31 Bhargava, R., Khanam, S., Mohanty, B., Ray, A. K., “Selection of optimal feed flow sequence for a multiple effect evaporator system”, *Computers and Chemical Engineering*, vol. 32, pp. 2203–2216, 2008.
- 2.32 Gautami, G., Khanam, S., “Selection of optimum configuration for multiple effect evaporator system”, *Desalination*, vol. 288, pp. 16–23, 2012.
- 2.33 Kouhikamal, R., Noori, S.M., Abadi, R., Hass, M., “Numerical investigation of falling film evaporation of multi-effect desalination plant”, *Applied Thermal Engineering*, vol. 70, pp. 477–485, 2014.
- 2.34 Chantasiriwan, S., “Optimum surface area distribution in co-current multiple effect evaporator”, *Journal of Food Engineering*, vol. 161, pp. 48–54, 2015.
- 2.35 Cyklis, P., “Industrial scale engineering estimation of the heat transfer in falling film juice evaporators,” *Applied Thermal Engineering*, vol. 123, pp. 1365–1373, 2017, doi: 10.1016/j.applthermaleng.2017.05.194.
- 2.36 Miranda, V., Simpson, R., “Modelling and simulation of an industrial multiple effect evaporator: tomato concentrate”, *Journal of Food Engineering*, vol. 66, pp. 203-210, 2005.
- 2.37 Simpson, R., Almonacid, S., López, D., and Abakarov, A., “Optimum design and operating conditions of multiple effect evaporators: Tomato paste,” *Journal of Food Engineering*, vol. 89, no. 4, pp. 488–497, Dec. 2008, doi: 10.1016/j.jfoodeng.2008.05.033.

- 2.38 Goula, A.M., and Adamopoulos, K.G., “Spray Drying of Tomato Pulp: Effect of Feed Concentration”, *Drying Technology*, vol. 22(10), pp. 2309–2330, 2004.
- 2.39 Schuck, P., Jeantet, R., Bhandari, B., Chen, X.D., Perrone, I. T., de Carvalho, A. F., Fenelon, M., & Kelly, P., “Recent advances in spray drying relevant to the dairy industry: A comprehensive critical review”, *Drying Technology*, vol 34(15), pp. 1773-1790, 2016, doi: 10.1080/07373937.2016.1233114.
- 2.40 Bhandari, B.R., Senoussi, A., Dumoulin, E.D., Lebert, A., “Spray drying of concentrated fruit juices”, *Drying Technology*, vol. 11 (5), pp. 1081-1092, 1993, <http://dx.doi.org/10.1080/07373939308916884>.
- 2.41 Goula, A.M., Adamopoulos, K.G., “A new technique for spray drying orange juice concentrate”, *Innovative Food Science and Emerging Technology*, vol. 11(2), pp. 342-351, 2010.
- 2.42 Fellows, P., “Tecnología del Procesado de los Alimentos”, *Principios y Prácticas Zaragoza, Spain*: Ed. Acribia, 2007.
- 2.43 Sánchez, J., Ruiz, Y., Auleda, J.M., Hernández, E., and Raventós, M., “Review. Freeze Concentration in the Fruit Juices Industry”, *Food Science and Technology International*, pp. 303-315, 2009.
- 2.44 Aider, M., Halleux, D., “Cryoconcentration technology in the bio-food industry: principles and applications”, *LWT*, vol. 42, pp. 679–685, 2009.
- 2.45 Maltini, E., and Mastrocola, D., “Preparazione di succo integro congelato di kiwifruit”, *Industria delle Bevande*, vol. 28(159), pp. 6-9, 1999.
- 2.46 Ghizzoni, C., Del Popolo, F., and Porretta, S., “Quality of cryoconcentrated red fruit juices as a function of volatile fraction”, *Rivista Italiana Eppos*, vol. 15, pp. 5–21, 1995.
- 2.47 Di Cesare, L.F., Nani, R., Brambilla, A., Tessari, D., and Fussari, E.L., “Volatile compounds and soluble substances in freeze concentrated feijoa juices [Feijoa sellowiana Berg]”, *Industria delle Bevande*, vol. 29(166), pp. 125-128, 2000.
- 2.48 Nazir, M., and Farid, M.M., “Modeling ice removal in fluidized-bed freeze concentration of apple juice”, *AIChE Journal*, vol. 54, pp. 2999–3006, 2008.

- 2.49 Hernández, E., Raventós, M., Auleda, J.M., & Ibarz, A., “Concentration of apple and pear juices in a multi-plate freeze concentrator”, *Innovative Food Science & Emerging Technologies*, vol. 10, pp. 348–355, 2009.
- 2.50 Braddock, R.J., and Marcy, J.E., “Quality of freeze concentrated orange juice”, *Journal of Food Science*, vol. 52, pp. 159–162, 1987.
- 2.51 Van Nistelrooij, M., “Bridging the cost barrier to freeze concentration”, *Food and Beverage Asia*, April/May 2005.
- 2.52 Cesare, Cortesi, and Maltini, E., “Studies on the concentration of model solutions and fruit distillates by “Freezing out”, *Fruit Processing*, vol. 3(12), pp. 442–445, 1993.
- 2.53 Hartel, R.W., and Espinel, L.A., “Freeze concentration of skim milk”, *Journal of Food Engineering*, vol. 20, pp. 101–120, 1993.
- 2.54 Putman, R., Vanderhasselt, B., Vanhamel, S., “Process for the preparation of beer of the “pilsener” or “lager” type”, *PCT – International-Patent-Application*, Belgium, 1997.
- 2.55 Raventós, M., Hernández, E., Auleda, J. M., & Ibarz, A., “Concentration of aqueous sugar solutions in a multi-plate cryoconcentrator”, *Journal of Food Engineering*, vol. 79, pp. 577–585, 2007.
- 2.56 Hernández, E., Raventós, M., Auleda, J. M., and Ibarz, A., “Freeze concentration of must in a pilot falling film cryoconcentrator”, *Innovative Food Science & Emerging Technologies*, vol. 11, pp. 130–136, 2010.
- 2.57 Sánchez, J., Ruiz, Y., Raventós, M., Auleda, J.M., Hernández, E., “Progressive freeze concentration of orange juice in a pilot plant falling film”, *Innovative Food Science & Emerging Technologies*, vol. 11(4), pp. 644-651, 2010.
- 2.58 Ramaswamy, H., and Marcotte, M., “Separation and Concentration. In Food processing Principles and Applications”, p.317-379. United States of America: CRC Press, 2006.
- 2.59 Aguiar, I.B., Miranda, M.G.M., Gomes, F.S., Santos, F.C.S., Freitas, D.d.G.C., Tonon, R.V., Cabral, L.M.C., “Physicochemical and sensory properties of apple juice concentrated by reverse osmosis and osmotic evaporation,” *Innovative*.

- Food Science and Emerging Technology*, vol. 16, pp. 137–142, Oct. 2012, doi: 10.1016/j.ifset.2012.05.003.
- 2.60 Castro, S.M., Saraiva, J.A., Lopes-da-Silva, J.A., Delgadillo, I., Van Loey, A., Smout, C., Hendrickx, M., “Effect of thermal blanching and of high-pressure treatments on sweet green and red bell pepper fruits (*Capsicum annum*L.)”, *Food Chemistry*, vol. 107 (4), pp. 1436-1449, 2008.
- 2.61 De Oliveira, R.C., Doce, R.C., and de Barros, S.T.D., “Clarification of passion fruit juice by microfiltration: Analyses of operating parameters, study of membrane fouling and juice quality”, *Journal of Food Engineering*, vol. 111(2), pp. 432–439, 2012.
- 2.62 Vaillant, F., Millan, P., Brien, G., and Decloux, M., “Cross-flow microfiltration of passion fruit juice after partial enzymatic liquefaction”, *Journal of Food Engineering*, vol. 42(4), pp. 215–225, 1999.
- 2.63 Vaillant, F., Millan, A., Dornier, M., Decloux, M., and Reynes, M., “Strategy for economical optimization of the clarification of pulpy fruit juices using cross flow microfiltration”, *Journal of Food Engineering*, vol. 48, pp. 83–90, 2001.
- 2.64 Rai, C., Rai, P., Majumdar, G.C., De, S., and Das Gupta, S., “Mechanism of permeate flux decline during microfiltration of watermelon (*Citrulluslanatus*) juice”, *Food and Bioprocess Technology*, vol. 3(4), pp. 545–553, 2010.
- 2.65 Gomes, F.A., Costa, P.A., Campos, M.B.D., Tonon, R.V., Couri, S., and Cabral, L.M.C., “Watermelon juice pretreatment with microfiltration process for obtaining lycopene”, *International Journal of Food Science and Technology*, vol. 48(3), pp. 601–608, 2013.
- 2.66 Chhaya, C., Rai, P., Majumdar, G.C., Dasgupta, S., and De, S., “Clarification of watermelon(*Citrulluslanatus*) juice by microfiltration”, *Journal of Food Process Engineering*, vol. 31(6), pp. 768–782, 2008.
- 2.67 Zarate-Rodriguez, E., Ortega-Rivas, E., and Barbosa-Canovas, G.V., “Effect of membrane pore size on quality of ultrafiltered apple juice”, *International Journal of Food Science and Technology*, vol. 36(6), pp. 663–667, 2001.
- 2.68 Youn, K.S., Hong, J.H., Bae, D.H., Kim, S.J., and Kim, S.D., “Effective clarifying process of reconstituted apple juice using membrane filtration with

- filter-aid pretreatment”, *Journal of Membrane Science*, vol. 228(2), pp. 179–186, 2004.
- 2.69 Vladisavljevic, G.T., Vukosavljevic, P., and Bukvic, B., “Permeate flux and fouling resistance in ultrafiltration of depectinized apple juice using ceramic membranes”, *Journal of Food Engineering*, vol. 60(3), pp. 241–247, 2003.
- 2.70 Onsekizoglu, P., Bahceci, K.S., and Acar, M.J., “Clarification and the concentration of apple juice using membrane processes: A comparative quality assessment”, *Journal of Membrane Science*, vol. 352(1–2), pp. 160–165, 2010.
- 2.71 De Bruijn, J., Venegas, A., and Borquez, R., “Influence of crossflow ultrafiltration on membrane fouling and apple juice quality”, *Desalination*, vol. 148(1), pp. 131–136, 2002.
- 2.72 Bhattacharjee, C., Saxena, V.K., & Dutta, S., “Watermelon juice concentration using ultrafiltration: Analysis of sugar and ascorbic acid”, *Food Science and Technology International*, (1082013217714672), 2017.
- 2.73 Cassano, A., Conidi, C., & Tasselli, F., “Clarification of pomegranate juice (*Punicagranatum L.*) by hollow fiber membranes: Analyses of membrane fouling and performance”, *Journal of Chemical Technology & Biotechnology*, vol. 90(5), pp. 859–866, 2015.
- 2.74 Bagci, P.O., “Effective clarification of pomegranate juice: A comparative study of pretreatment methods and their influence on ultrafiltration flux”, *Journal of Food Engineering*, vol. 141, pp. 58–64, 2014.
- 2.75 Tasselli, F., Cassano, A., and Drioli, E., “Ultrafiltration of kiwifruit juice using modified poly (ether ketone) hollow fibre membranes”, *Separation and Purification Technology*, vol. 57(1), pp. 94–102, 2007.
- 2.76 Mohammad, A., Ng, C., Lim, Y., and Ng, G., “Ultrafiltration in food processing industry: Review on application, membrane fouling, and fouling control”, *Food and Bioprocess Technology*, vol. 5(4), pp. 1143–1156, 2012.
- 2.77 Arriola, N.A., Dos-Santos, G.D., Prudencio, E.S., Vitali, L., Petrus, J.C.C., and Amboni, R.D.M.C., “Potential of nanofiltration for the concentration of bioactive compounds from watermelon juice”, *International Journal of Food Science and Technology*, vol. 49(9), pp. 2052–2060, 2014.

- 2.78 Conidi, C., Cassano, A., Caiazzo, F., and Drioli, E., “Separation and purification of phenolic compounds from pomegranate juice by ultrafiltration and nanofiltration membranes”, *Journal of Food Engineering*, vol. 195, pp. 1–13, 2017.
- 2.79 Warczok, J., Ferrando, M., Lopez, F., and Guell, C., “Concentration of apple and pear juices by nanofiltration at low pressures”, *Journal of Food Engineering*, vol. 63(1), pp. 63–70, 2004.
- 2.80 Jesus, D.F., Leite, M.F., Silva, L.F.M., Matta, V.M., Modesta, R.C.D., and Cabral, L.M.C., “Orange (*Citrus sinensis*) juice concentration by reverse osmosis”, *Journal of Food Engineering*, vol. 81(2), pp. 287–291, 2007.
- 2.81 Shaw, P. E., Lebrun, M., Dornier, M., Ducamp, M. N., Courel, M., and Reynes, M., “Evaluation of concentrated orange and passionfruit juices prepared by osmotic evaporation”, *LWT- Food Science and Technology*, vol. 34(2), pp. 60–65, 2001.
- 2.82 Gurak, P.D., Cabral, L.M., Rocha-Leao, M.H., Matta, V.M., and Freitas, S.P., “Quality evaluation of grape juice concentrated by reverse osmosis”, *Journal of Food Process Engineering*, vol. 96(3), pp. 421–426, 2010.
- 2.83 Bánvölgyi, S., Horváth, S., Stefanovits-Bányai, É., Békássy-Molnár, E., and Vatai, G., “Integrated membrane process for blackcurrant (*Ribesnigrum* L.) juice concentration”, *Desalination*, vol. 241(1), pp. 281–287, 2009.
- 2.84 Alvarez, V., Alvarez, S., Riera, E.A., Alvarez, R., “Permeate flux prediction in apple juice concentration by reverse osmosis”, *Journal of Membrane Science*, vol. 127, pp. 25-34, 1997.
- 2.85 Gostoli, C., Bandini, S., Di Francesca, R., and Zardi, G., “Concentrating fruit juices by reverse osmosis—the low retention—high retention method”, *Fruit Process*, vol. 6, pp. 183–193, 1995.
- 2.86 Matta, V.M., Moretti, R.H., and Cabral, L.M.C., “Microfiltration and reverse osmosis for clarification and concentration of acerola juice”, *Journal of Food Engineering*, vol. 61, pp. 477–482, 2004.
- 2.87 Rodrigues, R.B., Menezes, H.C., Cabral, L.M.C., Dornier, M., Rios, G.M., Reynes, M., “Evaluation of reverse osmosis and osmotic evaporation to

- concentrate camu–camu juice (Myrciariadubia)”, *Journal of Food Engineering*, vol. 63, pp. 97-102, 2004.
- 2.88 Vandana, T., Manjunath, S.S., and Das-Gupta, D.K., “Comparative evaluation of clarification and concentration technique for Kinnow fruit juice”, *Journal of Food Science and Technology*, vol. 41(4), pp. 382–385, 2004.
- 2.89 Walker, J.B., “Reverse osmosis concentration of juice products with improved flavor”, U.S. Patent 4.959.237, v.7
- 2.90 Kotsanopoulos, K.V., & Arvanitoyannis, I.S., “Membrane processing technology in the food industry: Food processing, wastewater treatment, and effects on physical, microbiological, organoleptic, and nutritional properties of foods”, *Critical Reviews in Food Science and Nutrition*, vol. 55, pp. 1147–1175, 2015.
- 2.91 Vera, E., Ruales, J., Dornier, M., Sandeaux, J., Persin, F., Pourcelly, G., Reynes, M., “Comparison of different methods for deacidification of clarified passion fruit juice”, *Journal of Food Engineering*, vol. 59, pp. 361–367, 2003a.
- 2.92 Vera, E., Ruales, J., Dornier, M., Sandeaux, J., Sandeaux, R., & Pourcelly, G., “Deacidification of the clarified passion fruit juice using different configurations of electrodialysis”, *Journal of Chemical Technology and Biotechnology*, vol. 78, pp. 918–925, 2003b.
- 2.93 Rozoy, E., Boudesocque, L., and Bazinet, L., “Deacidification of cranberry juice by electrodialysis with bipolar membranes”, *Journal of Agricultural and Food Chemistry*, vol. 63(2), pp. 642–651, 2015.
- 2.94 Serre, E., Rozoy, E., Pedneault, K., Lacour, S., and Bazinet, L., “Deacidification of cranberry juice by electrodialysis: Impact of membrane types and configurations on acid migration and juice physicochemical characteristics”, *Separation and Purification Technology*, vol. 163, pp. 228–237, 2016.
- 2.95 Adhikary, S.K., Harkare, W.P., Govindan, K.P., and Nanjundaswamy, A.M., “Deacidification of fruit juices by electrodialysis”, *Indian Journal of Technology*, vol. 21, pp. 120–123, 1983.

- 2.96 Kang, Y.J., and Rhee, K.C., “Deacidification of mandarin orange juice by electro dialysis combined with ultrafiltration”, *Nutraceuticals and Food*, vol. 7(4), pp. 411–416, 2002.
- 2.97 Andres, L.J., Riera, F.A., & Alvarez, R., “Skimmed milk demineralization by electro dialysis: Conventional versus selective membranes”, *Journal of Food Engineering*, vol. 26, pp. 57–66, 1995.
- 2.98 Boye, J.I., and Arcand, Y., “Green technologies in food production and processing”, Springer Science & Business Media, 2012.
- 2.99 Karlsson, H.O., and Tragardh, G., “Applications of pervaporation in food processing”, *Trends in Food Science & Technology*, vol. 7(3), pp. 78–83, 1996.
- 2.100 Catarino, M., Ferreira, A., and Mendes, A., “Study and optimization of aroma recovery from beer by pervaporation”, *Journal of Membrane Science*, vol. 341(1–2), pp. 51–59, 2009.
- 2.101 Cassano, A., Figoli, A., Tagarelli, A., Sindona, G., and Drioli, E., “Integrated membrane process for the production of highly nutritional kiwifruit juice”, *Desalination*, vol. 189, pp. 21–30, 2006.
- 2.102 Cassano, A., Conidi, C., and Drioli, E., “A membrane-based process for the valorization of the bergamot juice”, *Separation Science and Technology*, vol. 48(4), pp. 537–546, 2013.
- 2.103 Isci, A., Sahin, S., and Sumnu, G., “Recovery of strawberry aroma compounds by pervaporation”, *Journal of Food Engineering*, vol. 75(1), pp. 36–42, 2006.
- 2.104 Pereira, C.C., Rufino, J.R.M., Habert, A.C., Nobrega, R., Cabral, L.M.C., and Borges, C.P.J., “Aroma compounds recovery of tropical fruit juice by pervaporation: Membrane material selection and process evaluation”, *Journal of Food Engineering*, vol. 66, pp. 77–87, 2005.
- 2.105 Shepherd, A., Habert, A.C., and Borges, C.P., “Hollow fibre modules for orange juice aroma recovery using pervaporation”, *Desalination*, vol. 148(1), pp. 111–114, 2002.
- 2.106 Rajagopalan, N., and Cheryan, M., “Pervaporation of grape juice aroma”, *Journal of Membrane Science*, vol. 104, pp. 243–250, 1995.

- 2.107 Raisi, A., Aroujalian, A., and Kaghazchi, T., “Multicomponent pervaporation process for volatile aroma compounds recovery from pomegranate juice”, *Journal of Membrane Science*, vol. 322(2), pp. 339–348, 2008.
- 2.108 Takács, L., Vatai, G., and Korány, K., “Production of alcohol free wine by pervaporation”, *Journal of Food Engineering*, vol. 78(1), pp. 118–125, 2007.
- 2.109 Schafer, T., Bengtsem, G., Pingel, H., Bödeleker, K.W., and Crespo, J.P.S.G., “Recovery of aroma compounds from a wine-must fermentation by organophilic pervaporation”, *Biotechnology and Bioengineering*, vol. 62, pp. 412–421, 1999.
- 2.110 Lipnizki, F., “Cross-flow membrane applications in the food industry”, *Membranes for food applications*, K. V. Peinemann, S. Pereira, & L. Giorno (Eds.), Estados Unidos de América: Willey-VCH, pp. 1–23, 2010.
- 2.111 Klaassen, R., Feron, P.H.M., and Jansen, A.E., “Membrane contactors in industrial applications”, *Chemical Engineering Research and Design*, vol. 83(3), pp. 234–246, 2005.
- 2.112 Varavuth, S., Jiratananon, R., and Atcharyawut, S., “Experimental study on dealcoholisation of wine by osmotic distillation process”, *Separation and Purification Technology*, vol. 66, pp. 313–321, 2009.
- 2.113 Cassano, A., Conidi, C., Timpone, R., D'avella, M., and Drioli, E., “A membrane-based process for the clarification and the concentration of the cactus pear juice”, *Journal of Food Engineering*, vol. 80(3), pp. 914–921, 2007.
- 2.114 Lagana, F., Barbieri, G., and Drioli, E., “Direct contact membrane distillation: Modelling and concentration experiments”, *Journal of Membrane Science*, vol. 166(1), pp. 1–11, 2000.
- 2.115 Gunko, S., Verbych, S., Bryk, M., and Hilal, N., “Concentration of apple juice using direct contact membrane distillation”, *Desalination*, vol. 190(1–3), pp. 117–124, 2006.
- 2.116 Curcio, E., and Drioli, E., “Membrane distillation and related operations-a review”, *Separation and Purification Reviews*, vol. 34(1), pp. 35–86, 2005.
- 2.117 Calabro, V., Jiao, B., and Drioli, E., “Theoretical and experimental study on membrane distillation in the concentration of orange juice”, *Industrial and Engineering Chemistry Research*, vol. 33(7), pp. 1803–1808, 1994.

- 2.118 Diban, N., Voinea, O. C., Urtiaga, A., and Ortiz, I., “Vacuum membrane distillation of the main pear aroma compound: experimental study and mass transfer modelling”, *Journal of Membrane Science*, vol. 326(1), pp. 64–75, 2009.
- 2.119 Kozak, A., Bekassy-Molnar, E., and Vatai, G., “Production of blackcurrant juice concentrate by using membrane distillation”, *Desalination*, vol. 241(1–3), pp. 309–314, 2009.
- 2.120 Calabro, V., Jiao, B., & Drioli, E., “Theoretical and experimental study on membrane distillation in the concentration of orange juice”, *Industrial and Engineering Chemistry Research*, vol. 33(7), pp. 1803–1808, 1994.
- 2.121 Girard, B., & Fukumoto, L., “Membrane processing of fruit juices and beverages: A review”, *Critical Reviews in Biotechnology*, vol. 20(2), pp. 109–175, 2000.
- 2.122 Oliveira, C.S., Gomes, F.S., Constant, L.S., Silva, L.F.M., Godoy, R.L.O., Tonon, R.V., Cabral, L.M.C., “Integrated membrane separation processes aiming to concentrate and purify lycopene from watermelon juice”, *Innovative Food Science and Emerging Technology*, vol. 38 (Part A), pp. 149–154, 2016.
- 2.123 Koroknai, B., Csanádi, Z., Gubicza, L., and Bélafi-Bakó, K., “Preservation of antioxidant capacity and flux enhancement in concentration of red fruit juices by membrane processes”, *Desalination*, vol. 228(1–3), pp. 295–301, 2008.
- 2.124 Bottino, A., Capannelli, G., Turchini, A., Della Valle, P., Trevisan, M., “Integrated membrane processes for the concentration of tomato juice”, *Desalination*, vol. 148, pp. 73–77, 2002.
- 2.125 Echavarría, A.P., Falguera, V., Torras, C., Berduín, C., Pagán, J., Ibarz, A., “Ultrafiltration and reverse osmosis for clarification and concentration of fruit juices at pilot plant scale”, *LWT - Food Science and Technology*, vol. 46 (1), pp. 189–195, 2012, <https://doi.org/10.1016/j.lwt.2011.10.008>.
- 2.126 Quist-Jensen, C.A., Macedonio, F., Conidi, C., Cassano, A., Aljlil, S., Alharbi, O.A., Drioli, E., “Direct contact membrane distillation for the concentration of clarified orange juice”, *Journal of Food Engineering*, vol. 187, pp. 37–43, 2016.

- 2.127 Pap, N., Pongrácz, E., Jaakkola, M., Tolonen, T., Virtanen, V., Turkki, A., Horváth-Hovorka, Z., Vatai, G., Keiski, R.L., “The effect of pre-treatment on the anthocyanin and flavonol content of black currant juice (*Ribesnigrum* L.) in concentration by reverse osmosis”, *Journal of Food Engineering*, vol. 98(4), pp. 429-436, 2010.
- 2.128 Rektor, A., Vatai, G., Békássy-Molnár, E., “Multi-step membrane processes for the concentration of grape juice”, *Desalination*, vol. 191, pp. 446-453, 2006.
- 2.129 Ribeiro Jr, C.P., Lage, P., “Gas-Liquid Direct-Contact Evaporation: A Review”, *Chemical Engineering & Technology*, vol. 28(10), pp.1081 – 1107, 2005.
- 2.130 Ribeiro, C.P., Borges, C.P., and Lage, P.L.C., “Modelling of direct-contact evaporation using a simultaneous heat and multicomponent mass-transfer model for superheated bubbles,” *Chemical Engineering and Science*, vol. 60, no. 6, pp. 1761–1772, 2005, doi:10.1016/j.ces.2004.08.049.
- 2.131 Goswami, N., Basu, S., Bhowal, A., Datta, S., “Concentration of solution in cross-flow rotating packed bed contactor”, *Chemical Engineering Research and Design*, vol. 95, pp. 281-287, 2015.
- 2.132 Ramshaw, C., Mallinson, R.H., “Mass Transfer Process”, 1981, USPatent # 4, 283, 255.
- 2.133 Rao, D.P., Bhowal, A., Goswami, P.S., “Process intensification in Rotating Packed Beds (HIGEE): An Appraisal”, *Industrial Engineering Chemistry and Research*, vol. 43, pp. 1150-1162, 2004.
- 2.134 Jiao, W., Luo, S., He, Z., Liu, Y., “Applications of High Gravity Technologies for Wastewater Treatment: A Review”, *Chemical Engineering Journal*, vol. 313, pp. 912–927, 2017.

Chapter 3

Aims and objective

A crucial segment of the total processed fruit industry is represented by juice and juice products. Most of the fruits grow in a particular season and a specific climatic zone [3.1]. The fruits are usually processed in the forms of purees, juices, and pulps [3.2] to make them available in far-off geographical regions from their production sites throughout the year [3.3]. The high water content in fruit juice however reduces its stability and shelf life [3.2,3.3]. The concentration of raw juice has many benefits including increased shelf life, easy transportation, and packing, reduction in volume and weight of the product, increase in stability, and an overall reduction in cost [3.5-3.7].

Some of the methods studied in recent years for the concentration of fruit juice include membrane separation, filtration techniques, freeze concentration, and hydrate separation techniques. Membrane separation processes and filtration techniques are associated with high capital cost, capacity constraint, and decline of flux due to concentration polarization and membrane fouling. The disadvantages of spray-drying evaporators are their low thermal efficacy, lack of control over droplet size, and air humidity, among others [3.8]. In the case of freeze concentration, the disadvantages include large economy loss due to high energy consumption, difficult control of ice crystal growth for longer periods (capacity constraint), large energy consumption due to nonstop scraping blade rotation, and solids loss due to juice entrapped in ice crystals [3.8]. Furthermore, there is evidence that concentration procedures based on phase transitions have negative effects on product nutritional and sensory properties [3.9]. The nutritional and sensory attributes decline in the formation of hydrates in the hydrate

separation technique. Moreover, all the hydrates are not eco-friendly and may result in a bitter juice concentrate [3.8].

Fruit juice concentrates have been conventionally produced by removing water as vapor by application of thermal energy [3.10]. Falling film, wiped or agitated film evaporators are often used for heat-sensitive liquid foods. But the generation of local hotspots due to higher viscosity and nonuniform distribution of heat on the surface of the evaporators over which the solution flows results in fouling on the heating surface. Saravacos et al. [3.11] noted that liquid foods such as apple juice and soymilk among others cannot be concentrated at temperatures above 65 °C as precipitates from the liquid foods result in fouling of the tube. This solid layer also acts as a barrier to heat transfer and reduces the evaporation rate. This led Ribeiro et al. [3.12] to propose direct evaporation of fruit juices by dispersing heated gas bubbles through the fruit juice to enhance heat transfer. In this technique, the liquid is heated by gas bubbles. Water evaporates into the gas bubbles rising through the liquid.

The evaporation rate obtained with this technique would be further improved if the process is carried out in equipment associated with high values of volumetric mass transfer coefficient. Some of the traditional gas-liquid contactors are packed beds, spray columns, and tray columns wherein they flow continuously through the equipment in countercurrent contact. Figure 3.1 shows the schematic diagram of these devices. The spray column is a gas-liquid contactor that consists of nozzles that spray liquid into a steel or plastic empty cylindrical vessel. The gas stream typically enters at the bottom of the tower and goes upward. These columns are adaptable in handling liquids containing suspended particulates because they lack any internal structures. Packed columns are

usually hollow towers that are filled with different types of packing materials inside. The dispersed phase can coalesce and re-disperse with the aid of packing materials. The contact between the two phases (gas-liquid) takes place over perforated plates or trays in a tray column. A turbulent gas-liquid dispersion is generated as the gas bubbles rise through the layer of liquid flowing on the tray.

The range of volumetric mass transfer coefficients obtained in some of the above-mentioned extractors is given in Table 3.1.

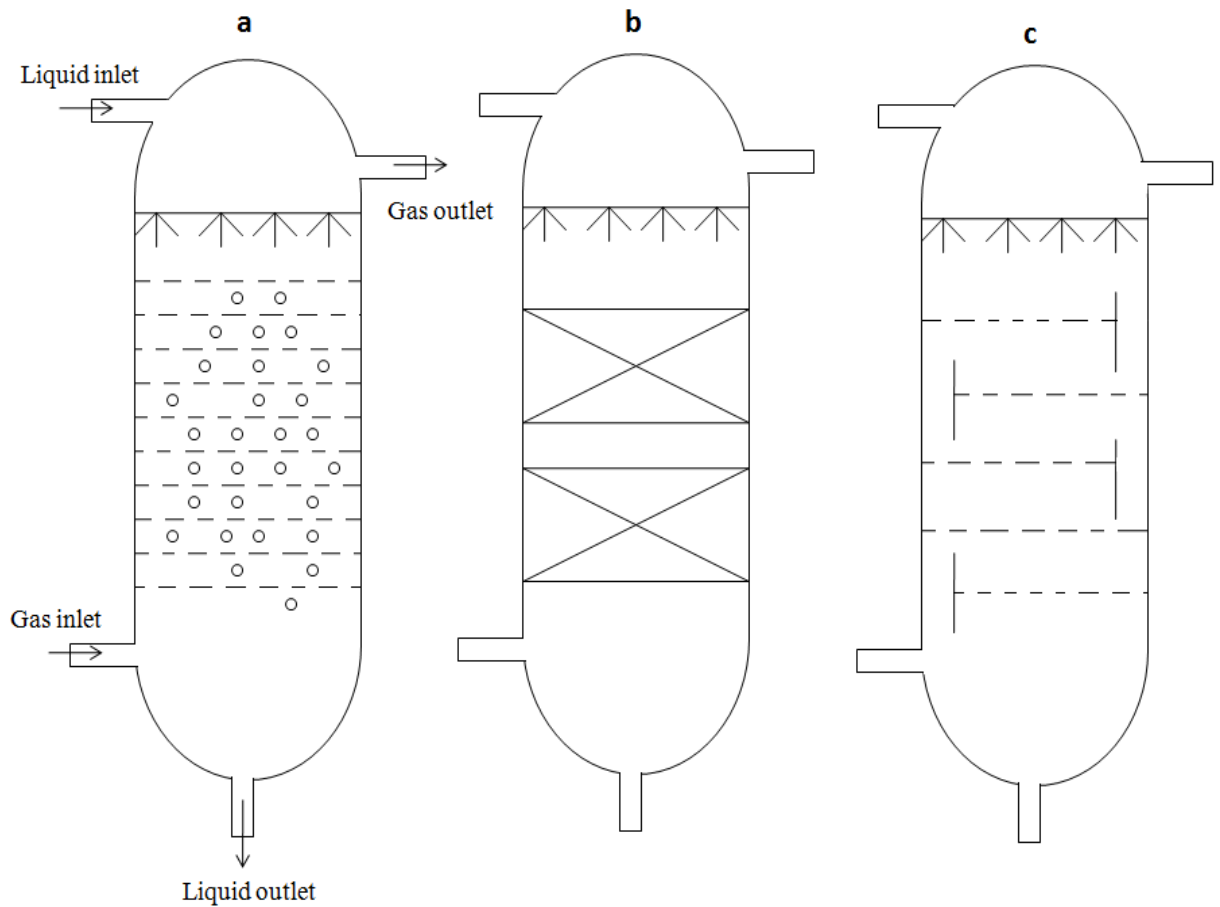


Fig. 3.1: Diagrams of conventional gas-liquid contactors (a. Spray column, b. packed column, c. tray column)

Table 3.1: Mass transfer coefficient in different gas-liquid contactors [3.13]

Contactors	Superficial gas velocity (m/s)	Mass Transfer parameters		
		$K_L * 10^{-4}$ (m/s)	$K_y * 10^3$ (kmol/sm ² Δy)	Interfacial area a (m ² /m ³)
Spray column	0.05 – 3	0.7-1.5	0.5-2	10-100
Packed column	0.1-1.2	1-20	0.03-2	10-350
Tray column	0.02-0.5	1-20	0.5-6	100-200
Bubble column	0.1-0.3	0.4-3	0.5-2	50-200
Mechanically agitated column	0.05-3	0.3-4	-	100-1000

Goswami et al. [3.14] used a rotating packed bed (RPB) for the concentration of sucrose solution. The volumetric mass transfer coefficient for gas-liquid operations in RPB is provided in Table 3.2.

Table 3.2: Mass transfer coefficient of different gas-liquid operations in rotating packed bed

System	Flow nature	$K_G a$ (s ⁻¹)	Reference
CO ₂ -MEA	Cross-flow	0.64-7.1	Jassim et al. [3.15]
CO ₂ -NaOH, CO ₂ -MEA, CO ₂ -MEA,AMP	Countercurrent flow	0.41-0.53, 0.5-0.75, 0.41-0.51.	Lin et al. [3.16]
CO ₂ - NaOH	Cross-flow	0.16-1.43	Lin et al. [3.17]
CO ₂ -MEA/PZ	Countercurrent flow	3.75-8.75	Cheng & Tan [3.18]
CO ₂ -NaOH	Countercurrent flow	0.68-2.62	Lin & Chu [3.19]
CO ₂ -DETA,PZ	Countercurrent flow	0.91-2.59	Sheng et al. [3.20]
CO ₂ -PZ/DETA	Countercurrent flow	1.54-4.29	Wu et al. [3.21]
CO ₂ -DETA	Countercurrent flow	1.12-7.44	Sheng et al. [3.22]
MEA - Mono Ethyl Alcohol, PZ - Piperazine, DETA - Diethylene triamine, AMP - Ammonium molybdophosphate			

The values are higher than in bubble column or other equipment reported in Table 3.1. Furthermore, centrifugal force would mitigate the adverse effect of increasing viscosity of the juice on the evaporation rate besides carrying precipitated particles away from the equipment.

The heart of a rotating contactor is the rotor that gives the contactor specific mass transfer characteristics. Various types of rotors viz. waveform discs, packed beds, spinning disc contactors, zigzag bed contactors, spiral discs, helical discs, and multistage spraying have been reported in the literature [3.23].

Split packed rotating packed bed

Two sets of alternate annular packing rings (Figure 3.2a) constitute the rotor of the device; one set was fixed to the top plate and the other set to the bottom plate. The rings were rotated in opposite directions to increase the tangential slip velocity between the gas and the packing.

Waveform discs

A waveform disc rotating bed with a set of concentric waveform discs on the rotor was created in order to successfully lower gas flow resistance (Figure 3.2b). In addition to the disk's surface area, this type of rotating bed can make use of the increased interfacial area produced by atomization.

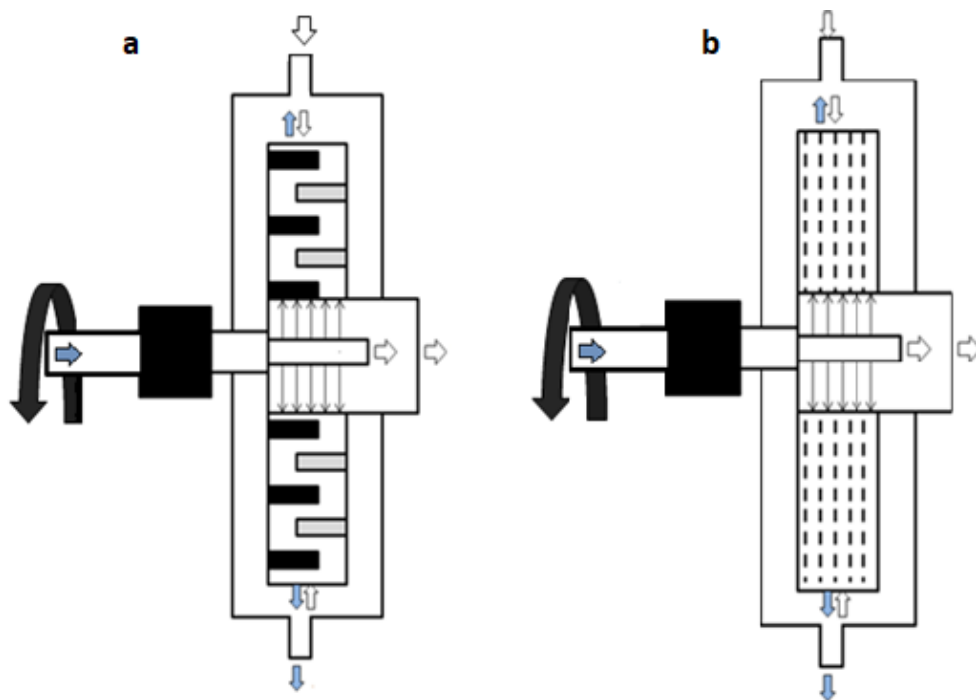


Fig. 3.2: **a.** Schematic diagram of split packed Rotating Packed bed, **b.** Schematic diagram of waveform disc.

Spinning Disk Contactor

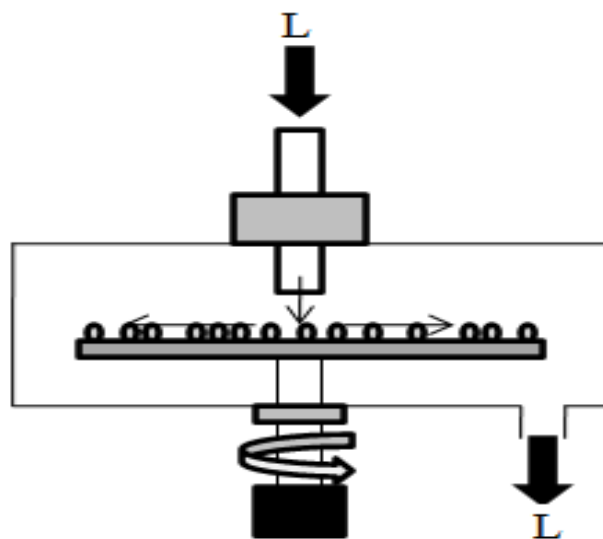


Fig. 3.3: Schematic diagram of Spinning Disk Contactor

This equipment (Figure 3.3) consists of a disk mounted either upon a horizontal or vertical rotating axis. Liquid is introduced near the center and due to high centrifugal force, it flows over the disc surface [3.24]. Centrifugal force helps in achieving highly sheared liquid film on the surface of the disc allowing high mass transfer rates as well as short residence time.

Rotating Spiral Bed

A rotating spiral bed comprises a motor, a sealed unit, and a spiral channel element. Figure 3.4 shows a schematic of a spiral bed. Inside this equipment, the liquid flows as a layer on the channel wall. The layered flow inside the rotating spiral channel is quite similar to that of the falling film inside a wetted-wall tower [3.25-3.28].

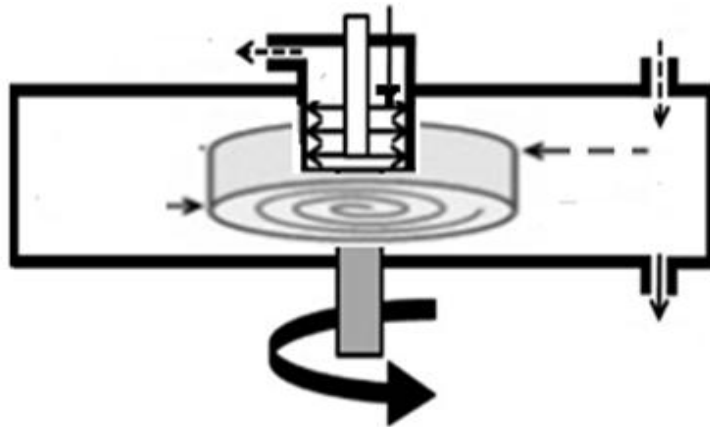


Fig.3.4: Schematic diagram of Rotating Spiral Bed

Rotating zigzag bed contactor

Among the rotor designs, the rotating zigzag bed (RZB) proposed by Ji et al. [3.29] has shown to be more effective in providing high mass transfer rates for absorption and distillation process. Rotating zigzag bed contactor combines a rotating disk and a stationary disk (shown in Figure 3.5). Concentric circular sheets are attached to both

disks. The rotational baffle is provided with holes fixed onto the lower (rotational) disk. The rotational disk is rotated by a motor through a vertical shaft [3.30-3.32].

In the rotor's interior, the dispersed liquid phase goes through numerous dispersion-accumulation cycles while the continuous gas phase travels in a zigzag pattern. Rotational baffles with a high rotational speed disperse the liquid into tiny droplets. These droplets are halted by stationary baffles. They aggregate as a liquid film on the baffle wall and fall once more onto the rotating disk. The liquid then disperses again radially outward by the subsequent rotational baffle. The gas enters the rotor from the outer radius and flows radially inward in a staggered manner. In comparison to RPB, the RZB features a considerably bigger liquid holdup caused by rotational and stationary baffles, which results in a longer residence time for the liquid phase, increasing mass transfer capacity.

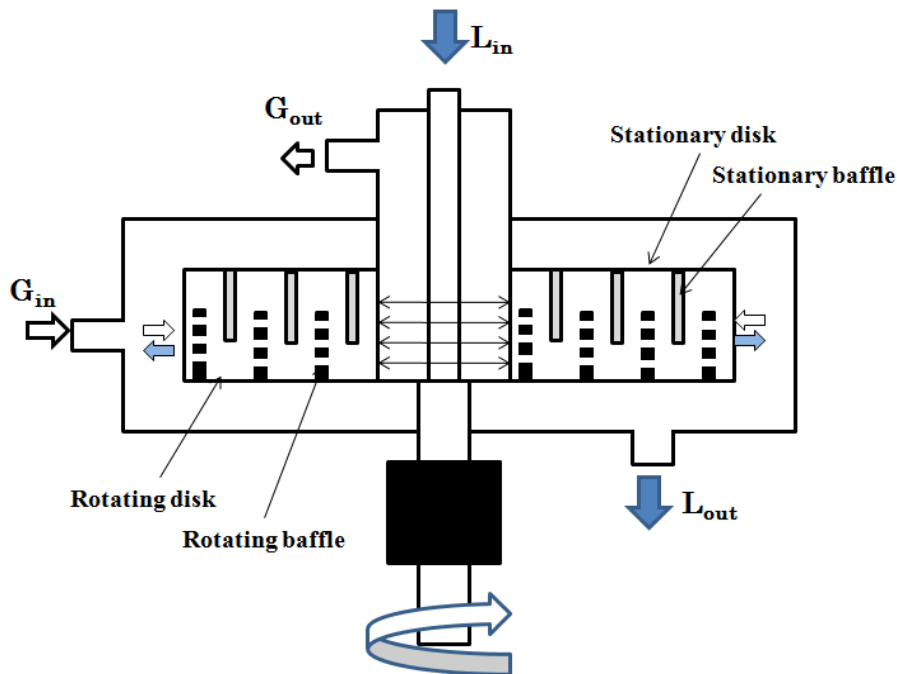


Fig 3.5: Schematic diagram of Rotating zigzag bed

Hangzhou Ke-Li Chemical Equipment Co. Ltd. in cooperation with the Zhejiang University of Technology has commercially manufactured distillation units using Rotating zigzag beds to recover organic solvents for chemical and pharmaceutical industries.

Various research on the hydrodynamics of rotating zigzag beds (RZB) [3.35], mass transfer characteristics [3.33], and performances [3.30] have been published in the past ten years. In a study conducted by Li et al. [3.32], it was shown that the liquid side mass transfer coefficient observed in RZB was 2.5 times more than that of conventional RPB. According to another investigation on distillation [3.31] in RZB, the volume needed for a packed bed operating under the same conditions was about ten times more than that of RZB. However, there are no available results on the feasibility of using rotating contactors for the concentration of fruit juice.

The major objective of this study has therefore been to explore the possibility of replacing traditional film evaporators for the concentration of fruit juice by air (unsaturated) stripping performed using rotating contactors. The traditional rotating packed bed used by Goswami et al. [3.14] for the concentration of sucrose solution has been used as one of the rotating contactors. The RZB was modified to serve as the second rotating contactor and has been named rotating baffle contactor. The main differences from shown that shown in Figure 3.5 are listed below.

- The rotor rotated about a horizontal axis
- Both the disks were rotating in the same direction
- There were no holes in the circular baffles of the rotating disk.

The presence of holes in the design of RZB could lead to gas passing through the holes rather than the zigzag pattern envisaged unless the liquid flow rate is high enough to ensure that only liquid flows through all the holes. This also increases the residence time of both phases in the contactor leading to more amount of mass transfer.

The following work has been done to achieve the objective

- (a) Experimental studies to determine the heat and mass transfer characteristics of Rotating Zigzag bed and Rotating packed bed using an air-water system.
- (b) Develop a mathematical model to estimate the overall volumetric mass transfer coefficient.
- (c) Experimental study for the concentration of a wide variety of fruit juice in the rotating contactor by air stripping.
- (d) Study the intensification achievable for concentration of fruit juice by comparing it with a conventional wiped film evaporator.

Physiochemical analysis of the feed juice and the concentrate was also done. Seven different fruits were used in the experimental study. According to their physiochemical characteristics, the fruits that were used are classified into 4 different groups –

- Citrus fruit - orange (*Citrus sinensis*)

Citrus fruits like orange are a rich source of vitamin C and dietary fibers which strengthens the immune system and keeps our skin good.

- Lycopene containing red fruits - tomato (*Solanum lycopersicum*) and watermelon (*Citrullus lanatus*),

A red-colored pigment (carotenoid) in plant derivatives is called lycopene. The pigment is responsible for the distinctive color of red and pink fruits including

tomatoes, watermelons, and pink grapefruit. Lycopene has been associated with health advantages ranging from heart health to defense against skin cancer and sunburn.

- High level of antioxidant-containing fruits - Black grapes (Black Muscat, *Vitis vinifera*) and pomegranate (*Punica granatum*),

Both Black grapes and Pomegranates are rich sources of antioxidants. Compared to green or red grapes, some black grape types have substantially more antioxidants. Pomegranate juice has been found to include large concentrations of anthocyanins and anthoxanthins, two compounds that promote heart health.

- Sugar-containing fruit and agronomic crop - Grapes (Thompson seedless, *Vitis vinifera*) and sugarcane (*Saccharum officinarum*).

Both grapes and sugarcane are rich sources of sugar where glucose is the variant obtained in grapes and sucrose is the variant obtained in sugarcane. Numerous antioxidants included in sugarcane juice protect the liver from damage and keep bilirubin levels under control. Excellent diuretic qualities of sugarcane juice aid in the body's removal of toxins and diseases.

The effect of operating parameters such as rotational speed, flow rate, and temperature on the concentration has been studied by continuously circulating a given volume of solution through the equipment. The details of the experimental studies are stated briefly in the next few chapters.

References

- 3.1 Sabanci, S., and Icier, F., "Applicability of ohmic heating assisted vacuum evaporation for concentration of sour cherry juice," *Journal of Food Engineering*, vol. 212, pp. 262-270, 2017, doi: 10.1016/j.jfoodeng.2017.06.004.

- 3.2 Keshani, S., LuqmanChuah, A., Nourouzi, M.M., Russly, A.R., and Jamilah, B., “Optimization of concentration process on pomelo fruit juice using response surface methodology (RSM),” *International Food and Research Journal*, vol. 17, pp. 733–742, 2010.
- 3.3 Berk, Z., “Production of citrus juice concentrates,” in *Citrus Fruit Processing*, Elsevier, pp. 187–217, 2016, doi: 10.1016/B978-0-12-803133-9.00009-6.
- 3.4 Echavarría, A.P., Falguera, V., Torras, C., Berdún, C., Pagán, J., and Ibarz, A., “Ultrafiltration and reverse osmosis for clarification and concentration of fruit juices at pilot plant scale,” *LWT - Food Science and Technology*, vol. 46, no. 1, pp. 189–195, 2012, doi: 10.1016/j.lwt.2011.10.008.
- 3.5 Aguiar, I.B., Miranda, N.G.M., Gomes, F.S., Santos, M.C.S., Freitas, D.G.C., Tonon, R.V., and Cabral, L.M.C., “Physicochemical and sensory properties of apple juice concentrated by reverse osmosis and osmotic evaporation,” *Innovative Food Science and Emerging Technology*, vol. 16, pp. 137–142, 2012, doi: 10.1016/j.ifset.2012.05.003.
- 3.6 Cassano, A., Drioli, E., Galaverna, G., Marchelli, R., Di Silvestro, G., and Cagnasso, P., “Clarification and concentration of citrus and carrot juices by integrated membrane processes,” *Journal of Food Engineering*, vol. 57, no. 2, pp. 153–163, 2003, doi: 10.1016/S0260-8774(02)00293-5.
- 3.7 Matta, V.M., Moretti, R.H., and Cabral, L.M.C., “Microfiltration and reverse osmosis for clarification and concentration of acerola juice,” *Journal of Food Engineering*, vol. 61, no. 3, pp. 477–482, 2004, doi: 10.1016/S0260-8774(03)00154-7.
- 3.8 Adnan, A., Mushtaq, M., and Islam, T.U., “Fruit Juice Concentrates,” in *Fruit Juices: Extraction, Composition, Quality and Analysis*, Elsevier Inc., pp. 217–240, 2018, doi: 10.1016/B978-0-12-802230-6.00012-6.
- 3.9 Onsekizoglu, P., Bahceci, K.S., and Acar, M.J., “Clarification and the concentration of apple juice using membrane processes: A comparative quality assessment”, *Journal of Membrane Science*, vol. 352(1–2), pp. 160–165, 2010.
- 3.10 Prost, J.S., González, M.T., and Urbicain, M.J., “Determination and correlation of heat transfer coefficients in a falling film evaporator,” *Journal of Food*

- Engineering*, vol. 73, no. 4, pp. 320–326, 2006, doi: 10.1016/j.jfoodeng.2005.01.032.
- 3.11 Saravacos, G., Moyer, J., and Wooster, G., “Concentration of liquid foods in a pilot-scale falling film evaporator,” *New York State Agricultural Experiment Station*, Sep. 1970, <https://ecommons.cornell.edu/handle/1813/4031>.
- 3.12 Ribeiro, C.P., Borges, C.P., and Lage, P.L.C., “Modelling of direct-contact evaporation using a simultaneous heat and multicomponent mass-transfer model for superheated bubbles,” *Chemical Engineering Science*, vol. 60, no. 6, pp. 1761–1772, 2005, doi:10.1016/j.ces.2004.08.049.
- 3.13 Dutta, B.K., “Principles of Mass Transfer and separation processes”, PHI Learning Pvt. Ltd., 2007.
- 3.14 Goswami, N., Basu, S., Bhowal, A., Datta, S., “Concentration of solution in cross-flow rotating packed bed contactor”, *Chemical Engineering Research and Design*, vol. 95, pp. 281-287, 2015.
- 3.15 Jassim, M.S., Rochelle, G., Eimer, D., Ramshaw, C., “Carbon dioxide absorption and desorption in aqueous monoethanolamine solutions in a rotating packed bed”, *Industrial Engineering Chemistry and Research* vol. 46, pp. 2823–2833, 2007.
- 3.16 Lin, C.C., Liu, W.T., Tan, C.S., “Removal of carbon dioxide by absorption in a rotating packed bed”, *Industrial Engineering Chemistry and Research* vol. 42, pp. 2381–2386, 2003.
- 3.17 Lin, C.C., Chen, B.C., Chen, Y.S., Hsu, S.K., “Feasibility of a cross-flow rotating packed bed in removing carbon dioxide from gaseous streams”, *Separation and Purification Technology*, vol. 62, pp. 507–512, 2008.
- 3.18 Cheng, H.H., Tan, C.S., “Removal of CO₂ from indoor air by alkanolamine in a rotating packed bed”, *Separation and Purification Technology*, vol. 82, pp. 156–166, 2011.
- 3.19 Lin, C.C., Chu, C.R., “Feasibility of carbon dioxide absorption by NaOH solution in a rotating packed bed with blade packings”, *International Journal of Greenhouse Gas Control*, vol. 42, pp.117–123, 2015.

- 3.20 Sheng, M.P., Sun, B.C., Zhang, F.M., Chu, G.W., Zhang, L.L., Liu, C.G., “Mass-transfer characteristics of the CO₂ absorption process in a rotating packed bed”, *Energy Fuels*, vol. 30, pp. 4215–4220, 2016.
- 3.21 Wu, W., Luo, Y., Chu, G.W., Liu, Y., Zou, H.K., Chen, J.F., “Gas flow in a multi liquid-inlet rotating packed bed: three-dimensional numerical simulation and internal optimization”, *Industrial Engineering Chemistry and Research* vol. 57, pp. 2031–2040, 2018.
- 3.22 Sheng, M.P., Xie, C.X., Zeng, X.F., Sun, B.C., Zhang, L.L., Chu, G.W., “Intensification of CO₂ capture using aqueous diethylenetriamine (DETA) solution from simulated flue gas in a rotating packed bed”, *Fuel*, vol. 234, pp. 1518–1527, 2018.
- 3.23 Wang, G.Q., Xu, O.G., Xu, Z.C., Ji, J.B., “New HIGEE-rotating zigzag bed and its mass transfer performance”, *Industrial & Engineering Chemistry Research*, vol.47, pp.8840-8846, 2008.
- 3.24 Wang, Y., Li, J., Jin, Y., Luo, J., Cao, Y., Chen, M., “Liquid-liquid extraction in a novel rotor-stator spinning disc extractor”, *Separation and Purification Technology*, vol. 207, 2018, doi:10.1016/j.seppur.2018.05.053.
- 3.25 MacInnes, J.M., Osorio, J., Jordan, P.J., Priestman, G.H., Allen, R.W.K., “Experimental demonstration of rotating spiral microchannel distillation”, *Chemical Engineering Journal*, vol. 159, pp. 159-169, 2010.
- 3.26 MacInnes, J.M., Pitt, M.J., Priestman, G.H., Allen, R.W.K., “Analysis of two-phase contacting in rotating spiral channel”, *Chemical Engineering Science*, vol. 69, pp. 304-315, 2012.
- 3.27 MacInnes, J.M., Zamberi, M.K.S., “Hydrodynamic characteristics of a rotating spiral fluid phase contactor”, *Chemical Engineering Science*, vol. 126, pp. 427-439, 2015.
- 3.28 MacInnes, J.M., Ayash, A.A., “Mass transfer characteristics of rotating spiral gas-liquid contacting”, *Chemical Engineering Science*, vol. 175, pp. 320-334, 2018.
- 3.29 Ji, J.B., Xu, Z.C., “Equipment of zigzag high-gravity rotating beds”, U.S. Pat., 7344126 (2008).

- 3.30 Wang, G.Q., Xu, Z.C., Yu, Y.L., Ji, J.B., “Performance of a rotating zigzag bed—a new HIGEE”, *Chemical Engineering Processing*, vol. 47, pp. 2131-2139, 2008.
- 3.31 Wang, G.Q., Xu, Z.C., Yu, Y.L., Ji, J.B., “Progress on HIGEE distillation-introduction to a new device and its industrial application”, *Chemical Engineering Research and Design*, vol. 89, pp.1434-1442, 2011.
- 3.32 Li, Y., Lu, Y., Liu, X., Wang, G., Ni, Y., Ji, J., “Mass transfer characteristics in a rotating zigzag bed as a HIGEE device”, *Separation and Purification Technology*, vol. 186, pp. 156-165, 2017.
- 3.33 Li, Y., Jianbing, L.I., Yunliang, Y.U., Zhichao, X.U., Xiaohua, L.I., “Hydrodynamic behavior in a rotating zigzag bed”, *Chinese Journal of Chemical Engineering*, vol. 18(1), pp. 34-38, 2010.

Chapter 4

Materials and Methods

4.1 Rotating Contactors

Two different rotating contactors were used for the experimental studies – Rotating baffled contactor (RC-1) and Rotating packed bed contactor (RC-2). The conventional wiped film evaporator was used for a comparative study between the rotating and the conventional equipment for the concentration of fruit juice. The schematic diagram (side view) of the space between the rotating disks through which the phases flow in the two rotating contactors (RC-1 and RC-2) used in the experimental study is shown in Figure 4.1.

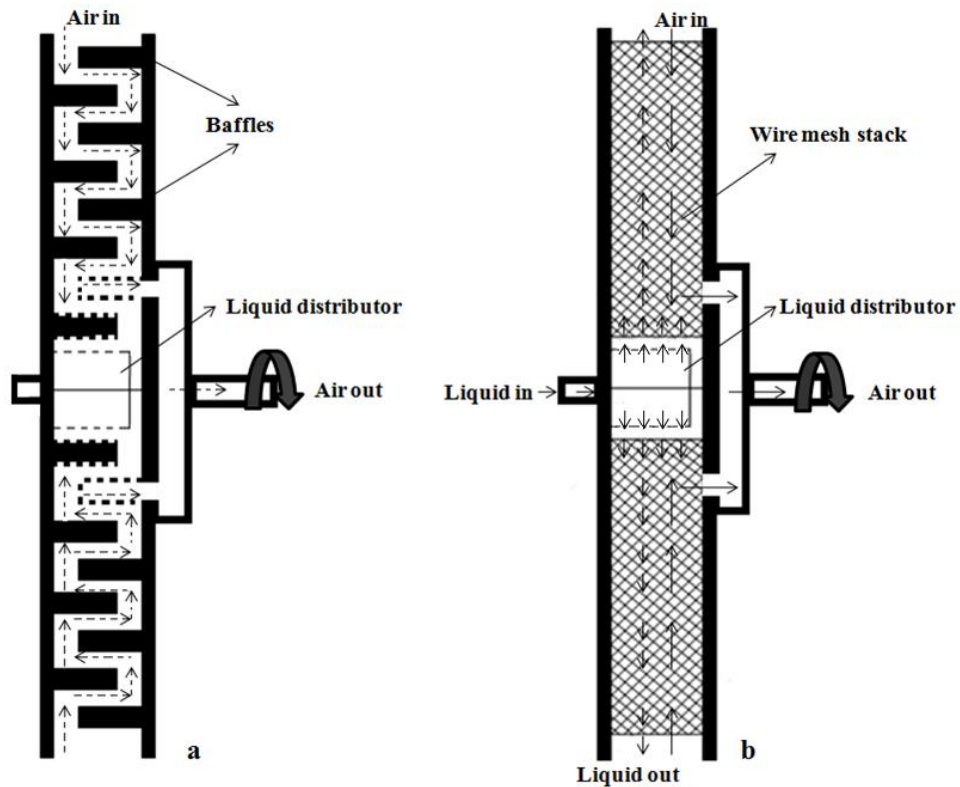


Fig 4.1: The internal schematic diagram (side view) of the two rotors

The gas and liquid phases were contacted within a rotor which is a pair of rotating stainless steel circular disks with an outer diameter of 0.360 m diameter and an inner diameter of 0.09 m. The disks were separated by spacers. The axial distance between the disks was 0.02 m. The disks were separated by spacers. The axial distance between the disks was 0.02 m. The rotor was encased in a stationary cylindrical casing made of stainless steel of diameter 0.4 m and rotated along a horizontal axis by a motor.

4.1.1 RC-1 (Rotating baffled contactor)

The photograph of the inner side of the two disks is provided in Figure 4.2. Circular baffles made of stainless steel of height 0.015 m were fitted on the inner surface of each of the disks of the rotor as shown in Figure 4.1. Five concentric baffles were fitted on both disks. In disk A, the radial distances of the baffles from the center are 0.03 m, 0.06 m, 0.09 m, 0.12 m, and 0.15 m respectively. In disk B, the radial distances are 0.045 m, 0.075 m, 0.105 m, 0.135 m, and 0.165 m respectively. The surface area in RC-1 was $\sim 80 \text{ m}^2/\text{m}^3$.



Fig 4.2: Pictorial representation of the Rotating baffled contactor (RC-1)

When the disks were fitted together, the gap between successive baffles was 0.015m. The space between the edge of the baffle and the disk through which the gas and liquid flow is 0.005m. The pictorial representation when the two disks are brought together is given in Figure 4.3.

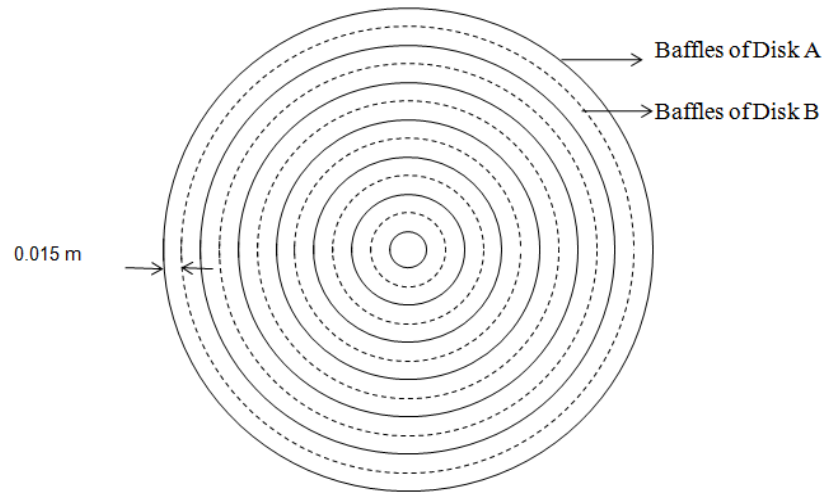


Fig 4.3: Front view of the Rotating baffled contactor (RC-1)

4.1.2 RC-2 (Rotating Packed bed)



Fig 4.4: Pictorial representation of the Rotating packed bed contactor (RC-2)

The photograph of RC-2 is provided in Figure 4.4. The dimension of the rotor was the same as that of RC-1. The space between the disks was packed with a stack of stainless steel wire mesh (20 meshes per linear inch). The wire mesh packing surface area and porosity of the rotating packed bed were $\sim 500 \text{ m}^2/\text{m}^3$ and 0.95 respectively.

4.2 Experimental setup for humidification using Air-Water

The schematic diagram of the experimental setup is shown in Figure 4.5 with RC-1. Air exiting an air compressor [Elgi Equipments Ltd, India] flowed through a filtration unit to remove particulate matter. The clean compressed air was introduced into the casing of the rotating contactor. It flows within the rotor under pressure from the outer periphery towards the center of the rotor. Warm water was kept in a $\sim 150 \text{ L}$ tank equipped with heaters, temperature controller, and mechanical stirrers. The liquid was introduced through a stationary liquid distributor at the eye of the rotor and flows outward under centrifugal force. The diameter and length of the distributor were 0.035 m and 0.02 m respectively and consisted of 11 numbers 1 mm diameter holes on its surface for uniform distribution of liquid inside the rotors. The liquid exited the equipment through an opening provided at the base of the casing wall.

Simultaneous heat and mass transfer within the equipment resulted in the humidification of air and cooling of water. Flow rates of air and water are measured with the help of air and liquid rotameters with 2% Full-scale (FS) accuracy. The temperatures of the liquid and air entering and leaving the contactor were measured using PT-100 thermocouples connected to a digital display unit. The moisture content of inlet and outlet air was calculated from the measurement of a hygrometer (Zeal, London, UK) with an accuracy of $\pm 1 \text{ }^\circ\text{C}$.

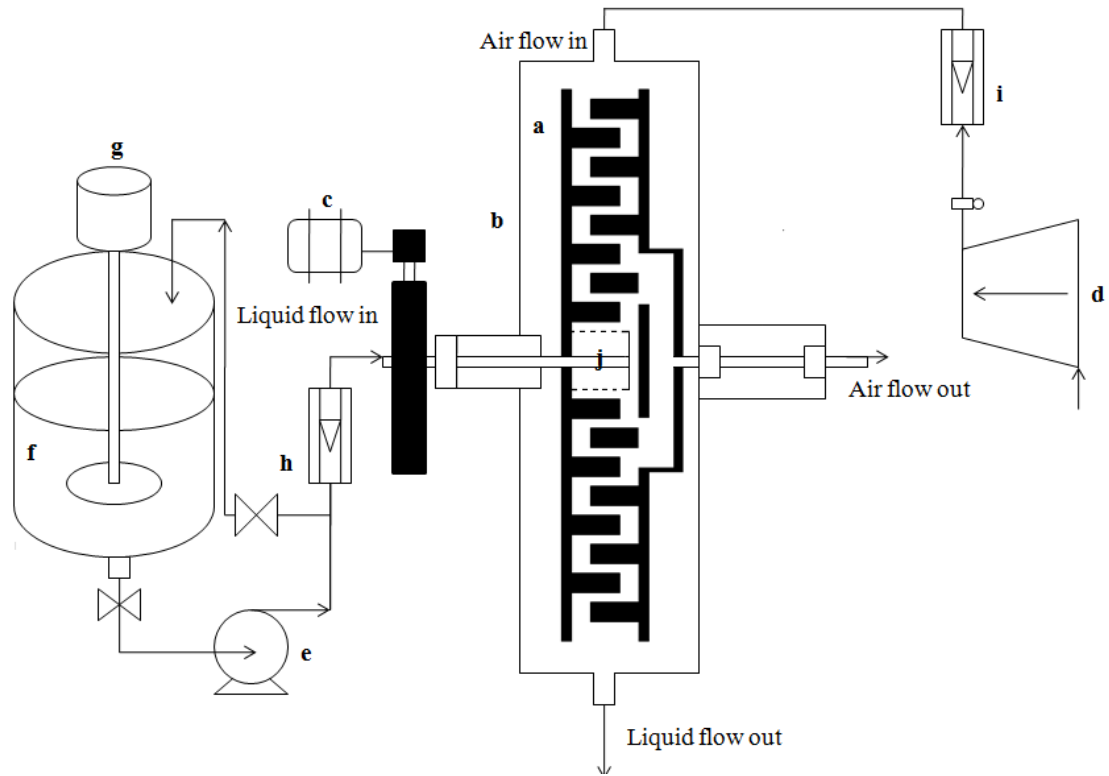


Fig 4.5: Schematic diagram of Experimental setup for air-water system (a. rotating baffled contactor, b. casing, c. motor, d. air compressor, e. liquid pump, f. solution tank, g. stirrer h. Liquid rotameter, i. air rotameter, j. liquid distributor)

4.3 Experimental setup for fruit juice

4.3.1 Preparation of fruit juice

Seven different fruits are used in the experiments – orange, green grapes, red grapes, pomegranate, tomato, watermelon, and sugarcane. All the fruits were bought from the commercial supermarket. They were sanitized with chlorinated water and then washed thoroughly thrice using de-ionized water followed by air drying to remove the dirt adhering to the surface of the fruits. Then the fruits were sliced, peeled, and deseeded manually. Juices were extracted by pressing the fruits in a juice extractor and homogenizing them in the blender for a few minutes. They were filtered using different

sieves and finally through a clean muslin cloth to remove the presence of arils or pulps. Finally, the obtained juice was centrifuged for 10 minutes at 9000 rpm. The clarified juice obtained was used for experimentation. Before each experiment, fresh juice was prepared and filtered. The total soluble solid content (in °Brix) and the pH of the fruit juices were recorded using a pocket refractometer (Atago, Japan) and a pH meter (Eutech pH tutor, US) respectively.

4.3.2 Experiment procedure

The experimental setup of the concentration of fruit juice is shown in Figure 4.6. The equipment RC-1 was replaced with RC-2 or wiped film evaporator as required. Three liters of fruit juice were kept in a double-jacketed feed tank provided with an agitator, heater, and temperature controller, and was preheated to the desired temperature. Heat was provided continuously to the juice to maintain the temperature. Clean compressed air enters the outer periphery of the casing of the rotating contactor and flows under pressure toward the inner radius of the rotor. The fruit juice was fed to the equipment by a sealless magnetic drive pump [PMD 85, Taha pump]. It flows outward in the rotor by centrifugal force after being introduced through a stationary liquid distributor at the eye of the rotor. The juice coming out from the contactor through an opening provided at the bottom of the casing wall was routed back to the feed tank. The juice was re-circulated continuously through the equipment.

Samples were collected in air-tight containers from the tank at regular intervals and brought to room temperature before measurement of total soluble solids. The total soluble solid content was measured using the refractometer with an accuracy of °Brix \pm 0.1%. All the experimental runs were performed in triplicates with a standard deviation of \pm

0.05. The schematic diagram and pictorial representation of the experimental setup for fruit juice are provided in Figures 4.6 and 4.7.

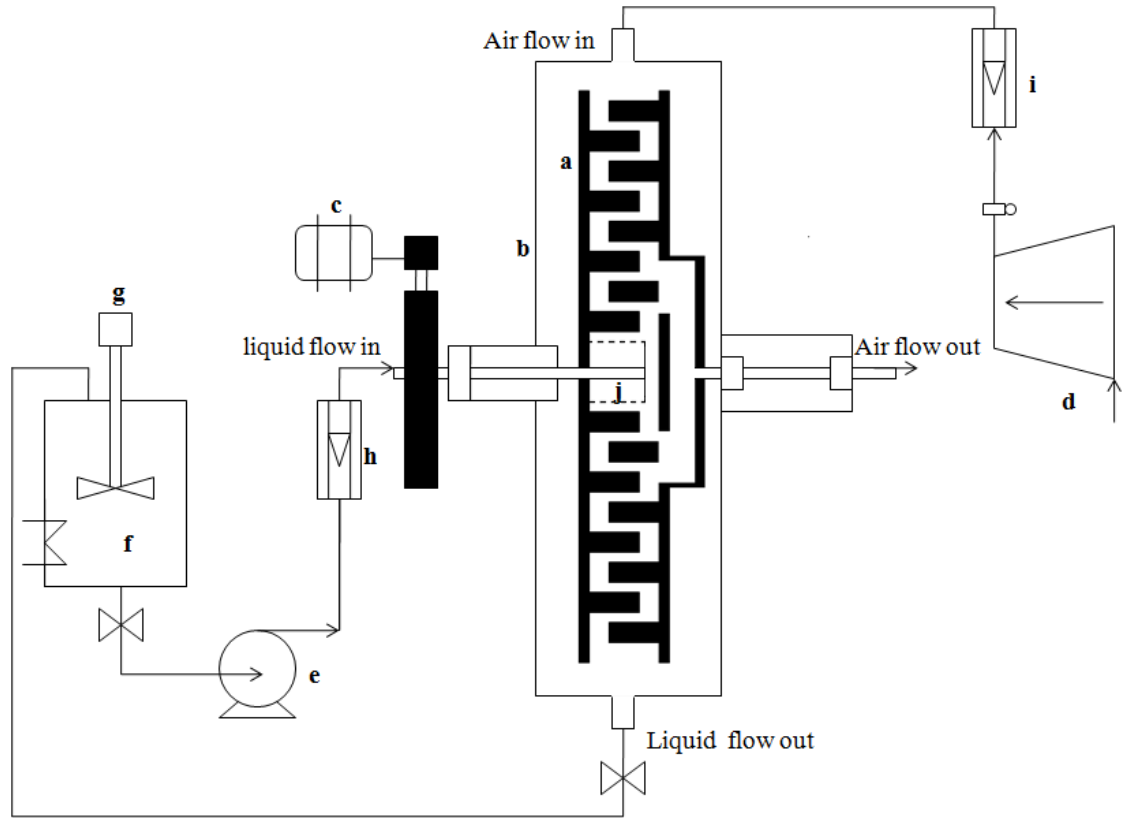


Fig 4.6: Schematic diagram of Experimental setup for fruit juice concentration (a. rotating baffled contactor, b. casing, c. motor, d. air compressor, e. liquid pump, f. solution tank, g. stirrer h. Liquid rotameter, i. air rotameter, j. liquid distributor)

4.4 Conventional evaporator

The conventional wiped film evaporator was a double-jacketed cylindrical stainless steel column with an outer diameter of 0.24 m and an inner diameter of 0.18 m. The length of the column is 0.7 m. Oil was heated in a hot oil bath (provided with a temperature controller and a stirrer) from where it is re-circulated in the outer hollow jacket of the evaporator to supply heat to the solution flowing over the inner wall. The schematic diagram is shown in Figure 4.8.

The liquid (water/ fruit juice) was preheated in a solution tank and pumped into the evaporator with the aid of a sealless drive pump. The warm solution was sprayed at the top of the column uniformly onto the walls with the aid of a ring-like stainless steel circular distributor (provided with 15 holes of 1.5 mm each). The solution flows down the wall under the action of terrestrial gravity. A vertical rotating shaft driven by a motor, provided with four wiper blades is mounted at the top of the column. The blades help in the formation of a uniform layer of fluid over the heating wall. Hot oil was continuously circulated through the jacket of the evaporator. The equipment was operated below ambient pressure (~ 670 mm Hg) to withdraw the vapor generated with the aid of a vacuum pump. The concentrated solution was again re-circulated back to the solution tank.



Fig 4.7: Pictorial representation of Experimental setup for fruit juice concentration

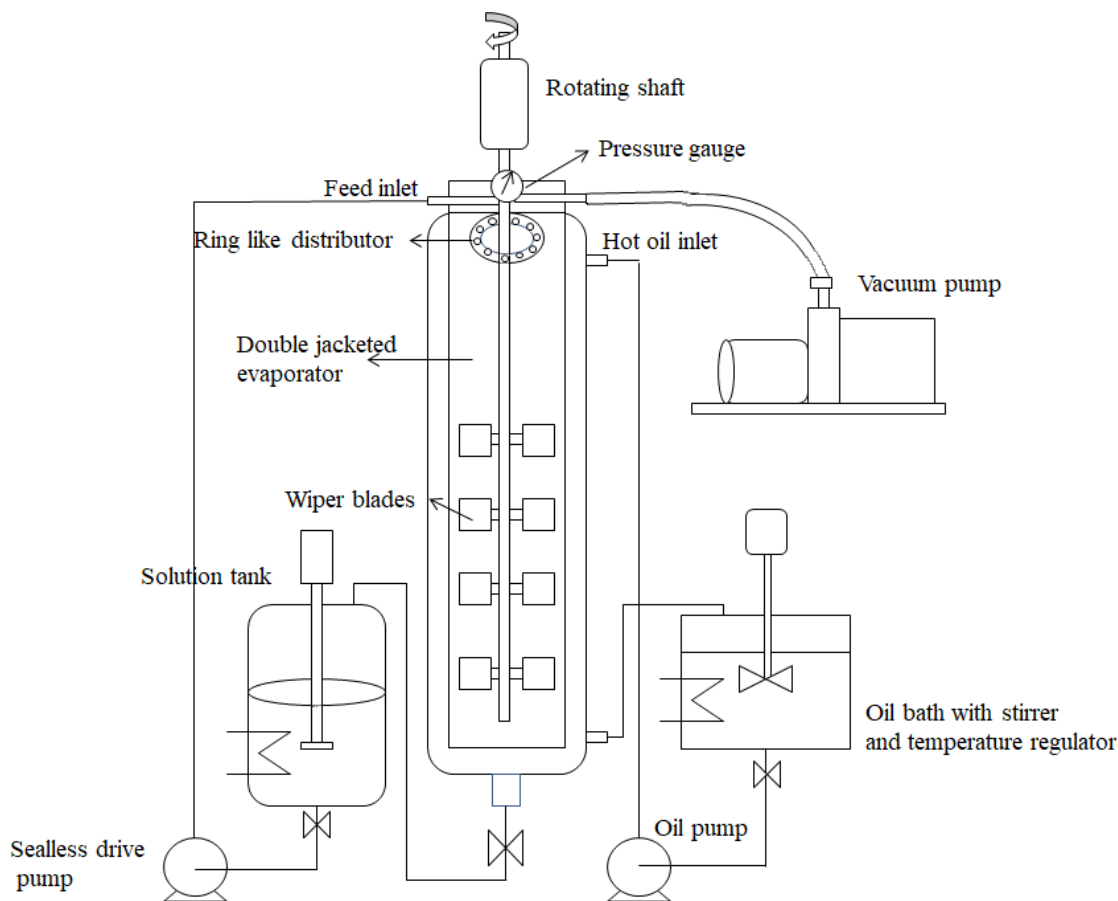


Fig 4.8: Schematic diagram of Wiped film evaporator setup

4.5 Physicochemical Analysis of fruit juices

4.5.1 Materials

Seven different fruits were used in the experiment. They include – oranges (*Citrus sinensis*), green grapes (Thompson seedless, *Vitis vinifera*), black grapes (Black Muscat, *Vitis vinifera*), pomegranate (*Punica granatum*), tomato (*Solanum lycopersicum*), watermelon (*Citrullus lanatus*) and sugarcane (*Saccharum officinarum*).

All the chemicals and reagents used in the study were of analytical grade. The reagents include - Sodium hydroxide (Merck), Phenolphthalein indicator (Merck), Acetone (ACS Reagent grade, Merck), Folin-Ciocalteu reagent (ACS Reagent grade, Merck), sodium

carbonate (Merck), gallic acid(Merck), sodium nitrite (Merck), aluminium chloride hexahydrate(Merck), Catechin (purity 97% HPLC grade, Merck), 2,6-dichlorophenol Indophenol dye (DCPIP) (Bioreagent, Sigma Aldrich), oxalic acid (purity 99%, Sigma Aldrich), Ascorbic acid (purity 99%, Sigma Aldrich), Hexane (purity 95%, anhydrous, Sigma Aldrich), Ethanol (purity >99, Merck), BHT (butylated hydroxyl toluene) (purity 99%, Sigma Aldrich), ABTS (2,2'-azino-bis(3-ethylbenzothiazoline-6-sulfonic acid)) (Merck), potassium persulfate (Merck), sodium acetate(Merck), Trolox solution (Merck), TPTZ [2,4,6 tris (2 pyridyl)- 1,3,5 triazine] (Sigma Aldrich), ferric chloride (Merck), Tris (hydroxymethyl)aminomethane hydrochloride (Tris-HCl) (purity 99%, Thermo Fisher Scientific), 2,2-diphenylpicrylhydrazyl (DPPH) (Merck).

4.5.2 Analysis methodology

During the processing of the fruit juices, the following samples were taken for analysis – fresh untreated juice clarified juice (after centrifuging for 10 minutes at 10000 rpm), and concentrated juice (at the end of two hours). According to A.O.A.C. 2006 [4.1], the analysis of the samples for pH, total and soluble solids, and total acidity was carried out.

- **pH content:** The pH of the fruit juice samples and their respective concentrates were measured using a digital pH meter (Eutech pH tutor, US).
- **Total acid content:** Total acidity of the feed and the product were measured by pipetting 10 ml of the solution in a clean conical flask and titrating it with 0.1 M NaOH solution in a burette using Phenolphthalein indicator until the color changes to pink or purple.
- **Total soluble solid content:** The TSS of the fruit juice as well as the concentrated product was measured using a pocket refractometer (Atago, Japan) with 0.1

resolutions. The unit is degrees Brix (symbol $^{\circ}\text{Brix}$) which is the sugar content of an aqueous solution. Each of the parameters was measured for the analysis using five replicates.

Extraction of the feed and the concentrated product for analysis

10 gm of the feed fruit juice is weighed and mixed with 80% Acetone (1:2 w/v) using a vortex mixer (Remicyclomixer CM-101, India) for around 5 minutes. The homogenates thus formed were filtered using No 1 Whatman Filter paper in a sterile atmosphere. The filtrate obtained was evaporated using a rotary vacuum evaporator (Rotavapor, Buchi, Switzerland) at a temperature of 45°C until only 10% of the product is left in the vessel. A similar method was used for obtaining the extracts for the concentrates of the respective juice samples. The extract obtained was stored at -40°C for further analysis [4.2].

- **Determination of total Phenolics compound**

The determination of total phenolic compound concentration was done spectrophotometrically using a modified Folin-Ciocalteu method [4.3]. An aliquot of the diluted extract (125 μL) was mixed with 125 μL Folin-Ciocalteu reagent. To the mixture, 1.25 mL of 7% sodium carbonate (Na_2CO_3) solution was added, and volume adjustment was done by adding 3mL of water. All the samples were incubated for 90 minutes at room temperature. Absorbances of the samples were then measured in a spectrophotometer (Thermo Scientific, USA) at 760 nm using water as a blank solution. The amount of total phenol content obtained was calculated using Gallic acid for calibrations. The values were expressed as mean [milligrams of GAE (Gallic acid equivalents) per liter of fruit/concentrate].

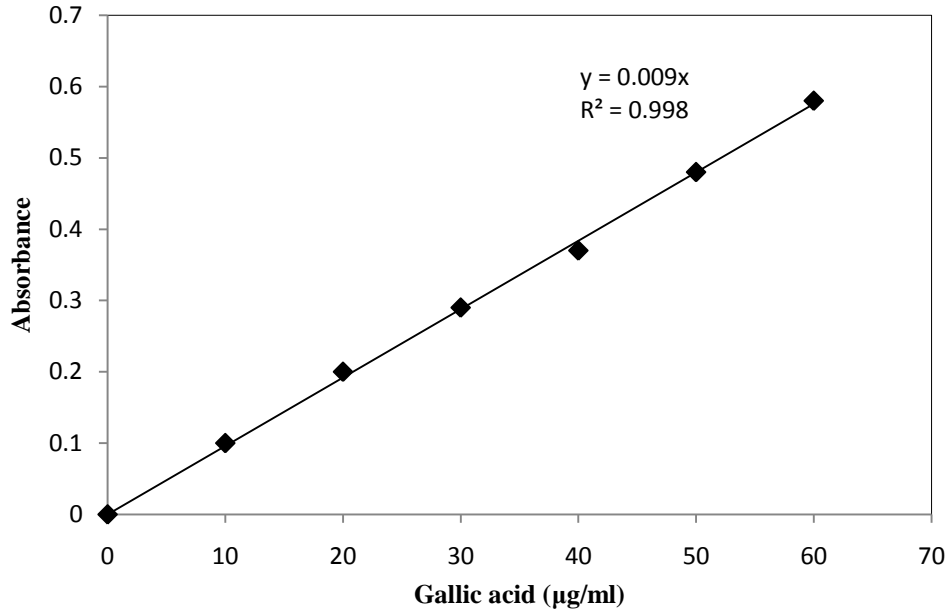


Fig 4.9: Gallic acid standard curve

Total phenolics content (TPC) in feed, clarified and concentrated juices were determined spectrophotometrically in a UV-Vis spectrophotometer (Thermo Scientific, USA) according to the Folin-Ciocalteu colorimetric method [4.3] using Gallic acid as the standard solution. To prepare the stock solution in a 10 mL test tube, 10 mg of dry gallic acid is dissolved in 1 mL of ethanol and then diluted to volume with water. To prepare a calibration curve, 0, 10, 20, 30, 40, 50, and 60 µL of the above phenol stock solution are added into 1000, 990, 980, 970, 960, 950, and 940 µL of water in test tubes. These solutions will have phenol concentrations of 0, 10, 20, 30, 40, 50, and 60 µg/mL gallic acid, which is the effective range of the assay. After creating the calibration curve with the standards and determining the levels in the samples, the results are reported as Gallic Acid Equivalent. The reagent consists of a mixture of sodium tungstate, and sodium molybdate, among other reagents. Upon reaction with phenols, the mixture produces a blue-colored complex Molybdenum

species which absorbs at 743 nm. After the determination of the λ_{\max} of the colored complex, the absorbances of all standards were taken to construct a calibration curve. The calibration formula obtained from 6 different concentrations of Gallic acid was $y = 0.009x$ ($R^2 = 0.998$).

- **Determination of total Flavonoids**

The Total flavonoid content was measured by using a colorimetric method [4.4]. An aliquot of 0.25 mL of the extracts was diluted with 1.25 mL of distilled water, followed by the addition of 75 μL of 5% Sodium nitrite (NaNO_2) solution. After keeping the solution at rest for 6 minutes, 150 μL of 10% Aluminium chloride ($\text{AlCl}_3 \cdot 6\text{H}_2\text{O}$) solution was added along with 0.5 mL of 1 M NaOH solution after 5 minutes. The volume adjustment was done using distilled water and samples were then measured against the blank at absorbance 510 nm in a UV-spectrophotometer (Thermo-scientific, USA) compared with standard similarly prepared with known Catechin concentrations. To prepare the stock solution, 10 mg of Catechin is mixed with 10 ml of water and 1 ml of methanol. The calibration curve is prepared by adding 0, 100, 200, 300, 400, and 600 μL of the above Catechin stock solution in 1000, 900, 800, 700, 600, and 400 μL of water in test tubes. The solutions were vortexed for 5 minutes for complete miscibility. These solutions will have flavonoid concentrations of 0, 100, 200, 300, 400, and 600 $\mu\text{g}/\text{mL}$ Catechin. The results obtained are expressed as milligrams of Catechin equivalent (CE) per gram of juice/concentrate.

Total flavonoid content in the feed, clarified and concentrated juices were determined spectrophotometrically in a UV-Vis spectrophotometer (Thermo Scientific, USA)

according to the method described by Zhishen et al. [3.4] using Catechin as the standard solution. Aluminium chloride forms an acid labile complex with the hydroxyl and keto groups of the flavonoids. At lower concentrations, the complex formed has a pale golden yellow color which intensifies with an increase in concentration. The calibration formula obtained from 6 different concentrations of Catechin was $y = 0.001x$ ($R^2 = 0.992$).

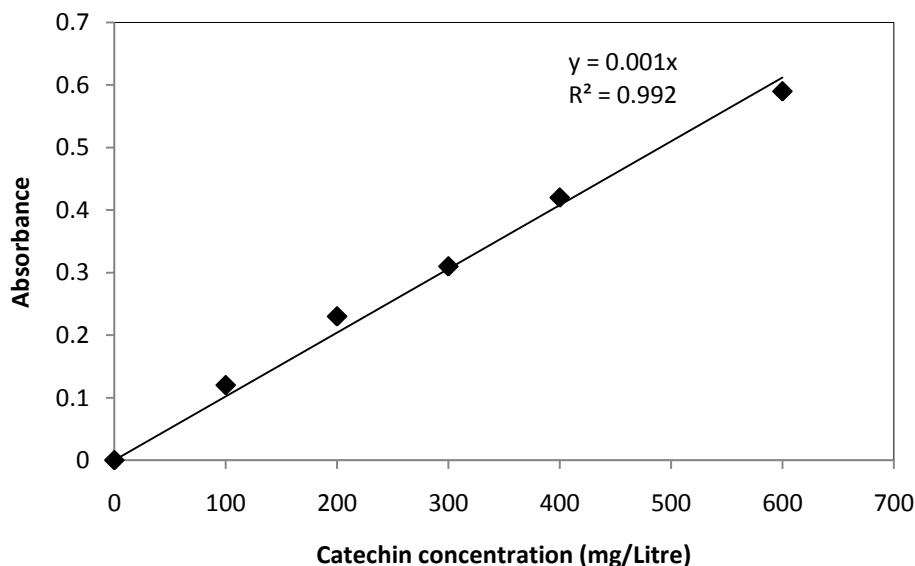


Fig 4.10: Catechin standard curve

- **L- Ascorbic Acid content determination**

The L-Ascorbic acid content was measured by visual titrimetry using 2,6-Dichlorophenol Indophenol dye (DCPIP) [4.5]. 10mL of the sample was pipetted in a clean conical flask and 25 mL 0.5% oxalic acid was added to it and then the solution was titrated against 2, 6-dichlorophenol indophenols dye. The endpoint was marked with the appearance of pink color that persisted for more than 30 seconds. Ascorbic acid (0.2g/L) was used as standard. Thus the amount of ascorbic acid present was calculated in

mg/100ml. The calibration formula obtained from 6 different concentrations of Ascorbic acid was $y = 0.010x$ ($R^2 = 0.992$).

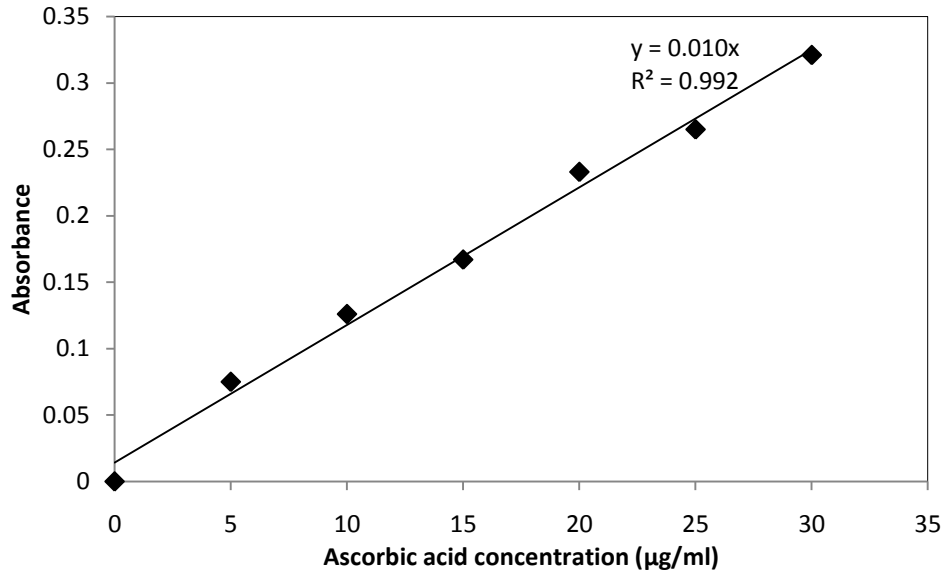


Fig 4.11: Ascorbic acid standard curve

- **Lycopene content determination**

The Lycopene content was extracted and measured using the method described by Fish et al. [4.6] by adding a mixture of Hexane: Ethanol: Acetone in a ratio 2:2:1 (by volume) containing 0.05 % BHT (butylated hydroxyl toluene) in the samples. After the extraction, the absorbance of the hydrophobic hexane phase was measured at 503 nm in a UV-Spectrophotometer [Thermo Scientific, USA]. Hexane was used as blank and precautions are taken by performing the analysis with the reduced luminosity of the room to prevent the photo-oxidation of Lycopene. The molar extinction coefficient value of Lycopene in hexane ($\epsilon = 17.2 \cdot 10^4 \text{ Lmole}^{-1} \text{ cm}^{-1}$) was used for the measurement and the values were expressed as milligrams per kg fw.

Determination of antioxidant activity

It is recommended by many researchers to estimate the antioxidant activity using several methods rather using a single one. In this study, three different standard methods were used (TEAC assay, FRAP assay, and DPPH radical scavenging).

- **Determination of Trolox equivalent antioxidant capacity (TEAC assay)**

The Trolox equivalent antioxidant capacity (TEAC) assay was estimated as described by Rice-Evans et al. [4.7] where ABTS was mixed with an acetate buffer and prepared by adding potassium persulfate. At pH 4.5, 20 mM sodium acetate ($C_2H_3NaO_2$) buffer was added for stability. $ABTS^+$ radical generation takes 12-16 hours. 3ml of the above $ABTS^+$ solution was mixed with 10 μ l of the juice and concentrated sample and the absorbance was determined at 734 nm. When the $ABTS^+$ radical (unstable form) accepts an electron from the antioxidant present in the sample, the blue-green color fades into a pale blue color which shows the regeneration of ABTS.

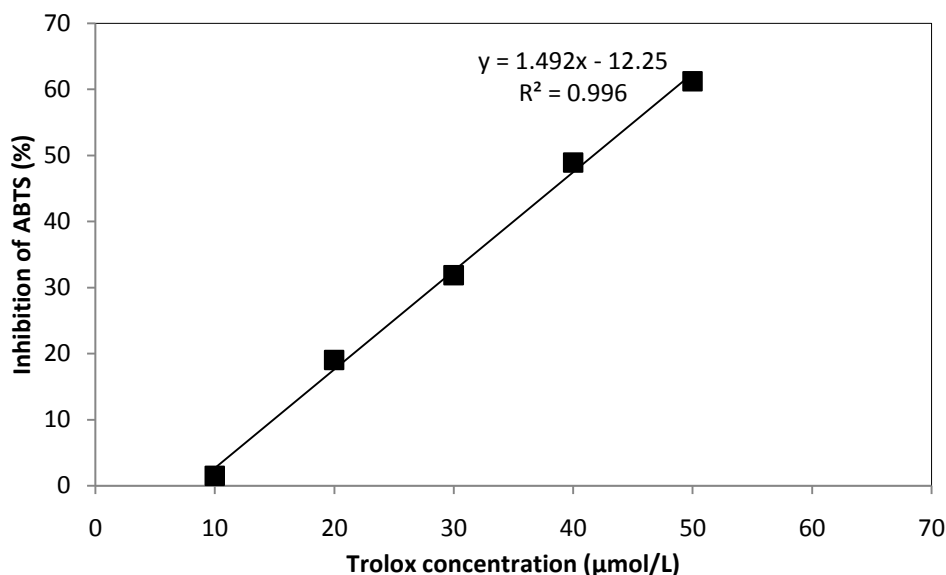


Fig 4.12: Trolox standard curve

The values obtained are expressed as mmol of Trolox equivalents/liter of juice/concentrate. The calibration formula obtained from 5 different concentrations of Trolox was $y = 1.472 x - 11.45$ ($R^2 = 0.997$).

- **Determination of antioxidant activity by FRAP (ferric reducing) assay**

FRAP assay of the sample is measured using the procedure by Benzie and Strain [4.8]. The stock solution consists of Acetate buffer (0.1M, pH 3.6) and 10 mM acidified TPTZ [2,4,6-tris (2 pyridyl)- 1,3,5 triazine] in the ratio 1000:3.3 (by volume). A 20 mM Ferric Chloride (III) solution is also prepared. Then the stock solutions were added in 10:1:1 ratio to prepare the FRAP reagent. Now, 30 μ L of the sample and 2.97 ml FRAP reagent are added for the assay. The amount of iron (II)-ferricyanide complex formed was determined by measuring the formation of Perl's Prussian blue at 700 nm after 10 minutes.

- **DPPH free radical scavenging assay for antioxidant measurement:**

The radical scavenging effect on the DPPH free radicals was used to measure the scavenging ability of fruit juices and concentrates as described by Kulkarni and Aradhya [4.9]. 0.1ml of the sample is mixed with 0.9ml of 100mM Tris-HCl buffer at pH 7.4. Now 1 ml of DPPH (prepared by adding 500 μ M in ethanol) is added to it. The tubes were shaken in a vortex and incubated at room temperature in dark for 30 minutes and the absorbance was measured at 517 nm using UV-Vis Spectrophotometer. The absorbance of DPPH control was also noted. The radial scavenging activity of the juices and concentrates was calculated using the formula: Scavenging activity (%) = $[(A - B) / A] \times 100$, where A is the absorbance of the control at 517nm and B is the absorbance of the sample at 517nm.

- **Color content**

The color of the juice and concentrate samples were measured in a Chroma Meter (Konica Minolta, Osaka, Japan) using the Hunter lab scale. All the juice and concentrate samples were placed in an optical glass cell and illuminated using artificial light and the temperature maintained is 25 °C. The values obtained from the chroma-meter were expressed as L* (Luminosity) for lightness/darkness, a* for redness/greenness, and b* for yellowness/blueness. The appearance of the fresh untreated juice clarified juice and concentrated juice was captured using a Sony Cybershot 20-megapixel digital camera.

References

- 4.1 A.O.A.C. (2006). Official methods of analysis (18th ed.). Gaithersburg, MD: Association of Official Analytical Chemists.
- 4.2 Dewanto, V., Wu, X., Adom, K., Liu, R., “Thermal Processing Enhances the Nutritional Value of Tomatoes by Increasing Total Antioxidant Activity”, *Journal of Agricultural and Food Chemistry*, vol. 50, pp. 3010–3014, 2002.
- 4.3 Singleton, V.L., Orthofer, R., Lamuela-Raventos, R.M., “Analysis of Total Phenols and Other Oxidation Substrates and Antioxidants by means of Folin-Ciocalteu Reagent”, *Methods in Enzymology, Oxidants and Antioxidants*, Part A, vol. 299, pp. 152-178, 1999.
- 4.4 Zhishen, J., Mengcheng, T., Jianming, W., “The Determination of Flavonoid Contents in Mulberry and their Scavenging Effects on Superoxide Radicals”, *Food Chemistry*, vol. 64, pp. 555-559, 1999, [http://dx.doi.org/10.1016/S0308-8146\(98\)00102-2](http://dx.doi.org/10.1016/S0308-8146(98)00102-2).
- 4.5 Helrich, K., Ed. *Official Methods of Analysis of the Association of Official Analytical Chemists*, 15th ed.; AOAC: Arlington, VA, pp. 1058-1059, 1990.
- 4.6 Fish, W.W., Perkins-Veazie, P., Collins, J.K., “A quantitative assay for lycopene that utilizes reduced volumes of organic solvents”, *Journal of Food Composition and Analysis*, vol. 15, pp. 309-317, 2002.90

- 4.7 Rice-evans, C.A., Miller, N.J., Bolwell, P.G., Bramley, P.M., Pridham, J.B., “The Relative Antioxidant Activities of Plant-Derived Polyphenolic Flavonoids”, *Free Radical Research*, vol. 22(4), pp. 375–383, 1995, doi: 10.3109/10715769509145649.
- 4.8 Benzie, I. F. F., & Strain, J. J., “The ferric reducing ability of plasma (FRAP) as a measure of “antioxidant power”: The FRAP assay”, *Annals of Biochemistry*, vol. 239, pp. 70–76, 1996.
- 4.9 Kulkarni, A. P., Aradhya, S. M., & Divakar, S., “Isolation and identification of a radical scavenging antioxidant punicalagin from pith and carpellary membrane of pomegranate fruit”, *Food Chemistry*, vol. 87, pp. 551–557, 2004.

Chapter 5

Simultaneous heat and mass transfer studies in rotating contactors

5.1 Introduction

The simultaneous heat and mass transfer characteristics of the rotating contactors are reported in this chapter. These experiments were carried out by contacting warm water with unsaturated air.

The aims of the study are

- To determine the mass transfer performance of rotating baffle and rotating packed bed contactor
- To evaluate the volumetric mass transfer coefficient.

5.2 Mathematical Modelling

The volumetric mass transfer coefficient was obtained through mathematical modelling of the simultaneous heat and mass transfer process. The derivation obtained from Treybal [5.1] for the cool tower was modified to account for the change in the geometry of the equipment. The enthalpy balance across the differential volume ($2\pi r dr h$) between two coaxial disks of the rotor at a steady state assuming the mass flow rate of liquid is constant is given by

$$LC_w \frac{dT_L}{dr} = G \frac{dH_G}{dr} \quad (5.1)$$

where, L , G , C_w , T_L , r and H_G represent the liquid flow rate, dry air flow rate, liquid heat capacity, liquid temperature, the radial distance from the centre of the rotor, and enthalpy of air respectively. The variation of gas enthalpy within the rotor by assuming

(i) the air-liquid heat transfer area per unit volume (a_H) and the mass transfer area per unit volume (a_M) are equal, and (ii) the Lewis number is unity, is given by

$$G \frac{dH_G}{dr} = -K_Y a (H_G^* - H_G) 2\pi r h \quad (5.2)$$

In the above equation, $K_Y a$, H_G^* and H is the volumetric mass transfer coefficient, enthalpy of air in equilibrium with liquid temperature and enthalpy of air in the bulk respectively.

The magnitude of the volumetric mass transfer coefficient for each experimental run was obtained by trial and error. It was done by comparing the temperature of the liquid and gas phase enthalpy exiting the equipment obtained by integrating equations (5.1) and (5.2) simultaneously with the experimental value.

5.3 Result and Discussion

5.3.1 Effect on Evaporation rate

The evaporation rate of water, \dot{m} reported in this study was calculated from the experimental data using the following expression

$$\dot{m} = \int G dY = G(Y_{out} - Y_{in}) \quad (5.3)$$

where, Y_{out} and Y_{in} are the absolute humidity of air at the outlet and inlet of the equipment respectively.

5.3.1.1 Effect of rotational speed

It is seen in Figure 5.1 that the value of evaporation rate of water (\dot{m}) increased from 0.0278 to 0.0372 Kg/min in the rotating baffle bed at air flow rate 400 LPM and from

0.0124 to 0.0188 Kg/min in rotating packed bed contactor at the same air flow rate when the rotational speed was increased from 400 to 1000 rpm, keeping the other parameters constant (water flow rate 1 LPM and inlet temperature 50 °C). In the rotating contactors, the liquid flows as films, rivulets, droplets, or ligaments. The increase in evaporation rate with rotational speed is partly due to the increase of gas-liquid interfacial area as a result of thinner films and smaller drops besides more vigorous mixing.

On impacting a surface, liquid drops either spread and form a liquid film or the droplet can splash and form secondary droplets at higher impact velocities [5.2]. The spreading diameter of the drop increases with impact velocity. In RC-1, the liquid flows outward over the edge of the baffles under centrifugal acceleration as drops and impacts the baffle wall in the direction of increasing radius. The velocity of the drops increases with rotational speed resulting in the increase of the surface area over which the drops spread.

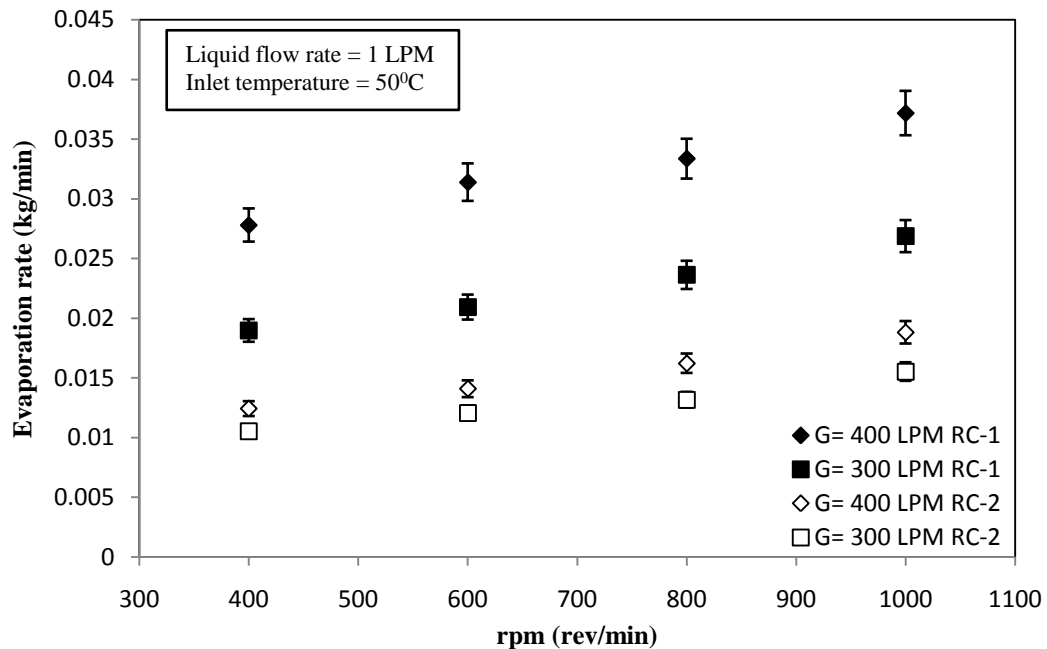


Fig 5.1: The influence of rotor speed on the evaporation rate of two rotating contactors

Therefore, increase in interfacial area is a key factor to the increase in evaporation rate in this contactor. The magnitude of \dot{m} obtained in RC-1 is nearly twice that in RC-2. This could be related to the changed internal structural design of the rotor that causes the gas and liquid to undergo a succession of directional changes. Sandilya et al [5.3] concluded from their experimental results that gas flow undergoes a solid body rotation in RC-2. Within RC-1, the gas and liquid undergo a succession of countercurrent and cross-current contact as the liquid flows as rivulets or film over the four baffle walls, and as droplets/ligaments in the intermediate space between two successive baffles respectively. The zig-zag path followed by the phases within RC-1 contributes to higher value of volumetric heat and mass transfer coefficient in comparison to RC-2.

5.3.1.2 Effect of air flow rate

The effect of the air flow rate on the evaporation rate of the rotating baffle bed and packed bed contactor for three different rotational speeds, keeping the water flow rate and inlet temperature constant is depicted in Figure 5.2. As the air flow rate was varied from 200 to 400 LPM, there is an increase in the evaporation rate from 0.017 to 0.037 Kg/min in RC-1 and 0.011 to 0.019 Kg/min in RC-2 at rotor speed 1000 rpm. At rotor speed of 600 rpm, the increase in the evaporation rate \dot{m} was from 0.015 to 0.031 Kg/min in RC-1 and 0.008 to 0.014 Kg/min in the case of RC-2.

Increase of gas flow rate has little effect on interfacial area. So the increase of evaporation rate is related to driving force and mass transfer coefficient. The turbulence in gas increase with air flow resulting in increase of mass transfer coefficient. Furthermore, the capacity of the gas phase for uptake of moisture also increases at a

higher flow rate [5.4]. This increases the driving force for mass transfer and consequently.

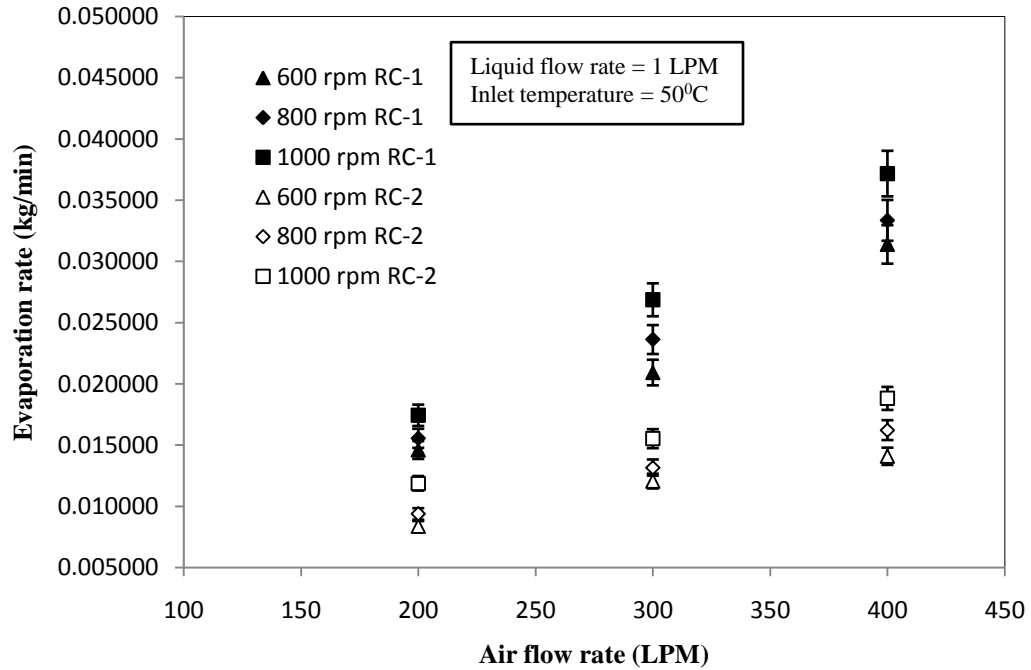


Fig 5.2: The influence of air flow rate on the evaporation rate of two rotating contactors

5.3.1.3 Effect of water flow rate

Figure 5.3 illustrates the influence of the water flow rate on the evaporation rate in the rotating contactors at two different air flow rates 300 and 400 LPM (keeping inlet temperature and the rotor speed constant). It was observed that there is an increase in the \dot{m} value from 0.026 to 0.039 Kg/min in case of RC-1 and 0.015 to 0.023 Kg/min in case of RC-2 (air flow rate 400 LPM) with increase in the water flow rate from 0.5 to 1.5 LPM. Whereas at air flow rate 300 LPM, the increase in the evaporation rate value is from 0.020 to 0.029 Kg/min and 0.013 to 0.018 Kg/min in RC-1 and RC-2 respectively.

At higher liquid flow rate more homogenous distribution of the liquid droplets takes place as more of the distributor openings become functional. This increases the gas-liquid

surface interfacial area [5.5] in both the contactors. In RC-1, the increase in interfacial area is due to the increase in the number of ligaments/streams of flying liquid droplets emitting from the edge of one baffle and striking the wall of the baffle located at immediate larger radial distance. The phenomenon is coupled with the increase of wetted fraction of the baffle wall on which the drops/ligaments are striking. Furthermore, the liquid holdup increases with liquid flow rate in rotating contactors [5.6].

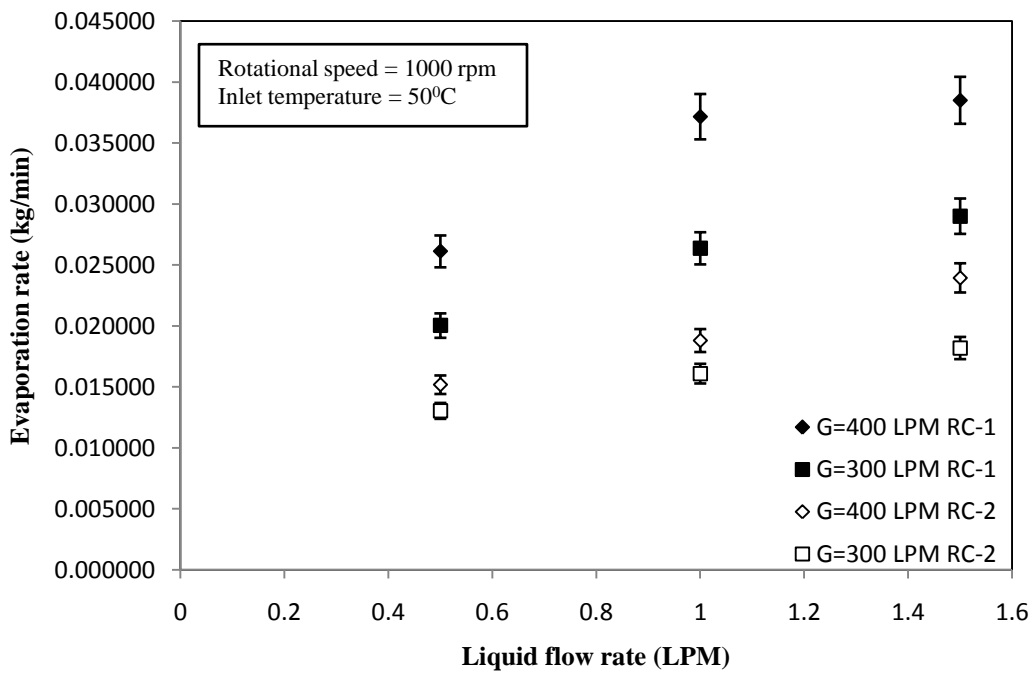


Fig 5.3: The influence of water flow rate on the evaporation rate of two rotating contactors

5.3.1.4 Effect of temperature

The effect of temperature on the evaporation rate of the water was also measured in both the rotating contactors at two different air flow rates (rotor speed 1000 rpm and liquid flow rate 1LPM). At air flow rate 400 LPM, as the temperature was varied from 40 to 60 °C, there was an increase in the evaporation rate from 0.020 to 0.045 Kg/min in the

rotating baffle bed and 0.013 to 0.028 Kg/min in the rotating packed bed. At air flow rate 300 LPM, the increase in the evaporation rate is from 0.014 to 0.032 Kg/min in RC-1 whereas it is 0.010 to 0.023 Kg/min in RC-2. Higher temperature enhances the mass transfer driving force due to increase in difference in partial pressure of water resulting in higher evaporation rates.

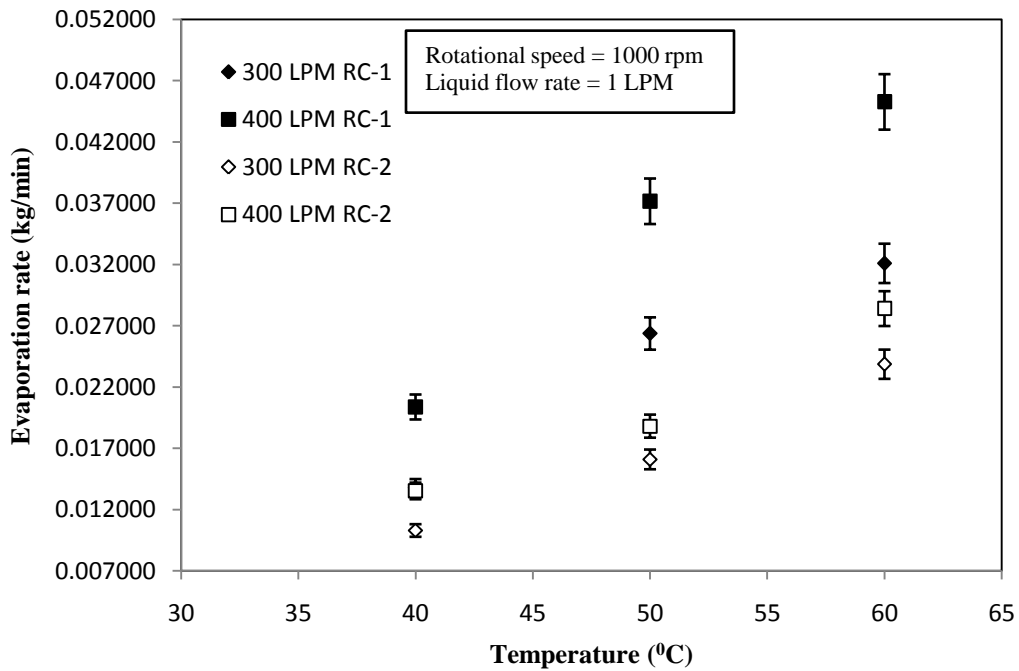


Fig 5.4: The influence of temperature on the evaporation rate of two rotating contactors

5.3.2 Effect on volumetric mass transfer coefficient ($K_Y a$)

Figures 5.5 – 5.7 depict the variation of $K_Y a$ in RC-1 and RC-2 with variation in rotor speed, air flow rate, and liquid flow rate respectively. There is a constant increase in the volumetric mass transfer coefficient of RC-1 from 8.25 kg/m³s to 20 kg/m³s, and from 6.53 kg/m³s to 13 kg/m³s as the rotational speed was varied from 600 rpm to 1000 rpm at a constant air flow rate of 400 L/min and 300 L/min respectively. In the case of RC-2, the volumetric mass transfer coefficient increased from 2.9 kg/m³s to 4.45 kg/m³s, and from

1.8 kg/m³s to 2.6 kg/m³s as the rotational speed was varied from 600 rpm to 1000 rpm at a constant air flow rate of 400 L/min and 300 L/min respectively.

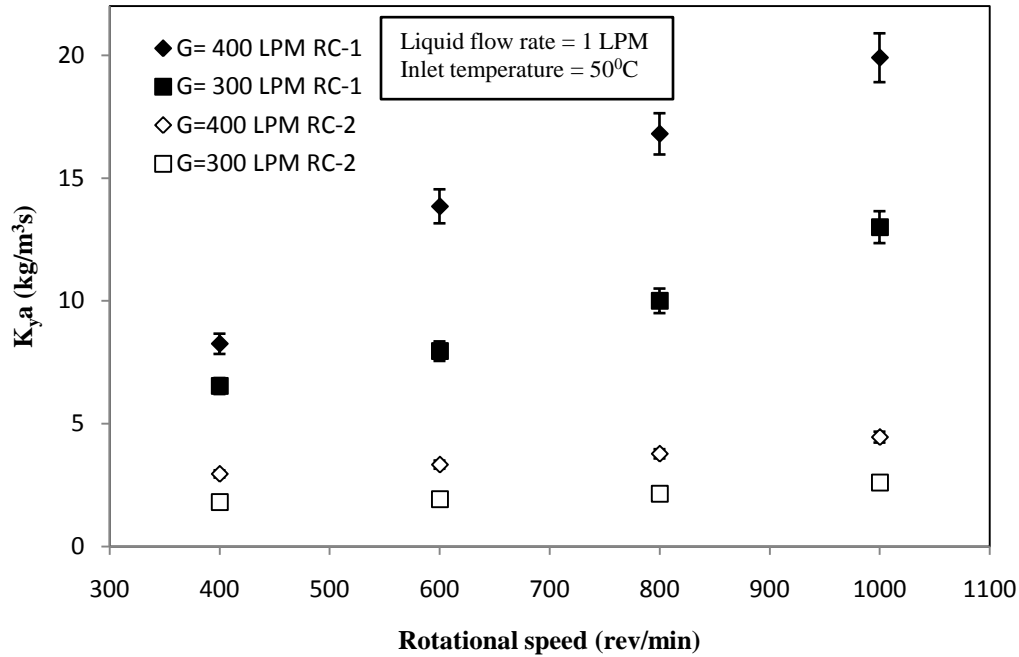


Fig 5.5: The influence of rotor speed on the volumetric mass transfer coefficient of two rotating contactors

The magnitude of $K_Y a$ increased with the increase in the air flow rate at two different rotational speeds. At rotational speed 1000 rpm, the $K_Y a$ value increased from 6.15 to 20 kg/m³s and 2.98 to 4.65 kg/m³s as the air flow rate varied from 200 to 400 LPM in RC-1 and RC-2 respectively. Again at rotational speed 600 rpm, the $K_Y a$ value increased from 4.2 to 14.05 kg/m³s and 1.7 to 2.43 kg/m³s as the air flow rate varied from 200 to 400 LPM in RC-1 and RC-2 respectively shown in Figure 5.6.

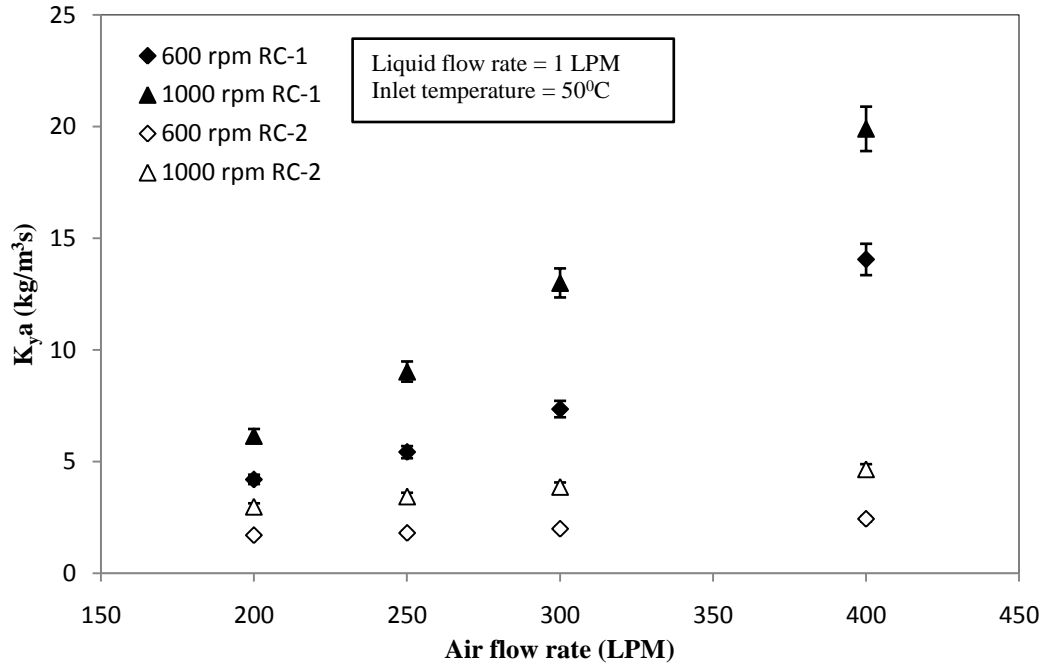


Fig 5.6: The influence of air flow rate on the volumetric mass transfer coefficient of two rotating contactors

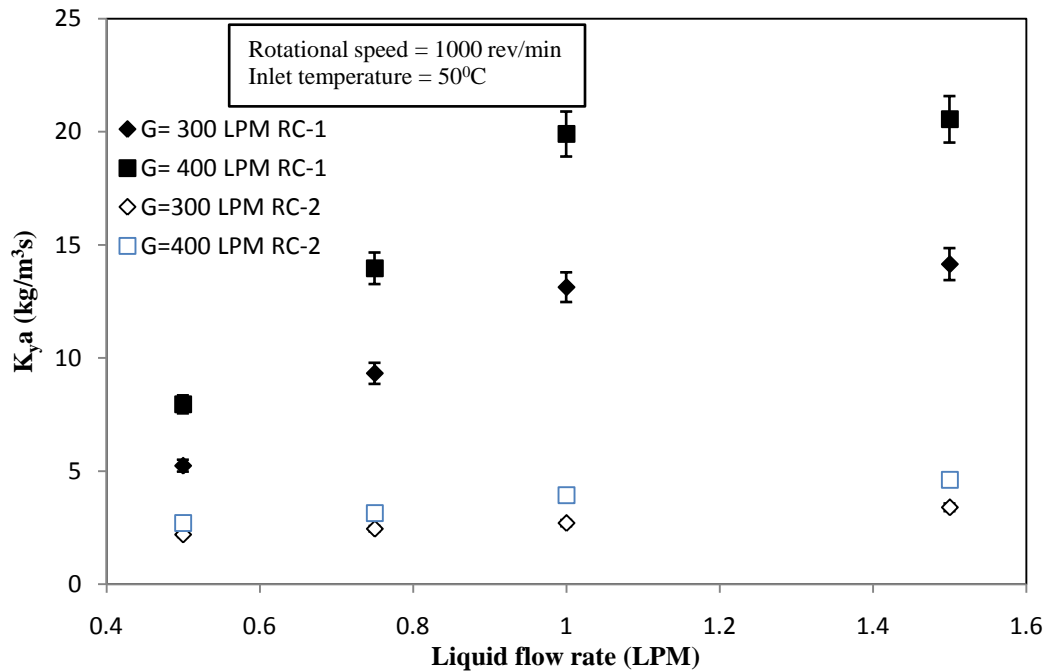


Fig 5.7: The influence of water flow rate on the volumetric mass transfer coefficient

The magnitude of $K_Y a$ increased from 8 kg/m³s at liquid flow rate = 0.5 L/min to 20.5 kg/m³s at 1.5 L/min (air flow rate = 400 L/min) and 3.26 to 5.42 kg/m³s in RC-1 and RC-2 respectively (Figure 5.7). The volumetric mass transfer coefficient of the rotor disk increased as a result of the increased air flow rate's enhancement of gas turbulence inside the contactor.

The volumetric mass transfer coefficient was noted to vary with rotor speed, air flow rate, and liquid flow rate. The coefficient $K_Y a$ was correlated to these experimental parameters through the following equation

$$K_Y a = P (\omega^2 r_{avg})^a (\dot{m}_w)^b (\dot{m}_a)^c \quad (5.4)$$

where $\omega^2 r_{avg}$ is the centrifugal acceleration at an average radius ($r_{avg} = \frac{r_i + r_o}{2}$), \dot{m}_w and \dot{m}_a are the mass flow rate of water and air per unit area at the mean value of the radius of the rotor respectively, r_i and r_o are the internal and external radius of the rotor respectively. The final form of Eq. (5.4) after regression analysis of the experimental data is given below

$$K_Y a = 18.9 (\omega^2 r_{avg})^{0.326} (\dot{m}_w)^{0.837} (\dot{m}_a)^{1.13} \quad (5.5)$$

The parity plot (Figure 5.8) obtained by plotting the experimental values of $K_Y a$ against the theoretical value showed deviations within $\pm 15\%$.

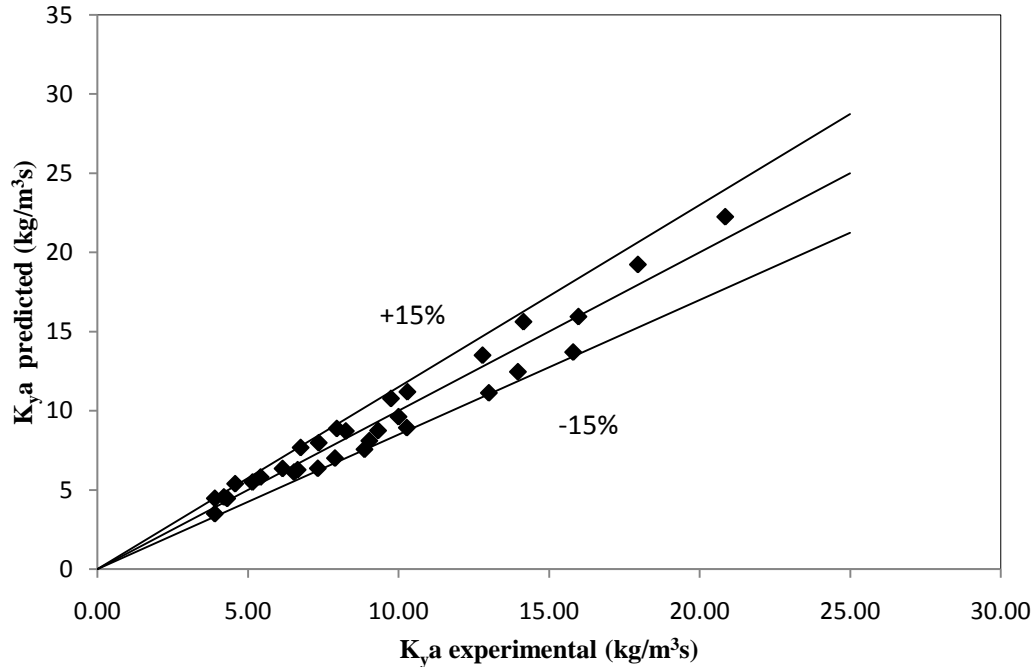


Fig 5.8: Volumetric mass transfer predicted vs. experimental

Wang et al. [5.7] reported the performance of rotating zigzag bed in terms of height equivalent of the theoretical plate (HETP). The parameter was estimated by dividing the radial depth of the rotor by the number of theoretical stages required for the separation. For comparison, the results of mass transfer performance have been reported in terms of HETP for this simultaneous heat and mass transfer process. Figures 5.9 shows the variation of HETP with rotor speed at water flow rate of 1.5 L/min and 1.0 L/min (air flow rate =400 L/min). The minimum value of HETP for this modified rotating zigzag contactor RC-1 is 0.055m. The HETP value for distillation in rotating zigzag bed is approximately between 0.045m and 0.06m [5.7].

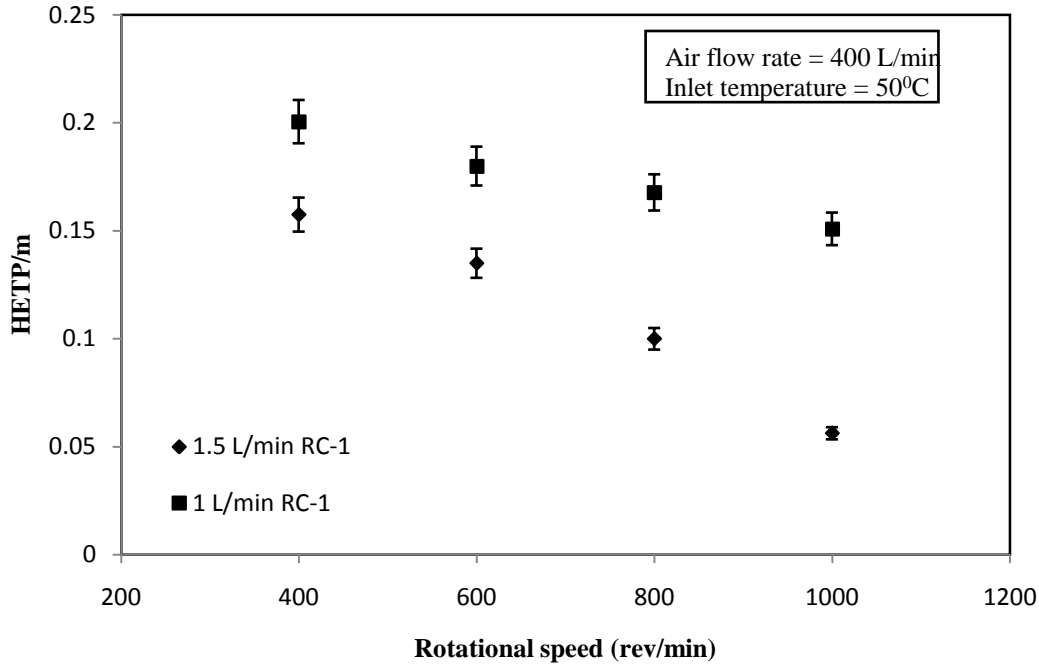


Fig 5.9: Variation of theoretical plate numbers with Rotational speed in RC-1

5.3.3 Comparison with other processes

Falling film-type evaporators are commonly used for the concentration of fruit juice. Figure 5.10 shows the ratio of the volume of the agitated film evaporator to that of RC-1 for obtaining water evaporation rate of 0.038 kg/min (obtained at 50 °C in the latter) for the range of overall heat transfer coefficient (500 W/m²K to 2200 W/m²K) reported in the literature [5.8]. The heat transfer to the liquid ($UA\Delta T$) at its boiling point results in its vaporization. The heat transfer surface area of the agitated film evaporator can be estimated from Eq. (5.6) obtained by equating the rate of heat transfer to the liquid to that carried away by the vapor

$$\dot{m}\gamma = UA\Delta T \quad (5.6)$$

where \dot{m} , γ , U , A , and ΔT represent the evaporation rate, latent heat of vaporization, heat transfer coefficient, surface area for heat transfer, and the temperature difference between heating medium and liquid respectively.

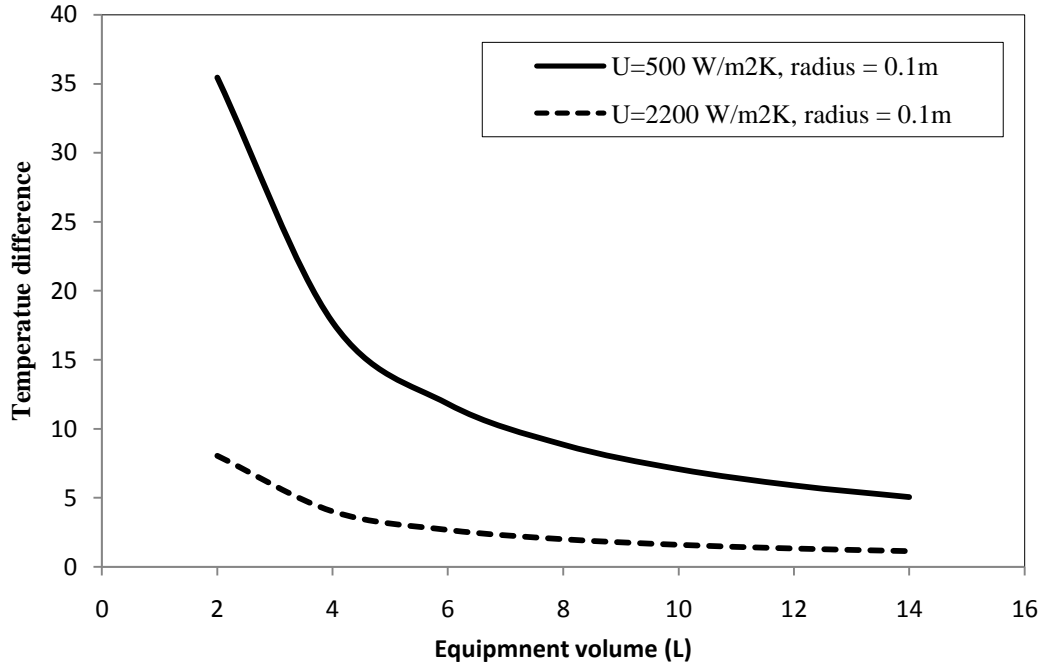


Fig 5.10: Relation between temperature difference, ΔT [eq. (5.6)] and calculated volume of the agitated film evaporator

The volume of the reactor ($A \times \frac{r}{2}$) was calculated by assuming the radius (r) of the heating surface to be 0.1 m. Falling film evaporators are useful for applications when the temperature difference between the surface of heat transfer and the liquid food does not exceed 8-9 °C [5.9]. At this temperature difference, the volume requirement of the evaporator is about 8 and 2 times that of RC-1. Thus, the equipment volume can be reduced by the proposed technique compared to falling film-type evaporators.

As noted earlier, Ribeiro et al. [5.10] proposed direct contact evaporation by bubbling hot air through the solution as an alternative to concentration in evaporators. The evaporation rates of ~ 15% sucrose solution reported by Ribeiro et al. [5.10] were approximately 0.7 g/min and 1.0 g/min at superficial air velocities of 3.5 cm/s and 6.5 cm/s when the temperature in the bubble column reaches 50 °C. These values are much lower than that obtained in RC-1 (38 g/min, superficial gas velocity = 53 cm/s) for pure water at the same inlet temperature even after accounting for the depression of vapor pressure due to sucrose. A given concentration of fruit juice can thus be achieved within a much shorter duration with the proposed technique.

The steam economy of single-effect evaporators has been reported to be ~1.25. In other words, a minimum of 2800 kJ of energy (1.25 kg steam) is required to evaporate 1 kg of water. The major requirement of energy in rotating contactors is the electric energy required to operate the rotor (~0.5 kW) and thermal energy to compensate for the cooling of the solution due to sensible heat exchange with air and latent heat transfer. In the equipment studied, the decrease in temperature across the rotor due to evaporative cooling of water is ~15 °C at 1.5 L/min water flowrate, air flow rate of 400 L/min, and rotational speed of 1000 rpm. Therefore, the theoretical energy required to raise the temperature of the re-circulating solution to the original value is ~1.6 kW. The energy requirement per kg of water evaporated (50 °C) for air-water system is ~3100 kJ. Energy efficiency was noted to improve with rotational speed, air, and liquid flow rate.

5.4 Conclusion

In this study, the mass transfer performance of two different rotating contactors under high gravity for air stripping of water was compared. It was illustrated that the rotating baffled bed contactor was more efficient than the rotating packed bed contactor. The equipment volume can also be reduced as compared to conventional thin-film evaporators. Internal design of the rotor plays a significant role in influencing the performance of this concentration technique. This comparative study would be useful in the selection of a suitable rotor design for stripping of water from an unsaturated gaseous stream.

Nomenclature

- A surface area for heat transfer (m^2)
- a effective interfacial area (m^2 / m^3)
- C_w heat capacity of water ($\text{kJ/kg } ^\circ\text{C}$)
- G dry air flow rate (kg/s)
- h axial distance between rotating disks (m)
- H_G enthalpy of air (kJ/kg)
- H_i enthalpy at the inlet of contactor (kJ/kg)
- H_o enthalpy at the outlet of contactor (kJ/kg)
- $H_{G,i}$ enthalpy of air at air-liquid interface (kJ/kg)
- $K_Y a$ volumetric mass transfer coefficient ($\text{kg/m}^3\text{s}$)
- L liquid flow rate (kg/s)
- \dot{m} evaporation rate (kg/h)
- P constant in Eq. (5.4)
- r radial distance (m)
- r_i inner radius of the rotor (m)

- r_o outer radius of the rotor (m)
- r_{avg} half of the radial path travelled by liquid within the rotor (m)
- R radius of the tube (m)
- \dot{m}_a mass flux of air (kg/m²s)
- \dot{m}_w mass flux of water (kg/m²s)
- T_L Temperature of liquid (⁰C)
- U Heat transfer coefficient (W/m².K)
- Y_{out} Absolute humidity of air at outlet (kg/kg of dry air)
- Y_{in} Absolute humidity of air at inlet (kg/kg of dry air)

Subscripts

- a air
- in inlet
- out outlet
- w water

Superscripts

- α_1 - α_6 exponential constant in Eq. (5.8)

Greek symbols

- ω rotational speed (rad/s)
- ΔT temperature difference between heating medium and liquid (⁰C)

References

- 5.1 Treybal, R.E., *Mass-Transfer Operations*; McGraw-Hill Book Co.: Singapore, 1981.
- 5.2 Šikalo, S., Tropea, C., Marengo, M., and Ganić, E.N., “Spreading of Droplets on Horizontal Surfaces,” in *New and Renewable Technologies for Sustainable Development*, N. H. Afgan and M. da Graça Carvalho, Eds. Boston, MA: Springer US, pp. 683–692, 2002, doi: 10.1007/978-1-4615-0296-8_54.

- 5.3 Sandilya, P., Rao, D.P., Sharma, A., Biswas, G., “Gas-phase mass transfer in a centrifugal contactor”, *Industrial & Engineering Chemistry Research*, vol. 40 (1), pp. 384–392, 2001.
- 5.4 Bhattacharyya, S., Mondal, A., Bhowal, A., Datta, S., “Evaporative cooling of water in a rotating packed bed (split packing)”, *Industrial Engineering Chemistry and Research*, vol. 49, pp. 847–851, 2010.
- 5.5 Li, Y., Lu, Y., Wang, G., Nie, Y., Ying, H., Ji, J., Liu, X., “Liquid Entrainment and Flooding in a Rotating Zigzag Bed”, *Industrial & Engineering Chemistry Research*, vol. 54, pp. 2554-2563, 2015.
- 5.6 Guo, K., Guo, F., Feng, Y., Chen, J., Zheng, C., and Gardner, N., “Synchronous visual and RTD study on liquid flow in rotating packed-bed contactor,” *Chemical Engineering and Science*, vol. 55, 2000, doi: 10.1016/S0009-2509(99)00369-3.
- 5.7 Wang, G.Q., Xu, Z.C., Yu, Y.L., Ji, J.B., “Performance of a rotating zigzag bed: A new HIGEE”, *Chemical Engineering Processing*, vol. 47 (12), pp. 2131–2139, 2008.
- 5.8 Glover, W., “Scaleup of agitated thin-film evaporators,” *Chemical Engineering Practice*, vol. 111, pp. 55–58, 2004.
- 5.9 Glover, W., “Selecting evaporators for process applications,” *Chemical Engineering Progress*, vol. 100, pp. 26–33, 2004.
- 5.10 Ribeiro, C.P., Borges, C.P., and Lage, P.L.C., “Modelling of direct-contact evaporation using a simultaneous heat and multicomponent mass-transfer model for superheated bubbles,” *Chemical Engineering Science*, vol. 60, no. 6, pp. 1761–1772, 2005, doi:10.1016/j.ces.2004.08.049.

Chapter 6

Concentration of citrus fruit juice in rotating contactors

6.1 Introduction

In this study, the results obtained on concentrating orange juice, a citrus fruit by evaporating water into an unsaturated gaseous stream was explored in a rotating baffled and a rotating packed bed contactor operating under high gravity has been reported. The objectives were

- To study the influence of process parameters such as air flow rate, water flow rate, rotor speed, and temperature on the concentration of orange juice in the equipment.
- Determine the optimum operational parameters utilizing experimental design, and response surface methodology using a four-factorial Box-Behnken design.
- Comparative study on performance between the rotating contactors, and traditional wiped film evaporator.
- To carry out physiochemical analysis of the orange juice (both feed and concentrates). Mean difference analysis of the data using a post hoc Tukey-Kramer multiple comparison test at $p \leq 0.05$

6.2 Materials and methods

6.2.1 Preparation of the juice

The peels of oranges were separated manually and the seeds were removed from the fruit. The juice was extracted using a juice extractor. The juice was then filtered using sieves and multilayered clean muslin clothes to ensure the absence of pulps or seeds in the juice.

Finally, the obtained juice was centrifuged for 10 minutes at 9000 rpm and the clarified juice so obtained was used for the experimental studies. Fresh juice was prepared for each of the experiments.

6.2.2 Experimental procedure

The experimental procedure has been described in detailed Chapter 4. Experiments were carried by continuously recirculating the fruit juice through the equipment wherein it was contacted with the gas phase.

6.3 Statistical Analysis

Statistical analysis was performed for RC-1 to determine the effect of different operating variables on the concentration of orange juice. A four-factorial Box-Behnken design was developed and analyzed to determine the optimal condition of the process.

$$y = \beta_0 + \sum_{i=1}^n \beta_i x_i + \sum_{i=1}^n \beta_{ii} x_i^2 + \sum_{i=1}^{n-1} \sum_{j=i+1}^n \beta_{ij} x_i x_j + \varepsilon \quad (6.1)$$

where y is the predicted response, β_0 is the constant coefficient, β_i is the linear coefficient, β_{ii} is the quadratic coefficient, β_{ij} is the interaction coefficient, ε represents a random error, and x_i & x_j are the coded values of the independent process variables. ANOVA test was further done to investigate the parametric significance with a significance level assumed at 5%.

6.4 Physiochemical Analytical methods

Samples were collected from the tank at regular intervals. The total soluble solid present was measured using the Refractometer (Atago, Japan). Various physiochemical parameters were measured in the feed and the final concentrate. The total acid content and viscosity were measured by titration and Contraves Rheomat 115. Vitamin C was

analyzed by titrating with 2,6-dichlorophenol indophenol. The color of the fruit juice was measured using a Konica Minolta colorimeter cr-400 using the Hunter system. The total phenolics content, flavonoid content, and antioxidant capacity using three different assays were also performed. The data shown in the table were recorded in five replicates and statistically analyzed using one-way ANOVA. Further, a post hoc Tukey Kramer HSD test was also performed to check the mean significant difference. In the table, the different alphabets (a, b, c) illustrate the significant difference in the means of the samples at $p \leq 0.05$.

6.5 Result and Discussions

The time-variant concentration of orange juice in wiped film evaporator (WPE) is presented in Figure 6.1 along with the results obtained in rotating packed contactor, RC-2. The juice could be concentrated to 15.4 °Brix and 24.6 °Brix after 2 hours of processing time in wiped film evaporator and rotating packed bed evaporator respectively. The surface area is ~5 times higher in RC-2 in comparison to WPE. This increases the gas-liquid interfacial area in the former for the evaporation of water to occur.

The effect of different operating parameters on the concentration of orange juice in the rotating contactors is shown in Figures 6.2 to 6.5.

6.5.1 Influence of rotor speed

It is seen that the total soluble solid increased to 19.9 °Brix after two hours of operation at rotor speed of 600 rpm (Figure 6.2) in RC-1. The corresponding concentration of orange juice was 30.6 °Brix at 1000 rpm. The final concentration of orange juice obtained in RC-2 at 600 rpm and 1000 rpm were 16.6 °Brix and 24.6 °Brix respectively.

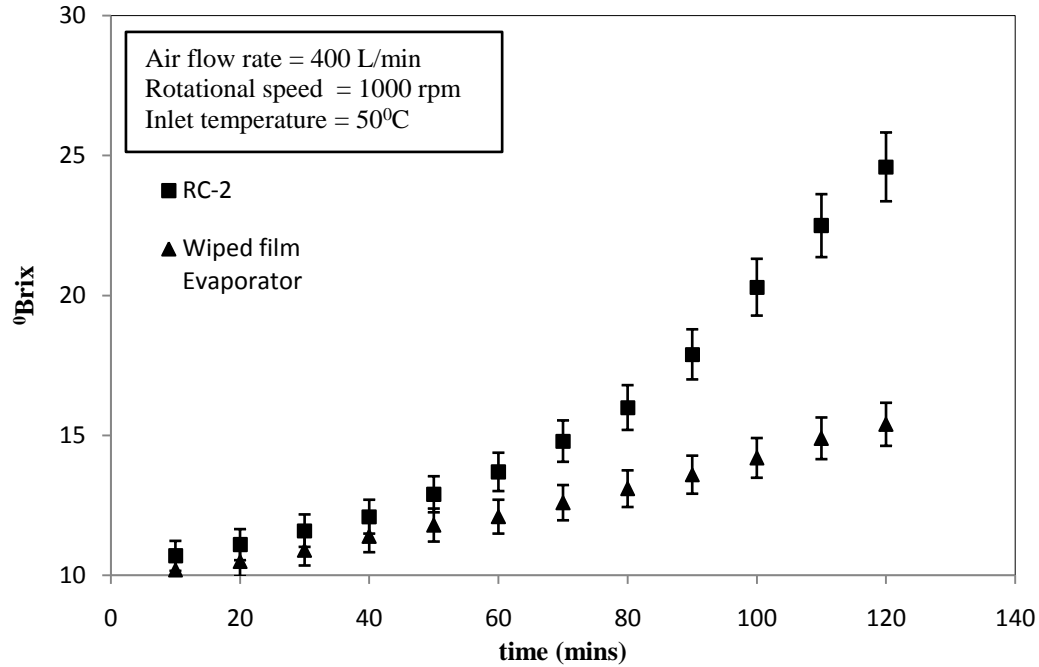


Fig 6.1: Comparative study in concentration of orange juice in Wiped film evaporator and Rotating packed bed RC-2

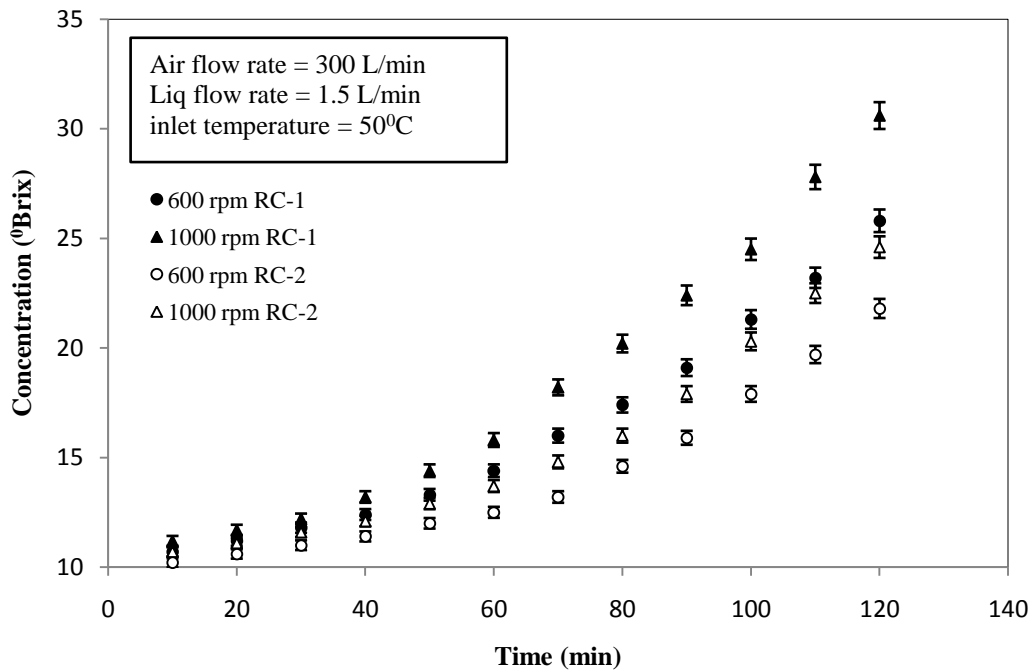


Fig 6.2: Influence of rotational speed on orange juice concentration in RC-1 and RC-2

6.5.2 Effect of juice flow rate

Figure 6.3 shows the effect of liquid flow rate on the concentration of fruit juice at liquid flow rates of 1.0 L/min and 1.5 L/min respectively. In RC-1, the final concentration of orange juice at liquid flow rates of 1.0 L/min and 1.5 L/min was 26.3 °Brix and 30.6 °Brix respectively after two hours of operation. The values obtained in RC-2 after the same duration of experiment were 22.3 °Brix and 24 °Brix from the initial 10 °Brix at fruit juice flow rates 1.0 L/min and 1.5 L/min respectively which is lower than RC-1.

The increase in the concentration of fruit juice at higher rotor speed and liquid flow rate is related to evaporation rate of water. It was noted in chapter 5 that evaporation rate of water increases with both these operational parameters. Consequently, more concentrated solution is obtained within a given processing time.

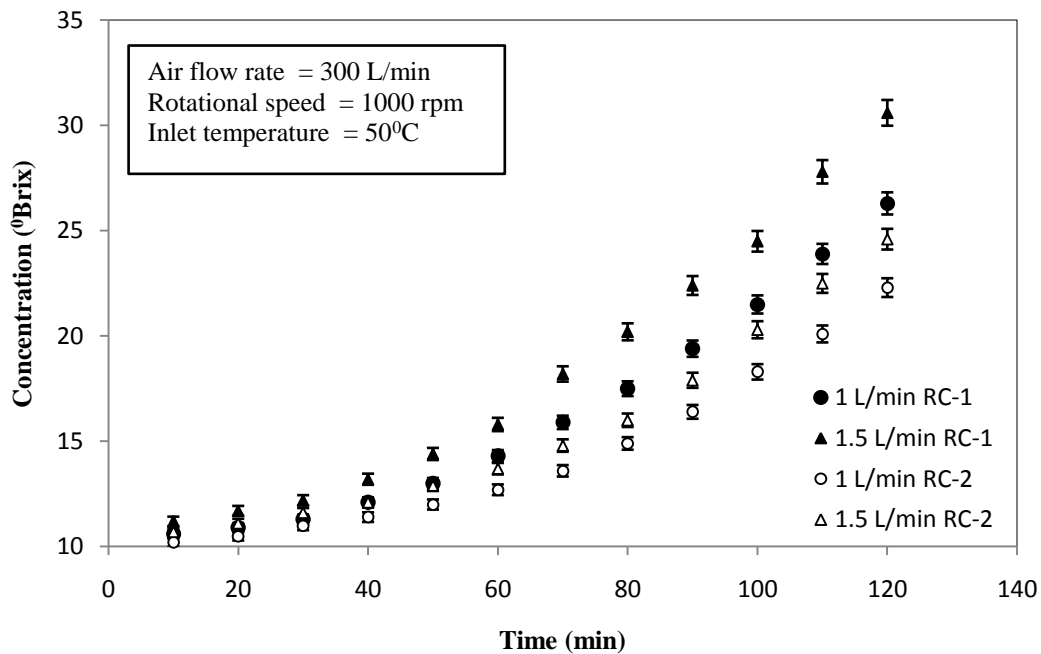


Fig 6.3: Effect of orange juice flow rate on the concentration in RC-1 and RC-2

6.5.3 Effect of air flow rate

The effect of variation of air flow rate on the concentration of fruit juice is depicted in Figure 6.4. It is seen that the concentration of orange juice increases to 22.9 °Brix and 32.8 °Brix at airflow rates of 200 L/min and 400 L/min respectively in RC-1. The final values of concentration at these flow rates obtained in RC-2 are 19.9 °Brix and 26.1 °Brix respectively which is significantly lower than RC-1.

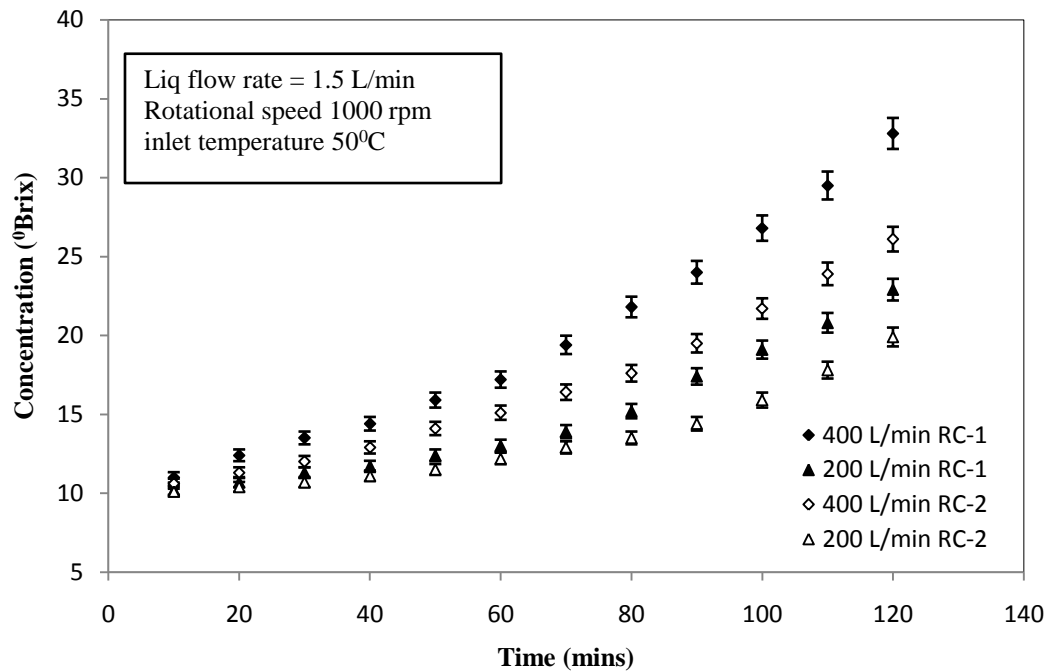


Fig 6.4: Influence of air flow rate on orange juice concentration in RC-1 and RC-2

The mole fraction of water in the juice was estimated to be around 0.975 at these °Brix readings assuming the soluble solids present in orange juice to be sucrose. The solution can then be considered to be pure water, and the mass transfer resistance to the transfer of water from solution to air lies entirely in the gas phase. An increase in air flow rate promotes turbulence and reduces the gas phase mass phase resistance. Furthermore, the capacity of the gas phase for the uptake of moisture also increases at a higher flow rate [6.1].

6.5.4 Effect of temperature

The influence of temperature on the concentration of the orange juice was studied in both RC-1 and RC-2 respectively (Figure 6.5). The concentration increased from 30.6 °Brix to 32.8 °Brix in RC-1 with the increase in the temperature from 50 °C to 60 °C due to the increase in vapor pressure of water and reduced viscosity. The corresponding concentrations observed in RC-2 were 24.3 °Brix and 25.9 °Brix respectively.

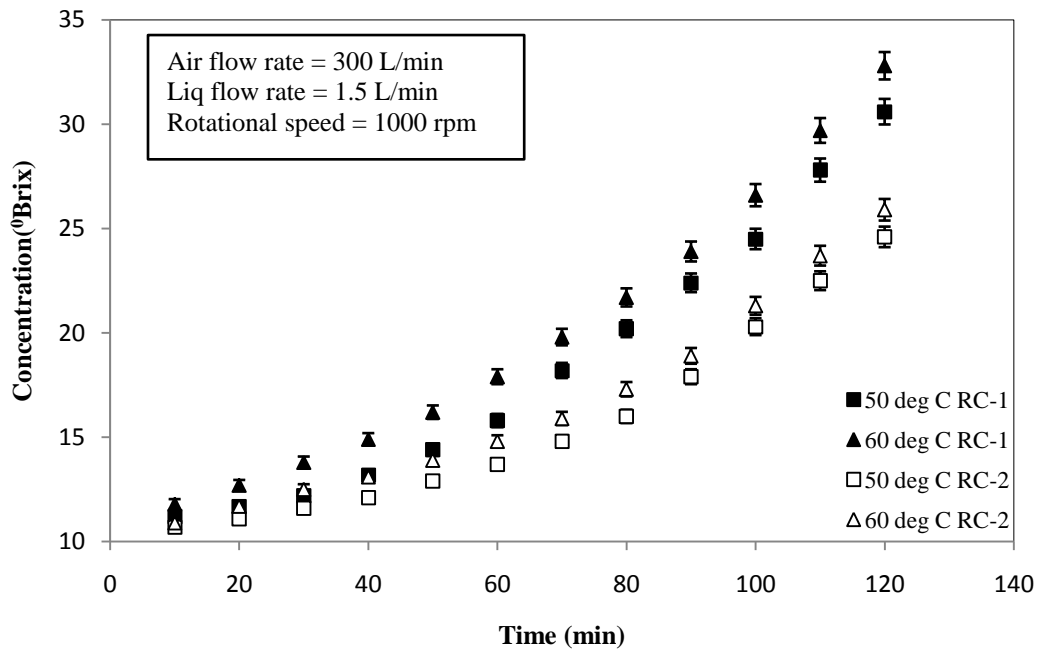


Fig 6.5: Influence of temperature on orange juice concentration in RC-1 and RC-2.

6.5.5 Optimization using Response surface methodology (RSM)

The variables were rotational speed (600, 800, and 1000 rpm), air flow rate (200, 300, and 400 LPM), liquid flow rate (0.5, 1, and 1.5 LPM), and temperature (45, 50, and 60 °C). These parameters were considered to be the independent variables in the study. Concentration of juice in °Brix was considered the response variable. Statistics-based software DOE version 8 (Design of experiment) was utilized to analyze experimental

results in terms of the regression coefficient. Furthermore, ANOVA (Analysis of variance) was also performed to determine the statistical significance of the model developed in the study. The predicted values were used to create a surface response and 3D graphs for the final optimization process. The ideal parameter levels for orange juice concentration were determined using a Box-Behnken experimental methodology. This method involves the following three basic steps: experimental design, modeling, and optimization. Previous studies have shown that the rotational speed, liquid flow rate, and airflow rate affect the performance of rotating contactors. In addition to these, the temperature of the feed would affect the water vapor pressure and, consequently, the effectiveness of the liquid concentration process in the equipment. Twenty-seven experiments were carried out using the RSM combination with factorial points, axial points, and the centre point (0).

The experimental ranges and different levels of the independent variables are listed in Table 6.1. It is shown that the four different factors chosen for optimization are rotational speed, air flow rate, liquid flow rate, and temperature of concentration. Symbolically the variables were represented by A, B, C, and D for air flow rate, liquid flow rate, rotational speed, and temperature respectively. The prescribed levels for high, intermediate, and low values were represented by -1, 0, and 1.

Table 6.1: Experimental range and various levels of independent variables

Variables	Symbol	Coded levels		
		-1	0	+1
Air Flow rate	A	200	300	400
Liquid Flow rate	B	0.5	1	1.5
Rotational speed	C	600	800	1000
Temperature	D	45	50	60

Due to the use of fewer experiments than other experimental models, the Box-Behnken experimental design is significantly better for response surface methods and statistical analysis. It is one of the most effective methods for determining the optimal level of process parameters.

6.5.6 Model fitting and ANOVA analysis

For the model development experiment, Table 6.1 lists the actual and coded values for the air flow rate, liquid flow rate, rotor speed, and temperature. Tables 6.2 and 6.3 present the findings of the analysis of variance (ANOVA), which ensures the developed model's fit. Equation 6.2 represents the predictive quadratic equation model for the concentration of orange juice as a function of rotor speed, water flow rate, and air flow rate as determined by the experimental investigation.

$$\begin{aligned}
 C_{orange} = & 28.75 + 6.1A + 2.448B + 1.166C + 2.519D + 1.228AB \\
 & + 0.055AC + 0.0675AD + 1.0025BC + 0.095BD \\
 & - 0.275CD - 1.7629A^2 - 2.5079B^2 - 0.5542C^2 \\
 & - 0.4792D^2
 \end{aligned} \tag{6.2}$$

where, C_{orange} is the predicted concentration of orange juice ($^{\circ}$ Brix), A , B and C , and D are the coded terms for air flow rate (Litre/min), liquid flow rate (Litre/min), rotational speed (rev/min) and temperature ($^{\circ}$ C) respectively.

All the linear term (A , B , C , D) coefficients showed a positive, favorable and significant effect on response. The quadratic terms A^2 , B^2 , C^2 , and D^2 showed an unfavorable effect on response C . Interaction terms (AB , AC , AD , BC , BD) of the same parameter indicated positive and favorable effects, while CD showed a negative and unfavorable effect on the concentration of orange juice. Anova results were given in Tables 6.2 and 6.3. The

coefficient of determination (R^2) value obtained was 0.9766 which can be considered a good agreement between the predicted values and the experimental ones. The adjusted R^2 value was also calculated (0.9495) to assure the reliability of the regression model, which was in reasonable agreement with the R^2 value. The model may be used to accurately predict the response variable, as shown by the F test result. The model is suggested to be significant by the model's F-value of 35.91. There is only a 0.01% chance that a “Model F-value” with such a large value could occur due to noise. The “Prob> F” value of less than 0.05 also ensured that the study is significant. In this case, A, B, C, D, A^2 , B^2 , C^2 , D^2 , AB, CD, and BC are significant model terms (with p value less than 0.005). The "Predicted R-Squared" of 0.8657 and the "Adj R-Squared" of 0.9495 are reasonably in accord. This shows that the model can accurately predict and explain the total variation in the measured response. The signal-to-noise ratio was measured using "Adeq Precision," which was 21.067. The value, therefore, denotes an adequate signal.

The predicted vs. actual juice concentration plot is shown in Figure 6.6. While the predicted values were computed using the model, the actual values were obtained from experimentation. It is seen in the figure that Eq. (6.2) predicted the experimental values obtained in the contactor within $\pm 10\%$.

Table 6.2: Statistics used in the evaluation of the goodness-of-fit of the responses to the models in orange juice.

RSM Statistics	
Coefficient of Variation (C.V.) %	4.352
Determination coefficient R^2	0.976687
Adjusted R^2	0.949489
Predicted R^2	0.865718
Adequate precision	21.06688

Table 6.3: Analysis of variance for the response surface quadratic model in orange juice.

Table 3 –ANOVA for the response surface quadratic model.						
Source	Sum of squares	df	Mean square	F Value	P value Prob> F	
Model	663.294	14	47.37814	35.90985	< 0.0001	significant
A	446.52	1	446.52	338.436	< 0.0001	significant
B	71.93203	1	71.93203	54.52027	< 0.0001	significant
C	16.31001	1	16.31001	12.36203	0.0043	significant
D	76.15441	1	76.15441	57.72058	< 0.0001	significant
AB	6.027025	1	6.027025	4.568132	0.0438	significant
AC	0.0121	1	0.0121	0.009171	0.9253	
AD	0.018225	1	0.018225	0.013813	0.9084	
BC	4.020025	1	4.020025	3.046943	0.0106	significant
BD	0.0361	1	0.0361	0.027362	0.8714	
CD	0.3025	1	0.3025	0.229277	0.0440	significant
A ²	16.57533	1	16.57533	12.56313	0.0040	significant
B ²	33.54478	1	33.54478	25.42498	0.0003	significant
C ²	1.63787	1	1.63787	1.24141	0.0287	significant
D ²	1.224537	1	1.224537	0.928127	0.0354	significant
Residual	15.83236	12	1.319363			
Lack of Fit	15.83236	10	1.583236			
Pure error	0	2	0			
Cor total	679.1263	26				

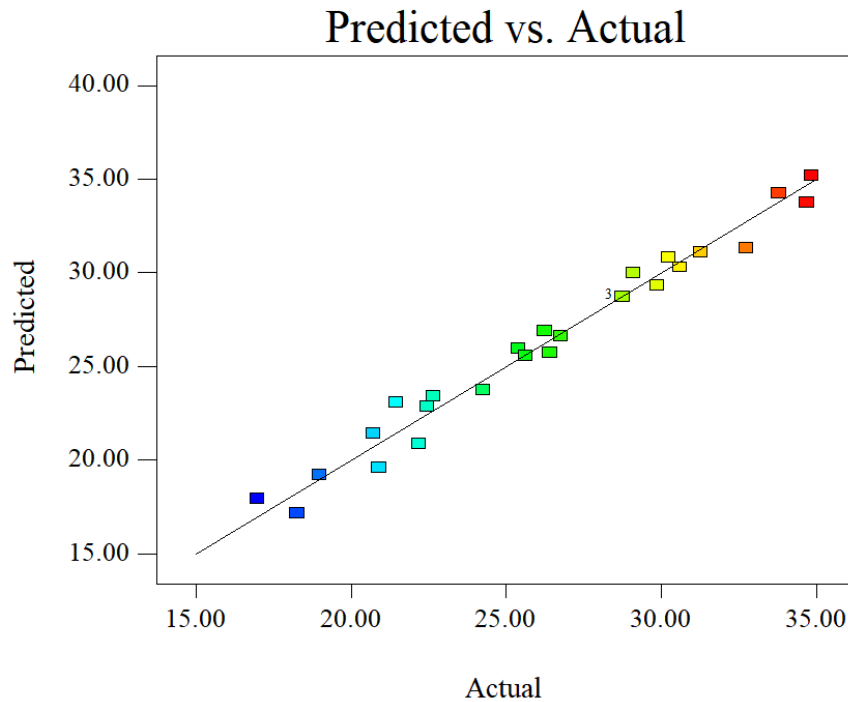


Fig 6.6: Predicted value vs actual value of concentration of orange juice

6.5.7 Interaction among variables

Figures 6.7–6.12 illustrate the interactional influence of air flow rate, liquid flow rate, rotor speed, and temperature on the concentration of orange juice graphically in three dimensions. The surface plots are achieved for the mutual effect on a pair-wise combination whereas the other factors are set at their middle level. The interaction between liquid flow rate and air flow rate on juice concentration is depicted in Figure 6.7. The positive value for the linear coefficient of the air and liquid flow rates in Eq. (6.2), suggests that both the air and liquid flow rates increase the concentration value. This is supported by the gradual ascent along the liquid flow rate and air flow rate axes in the 3D response support.

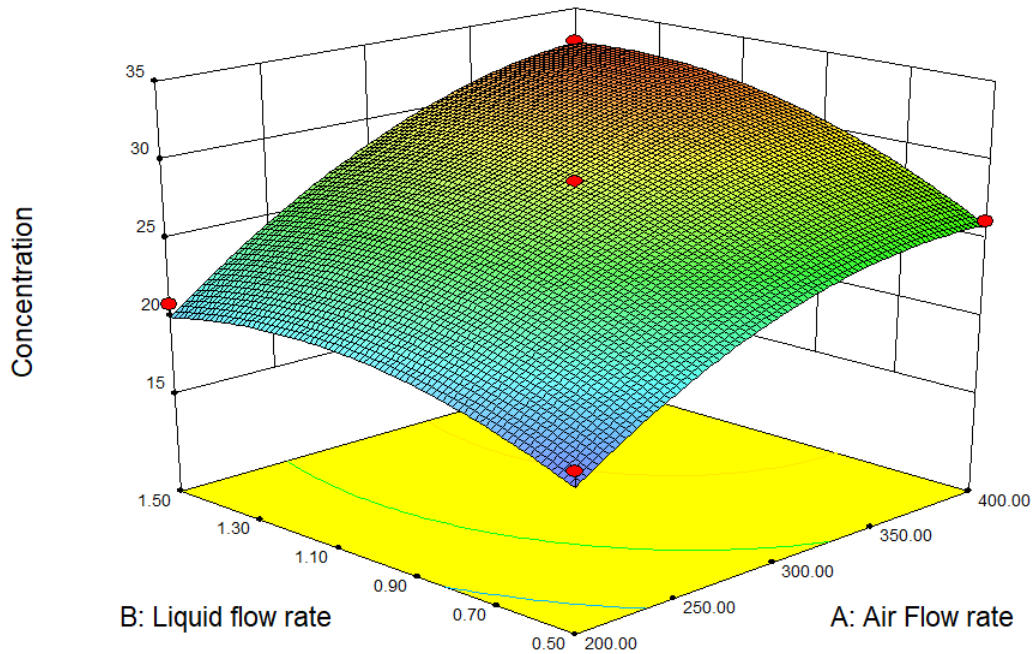


Fig. 6.7: Interactive effect of air flow rate (Litre/min) and liquid flow rate (Litre/min) on the concentration of juice.

Figure 6.8 illustrates the interaction between rotor speed and air flow rate. These parameters have a strong influence on the concentration of orange juice as indicated by the curvatures along their respective axes. The positive values of the linear coefficient in Eq. (6.2) suggested that the concentration value in $^{\circ}\text{Brix}$ increased with rotor speed and air flow rate. On the other hand, a rise in the volumetric mass transfer coefficient $K_Y a$ is suggested by the interaction coefficient's positive value. This is in keeping with the finding in chapter 5 where it was noted that $K_Y a$ increases with the gas flow rate. The p -value greater than 0.05 in this study indicated that the interactive effect between rotor speed and air flow rate is not significant.

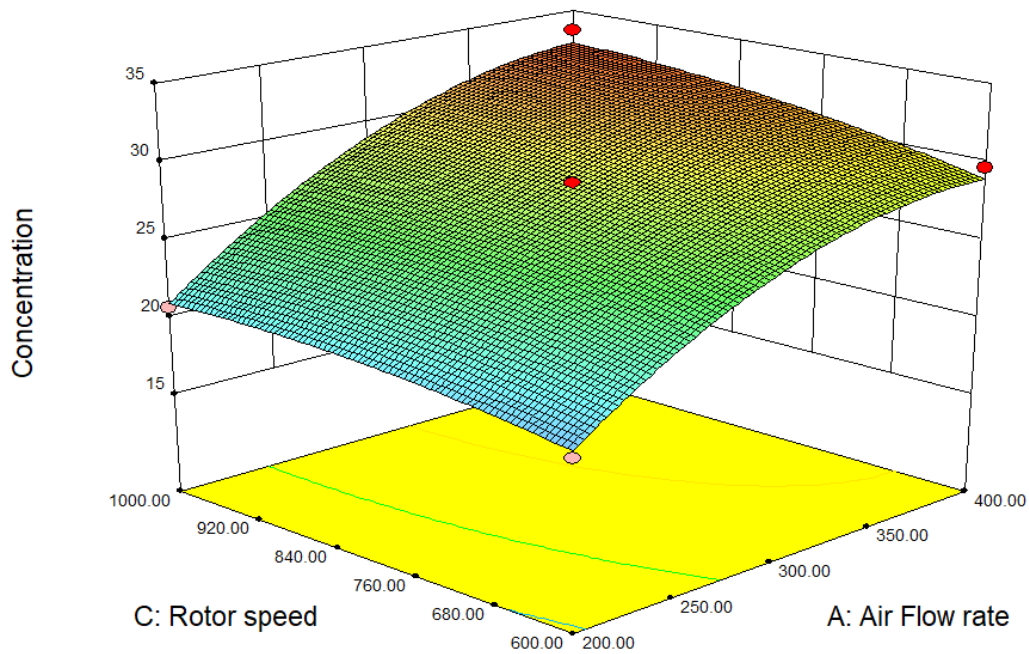


Fig. 6.8: Interactive effect of air flow rate (Litre/min) and rotor speed (rev/min) on the concentration of orange juice.

Figure 6.9 illustrates the relationship between rotor speed and liquid flow rate. The linear and interactive coefficient's positive value indicates that concentration rises with both

rotor speed and liquid flow rate. The gas-liquid interfacial area increases with both liquid flow rate and rotational speed [6.2]. As a result, the evaporation rate of water and juice concentration both increase with these.

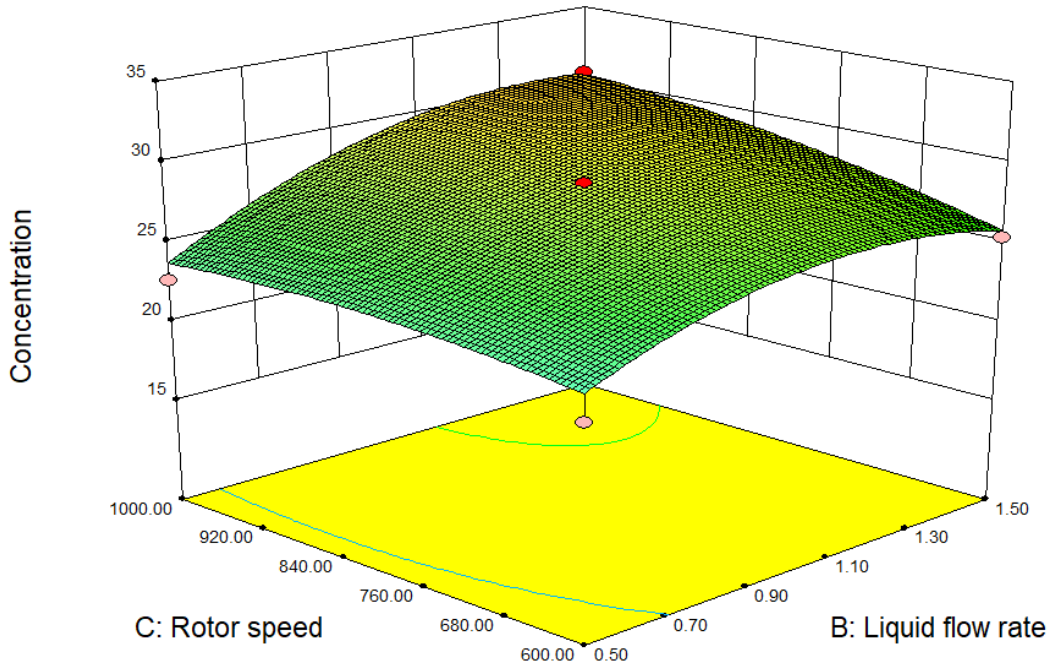


Fig. 6.9: Interactive effect of liquid flow rate (Litre/min) and rotor speed (rev/min) on the concentration of juice.

Figure 6.10 indicated the interactive relationship between rotor speed and temperature. The positive value of the linear coefficient suggested that concentration rises with both rotor speed and temperature. Liquid droplets split apart into smaller droplets, thinner films, and long ligaments as the rotational speed increased [6.3]. This results in the development of a larger solid-liquid contact area and a higher rate of gas-liquid interface renewal. As a result, the mass transfer rate is enhanced, increasing the juice concentration.

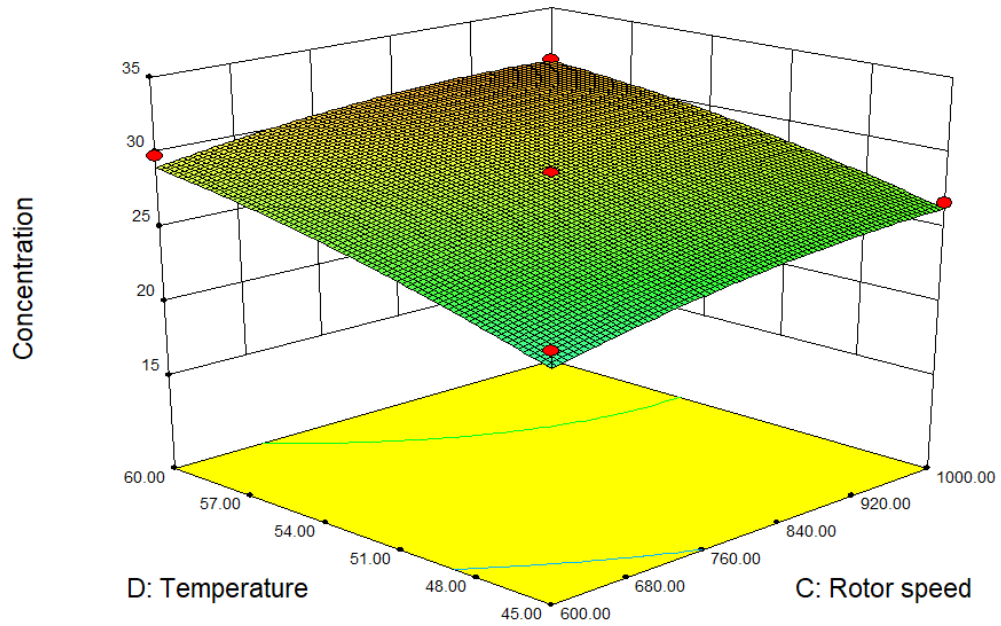


Fig. 6.10: Interactive effect of rotor speed (rev/min) and temperature ($^{\circ}\text{C}$) on the concentration of orange juice.

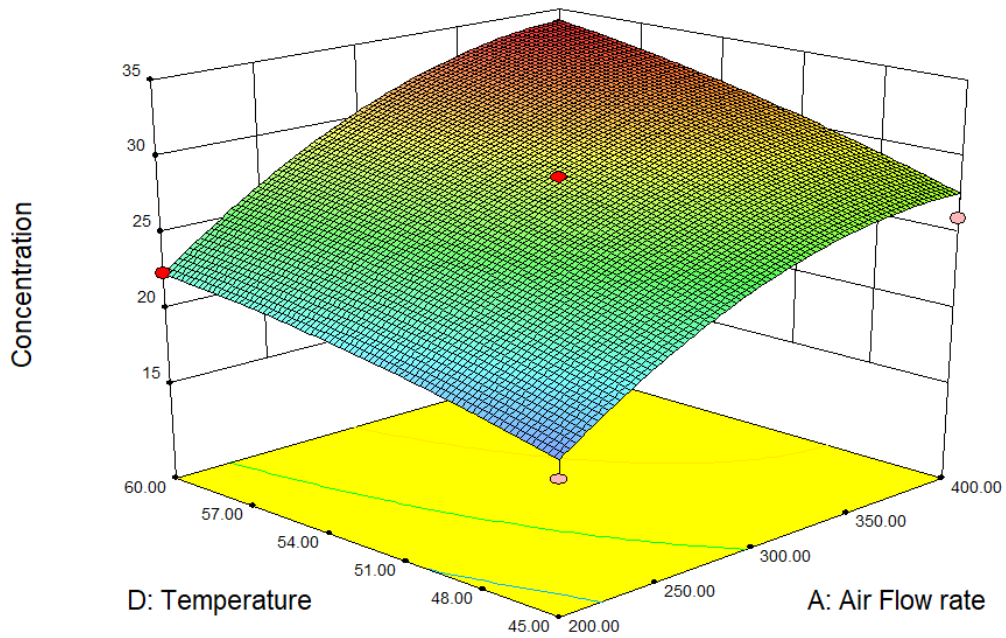


Fig. 6.11: Interactive effect of rotor speed (rev/min) and temperature ($^{\circ}\text{C}$) on the concentration of orange juice.

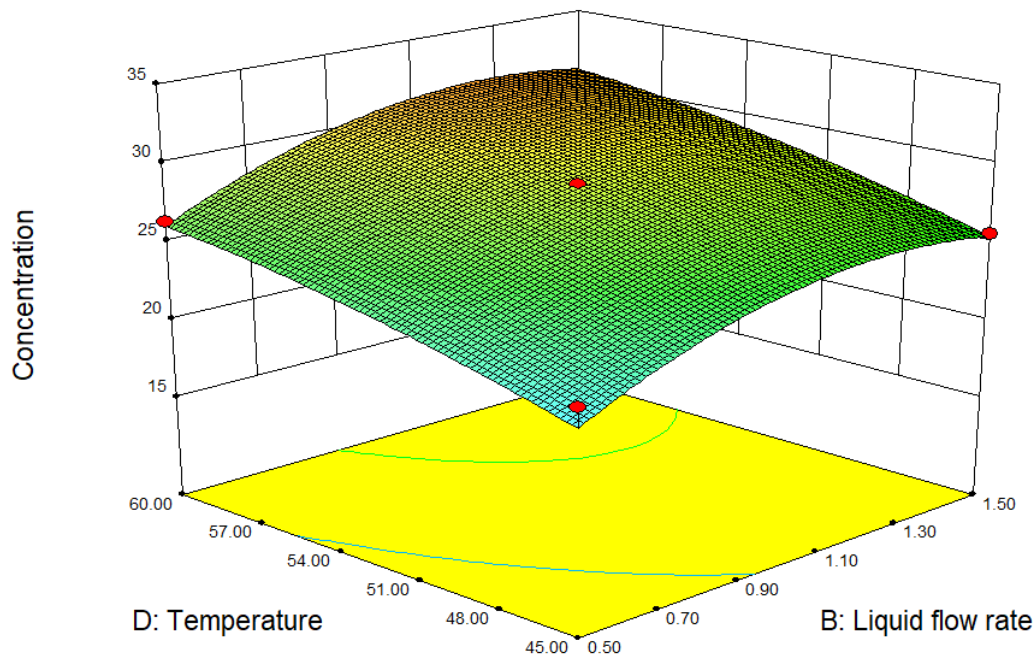


Fig. 6.12: Interactive effect of temperature ($^{\circ}\text{C}$) and liquid flow rate (Litre/min) on the concentration of orange juice.

The interactive effects of temperature and flow rates are shown in Figures 6.11 and 6.12. The positive value of the interaction suggested that there is an increase in the concentration owing to better mass transfer rates.

Membrane processes have also been explored for the concentration of fruit juice as an alternative to the thermal evaporation of fruit juice. Shaw et al. [6.4] studied the concentration of orange juice using microfiltration (membrane surface area = 1.3 m^2) followed by osmotic evaporation (membrane surface = 10.3 m^2). They reported that it took 21 hours to increase the concentration from 10.3 to 33.5 $^{\circ}\text{Brix}$. The same concentration was achieved within 2 hours by stripping the juice with an unsaturated gas

stream in RC-1. Other major limitations of membrane processes are the high osmotic pressure and fouling of the membrane surface [6.5, 6.6].

6.5.8 Physicochemical Analysis results

Tables 6.4 and 6.5 show the physicochemical evaluation of the feed, clarified, and concentrated juices. The difference in pH of the fresh juice clarified juice and concentrated juice was not significant. In fresh juice, the pH was 4.2 whereas in the clarified and concentrated juice the pH was 4.1 and 4.4 respectively. The total acid content of the feed and the final concentrate was measured by titration of a base using a phenolphthalein indicator. The acid content increased from 0.998 to 1.874 gm/100 ml in feed and concentrated juice. The total soluble solid content was measured for both the juice and the concentrated juice. The initial soluble solid content was 10 °Brix which after the experimentation of 2 hours in RC-1 became 32.6 °Brix. The viscosity increased three folds from a value of 1.7 mPa.s in the feed to 5.5 mPa.s in the concentrated juice.

Table 6.4: Physicochemical data of the feed, clarified juice, and concentrate.

Physicochemical analysis	Feed juice	Clarified juice	Concentrate
pH	4.2±0.01 ^a	4.1±0.01 ^b	3.93±0.01 ^c
Total acid content (gm/100 ml)	0.998±0.5 ^b	0.985±0.02 ^b	1.874±0.01 ^a
Total soluble solid (°Brix)	10±0.54 ^b	9.9±0.39 ^b	32.6±0.25 ^a
Viscosity (mPa.s)	1.7±0.01 ^b	1.6±0.23 ^c	5.5±0.57 ^a
Ascorbic acid (mg/100 ml)	50.5±0.66 ^b	50.5±0.01 ^b	65.7±0.19 ^a
a(Hunter system)	1.8±0.54 ^b	1.72±0.66 ^b	2.0±0.03 ^a
B (hunter system)	9.8±0.27 ^a	9.69±0.29 ^b	9.6±0.45 ^c
Luminosity (L)	15.4±0.01 ^a	15.2±1.12 ^b	14.9±0.59 ^b

The results are provided in arithmetic means ± standard deviations form calculated for five replicates. Different letters (a, b, c) indicate a significant difference between different samples (p≤0.05) determined by Tukey HSD test.

The Ascorbic acid content of the fresh and the concentrated juice was measured using visible titrimetry using 2,6 dichlorophenol indophenol dye (DCPIP dye technique). The value was 50.5 mg Ascorbic acid/100 ml in the feed juice and 65.7 mg Ascorbic acid/100 ml in the concentrated juice. The color content of the orange juice and concentrate was observed using the Hunters method in a Konica Minolta colorimeter. The Luminosity value decreased from 15.4 to 14.9 in the case of the concentrate whereas there is not much change in the 'a' and 'b' values of the feed and the concentrate. The value of 'a' in feed and concentrated fruit juice is 1.8 and 2.0 respectively and that of 'b' was 9.8 and 9.6 respectively. A similar trend for ascorbic acid content, viscosity, and color content was observed in single-strength and concentrated juice obtained by Jesus et al. [6.7] while concentrating orange juice by reverse osmosis.

The Total phenolic content in the orange juice was measured using the Gallic acid standard calibration curve. The concentration was 717 mg GAE/Litre in the feed juice which increased 1.5 times in the concentrated juice (1071 mg GAE/Litre). The total flavonoid content was measured using Catechin as the standard solution. The concentration was 244 mg Catechin equivalent (CE)/Litre in the feed orange juice which increased a little in the concentrated juice (336 mg CE/Litre). The antioxidant capacity was measured using three different assays. In TEAC assay, the antioxidant capacity of the feed, clarified juice and concentrate were 10.5, 9.69, and 14.61 mmol of Trolox equivalents (TE)/Litre of sample. In the FRAP assay, the antioxidant capacity of the feed, clarified juice and concentrate were 4.48, 4.15, and 5.74 mmol of Trolox equivalents (TE)/Litre of sample. The DPPH % inhibition after 30 minutes was 56.72 %, 54.75%, and 58.016 % respectively. All the data shown in the table were recorded in five

replicates and statistically analyzed using one-way ANOVA. Further, a post hoc Tukey Kramer HSD test was also performed to check the mean significant difference. In the table, the different alphabets (a,b,c) illustrate the significant difference in the means of the samples at $p \leq 0.05$.

6.6 Conclusion

Reducing the water content of fruit juice by stripping with an unsaturated gaseous stream under high gravity was studied in a baffled rotating contactor operating and rotating packed bed contactor. The salient findings are:

- This strategy of direct contact evaporation is more efficient for the concentration of fruit juice than bubbling hot air through the solution proposed in the literature for overcoming the limitations of conventional evaporators.
- The concentration achieved in orange juice was 32.8 °Brix from an initial 10 °Brix after 2 hours of operation which is quite significant.
- Higher concentration was achieved in RC-1 compared to RC-2 at the same operating parameters.
- Experimental results obtained with orange juice suggest that the proposed strategy using high-gravity contactors can be further explored for the concentration of fruit juice.

Table 6.5: Total Phenolics, Flavonoids, and Antioxidant capacity of the feed, clarified juice, and the concentrate.

Fruits		Antioxidant capacity				
		Total phenolics* (mg GAE/litre)	Total flavonoids** (mg CE/litre)	TEAC*** (mmol TE/l)	FRAP**** (mmol TE/l)	DPPH***** (%Inhibition) After 30 minutes
Orange	Fresh juice	717.004±0.48 ^b	244.01±1.12 ^b	10.5±0.42 ^b	4.48±0.318 ^b	56.72±0.212 ^b
	Clarified juice	702.28±0.46 ^b	228.02±0.488 ^b	9.69±0.36 ^b	4.146±0.102 ^c	54.75±0.166 ^c
	concentrate	1071.12±0.309 ^a	336.02±4.117 ^a	14.61±0.65 ^a	5.74±0.287 ^a	58.016±0.173 ^a

*Total Phenolics content was measured using Folin –Ciocalteu assay [Singleton, 1999] and the values are expressed in mg Gallic acid equivalents (GAE)/Litre of juice/concentrate
**Total Flavonoids content was estimated using the method of Zhisen et al, 1999 and the values are expressed in mg Catechin equivalents (CE)/Litre of juice/concentrate.
***TEAC assay values are determined using the method by Re, 1999 and the values are expressed in mmol of trolox equivalents (TE)/litre of juice/concentrate.
****FRAP assay values are determined by the method of Benzie and Strain, 1996 and the values are expressed in mmol of trolox equivalents (TE)/Litre of juice/concentrate.
*****DPPH assay values were determined using the method by Moon and Terrao, 1998 and the values are expressed in % Inhibition after 30 minutes for both juice and concentrate

Nomenclature

y	objective to optimize the response in Eqn. 6.1
β_0	constant coefficient in Eqn. 6.1
β_i	linear coefficient in Eqn. 6.1
β_{ii}	quadratic coefficient in Eqn. 6.1
β_{ij}	interaction coefficient in Eqn. 6.1
ε	random error in Eqn. 6.1
x_i	coded value of the independent process variable in Eqn. 6.1
x_j	coded value of the independent process variable in Eqn. 6.1
C_{orange}	predicted concentration of orange juice ($^{\circ}$ Brix) in Eqn. 6.2
A	coded term for air flow rate (Litre/min) in Eqn. 6.2
B	coded term for juice flow rate (Litre/min) in Eqn. 6.2
C	coded term for rotational speed (rev/min) in Eqn. 6.2
D	coded term for temperature ($^{\circ}$ C) in Eqn. 6.2
A^2	quadratic term in Eqn. 6.2
B^2	quadratic term in Eqn. 6.2
C^2	quadratic term in Eqn. 6.2
D^2	quadratic term in Eqn. 6.2
AB	interactive term in Eqn. 6.2
AC	interactive term in Eqn. 6.2
AD	interactive term in Eqn. 6.2
BC	interactive term in Eqn. 6.2
BD	interactive term in Eqn. 6.2
CD	interactive term in Eqn. 6.2
R^2	Coefficient of determination
<i>Superscript</i>	
a	significant difference in the means of the samples at $p \leq 0.05$ in Tables 6.4 and 6.5
b	significant difference in the means of the samples at $p \leq 0.05$ in Tables 6.4 and 6.5
c	significant difference in the means of the samples at $p \leq 0.05$ in Tables 6.4 and 6.5

References

- 6.1 Bhattacharyya, S., Mondal, A., Bhowal, A., Datta, S., “Evaporative cooling of water in a rotating packed bed (split packing)”, *Industrial Engineering Chemistry and Research*, vol. 49, pp. 847–851, 2010.
- 6.2 Munjal, S., Dudukovic, M.P., Ramachandran, P., “Mass transfer in rotating packed beds II. Experimental results and comparison with theory and gravity flow”, *Chemical Engineering and Science*, vol. 44, pp. 2257, 1989.
- 6.3 Rao, D.P., Bhowal, A., Goswami, P.S., “Process intensification in Rotating Packed Beds (HIGEE): An Appraisal”, *Industrial Engineering Chemistry and Research*, vol. 43, pp. 1150-1162, 2004.
- 6.4 Shaw, P.E., Lebrun, M., Dornier, M., Ducamp, M.N., Courel, M., and Reynes, M., “Evaluation of Concentrated Orange and Passionfruit Juices Prepared by Osmotic Evaporation,” *LWT - Food Science and Technology*, vol. 34, no. 2, pp. 60–65, 2001.
- 6.5 Cassano, A., Marchio, M., and Drioli, E., “Clarification of blood orange juice by ultrafiltration: Analyses of operating parameters, membrane fouling and juice quality,” *Desalination*, vol. 212, pp. 15–27, 2007.
- 6.6 Echavarría, A.P., Falguera, V., Torras, C., Berdún, C., Pagán, J., and Ibarz, A., “Ultrafiltration and reverse osmosis for clarification and concentration of fruit juices at pilot plant scale,” *LWT - Food Science and Technology*, vol. 46, no. 1, pp. 189–195, 2012.
- 6.7 Jesus, D.F., Leite, M.F., Silva, L.F.M., Modesta, R.D., Matta, V.M., and Cabral, L.M.C., “Orange (*Citrus sinensis*) juice concentration by reverse osmosis,” *Journal of Food Engineering*, vol. 81, no. 2, pp. 287–291, 2007.

Chapter 7

a. Concentration of Lycopene containing red fruit juices

7a.1 Introduction

In this study, the influence of process parameters such as air flow rate, water flow rate, rotor speed, and temperature on the concentration of Lycopene containing red juice (tomato and watermelon) in both RC-1 and RC-2 contactors was explored under high gravity. The optimum operating parameters (rotor rotational speed, temperature, liquid, and air flow rates) have been identified using a four-factorial Box-Behnken design by Response Surface Methodology.

7a.2 Preparation of the juice

Tomato and Watermelon were bought from a commercial supermarket and washed thoroughly to remove any kind of dirt in the outer layer. The outer peels of watermelons were cut off manually and both fruits were chopped into small pieces separately. Juice was extracted using a juice extractor. The juice was then filtered using sieves and a multilayered clean muslin cloth to ensure the absence of pulps or seeds in the juice. Finally, the obtained juice was centrifuged for 10 minutes at 9000 rpm and clarified juice is obtained which was used for experimentation. Before each experiment, fresh juice was prepared and filtered

The experimental procedure, statistical analysis of the data, and the physicochemical analysis of both the juices followed here were described elaborately in chapter 4 and chapter 6.

7a.3 Result and Discussion

The effect of four operating parameters (air flow rate, juice flow rate, rotational speed,

and temperature) on the concentration of tomato and watermelon juices in the RC-1 and RC-2 contactors was shown in figures 7a.1 to 7a.4.

7a.3.1 Effect of Rotor speed

The influences of the rotor speed on the concentration of the tomato and watermelon fruit juices are shown in Figure 7a.1. It is seen that in RC-1 the concentration increased to 8.8 °Brix for tomato juice and 16.9 °Brix for watermelon juice after two hours of operation at rotor speed of 600 rpm. The corresponding final concentrations of tomato and watermelon juice were 14.2 °Brix and 24.5 °Brix at 1000 rpm. The final concentration of tomato juice obtained in RC-2 at 600 rpm and 1000 rpm were 7.9 °Brix and 10.9 °Brix respectively. The concentration of watermelon juice obtained in RC-2 at 600 rpm and 1000 rpm were 15.4 °Brix and 19.8 °Brix respectively.

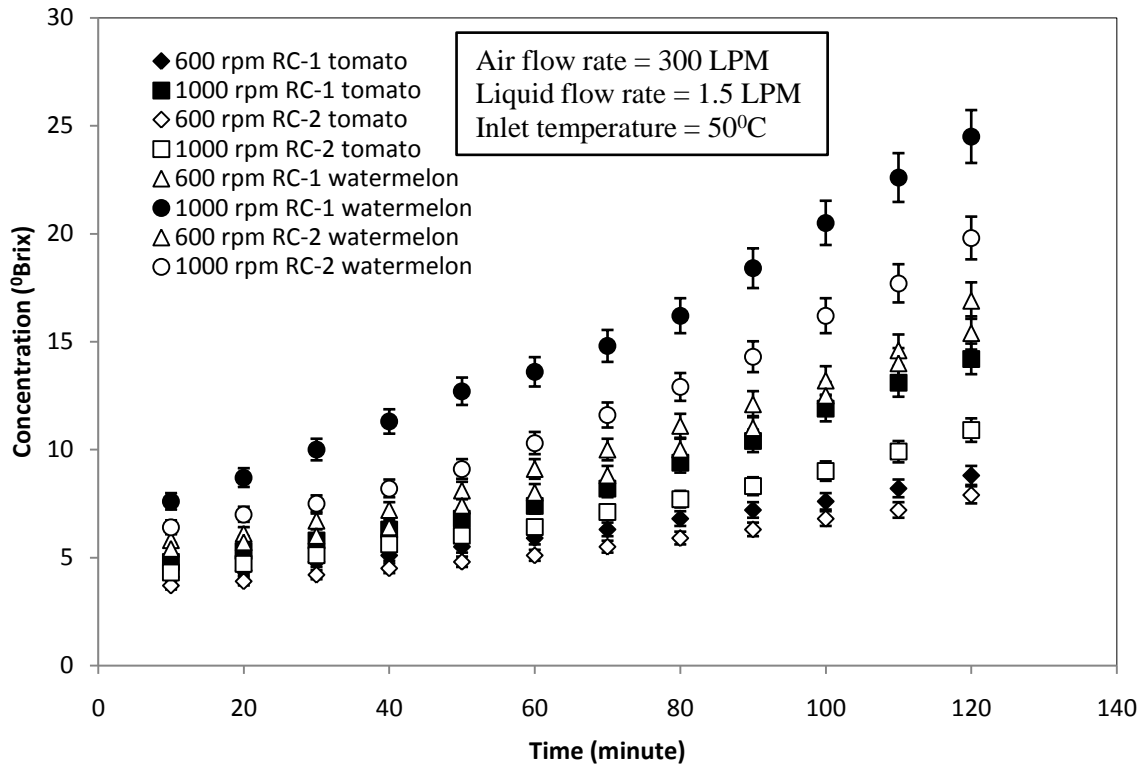


Fig 7a.1: Influence of rotational speed on red fruit juice concentration in RC-1 and RC-2

7a.3.2 Effect of Air flow rate

Figure 7a.2 shows the effect of air flow rate on the concentration of tomato and watermelon juice at air flowrates of 400 L/min and 300 L/min respectively. In RC-1, the final concentrations of tomato juice at air flow rate of 300 L/min and 400 L/min were 11.3 °Brix and 15.2 °Brix respectively after two hours of operation. Whereas the final concentration of watermelon juice at these airflow rates were 20 °Brix and 26.8 °Brix respectively after two hours of operation. These values are higher than that obtained in RC-2 after the same duration of experimental time (9.1 °Brix and 12.2 °Brix at air flow rate 300 L/min and 400 L/min for tomato juice and 17.4 °Brix and 18.9 °Brix at air flow rate 300 L/min and 400 L/min for watermelon juice respectively).

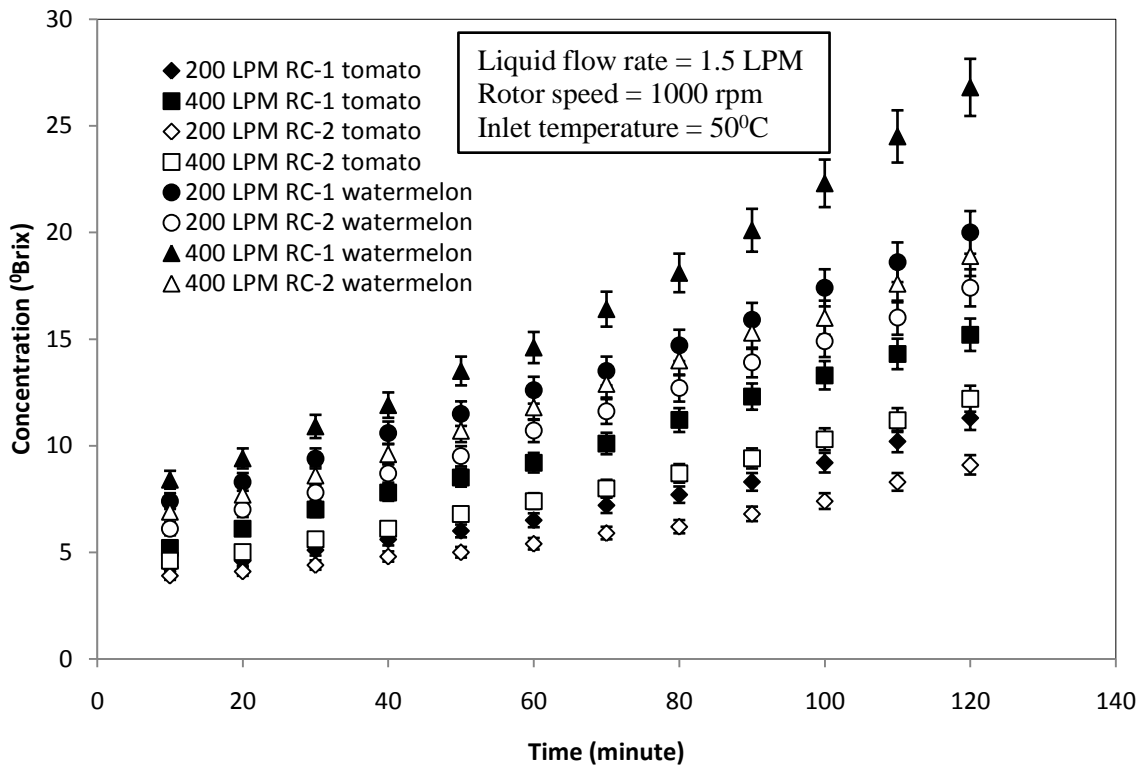


Fig 7a.2: Influence of air flow rate on red fruit juice concentration in RC-1 and RC-2

7a.3.3 Effect of Juice flow rate

Figure 7a.3 shows the effect of liquid flow rate on the concentration of fruit juice at liquid flow rates of 0.5 L/min and 1.5 L/min respectively. In RC-1, the final concentration of tomato juice at liquid flow rates of 0.5 L/min and 1.5 L/min were 9.5 °Brix and 14.2 °Brix respectively from the initial concentration of 4.2 °Brix. In the same baffled bed contactor, the final concentration of watermelon juice at liquid flow rates of 0.5 L/min and 1.5 L/min were 19.8 °Brix and 24.5 °Brix respectively from an initial concentration of 5.9 °Brix. The concentrations obtained in RC-2 after the same duration of experiment were 7.5 °Brix and 10.9 °Brix at tomato juice flow rate of 0.5 L/min and 1.5 L/min and 15.9 °Brix and 18.9 °Brix at watermelon juice flow rate 0.5 L/min and 1.5 L/min respectively.

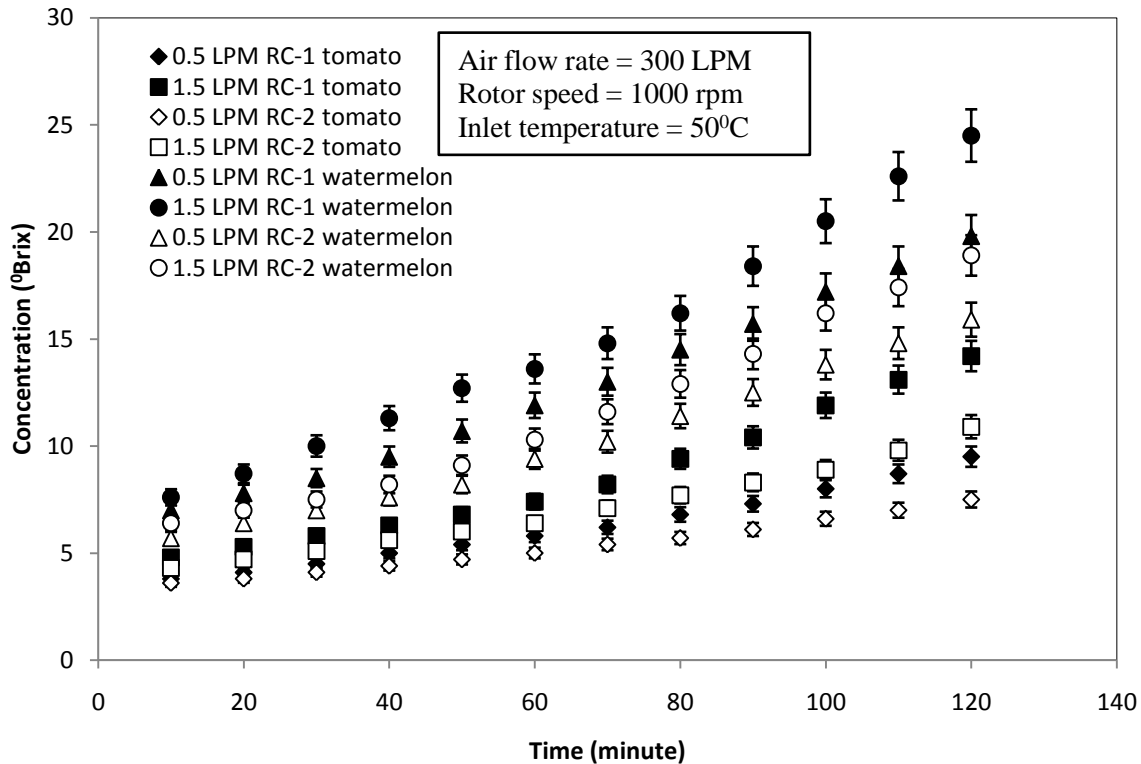


Fig 7a.3: Influence of juice flow rate on red fruit juice concentration in RC-1 and RC-2

7a.3.4 Effect of Temperature

The influence of temperature on the concentration of the tomato and watermelon juice was studied in both RC-1 and RC-2 respectively (Figure 7a.4). The concentration increased from 11 °Brix to 15.7 °Brix in RC-1 for tomato juice and from 19.9 °Brix to 27.5 °Brix in watermelon juice with an increase in the temperature from 45 °C to 60 °C due to the increase in vapor pressure of water and reduced viscosity. The corresponding concentrations observed in RC-2 were 9.4 °Brix and 12.2 °Brix for tomato juice and 17.4 °Brix and 21.9 °Brix for watermelon juice respectively which were significantly lower than that obtained in RC-1.

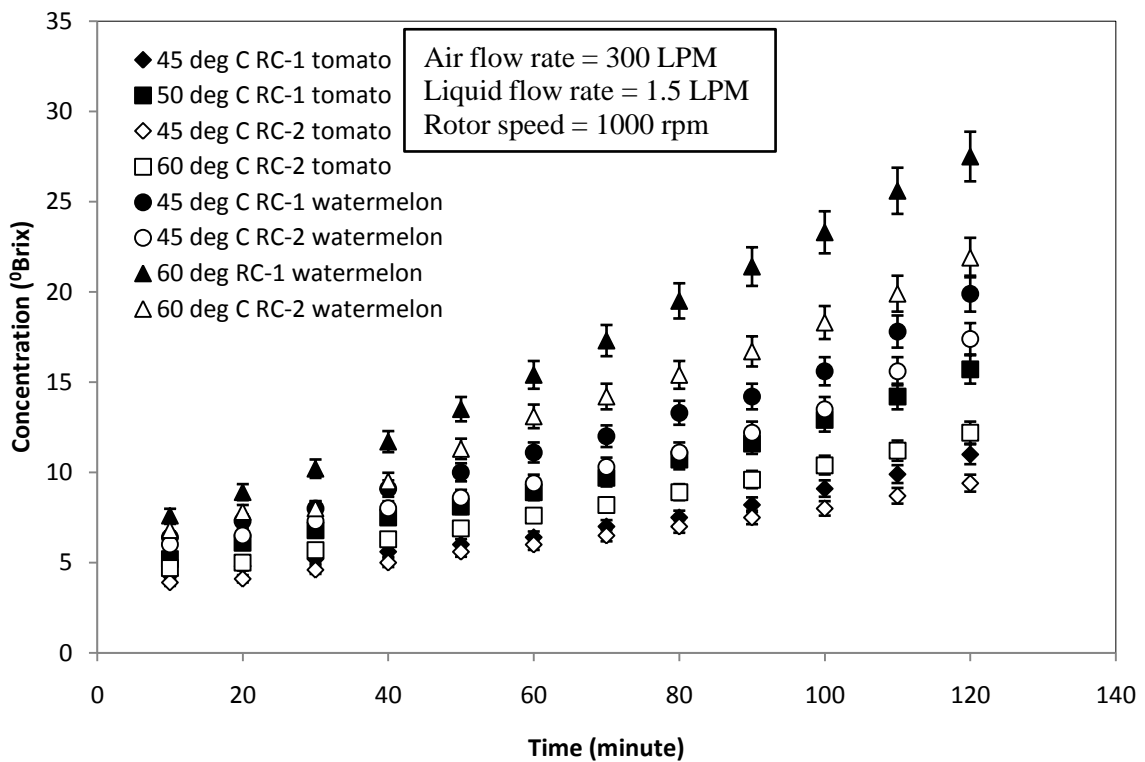


Fig 7a.4: Influence of temperature on red fruit juice concentration in RC-1 and RC-2

7a.3.5 Comparative study of red fruit juices

A comparative study was performed between the two rotating contacts RC-1 and RC-2 and a conventional wiped film evaporator at optimum operating conditions (air flow rate = 300 L/min, juice flow rate = 1.5 L/min, inlet temperature = 50°C, and rotor speed = 1000 revolutions/min) for both tomato and watermelon juices for a span of two hours. The results are shown in Figures 7a.5 and 7a.6.

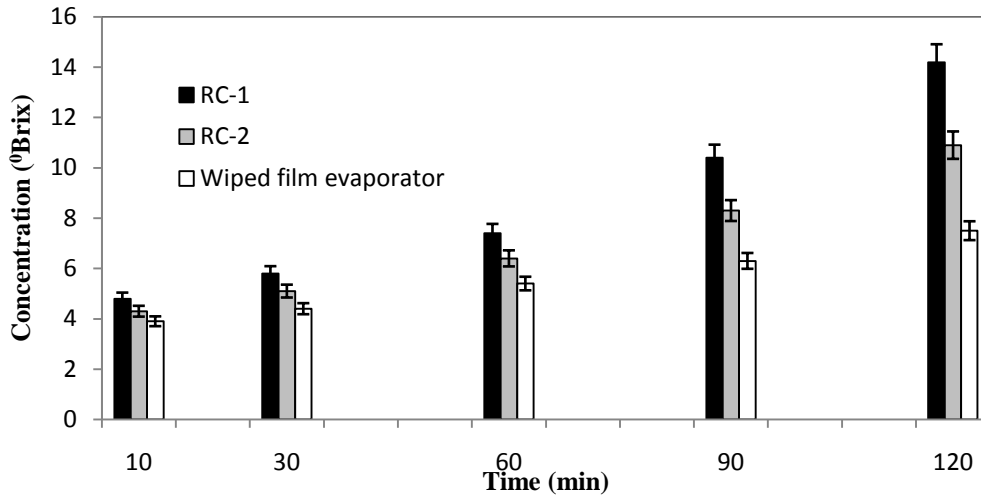


Fig. 7a.5: Comparative study of the concentration of tomato juice in three different contactors

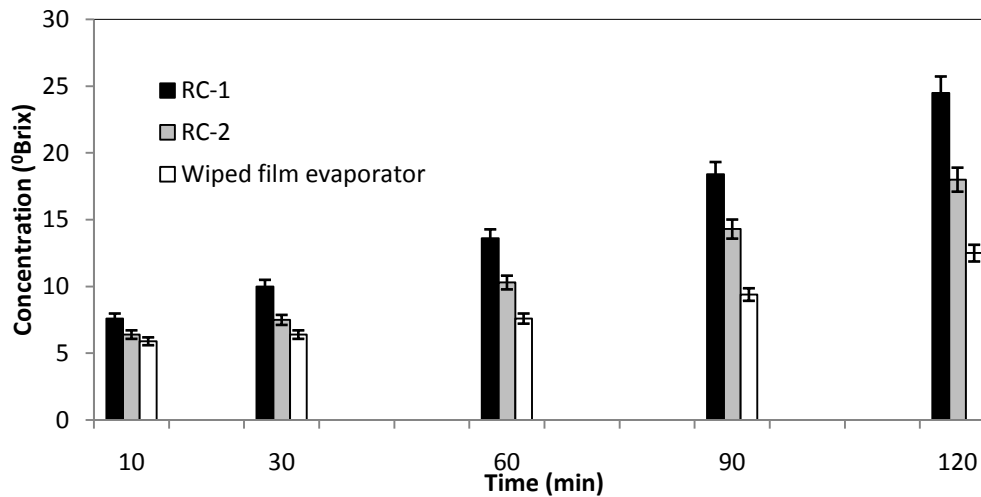


Fig. 7a.6: Comparative study of the concentration of watermelon juice in three different contactors

7a.3.6 Optimization using Response surface methodology (RSM)

The independent variables assumed in the Response surface method and the list of experimental ranges are similar to the one described in the previous chapter. Only the quadratic models developed for both tomato and watermelon juice are shown below.

7a.3.7 Model fitting and ANOVA analysis

$$\begin{aligned} C_{Tomato} = & 11.47 + 3A + 1.4541B + 0.9825C + 1.3266D - 0.13AB \\ & - 0.42AC - 0.17AD - 0.1275BC + 0.275BD + 0.005CD \quad (7a.1) \\ & - 0.10581A^2 - 0.79335B^2 - 0.063C^2 - 0.1345D^2 \end{aligned}$$

$$\begin{aligned} C_{Watermelon} = & 22.85 + 4.2758A + 1.4558B + 1.22C + 1.7866D \quad (7a.2) \\ & + 0.71AB + 0.3825AC + 0.445AD + 0.8BC + 0.7725BD \\ & + 0.0275CD - 1.4792A^2 - 1.6692B^2 - 0.1104C^2 \\ & - 0.1846D^2 \end{aligned}$$

where, C_{Tomato} and $C_{Watermelon}$ are the predicted concentration of tomato and watermelon juice ($^{\circ}$ Brix), A , B , C , and D are the coded terms for air flow rate (Litre/min), liquid flow rate (Litre/min), rotational speed (rev/min) and temperature ($^{\circ}$ C) respectively.

Tables 7a.2 and 7a.3 present the findings of the analysis of variance (ANOVA) for tomato and watermelon juices, which ensures the significance of the developed model. In both the juices the linear terms (A , B , C , and D) showed a positive and significant effect on the response C . The quadratic terms A^2 , B^2 , C^2 , and D^2 in both the juice showed an unfavorable effect on response C . The interactive terms (AB , AC , AD , and BC) are negative in tomato juice and the terms BD and CD are positive. Whereas, the interactive terms obtained were all positive in the case of watermelon juice. Positive regression

coefficients show a synergistic impact, whilst negative values show an antagonistic effect.

Table 7a.1: Statistics used in the evaluation of the goodness-of-fit of the responses to the models in red fruit juices.

RSM Statistics obtained from the models.		
	Tomato juice	Watermelon juice
Coefficient of Variation (C.V.) %	6.581575	3.992434
Determination coefficient R^2	0.9646	0.9745
Adjusted R^2	0.9234	0.9447
Predicted R^2	0.7964	0.8529
Adequate precision	17.4495	20.9334

The model obtained in tomato juice had a p -value of less than 0.0001 and an F value of 23.39, according to Table 7a.1. In watermelon juice, the F value obtained is 32.72 with a p -value of less than 0.0001. The R^2 values obtained in tomato and watermelon juices are 0.9646 and 0.9745 respectively which is a good agreement between the predicted and actual values. The significant model terms in tomato juice were A, B, C, D, B^2 , C^2 , AC, AD, and BD. In watermelon juice, the significant model terms with p -value less than 0.05 are A, B, C, D, A^2 , B^2 , AB, AC, and AD. The "Predicted R-Squared" values of 0.7964 and 0.8529 and their "Adj R-Squared" values of 0.9234 and 0.9447 are reasonably in agreement. This demonstrates how well the model can predict and accounts for all of the variations in the measured response.

Figure 7a.7 and 7a.8 display the plot of tomato and watermelon juice concentrations between expected and actual values. The deviations in predicted vs actual values in both the red fruit juice obtained from Eqs. (7a.1 and 7a.2) are within $\pm 10\%$.

Table 7a.2: Analysis of variance for the response surface quadratic model (Tomato juice).

ANOVA for the response surface quadratic model (Tomato juice).						
Source	Sum of squares	df	Mean square	F Value	P value Prob> F	
Model	171.0281	14	12.2163	23.38927	< 0.0001	significant
A	108	1	108	206.7763	< 0.0001	significant
B	25.37521	1	25.37521	48.58327	< 0.0001	significant
C	11.58368	1	11.58368	22.17805	0.0005	significant
D	21.12053	1	21.12053	40.43728	< 0.0001	significant
AB	0.0676	1	0.0676	0.129427	0.07253	
AC	0.7056	1	0.7056	1.350939	0.02677	significant
AD	0.1156	1	0.1156	0.221327	0.0465	significant
BC	0.065025	1	0.065025	0.124497	0.7303	
BD	0.3025	1	0.3025	0.579165	0.04613	significant
CD	0.0001	1	0.0001	0.000191	0.9892	
A ²	0.064045	1	0.064045	0.122621	0.7323	
B ²	3.356681	1	3.356681	6.426688	0.0262	significant
C ²	0.021393	1	0.021393	0.040958	0.0084	significant
D ²	0.096601	1	0.096601	0.184952	0.6748	
Residual	6.267642	12	0.522303			
Lack of Fit	6.267642	10	0.626764			
Pure error	0	2	0			
Cor total	177.2958	26				

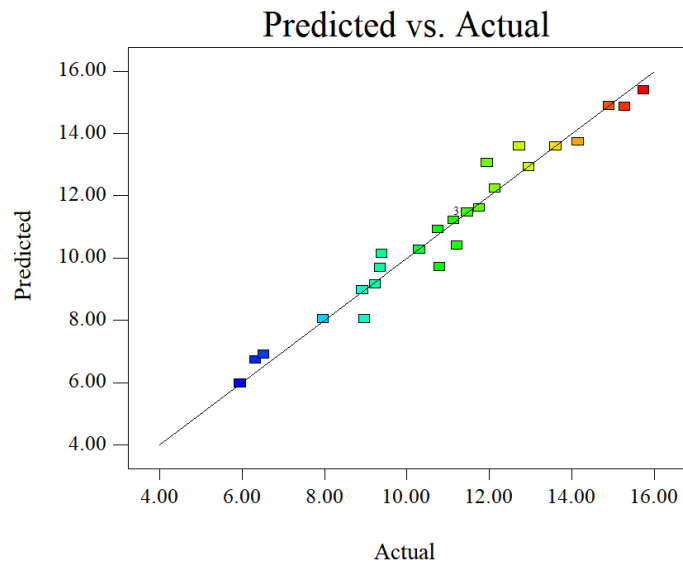


Fig. 7a.7: Predicted value vs actual value of concentration of tomato juice

Table 7a.3: Analysis of variance for the response surface quadratic model (Watermelon juice).

ANOVA for the response surface quadratic model (watermelon juice).						
Source	Sum of squares	df	Mean square	F Value	P value Prob> F	
Model	336.9634	14	24.06881	32.71605	< 0.0001	significant
A	219.393	1	219.393	298.2147	< 0.0001	significant
B	25.43341	1	25.43341	34.57091	< 0.0001	significant
C	17.8608	1	17.8608	24.27768	0.0003	significant
D	38.30613	1	38.30613	52.06844	< 0.0001	significant
AB	2.0164	1	2.0164	2.740835	0.01237	significant
AC	0.585225	1	0.585225	0.79548	0.039	significant
AD	0.7921	1	0.7921	1.076679	0.03199	significant
BC	2.6244	1	2.6244	3.567272	0.0833	
BD	2.387025	1	2.387025	3.244615	0.0968	
CD	0.003025	1	0.003025	0.004112	0.9499	
A ²	11.66898	1	11.66898	15.86131	0.0018	significant
B ²	14.85929	1	14.85929	20.19781	0.0007	significant
C ²	0.065023	1	0.065023	0.088384	0.7713	
D ²	0.181712	1	0.181712	0.246996	0.6282	
Residual	8.828258	12	0.735688			
Lack of Fit	8.828258	10	0.882826			
Pure error	0	2	0			
Cor total	177.2958	26				

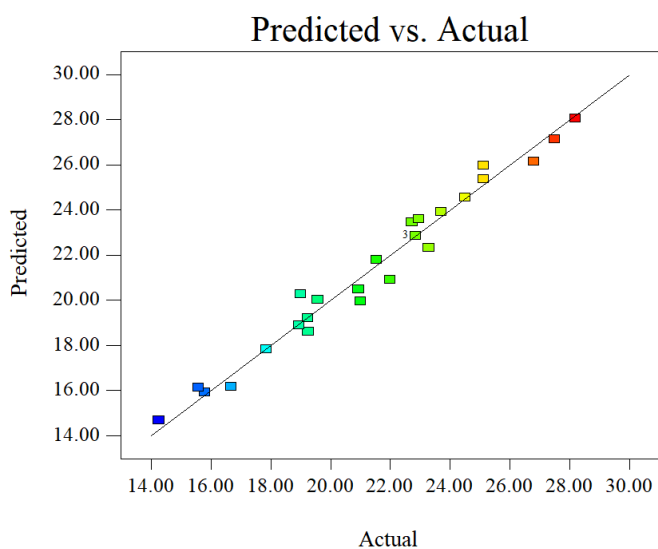


Fig 7a.8: Predicted value vs actual value of concentration of watermelon juice

7a.3.8 Interaction among variables

The interactive impact of air flow rate, liquid flow rate, rotor speed, and temperature on tomato and watermelon juice concentration is graphically depicted in three dimensions in Figures 7a.9–7a.14. Figure 7a.9 illustrates the relationship between liquid flow rate and air flow rate on juice concentration for both tomato and watermelon juices. Both the air and liquid flow rates raise the concentration value, as indicated by the positive value of the linear coefficient of both parameters in Eq. (7a.2) for watermelon juice. This is supported by the 3D response's gradual ascent along the liquid flow rate and air flow rate axes. Whereas, in the case of tomato juice the interactive effect of air and liquid flow rate lowers the concentration of juice.

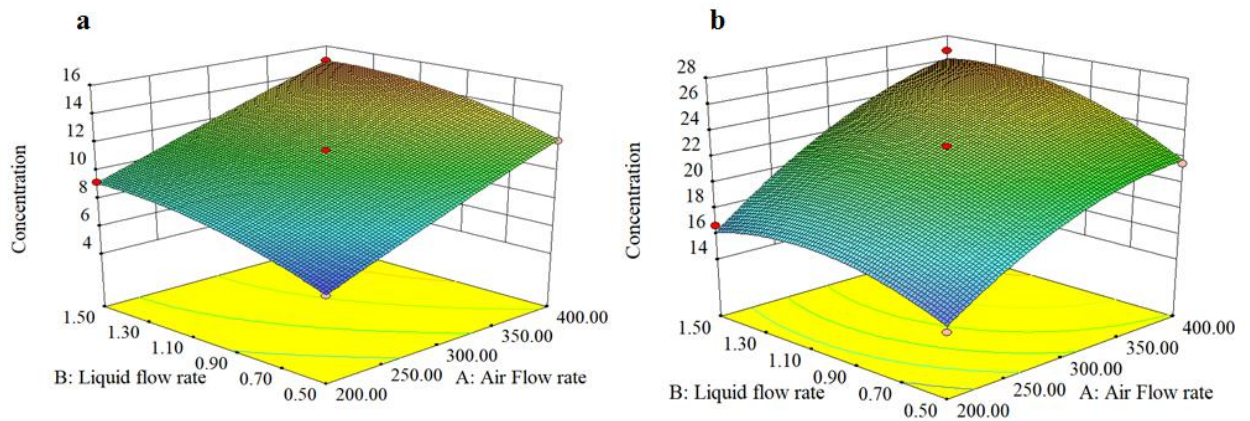


Fig. 7a.9: Interactive effect of air flow rate (Litre/min) and liquid flow rate (Litre/min) on the concentration of tomato juice (a) and watermelon juice (b).

The relationship between rotor speed and air flow rate is depicted in Fig. 7a.10. The curvatures along the corresponding axes of rotor speed and airflow rate show considerable quadratic influences on watermelon juice concentration. The positive values of the linear coefficient in Eqn. 7a.2 indicate that the concentration value in $^{\circ}\text{Brix}$ increases with rotor speed and air flow rate. But the negative value of the interactive

coefficient denotes that the concentration of tomato juice decreases with the combined effect of rotor speed and air flow rate. The correlation between air flow rate and temperature is seen in Figure 7a.11. The positive value of the linear and interaction coefficient denotes a concentration increase with temperature and air flow rate in watermelon juice. But the interactive effect of air flow rate and temperature shows a negative effect on concentration in tomato juice.

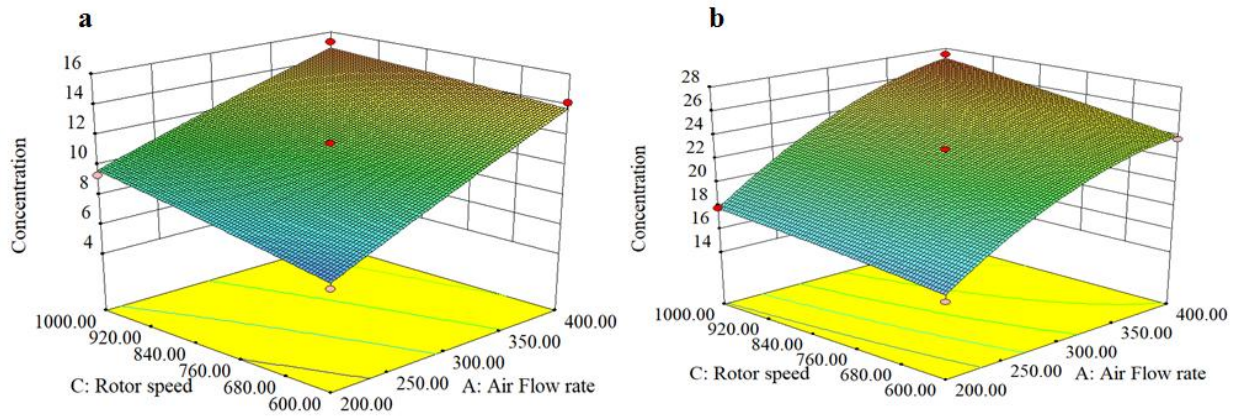


Fig. 7a.10: Interactive effect of air flow rate (Litre/min) and rotor speed (rev/min) on the concentration of tomato juice (a) and watermelon juice (b).

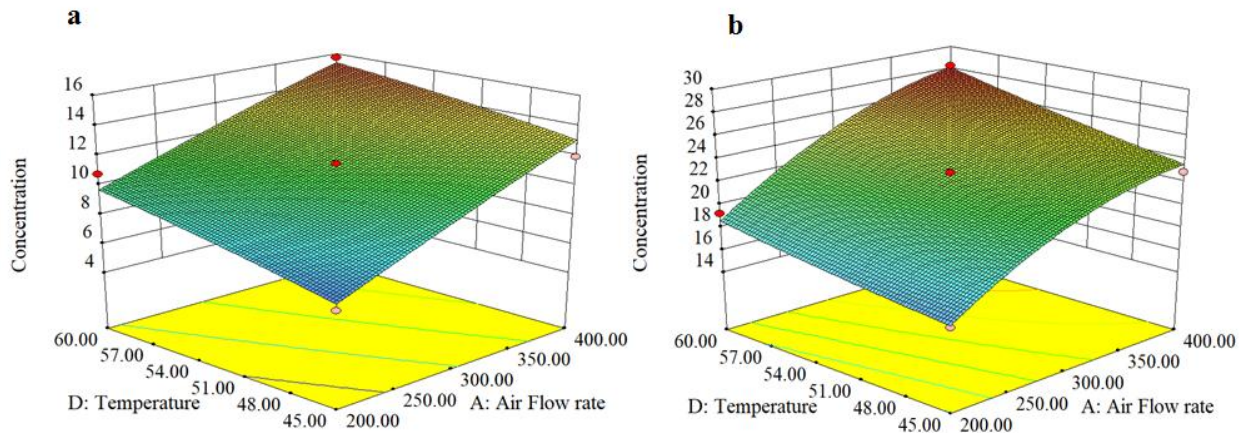


Fig. 7a.11: Interactive effect of air flow rate (Litre/min) and temperature ($^{\circ}$ C) on the concentration of tomato juice (a) and watermelon juice (b).

The interactive relationship between rotor speed and liquid flow rate was shown in Figure 7a.12. The linear coefficient's positive value indicated that concentration increases with both rotor speed and liquid flow rate. However, the interaction's negative value in tomato juice indicates that there is a decline in mass transfer rates, which results in a reduction in juice concentration. However, in watermelon juice, both linear and interaction coefficients showed positive values.

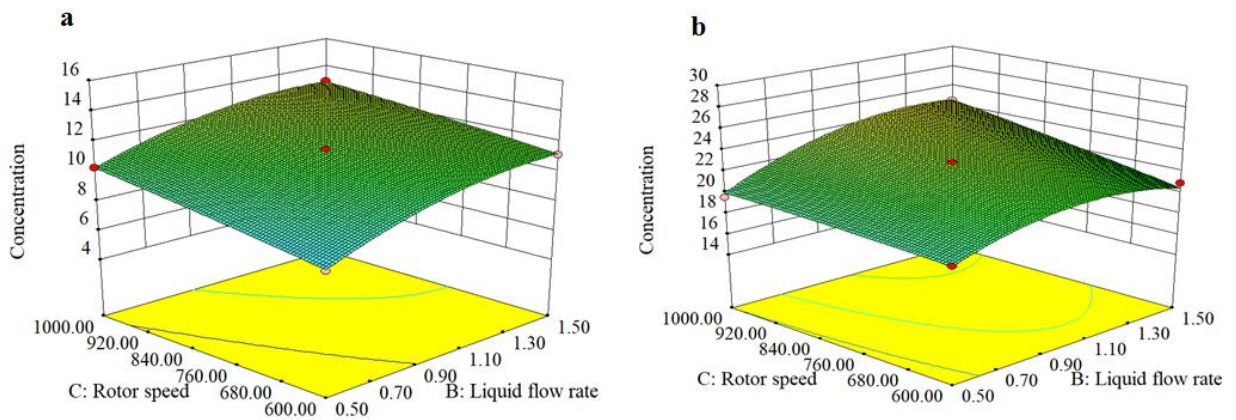


Fig. 7a.12: Interactive effect of rotor speed (rev/min) and liquid flow rate (Litre/min) on the concentration of tomato juice (a) and watermelon juice (b).

The interactive relationship between rotor speed and liquid flow rate with temperature for both tomato and watermelon juices were shown in Figures 7a.13 and 7a.14 respectively. A similar trend was observed in both juices. The positive value of both linear and interaction coefficients indicated that the concentration increases with both rotor speed and temperature and also with liquid flow rate and temperature respectively.

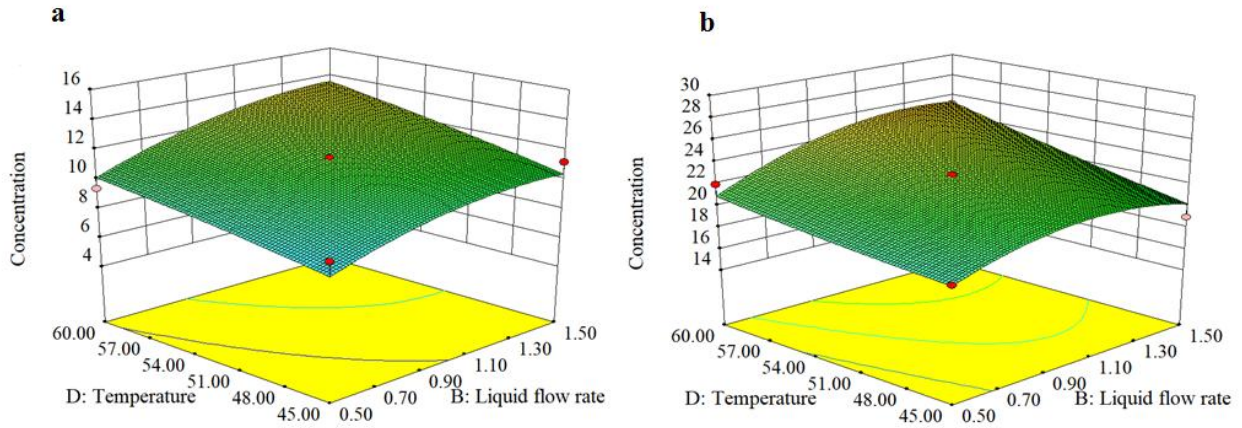


Fig. 7a.13: Interactive effect of temperature ($^{\circ}\text{C}$) and liquid flow rate (Litre/min) on the concentration of tomato juice (a) and watermelon juice (b).

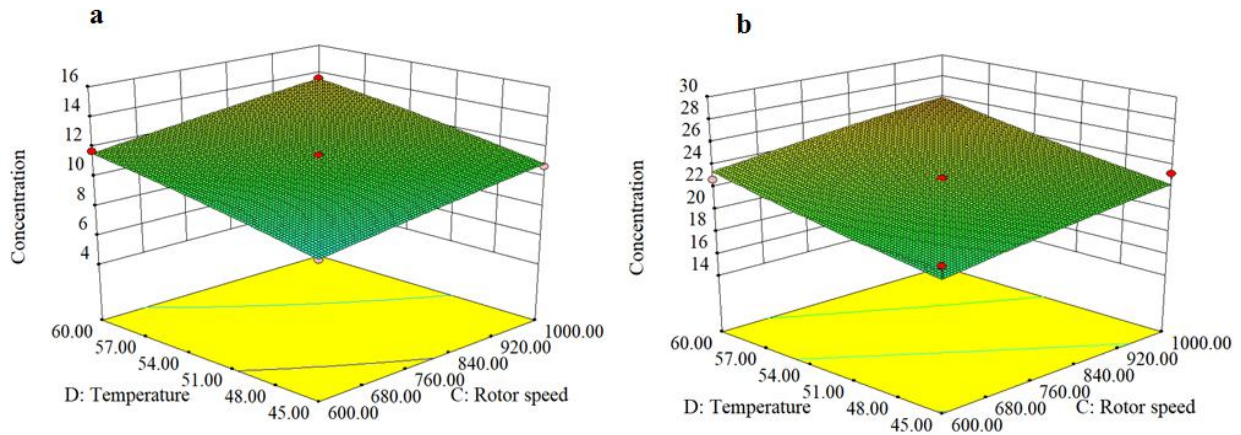


Fig. 7a.14: Interactive effect of rotor speed (rev/min) and temperature ($^{\circ}\text{C}$) on the concentration of tomato juice (a) and watermelon juice (b).

7a.3.9 Physicochemical analysis results

There is no significant change in the pH value of the feed and final concentrates in both tomato and watermelon juice. The total acid content increased from 0.93 to 1.63 gm/100 ml in concentrated tomato juice. The increase in total acid is 0.30 to 0.32 gm/100 ml in concentrated watermelon juice which is negligible. The initial soluble solid content was 4.24 $^{\circ}\text{Brix}$ and 5.9 $^{\circ}\text{Brix}$ for both the red juices which after the experimentation of 2 hours in RC-1 became 14.4 $^{\circ}\text{Brix}$ and 24.8 $^{\circ}\text{Brix}$. The ascorbic acid content increases two times

in tomato concentrates (changed from 15.5 to 34.9 mg Ascorbic acid/100 ml), whereas no significant change was observed in watermelon juice. The difference observed in the color content in both red juices is also insignificant. The total phenol content was increased from 157.2 to 198.9 mg GAE/Litre in tomato concentrate and from 585.2 to 787.2 mg GAE/Litre in watermelon concentrate. The flavonoid content increased from 37.24-47.8 mg Catechin equivalent (CE)/Litre in tomato concentrate and 28.9-31.3 mg CE/Litre in watermelon concentrate. The antioxidant capacity was measured using three different assays are shown in Table 7a.4.

7a.4 Conclusion

Concentration of tomato and watermelon juices by stripping with an unsaturated gaseous stream was studied in a rotating baffled rotating contactor and rotating packed bed contactor in this chapter. The maximum concentration of tomato and watermelon juices attained in the rotating contactor RC-1 within two hours with continuous recirculation of the solution were 15.7 °Brix and 27.5 °Brix from the initial 4.2 °Brix and 5.9 °Brix respectively. The values for concentration in both juices achieved in RC-2 (10.9 °Brix and 15.9 °Brix) are significantly low than RC-1. Experimental results obtained with tomato and watermelon juice juices suggested that the proposed strategy using high-gravity contactors can be further explored for the concentration of fruit juice.

Table 7a.4 Physiochemical test results for red feed juice and their respective concentrates

Physiochemical Analysis							
Fruits		pH	TSS (⁰ Brix)	Titrateable acidity (gm/100ml)	Total phenolics* (mg GAE/Litre)	Total flavonoids** (mg CE/Litre)	L-Ascorbic acid*** (mg/100ml)
Tomato	Fresh juice	4.25±0.02 ^a	4.24±0.09 ^b	0.929±0.004 ^b	157.16±6.20 ^b	37.24±0.796 ^b	15.52±0.221 ^a
	Clarified juice	4.17±0.03 ^b	3.94±0.11 ^b	0.917±0.003 ^c	146.12±4.33 ^c	35.52±0.57 ^c	15.276±0.161 ^a
	concentrate	4.02±0.023 ^c	14.36±0.31 ^a	1.633±0.005 ^a	198.90±4.80 ^a	42.77±1.002 ^a	34.908±0.119 ^b
Watermelon	Fresh juice	7.92±0.04 ^a	5.84±0.46 ^b	0.302±0.003 ^b	585.248±8.14 ^b	28.99±0.865 ^b	8.29±0.153 ^a
	Clarified juice	7.82±0.03 ^b	5.36±0.11 ^b	0.296±0.002 ^c	547.22±13.64 ^c	25.56±0.496 ^c	7.998±0.141 ^b
	concentrate	7.3±0.02 ^c	24.82±0.3 ^a	0.319±0.003 ^a	797.18±12.84 ^a	31.29±0.746 ^a	7.776±0.195 ^b

Antioxidant capacity								
Fruits		Lycopene Content (mg/kg fw)	TEAC**** (mmol TE/l)	FRAP***** (mmol TE/l)	DPPH***** (%Inhibition) After 30 minutes	L	Color content	
							a*	b*
Tomato	Fresh juice	39.296±0.72 ^a	14.32±0.31 ^b	5.828±0.071 ^b	53.516±0.22 ^b	33.45±0.14 ^b	24.83±0.08 ^b	16.64±0.15 ^b
	Clarified juice	37.304±0.56 ^b	13.48±0.34 ^b	5.22±0.082 ^c	53.12±0.08 ^c	33.12±0.08 ^c	24.32±0.13 ^c	16.22±0.08 ^c
	concentrate	36.91±0.186 ^b	28.77±0.82 ^a	7.704±0.131 ^a	54.91±0.119 ^a	34.83±0.11 ^a	25.26±0.05 ^a	16.95±0.093 ^a
Watermelon	Fresh juice	81.36±1.116 ^a	16.06±0.19 ^b	5.616±0.213 ^b	39.49±0.37 ^b	37.11±0.14 ^b	21.35±0.12 ^b	7.67±0.05 ^b
	Clarified juice	78.54±0.48 ^b	14.99±0.22 ^c	5.12±0.081 ^c	38.94±0.144 ^c	36.76±0.15 ^c	21.08±0.05 ^c	7.33±0.09 ^c
	concentrate	77.40±0.275 ^b	23.55±0.85 ^a	8.74±0.139 ^a	40.78±0.195 ^a	37.72±0.21 ^a	22.26±0.07 ^a	7.88±0.08 ^a

The results are provided in arithmetic means ± standard deviations form calculated for five replicates. Different letters (a, b, c) indicate significant difference between different samples (p≤0.05) determined by Tukey HSD test.

*Total Phenolics content was measured using Folin –Ciocalteu assay [Singleton, 1999] and the values are expressed in mg Gallic acid equivalents (GAE)/litre of juice/concentrate.

**Total Flavonoids content was estimated using the method of Jia et al, 1999 and the values are expressed in mg Catechin equivalents (CE)/litre of juice/concentrate.

***L- Ascorbic acid content was measured using Dichlorophenol-Indophenol (DCPIP) titrimetric method and the values are expressed as mg Ascorbic acid/100 ml juice/concentrate

Lycopene content was determined using the Calorimetric method by Fish et al, 2002 and the values are expressed as mg/ kg fw.

****TEAC assay values are determined using the method by Re, 1999 and the values are expressed in mmol of trolox equivalents (TE)/litre of juice/concentrate.

*****FRAP assay values are determined by the method of Benzie and Strain, 1996 and the values are expressed in mmol of trolox equivalents (TE)/litre of juice/concentrate.

*****DPPH assay values were determined using the method by Moon and Terraio, 1998 and the values are expressed in % Inhibition after 30 minutes for both juice and concentrate

7b. Concentration of antioxidant-rich fruit juices

7b.1 Introduction

In this work, the effects of processing parameters on the concentration of black grapes and pomegranate juice in both RC-1 and RC-2 contactors at high gravity were investigated. The response surface Method was used to study the optimum parameters and ANOVA studies were done to study the statistical significance.

7b.2 Preparation of the juice

Black grapes and pomegranates were purchased from a commercial supermarket and thoroughly cleansed to get rid of any form of dirt on the exterior layer. Manually cutting off the pomegranate's outer skins allowed the arils to be separated from the peels. On the other hand, green grapes were cleaned and separated from their pedicel. For each of the two fruits, juice was extracted using a juice extractor. To guarantee that there were no pulps or seeds in the juice, the juice was subsequently filtered using sieves and multiple layers of clean muslin fabric. The acquired juice was then clarified by centrifuging it for 10 minutes at 9000 rpm, producing the juice that was used in the experiment. The juice was made fresh and filtered before each trial.

The experimental procedure, statistical analysis of the data, and the physicochemical analysis of both juices were elaborately described in chapters 4 and 6.

7b.3 Result and Discussion

The effect of four operating parameters (air flow rate, juice flow rate, rotational speed and temperature) on the concentration of Black grapes and pomegranate juices in the RC-1 and RC-2 contactors was studied and shown in figures 7b.1 to 7b.4.

7b.3.1 Effect of rotor speed

The effect of the rotor speed on the concentration of the black grapes and pomegranate fruit juices are shown in Figure 7b.1a and 7b.1b respectively for two different rotors RC-1 and RC-2. It is seen in figure 7b.1a, at rotor speed of 600 rpm, the concentration increased from 15.3 °Brix to 29.3 °Brix for black grapes juice and from 16.2 °Brix to 38.8 °Brix for pomegranate juice in RC-1. The corresponding final concentrations of black grapes and pomegranate juices at 1000 rpm in the same contactor were 41.8 °Brix and 53.9 °Brix.

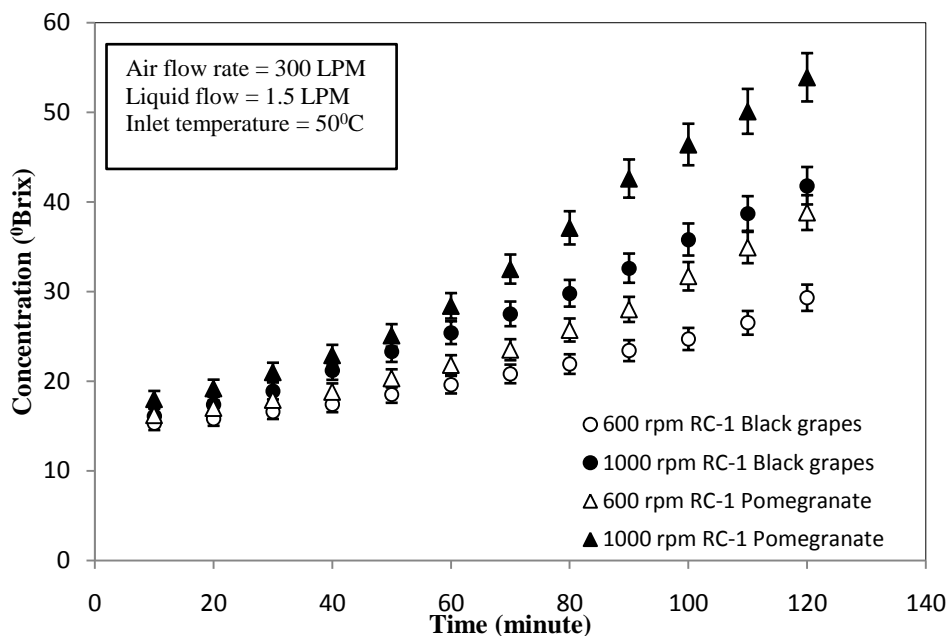


Fig 7b.1a: Influence of rotational speed on black grapes and pomegranate fruit juices concentration in RC-1

In the rotating packed bed RC-2, the concentration of black grapes juice obtained at 600 rpm and 1000 rpm were 25.9 °Brix and 34.4 °Brix respectively. The final concentration of pomegranate juice obtained in RC-2 at 600 rpm and 1000 rpm were 29.7 °Brix and 44.9 °Brix respectively (shown in figure 7b.1b).

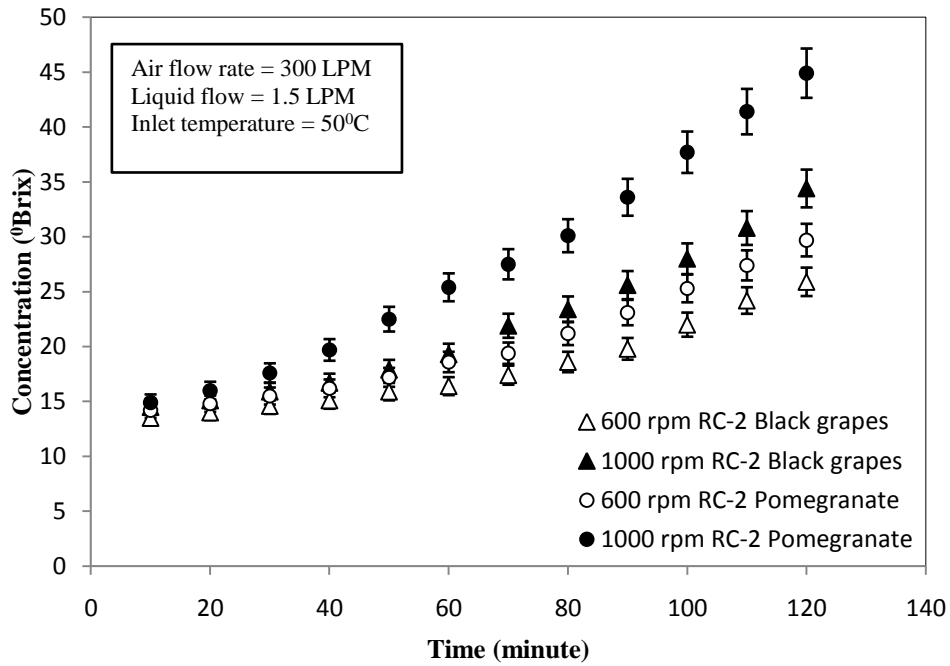


Fig 7b.1b: Influence of rotational speed on black grapes and pomegranate fruit juices concentration in RC-2

7b.3.2 Effect of air flow rate

Figure 7b.2a and 7b.2b show the influence of air flow rate on the concentration of black grapes and pomegranate juice at two different air flowrates of 400 L/min and 200 L/min respectively. In RC-1 (figure 7b.2a), the concentration achieved in black grapes juice at air flow rates of 200 L/min and 400 L/min were 30.5 °Brix and 45.8 °Brix respectively after two hours of operation. Whereas in RC-1, the concentration of pomegranate juice at air flow rates of 200 L/min and 400 L/min was 42.6 °Brix and 59 °Brix respectively. So, in both juices, there is a significant increase in the concentration with the increase in air flow rate.

The values obtained in RC-2, at air flow rates 200 L/min and 400 L/min for black grapes juice were 28.5 °Brix and 35.8 °Brix. And the increase in concentration was from 33.4 °Brix and 47 °Brix at air flow rates 200 L/min and 400 L/min for pomegranate juice.

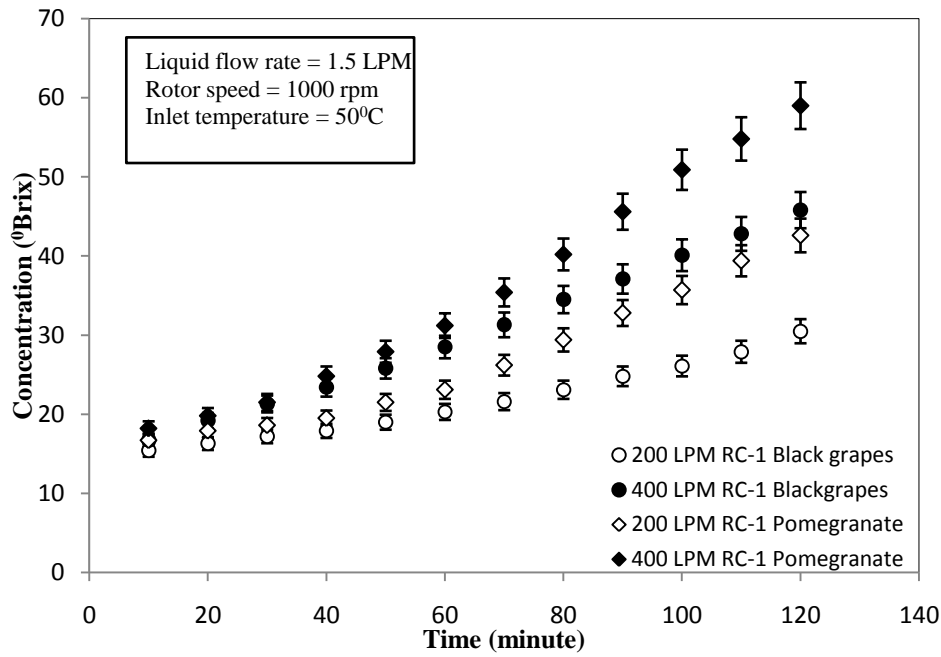


Fig 7b.2a: Influence of air flow rate on black grapes and pomegranate fruit juices concentration in RC-

1

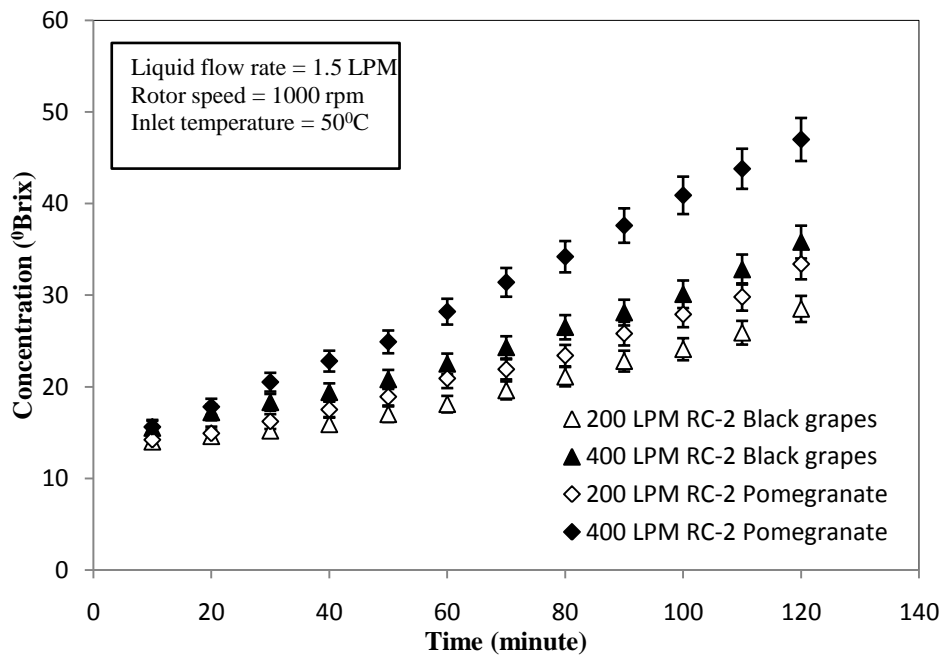


Fig 7b.2b: Influence of air flow rate on black grapes and pomegranate fruit juices concentration in RC-

2

7b.3.3 Effect of juice flow rate

Figure 7b.3a and 7b.3b show the influence of liquid flow rate on the concentration of two antioxidant-rich fruit juices at liquid flow rates of 0.5 L/min and 1.5 L/min in RC-1 and RC-2 respectively. In RC-1, the final concentration of black grapes juice increased from 27.3 °Brix to 41.8 °Brix as liquid flow rate was increased from 0.5 L/min and 1.5 L/min. A similar trend was achieved in pomegranate juice where the concentration increased from 37.8 °Brix to 53.9 °Brix at the same liquid flow rates after two hours of operation.

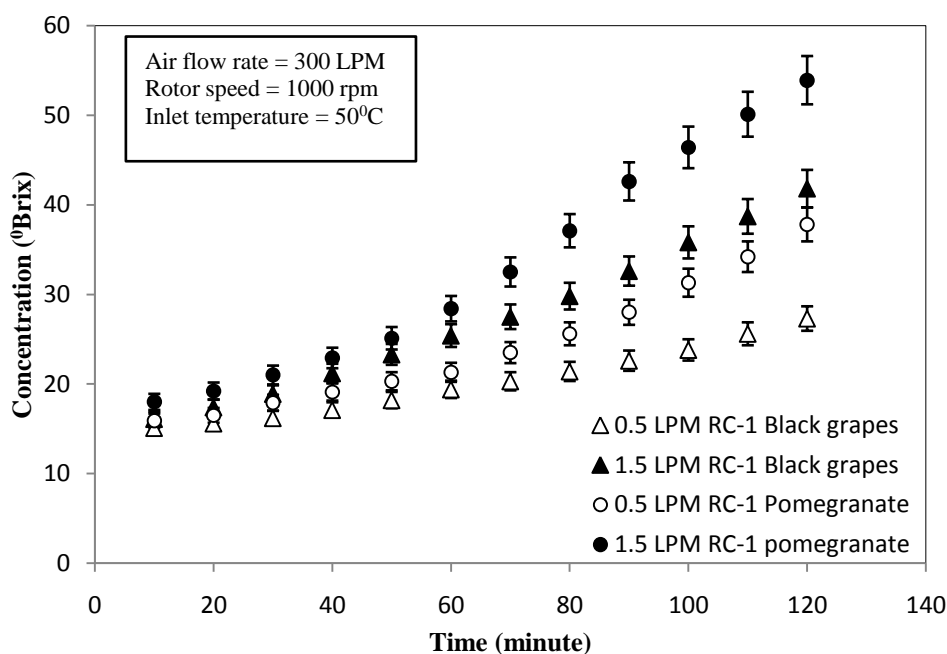


Fig 7b.3a: Influence of liquid flow rate on black grapes and pomegranate fruit juices concentration in RC-1

The values obtained in RC-1 are relatively higher than that obtained in RC-2 after the same duration of experiment (concentration increased from 25.9 °Brix to 34.4 °Brix in black grapes and from 29.8 °Brix to 44.9 °Brix in pomegranate juice as the liquid flow rate was increased from 0.5 L/min to 1.5 L/min (shown in figure 7b.3b).

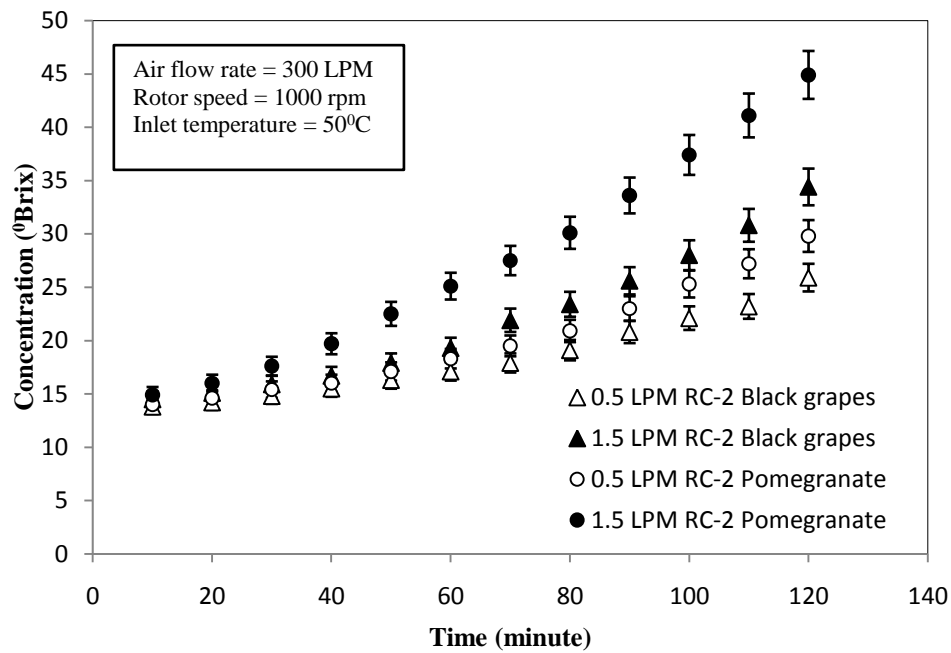


Fig 7b.3b: Influence of liquid flow rate on black grapes and pomegranate fruit juices concentration in RC-2

7b.3.4 Effect of temperature

The effect of temperature on the concentration of the black grapes and pomegranate juice was studied in both RC-1 and RC-2 respectively (Figure 7b.4a and 7b.4b). The concentration increased from 34.8 °Brix to 45.7 °Brix in RC-1 for black grapes juice and from 43.2 °Brix to 59.4 °Brix in pomegranate juice with an increase in the temperature from 45 °C to 60 °C. The corresponding concentrations observed in RC-2 were 28.9 °Brix and 36.2 °Brix for black grapes juice and 37.8 °Brix and 47.6 °Brix for pomegranate juice respectively. The results obtained in RC-1 are significantly higher than that of RC-2.

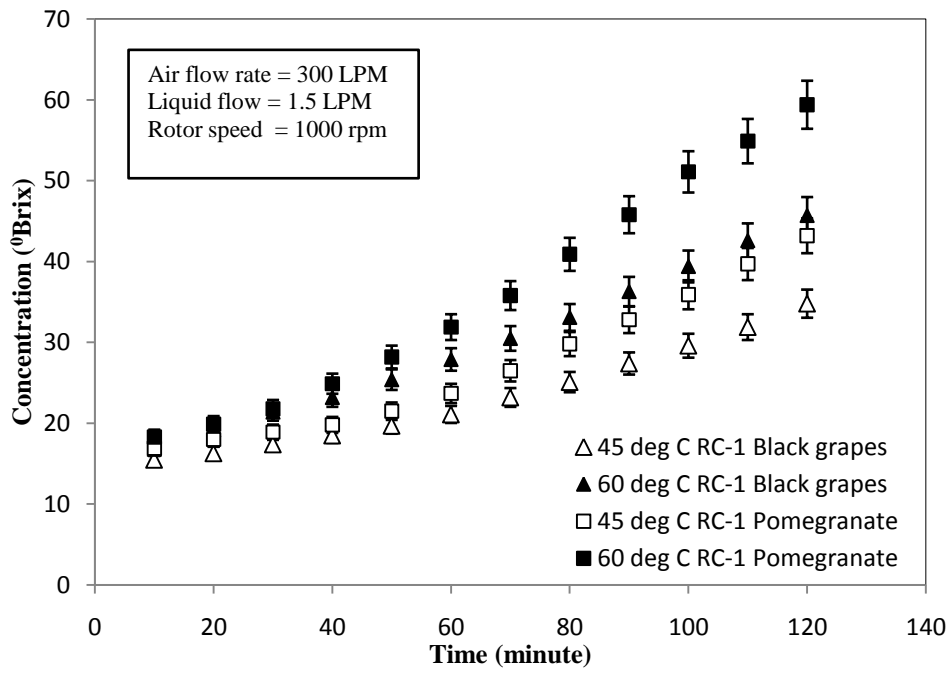


Fig 7b.4a: Influence of temperature on black grapes and pomegranate fruit juices concentration in RC-

1

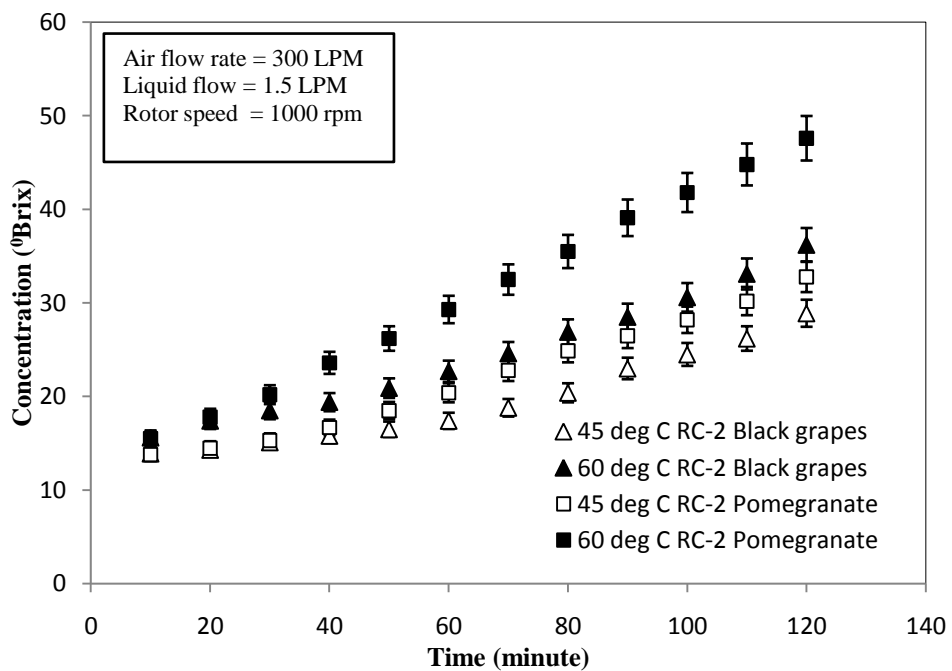


Fig 7b.4b: Influence of temperature on black grapes and pomegranate fruit juices concentration in RC-

2

7b.3.5 Comparative study of antioxidant-rich fruit juices

A comparative study for the concentration of pomegranate and black grapes juices in three different contactors was performed for a span of two hours (Figure 7b.5a and 7b.5b).

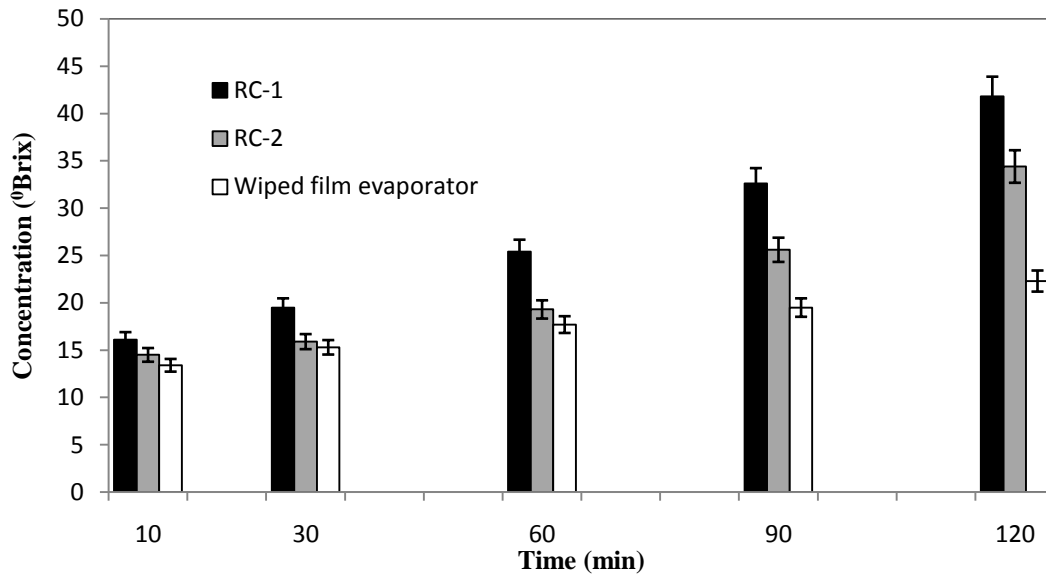


Fig. 7b.5a: Comparative study of the concentration of black grapes juice in three different contactors

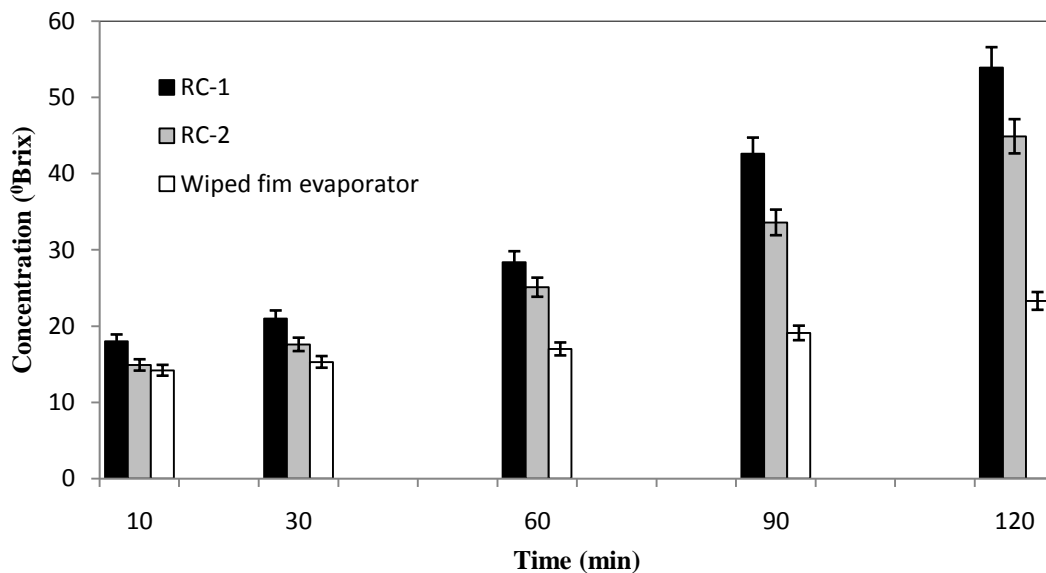


Fig. 7b.5b: Comparative study of the concentration of pomegranate juice in three different contactors

The optimum parameters were air flow rate 300 Litre/min, juice flow rate 1.5 Litre/min, rotor speed 1000 revolutions/min, and inlet temperature of 50 °C. It was observed that the concentration achieved in 2 hours is quite negligible in a conventional wiped film evaporator and maximum in RC-1. So the study shows the feasibility and effectiveness of the rotating contactor RC-1 in concentration of juice.

7b.3.6 Statistical analysis

The experimental range and the levels of independent variables used are similar to the ones used in the previous chapter (chapter 6). Box-Behnken experimental design was utilized for optimization using Response surface methodology. An elaborate explanation of the design was given in the previous chapter (chapters 4 and 6). The quadratic model obtained and the ANOVA analysis results obtained for the study are briefly provided below.

$$\begin{aligned}
 C_{Blackgrapes} = & 39.62 + 7.31A + 2.4558B + 1.68666C + 2.143D \\
 & + 0.455AB + 0.3825AC + 0.3825AD + 0.27BC \\
 & + 0.1275BD + 0.4225CD - 1.8758A^2 - 1.247B^2 \\
 & - 1.6808C^2 - 1.1046D^2
 \end{aligned} \tag{7b.1}$$

$$\begin{aligned}
 C_{Pomegranate} = & 47.5 + 8.866A + 3.71668B + 1.6916C + 3.6416D \\
 & - 0.55AB + 0.525AC + 0.475AD + 0.4BC + 0.95BD \\
 & - 0.45CD - 0.0583A^2 - 1.633B^2 - 0.5042C^2 - 0.1542D^2
 \end{aligned} \tag{7b.2}$$

where, $C_{Blackgrapes}$ and $C_{Pomegranate}$ is the predicted concentration of black grapes and pomegranate juices (⁰Brix), A , B , and C and D are the coded terms for air flow rate (Litre/min), liquid flow rate (Litre/min), and rotational speed (rev/min) and temperature (⁰C) respectively.

The results showed that the model obtained for pomegranate juice had an F value of 43.34 with p -value less than 0.0001. The F value for black grapes juice was 37.93, and the p -value was less than 0.0001. The coefficient of determination (R^2 value) in

pomegranate and black grapes juices were 0.9806 and 0.9779, respectively, showing good agreement between expected and observed values. The suitable model terms for pomegranate juice were A, B, C, D, B², C², AB, AC, and BD (with *p*-value less than 0.05). In the case of black grapes juice, the suitable model terms were A, B, C, D, AB, AC, A², B², C², and D². The "Predicted R-Squared" values for pomegranate and black grapes juices are 0.8883 and 0.8727, while their "Adj R-Squared" values are 0.9579 and 0.9521 respectively. This shows how accurately this model forecasted and explained every variance in the measured response.

Table 7b.1: Statistics used in the evaluation of the goodness-of-fit of the response to the models in antioxidant-rich fruit juices.

RSM Statistics		
	Pomegranate juice	Black grapes juice
Coefficient of Variation (C.V.) %	3.1508	3.3842
Determination coefficient R ²	0.9806	0.9779
Adjusted R ²	0.9579	0.9521
Predicted R ²	0.8883	0.8727
Adequate precision	25.2582	20.9304

Table 7b.2: Analysis of variance for the response surface quadratic model (Pomegranate juice).

ANOVA for the response surface quadratic model (Pomegranate juice).						
Source	Sum of squares	df	Mean square	F Value	P value Prob> F	
Model	1333.103	14	95.22162	43.34412	< 0.0001	significant
A	943.4133	1	943.4133	429.4342	< 0.0001	significant
B	165.7633	1	165.7633	75.45415	< 0.0001	significant
C	34.34083	1	34.34083	15.63167	0.0019	significant
D	159.1408	1	159.1408	72.43964	< 0.0001	significant
AB	1.21	1	1.21	0.550782	0.0047	significant
AC	1.1025	1	1.1025	0.501849	0.0049	significant
AD	0.9025	1	0.9025	0.410811	0.5336	
BC	0.64	1	0.64	0.291323	0.5992	
BD	3.61	1	3.61	1.643243	0.0022	significant
CD	0.81	1	0.81	0.368706	0.555	
A ²	0.018148	1	0.018148	0.008261	0.9291	
B ²	14.22815	1	14.22815	6.47654	0.0257	significant
C ²	1.355648	1	1.355648	0.61708	0.0474	significant
D ²	0.126759	1	0.126759	0.0577	0.8142	
Residual	26.3625	12	2.196875			
Lack of Fit	26.3625	10	2.63625			
Pure error	0	2	0			
Cor total	1359.465	26				

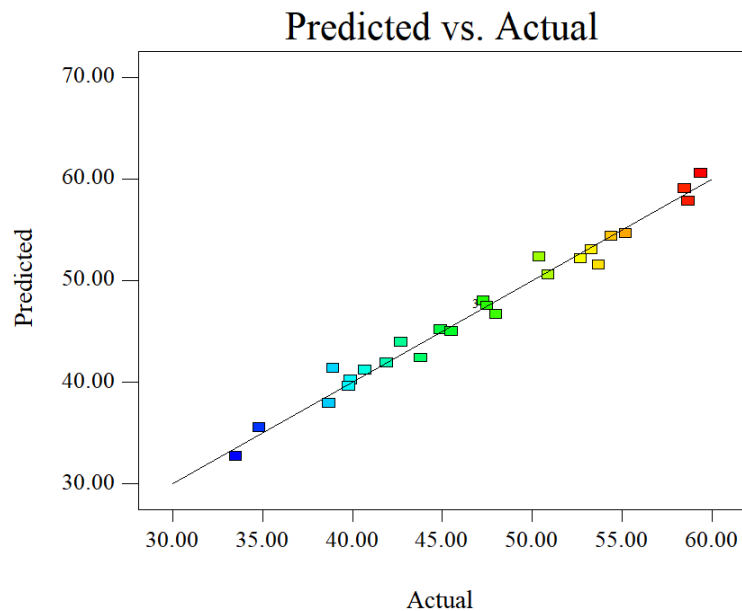


Fig 7b.6: Predicted value vs actual value of concentration of pomegranate juice

Table 7b.3: Analysis of variance for the response surface quadratic model (Black grapes juice).

ANOVA for the response surface quadratic model (Black Grapes juice).						
Source	Sum of squares	df	Mean square	F Value	P value Prob> F	
Model	832.3073	14	59.45052	37.92819	< 0.0001	significant
A	641.2332	1	641.2332	409.0934	< 0.0001	significant
B	72.37341	1	72.37341	46.17273	< 0.0001	significant
C	34.13813	1	34.13813	21.77942	0.0005	significant
D	55.08368	1	55.08368	35.14224	< 0.0001	significant
AB	0.8281	1	0.8281	0.528311	0.0481	significant
AC	0.585225	1	0.585225	0.373361	0.0426	significant
AD	0.585225	1	0.585225	0.373361	0.5526	
BC	0.2916	1	0.2916	0.186035	0.6739	
BD	0.065025	1	0.065025	0.041485	0.842	
CD	0.714025	1	0.714025	0.455533	0.5125	
A ²	18.76667	1	18.76667	11.97274	0.0047	significant
B ²	8.29449	1	8.29449	5.291712	0.0402	significant
C ²	15.06774	1	15.06774	9.612902	0.0092	significant
D ²	6.507223	1	6.507223	4.151473	0.0343	significant
Residual	18.80939	12	1.567449			
Lack of Fit	18.80939	10	1.880939			
Pure error	0	2	0			
Cor total	851.1167	26				

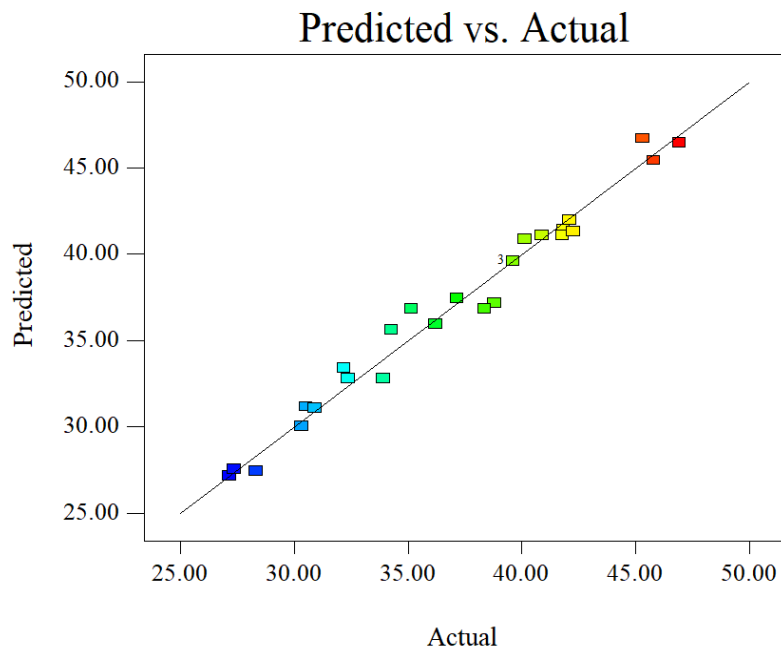


Fig 7b.7: Predicted value vs actual value of concentration of Black grapes juice

The plot of pomegranate and black grapes juice concentrations between expected and actual values are shown in Figures 7b.6 and 7b.7. Eqs. (7b.1 and 7b.2) predicted that the deviation of experimental values for both juices from the actual ones would be approximately 10%.

7b.3.7 Interactive variables

A three-dimensional graphic representation of the interactional impact of air flow rate, liquid flow rate, rotor speed, and temperature on pomegranate and black grapes juice concentration is shown in figures 7b.8–7b.13.

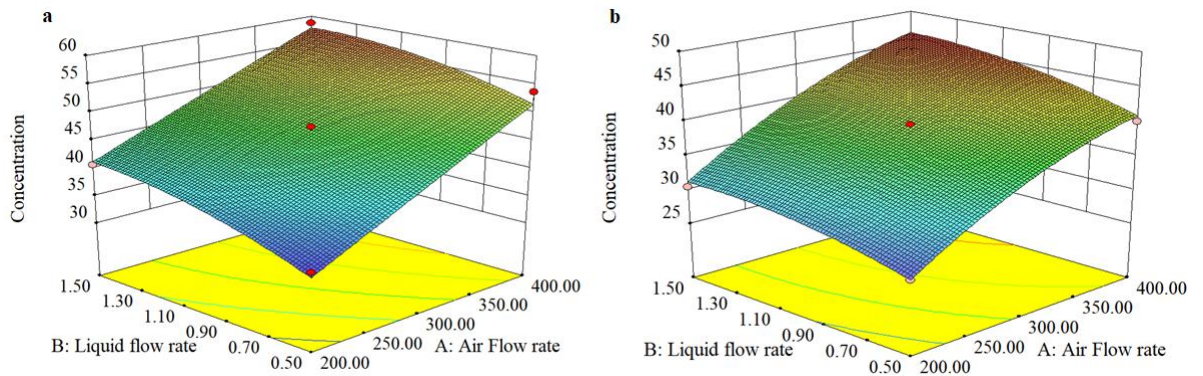


Fig. 7b.8: Interactive effect of air flow rate (Litre/min) and liquid flow rate (Litre/min) on the concentration of pomegranate juice (a) and black grapes juice (b).

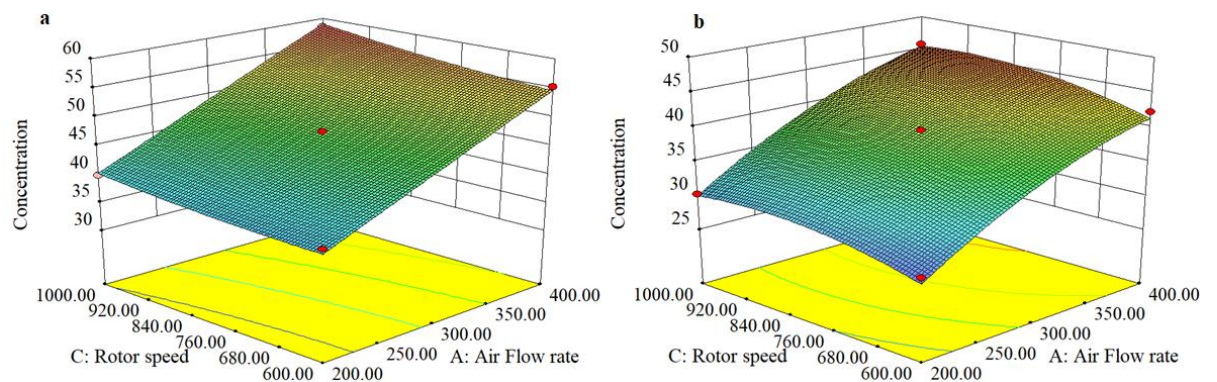


Fig. 7b.9: Interactive effect of air flow rate (Litre/min) and rotor speed (rev/min) on the concentration of pomegranate juice (a) and black grapes juice (b).

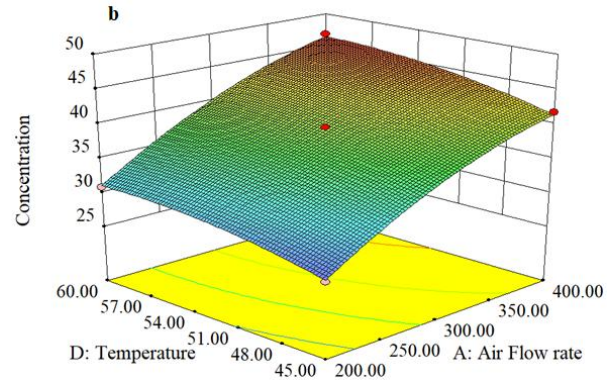
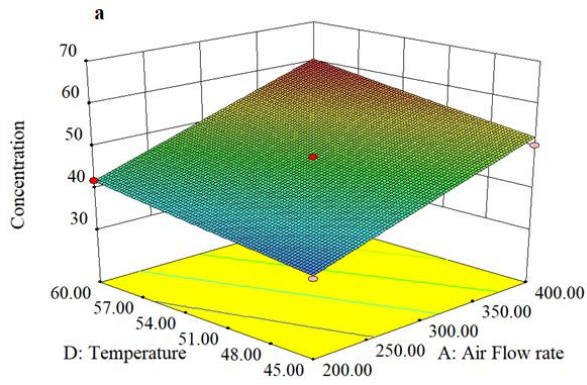


Fig. 7b.10: Interactive effect of air flow rate (Litre/min) and temperature ($^{\circ}$ C) on the concentration of pomegranate juice (a) and black grapes juice (b).

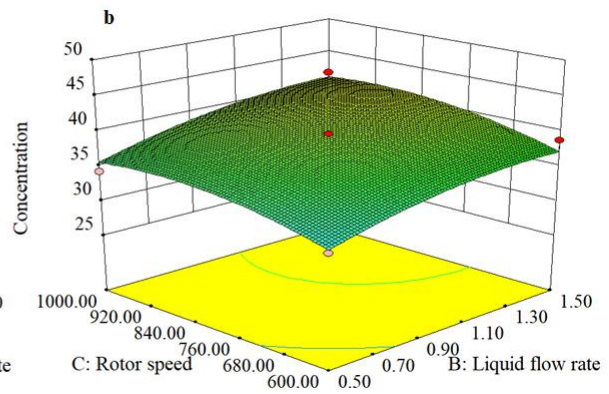
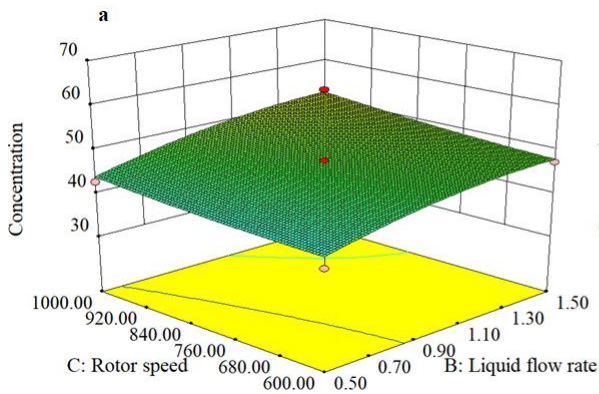


Fig. 7b.11: Interactive effect of rotor speed (rev/min) and liquid flow rate (Litre/min) on the concentration of pomegranate juice (a) and black grapes juice (b).

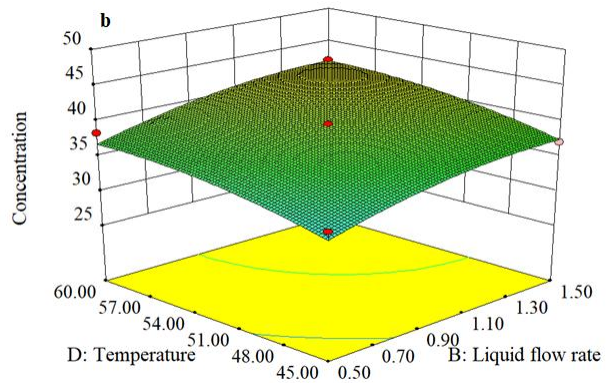
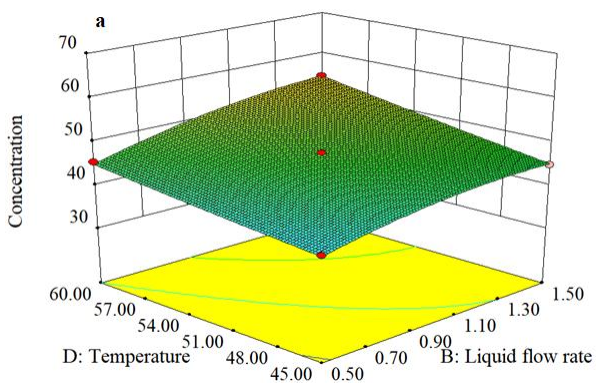


Fig. 7b.12: Interactive effect of temperature ($^{\circ}$ C) and liquid flow rate (Litre/min) on the concentration of pomegranate juice (a) and black grapes juice (b).

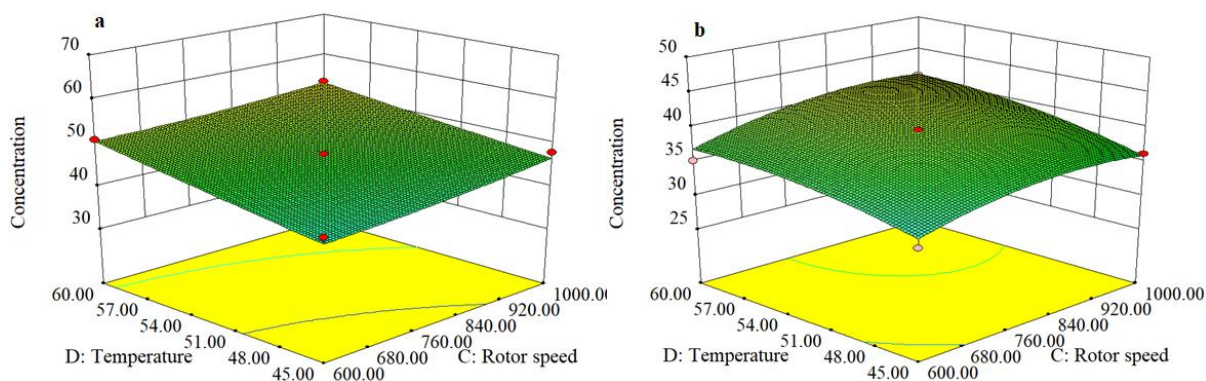


Fig. 7b.13: Interactive effect of rotor speed (rev/min) and temperature ($^{\circ}\text{C}$) on the concentration of pomegranate juice (a) and black grapes juice (b).

7b.3.8 Physicochemical analysis results

Table 7b.4 shows the physicochemical evaluation of the feed, clarified and concentrated juice of the antioxidant-rich fruits. The pH of the fresh juice, and the concentrated juice showed a very negligible difference. In fresh black grapes juice, the pH was 4.03 whereas in concentrated juice the pH was 3.81. In fresh pomegranate juice, the pH was 3.37 whereas in concentrated juice the pH was 3.24. The total acid content increased from 0.93 to 1.27 gm/100 ml in black grapes concentrated juice. In pomegranate juice, the value increased from 0.83 to 1.18 gm/100 ml in concentrated juice. The initial soluble solid content was 15.36 $^{\circ}\text{Brix}$ and 17.88 $^{\circ}\text{Brix}$ for both the antioxidant-rich juices which after concentration increased ~ 3 folds in both juices (the TSS value became 41.88 $^{\circ}\text{Brix}$ and 54.02 $^{\circ}\text{Brix}$ in black grapes and pomegranate respectively). The feed juice had 43.58 mg Ascorbic acid/100 ml and the concentrated juice had 59.22 mg Ascorbic acid/100 ml which is higher than the feed. In pomegranate, the feed juice had 19.86mg Ascorbic acid/100 ml and in the concentrated juice, the ascorbic acid content was 38.01 mg Ascorbic acid/100 ml which is twice that of the feed value. Negligible change in the color content was observed in the feed and concentrate in both fruit juices.

The total phenol content and total flavonoid content were measured in both black grapes and pomegranate juices. The concentration increased from 699.8 to 1075.3 mg GAE/Litre in the black grapes concentrate. In pomegranate juice, the increase in concentration was 999.13 - 1632.13 mg GAE/Litre. The antioxidant capacity was measured using three different assays reported in Table 7b.4. All the data shown in the table were recorded in five replicates and statistically analyzed using one-way ANOVA and further mean difference analysis was performed.

7b.4 Conclusion

In this chapter air stripping in rotating packed bed and rotating baffled bed for the concentration of pomegranate and black grapes juices.

The concentration achieved in black grapes juice was 45.8 °Brix and in pomegranate juice was 59.4 °Brix after two hours of operation in the rotating baffled contactor. The statistical analysis and ANOVA results showed the significant contribution of the operating parameters in the concentration of juice. Furthermore, the physicochemical analysis of the feed and the concentrated juice was evaluated and the highest antioxidant content was observed in pomegranate juice. Thus the feasibility of concentrating juice with this novel technique was hence proved.

Physicochemical Analysis							
Fruits		pH	TSS (⁰ Brix)	Titratable acidity (gm/100ml)	Total phenolics* (mg GAE/Litre)	Total flavonoids** (mg CE/Litre)	L-Ascorbic acid*** (mg/100ml)
Black grapes	Fresh juice	4.03±0.03 ^a	15.36±0.17 ^b	0.928±0.002 ^b	699.83±17.77 ^b	98.13±1.15 ^b	43.584±2.625 ^a
	Clarified juice	3.97±0.02 ^b	14.74±0.11 ^c	0.925±0.003 ^b	672.75±5.94 ^c	96.61±0.696 ^b	42.93±1.748 ^a
	concentrate	3.81±0.02 ^c	41.88±0.15 ^a	1.265±0.004 ^a	1075.34±14.86 ^a	108.88±6.32 ^a	59.22±0.937 ^b
Pomegranate	Fresh juice	3.37±0.02 ^a	13.88±0.33 ^b	0.833±0.003 ^b	999.13±9.34 ^b	100.01±1.12 ^b	19.86±0.265 ^a
	Clarified juice	3.31±0.01 ^b	13.08±0.18 ^c	0.822±0.003 ^c	981.5±5.21 ^b	97.02±0.488 ^b	18.57±0.284 ^b
	concentrate	3.24±0.03 ^c	45.02±0.24 ^a	1.184±0.003 ^a	1632.13±19.18 ^a	134.02±4.117 ^a	38.01±0.236 ^c
Antioxidant capacity							
Fruits		TEAC** (mmol TE/l)	FRAP*** (mmol TE/l)	DPPH**** (%Inhibition) After 30 minutes	L	Color content a* b*	
Black grapes	Fresh juice	19.58±0.59 ^b	9.23±0.063 ^b	49.98±0.521 ^b	22.05±0.203 ^b	9.74±0.13 ^b	7.94±0.06 ^b
	Clarified juice	18.13±0.29 ^c	8.97±0.056 ^b	49.046±0.416 ^c	21.84±0.11 ^b	9.37±0.08 ^b	7.74±0.09 ^c
	concentrate	33.82±0.86 ^a	12.22±0.256 ^a	52.18±0.272 ^a	23.18±0.27 ^a	9.91±0.09 ^a	8.23±0.09 ^a
Pomegranate	Fresh juice	17.89±0.68 ^b	10.06±0.43 ^b	68.85±0.895 ^b	31.84±0.24 ^b	33.99±0.07 ^b	14.15±0.068 ^b
	Clarified juice	16.84±0.28 ^c	8.77±0.394 ^c	66.94±0.099 ^b	31.07±0.10 ^c	33.73±0.05 ^c	14.01±0.03 ^c
	concentrate	36.17±0.42 ^a	19.41±0.515 ^a	69.21±0.28 ^a	32.72±0.17 ^a	34.34±0.109 ^a	14.57±0.09 ^a

Table 7b.4:Physicochemical analysis of the feed and concentrated pomegranate and black grapes juices.

7c. Concentration of sugar-containing fruit juices

7c.1 Introduction

In this study, the feasibility of the concentration of sugar-containing fruit juices (green grapes and sugarcane juice) by air stripping water into an unsaturated gaseous stream was explored in a rotating baffled and a rotating packed bed contactor operating under high gravity. The influence of process parameters on the concentration of green grapes and sugarcane juice was performed. Response Surface Methodology was used to check the statistical significance of the study. Comparative study on performance between the rotating contactors, and traditional wiped film evaporator was also done.

7c.2 Preparation of the juice

Green grapes and sugarcane were bought from a commercial supermarket and washed thoroughly to remove any kind of dirt in the outer layer. The outer peels of sugarcane were cut off manually and the agronomic crop was chopped into small pieces. Green grapes, on the other hand, were cleaned and detached from their pedicel. Juice was extracted using a juice extractor for both fruits separately. The juice was then filtered using sieves and a multilayered clean muslin cloth to ensure the absence of pulps or seeds in the juice. Finally, the obtained juice was centrifuged for 10 minutes at 9000 rpm and clarified juice is obtained which was used for experimentation. Before each experiment, fresh juice was prepared and filtered

The experimental procedure, statistical analysis, and physicochemical analysis of both juices were performed (the method is described in Chapters 4 and 6).

7c.3 Result and Discussion

The effect of four operating parameters (air flow rate, juice flow rate, rotational speed,

and temperature) on the concentration of tomato and watermelon juices in the RC-1 and RC-2 contactors was studied and shown in figures 7c.1 to 7c.4.

7c.3.1 Effect of Rotor speed

The total soluble solid content increased from 30.1 °Brix to 42.5 °Brix as the rotor speed was changed from 600 rpm to 1000 rpm in grapes juice. The corresponding values in sugarcane juice increased from 13.1 °Brix to 27.1 °Brix in RC-1. The concentration of grapes juice obtained in RC-2 at 600 rpm and 1000 rpm were 29.2 °Brix and 36.3 °Brix respectively. And the concentration of sugarcane juice obtained in RC-2 at 600 rpm and 1000 rpm were 16.3 °Brix and 21.5 °Brix respectively.

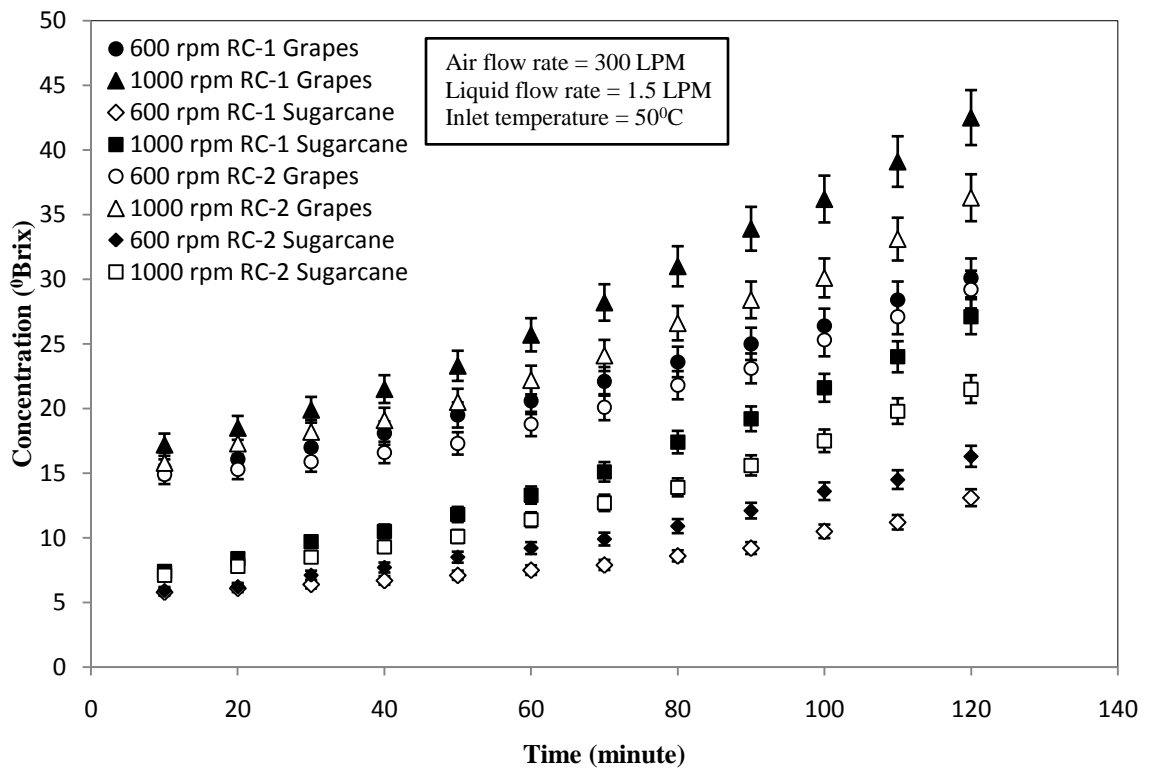


Fig 7c.1: Influence of rotational speed on sugar-containing fruit juice concentration in RC-1 and RC-2

7c.3.2 Effect of air flow rate

In RC-1, the total soluble solid content of grapes juice at air flow rates of 200 L/min and 400 L/min were 31.8 °Brix and 45.2 °Brix respectively after two hours of operation. Whereas the final concentration of sugarcane juice at the same airflow rates were 21.2 °Brix and 27.9 °Brix respectively. These values obtained in RC-1 are higher than that obtained in RC-2 (TSS content reported were 28.8 °Brix and 38.2 °Brix at air flow rates 200 L/min and 400 L/min for grapes juice and 19.2 °Brix and 23.9 °Brix for sugarcane juice respectively).

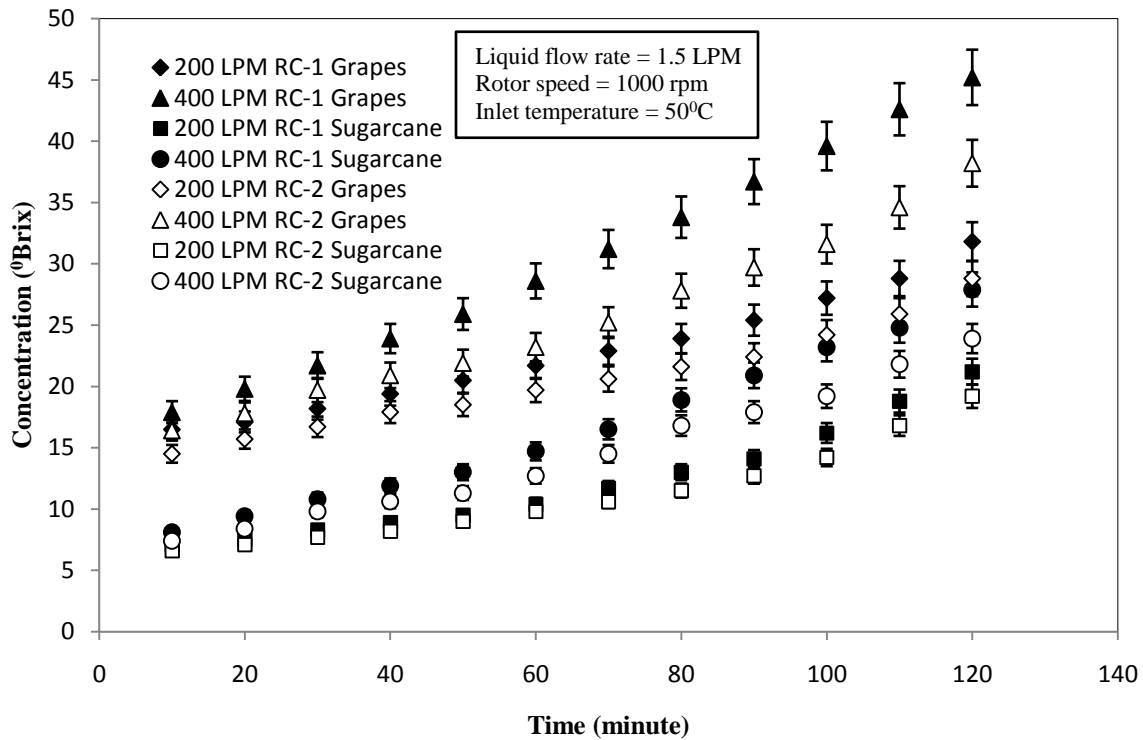


Fig 7c.2: Influence of air flow rate on sugar-containing fruit juice concentration in RC-1 and RC-

7c.3.3 Effect of juice flow rate

In RC-1, the final concentration of grapes juice at liquid flow rates of 0.5 L/min and 1.5 L/min were 28.8 °Brix and 42.7 °Brix respectively. And in RC-1, the final concentration of sugarcane juice at liquid flow rates of 0.5 L/min and 1.5 L/min were 14.9 °Brix and 27.1 °Brix respectively. A similar increasing trend of juice flow rate was also observed in RC-2 (TSS content increased from 25.4 °Brix - 36.3 °Brix in grapes juice flow rate 0.5 L/min and 1.5 L/min and 11.9 °Brix -21.5 °Brix in sugarcane juice).

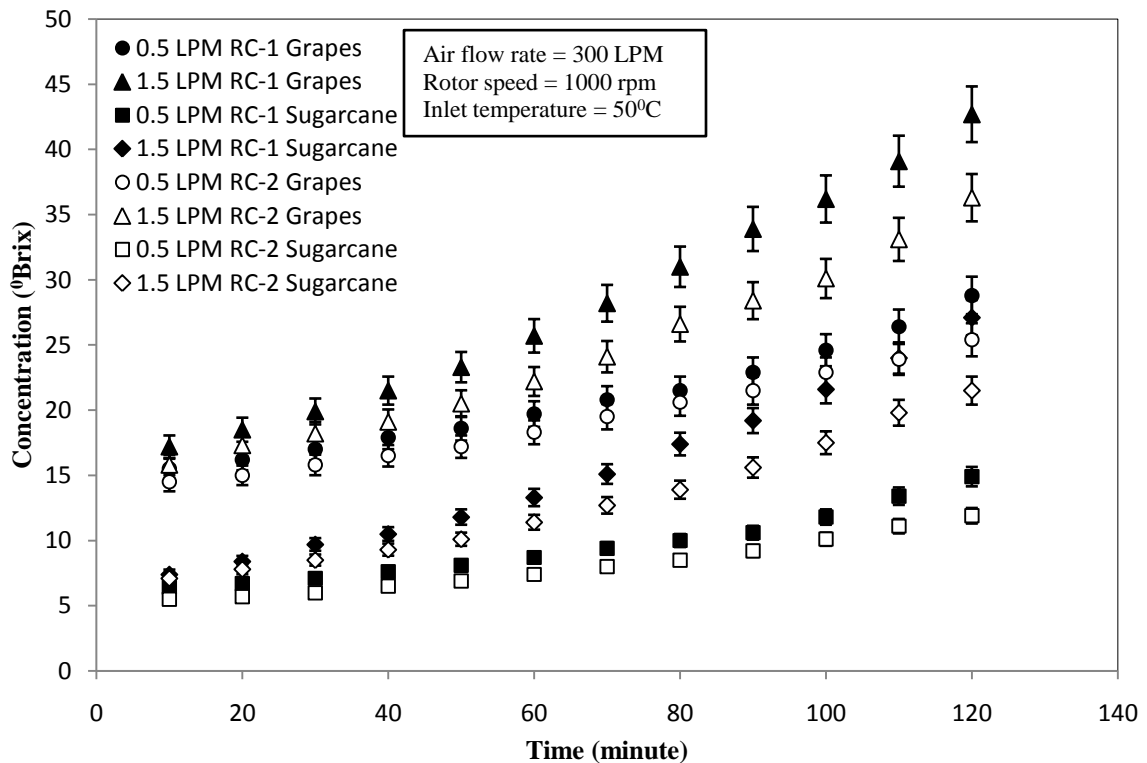


Fig 7c.3: Influence of juice flow rate on sugar-containing juice concentration in RC-1 and RC-2

7c.3.4 Effect of Temperature

The influence of temperature on the concentration of the grapes and sugarcane juice was studied in both RC-1 and RC-2 respectively (Figure 7c.4). The TSS content increased from 39.8 °Brix to 45.6 °Brix in RC-1 for grapes juice and from 21.4 °Brix to 29.3 °Brix

in sugarcane juice with an increase in the temperature from 45 °C to 60 °C. The corresponding concentrations observed in RC-2 were 32.8 °Brix and 37.7 °Brix for grapes juice and 16.9 °Brix and 24.2 °Brix for sugarcane juice respectively. The trend of the curve in both contactors was similar but values obtained in RC-1 were higher.

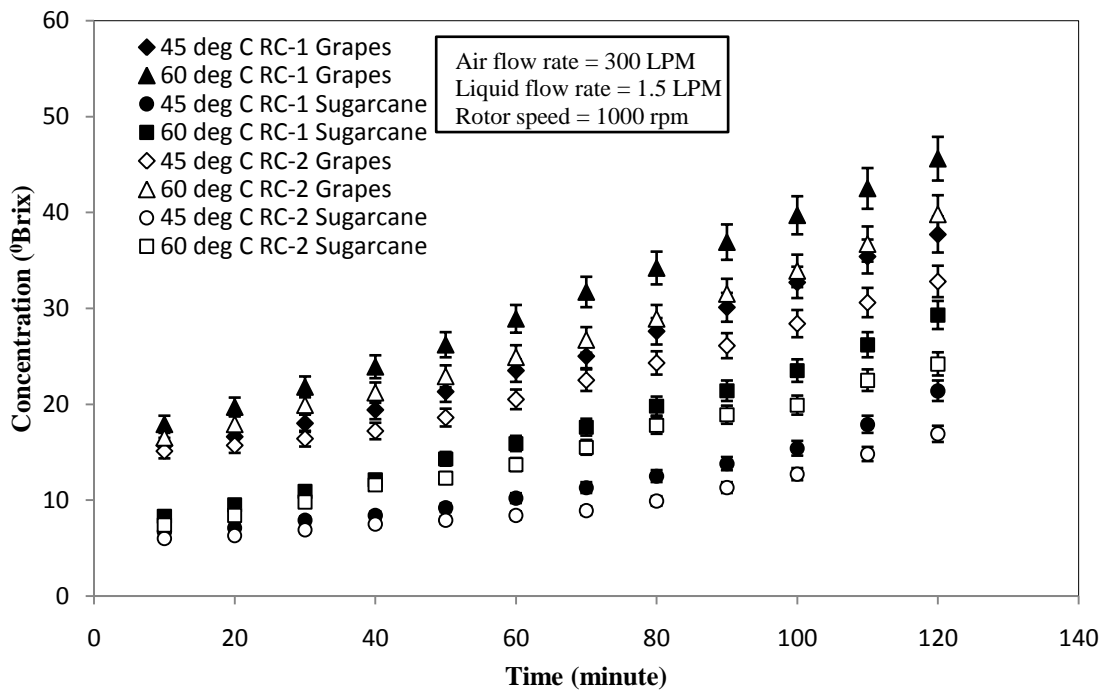


Fig 7c.4: Influence of temperature on sugar-containing juice concentration in RC-1 and RC-2

7c.3.5 Comparative study of sugar-rich fruit juices

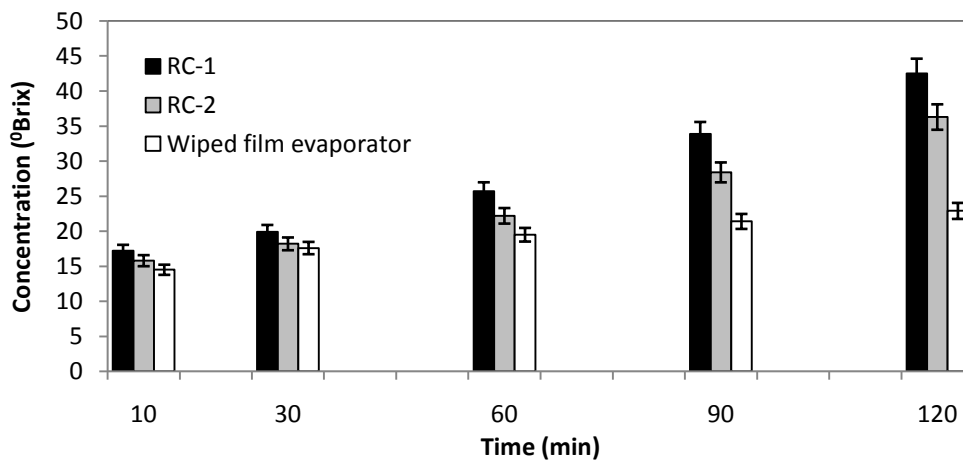


Fig. 7c.5a: Comparative study of the concentration of grapes juice in three different contactors

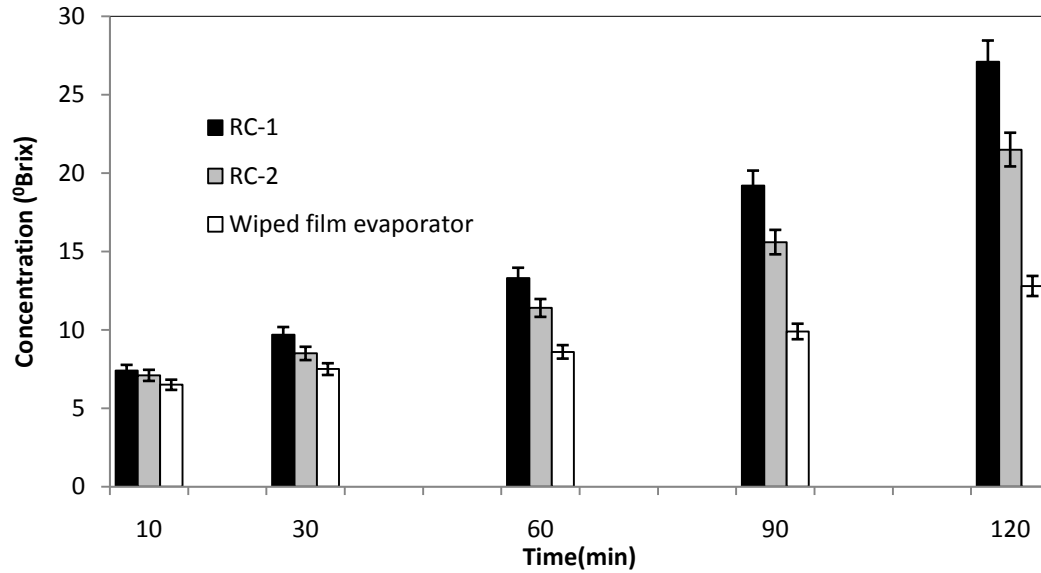


Fig. 7c.5b: Comparative study of the concentration of sugarcane juice in three different contactors

A comparative study for the concentration of sugar-rich grapes and sugarcane juices in three different contactors was performed for two hours at optimum operating parameters (Figure 7c.5a and 7c.5b).

7c.3.6 Response Surface Method

The experimental range and the levels of the independent variables employed are comparable to those in earlier chapters (chapter 6).

Response surface methodology using Box-Behnken experimental design in Design Expert 8.0 software was utilized for optimization. The quadratic model obtained and the Anova analysis results obtained for the study are briefly described.

$$\begin{aligned}
C_{Grapes} = & 42.24 + 7.644A + 3.4466B + 1.2225C + 2.7283D \\
& - 0.0625AB + 0.175AC - 0.105AD + 0.9975BC \\
& - 1.225BD + 0.95CD - 4.361A^2 - 3.0975B^2 \\
& - 2.1512C^2 - 1.195D^2
\end{aligned} \tag{7c.1}$$

$$\begin{aligned}
C_{Sugarcane} = & 25.23 + 4.8392A + 2.6292B + 1.025C + 2.16D \\
& - 0.0475AB + 0.59AC - 0.285AD + 0.69BC - 0.465BD \\
& + 0.03CD - 1.6408A^2 - 1.43085B^2 - 0.8796C^2 \\
& - 0.8796D^2
\end{aligned} \tag{7c.2}$$

where, C_{Grapes} and $C_{Sugarcane}$ are the predicted concentrations of black grapes and pomegranate juices ($^{\circ}$ Brix), A , B and C and D represent the coded terms for air flow rate (litre/min), liquid flow rate (litre/min) and rotational speed (rev/min) and temperature ($^{\circ}$ C) respectively. Comparison between the actual and predicted value was also done using Analysis of Variance. The results showed that the quadratic model obtained for both grapes and sugarcane juice had an F value of 34.49 and 37.25 with p-value less than 0.0001. The coefficient of determination (R^2 value) for grapes and sugarcane juice were 0.976 and 0.978 respectively. The statistical data and the ANOVA chart for both the juices were provided to check the statistical significance of the study in tabular form (Table 7c.2, 7c.3 and 7c.4) respectively. The parity plot obtained in both the juices (Figure 7c.6 and 7c.7) showed a deviation of the actual values from the predicted one to be approximately 10%.

Table 7c.1: Statistics used in the evaluation of the goodness-of-fit of the response to the models for grapes and sugarcane juice.

RSM Statistics		
	Grapes juice	Sugarcane juice
Coefficient of Variation (C.V.) %	4.01	4.05
Determination coefficient R ²	0.9758	0.9775
Adjusted R ²	0.9475	0.9512
Predicted R ²	0.8604	0.8704
Adequate precision	20.863	21.424

Table 7c.2: Analysis of variance for the response surface quadratic model (Grapes juice).

ANOVA for the response surface quadratic model (Grapes juice).						
Source	Sum of squares	df	Mean square	F Value	P value Prob> F	
Model	1086.491	14	77.60652	34.49916	< 0.0001	significant
A	701.1994	1	701.1994	311.7109	< 0.0001	significant
B	142.5541	1	142.5541	63.37095	< 0.0001	significant
C	17.93408	1	17.93408	7.972405	0.0154	significant
D	89.32563	1	89.32563	39.70877	< 0.0001	significant
AB	0.015625	1	0.015625	0.006946	0.9350	
AC	0.1225	1	0.1225	0.054456	0.8194	
AD	0.0441	1	0.0441	0.019604	0.8910	
BC	3.980025	1	3.980025	1.769278	0.2082	significant
BD	6.0025	1	6.0025	2.668349	0.1283	significant
CD	3.61	1	3.61	1.604788	0.2293	
A ²	101.4427	1	101.4427	45.09528	< 0.0001	significant
B ²	51.1707	1	51.1707	22.7474	0.0005	significant
C ²	24.68201	1	24.68201	10.97213	0.0062	significant
D ²	7.616133	1	7.616133	3.385672	0.0906	
Residual	26.99423	12	2.249519			
Lack of Fit	26.99423	10	2.699423			
Pure error	0	2	0			
Cor total	1113.485	26				

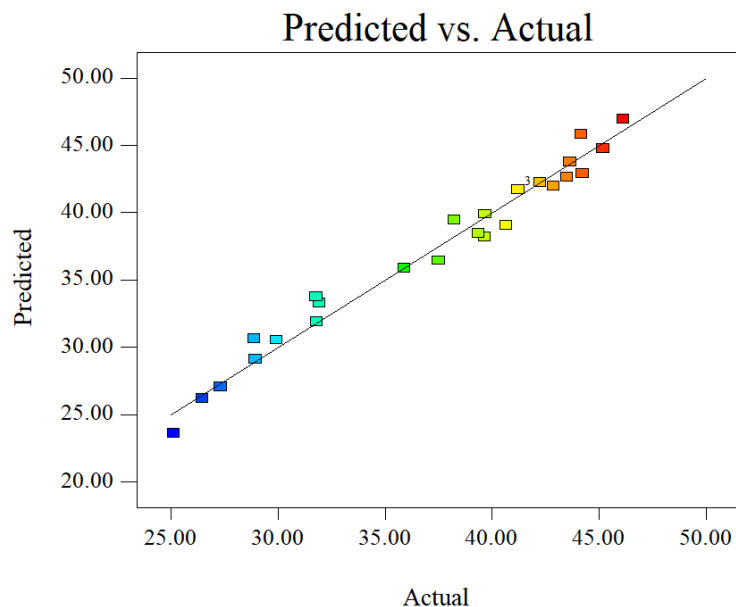


Fig 7c.6: Predicted value vs actual value of concentration of Grapes juice

Table 7c.3: Analysis of variance for the response surface quadratic model (Sugarcane juice).

ANOVA for the response surface quadratic model (Sugarcane juice).						
Source	Sum of squares	df	Mean square	F Value	P value Prob> F	
Model	456.2342	14	32.58816	37.24665	< 0.0001	significant
A	281.0104	1	281.0104	321.181	< 0.0001	significant
B	82.95021	1	82.95021	94.80799	< 0.0001	significant
C	12.6075	1	12.6075	14.40975	0.0025	significant
D	55.9872	1	55.9872	63.9906	< 0.0001	significant
AB	0.009025	1	0.009025	0.010315	0.9208	
AC	1.3924	1	1.3924	1.591444	0.0231	significant
AD	0.3249	1	0.3249	0.371345	0.5536	
BC	1.9044	1	1.9044	2.176635	0.0165	significant
BD	0.8649	1	0.8649	0.988538	0.0339	significant
CD	0.0036	1	0.0036	0.004115	0.9499	
A ²	14.35911	1	14.35911	16.41176	0.0016	significant
B ²	10.91885	1	10.91885	12.4797	0.0041	significant
C ²	4.126223	1	4.126223	4.716069	0.0406	significant
D ²	4.126223	1	4.126223	4.716069	0.0456	significant
Residual	10.49914	12	0.874928			
Lack of Fit	10.49914	10	1.049914			
Pure error	0	2	0			
Cor total	466.7334	26				

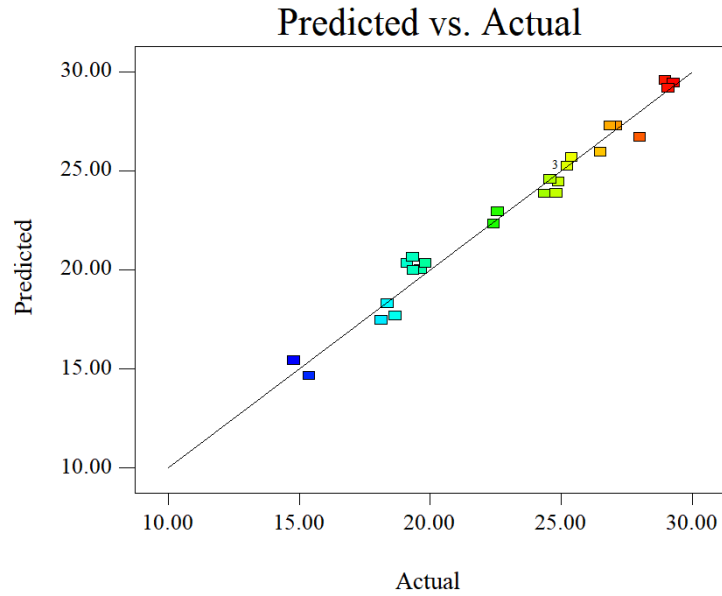


Fig 7c.7: Predicted value vs actual value of concentration of sugarcane juice

7c.3.7 Interactive effect of the variables

The interaction among the four operational parameters was studied by a 3-dimensional graphical representation shown in figure 7c.8 to 7c.13.

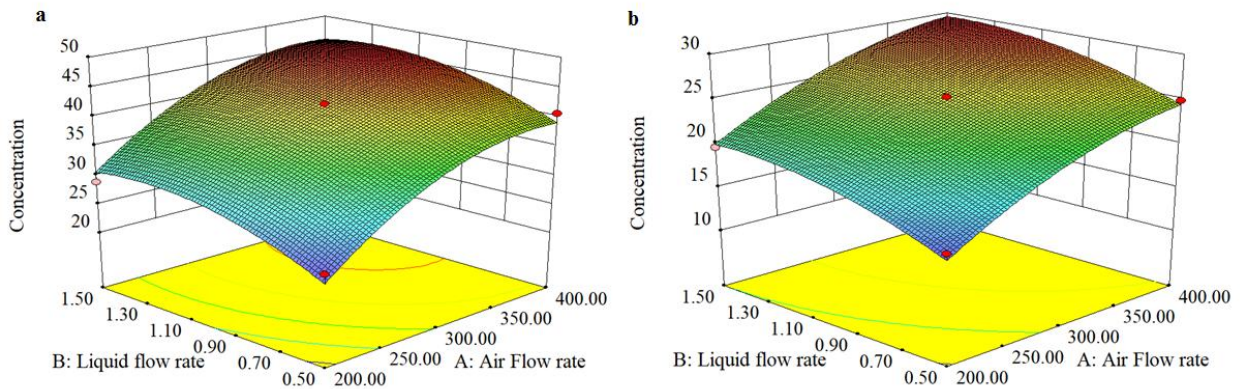


Fig. 7c.8: Interactive effect of air flow rate (Litre/min) and liquid flow rate (Litre/min) on the concentration of grapes juice (a) and sugarcane juice (b).

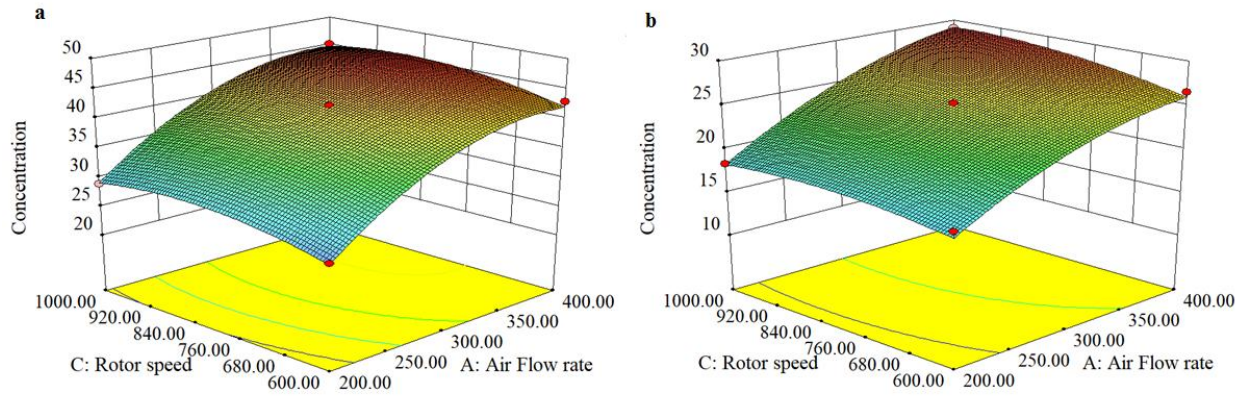


Fig. 7c.9: Interactive effect of air flow rate (Litre/min) and rotor speed (rev/min) on the concentration of grapes juice (a) and sugarcane juice (b).

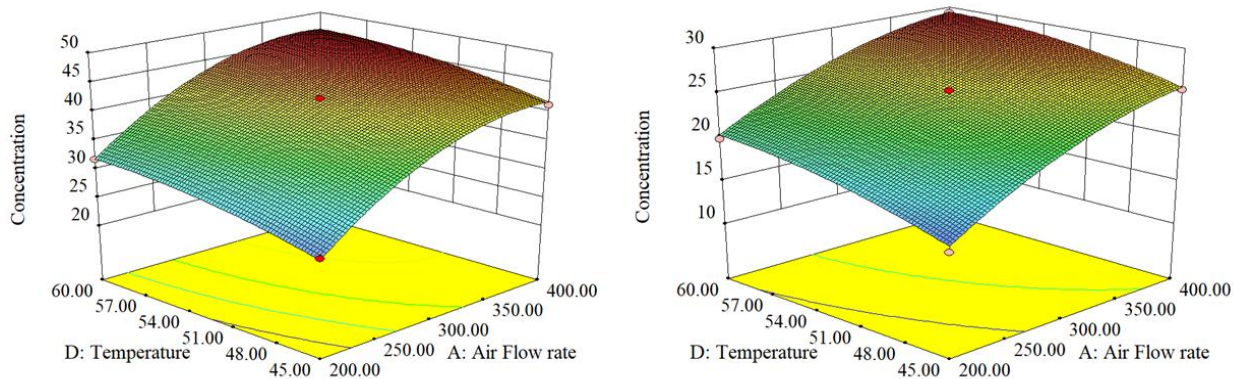


Fig. 7c.10: Interactive effect of air flow rate (Litre/min) and temperature ($^{\circ}$ C) on the concentration of grapes juice (a) and sugarcane juice (b).

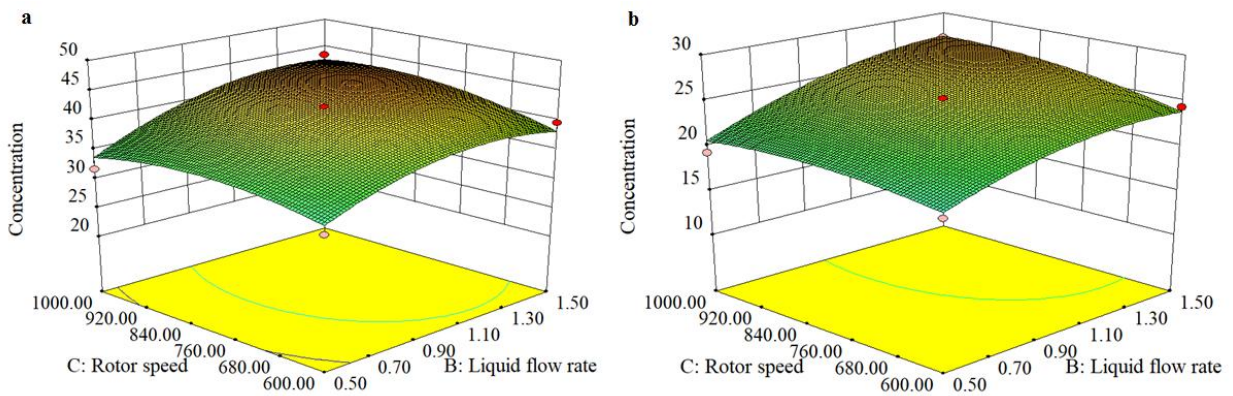


Fig. 7c.11: Interactive effect of rotor speed (rev/min) and liquid flow rate (Litre/min) on the concentration of grapes juice (a) and sugarcane juice (b).

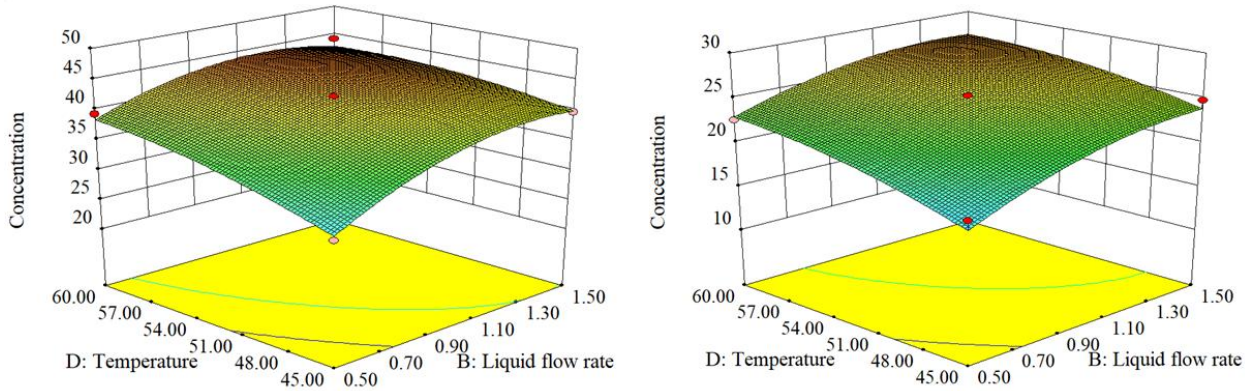


Fig. 7c.12: Interactive effect of temperature ($^{\circ}\text{C}$) and liquid flow rate (Litre/min) on the concentration of grapes juice (a) and sugarcane juice (b).

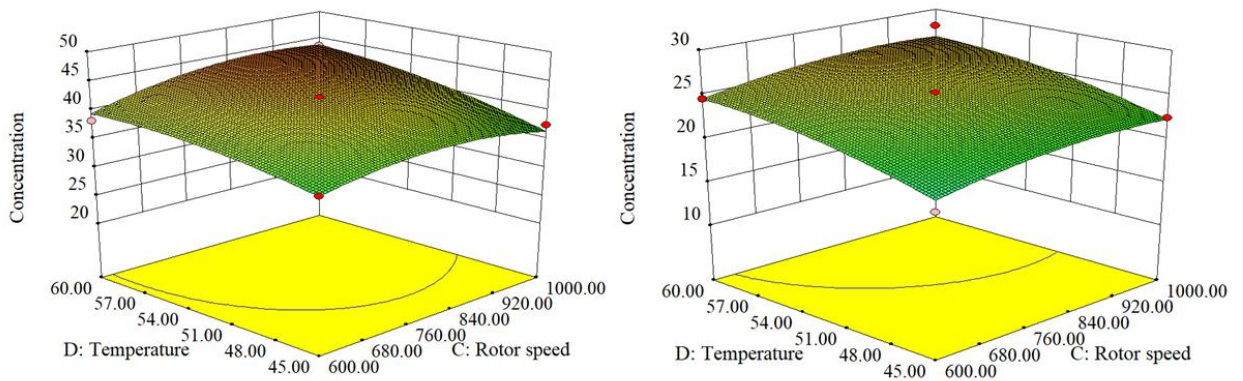


Fig. 7c.13: Interactive effect of rotor speed (rev/min) and temperature ($^{\circ}\text{C}$) on the concentration of grapes juice (a) and sugarcane juice (b).

7c.3.8 Physicochemical analysis results

The pH of the fresh juice and the concentrated juice showed a very negligible difference. In fresh grapes juice, the pH value reported was 3.63 whereas in concentrated juice the pH was 3.51. In sugarcane juice, the reported value of pH was 5.57 whereas in concentrated juice the pH was 5.42. The acid content increased from 0.895 to 1.46 gm/100 ml in grapes concentrated juice. However, there is no significant change in the acid content in sugarcane juice. The initial soluble solid content reported in this study was 14.9 $^{\circ}\text{Brix}$ and 10.4 $^{\circ}\text{Brix}$ for both the sugar-rich juices. The final concentrations

after 2 hours of operation noted were 42.6 °Brix and 34.4 °Brix. In grapes, the feed juice had 42.02 mg Ascorbic acid/100 ml and in the concentrated juice, the ascorbic acid content was 56.22 mg Ascorbic acid/100 ml which is quite significant. In sugarcane, the feed juice had 6.85 mg Ascorbic acid/100 ml and in the concentrated juice, the ascorbic acid content was 7.58 mg Ascorbic acid/100 ml which is negligible. Negligible change in the color content was observed in the feed and concentrate in both fruit juices.

The total phenol content and total flavonoid content were measured in both black grapes and pomegranate juices. The concentration increased from 574.66 to 941.72 mg GAE/Litre in the grapes concentrate. In sugarcane juice, the increase in concentration was reported from 95.89 to 145.99 mg GAE/Litre. In the feed grapes juice, the concentration was 63.64 mg Catechin equivalent (CE)/Litre which increased a little in the concentrated juice (74.42 mg CE/Litre). Similarly in the feed sugarcane juice, the concentration was 25.89 mg Catechin equivalent (CE)/Litre which increased a little in the concentrated juice (35.99 mg CE/Litre). The antioxidant capacity was measured using three different assays reported in Table 7c.4.

7c.4 Conclusion

In this chapter, the air stripping of water from two sugar-rich fruit juices was performed by contacting the juice directly to that of an unsaturated gaseous stream. The concentration achieved in grapes juice was 45.6 °Brix and in sugarcane juice was 29.3 °Brix after two hours of operation in the rotating baffled contactor. The statistical analysis showed the significant contribution of the operating parameters in the concentration of juice. Furthermore, the physicochemical analysis of the feed and the concentrated juice

was evaluated. Thus the feasibility of concentrating juice with this novel technique was proved.

Nomenclature

C_{Tomato}	predicted concentration of tomato juice ($^{\circ}$ Brix) in Eqn. 7a.1
$C_{Watermelon}$	predicted concentration of watermelon juice ($^{\circ}$ Brix) in Eqn. 7a.2
$C_{pomegranate}$	predicted concentration of pomegranate juice ($^{\circ}$ Brix) in Eqn. 7b.1
$C_{Black\ grapes}$	predicted concentration of black grapes juice ($^{\circ}$ Brix) in Eqn. 7b.2
C_{Grapes}	predicted concentration of grapes juice ($^{\circ}$ Brix) in Eqn. 7c.1
$C_{Sugarcane}$	predicted concentration of watermelon juice ($^{\circ}$ Brix) in Eqn. 7c.2
A	coded term for air flow rate (Litre/min)
B	coded term for juice flow rate (Litre/min)
C	coded term for rotational speed (rev/min)
D	coded term for temperature ($^{\circ}$ C)
A^2	quadratic term
B^2	quadratic term
C^2	quadratic term
D^2	quadratic term
AB	interactive term
AC	interactive term
AD	interactive term
BC	interactive term
BD	interactive term
CD	interactive term
R^2	Coefficient of determination

Superscript

- a significant difference in the means of the samples at $p \leq 0.05$ in Table 7a.4, 7b.4, 7c.4
- b significant difference in the means of the samples at $p \leq 0.05$ in Table 7a.4, 7b.4, 7c.4
- c significant difference in the means of the samples at $p \leq 0.05$ in Table 7a.4, 7b.4, 7c.4

Physicochemical Analysis							
Fruits		pH	TSS (⁰ Brix)	Titratable acidity (gm/100ml)	Total phenolics* (mg GAE/Litre)	Total flavonoids** (mg CE/Litre)	L-Ascorbic acid*** (mg/100ml)
Grapes	Fresh juice	3.63±0.01 ^a	14.92±0.52 ^b	0.895±0.003 ^b	547.66±8.79 ^b	63.64±1.82 ^b	42.016±1.772 ^a
	Clarified juice	3.58±0.01 ^b	14.7±0.23 ^b	0.885±0.002 ^c	528.13±4.18 ^c	60.92±0.66 ^b	41.23±1.564 ^b
	concentrate	3.51±0.01 ^c	42.58±0.24 ^a	1.4612±0.005 ^a	941.72±15.6 ^a	70.42±2.83 ^a	56.22±1.29 ^b
Sugarcane	Fresh juice	5.57±0.015 ^a	10.4±0.32 ^b	0.227±0.002 ^b	95.89±3.78 ^b	25.89±3.78 ^b	6.85±0.09 ^a
	Clarified juice	5.50±0.011 ^b	9.66±0.27 ^c	0.218±0.003 ^c	87.102±3.65 ^c	25.102±3.65 ^c	5.92±0.204 ^b
	concentrate	5.42±0.019 ^c	34.44±0.34 ^a	0.277±0.005 ^a	145.99±6.58 ^a	35.99±6.58 ^a	7.586±0.305 ^b

Antioxidant capacity							
Fruits		TEAC** (mmol TE/l)	FRAP*** (mmol TE/l)	DPPH**** (%Inhibition) After 30 minutes	L	Color content	
						a*	b*
Grapes	Fresh juice	15.5±0.42 ^b	4.98±0.318 ^b	43.72±0.212 ^b	35.66±0.33 ^b	4.78±0.12 ^a	3.72±0.1 ^b
	Clarified juice	14.69±0.36 ^b	4.146±0.102 ^c	42.75±0.166 ^c	34.81±0.198 ^c	4.37±0.11 ^b	3.45±0.06 ^c
	concentrate	27.61±0.65 ^a	7.024±0.287 ^a	45.016±0.173 ^a	36.46±0.45 ^a	4.25±0.06 ^c	3.99±0.09 ^a
Sugarcane	Fresh juice	9.72±0.24 ^b	3.09±0.314 ^b	35.49±0.385 ^b	23.69±0.26 ^b	3.16±0.12 ^b	5.37±0.096 ^b
	Clarified juice	9.054±0.08 ^c	2.28±0.329 ^c	34.802±0.244 ^c	23.22±0.09 ^c	2.96±0.07 ^c	5.14±0.054 ^c
	concentrate	17.20±0.49 ^a	5.56±0.344 ^a	36.51±0.29 ^a	26.34±0.36 ^a	3.26±0.07 ^a	5.74±0.11 ^a

Table 7c.4: Physicochemical analysis of the feed and concentrated grapes and sugarcane juice.

Chapter 8

Overall Conclusion and Future scope

8.1 Overall Conclusion

Reducing the water content in fruit juices is a promising step to facilitate storage as well as transportation. The conventional method is thermal evaporation carried out in film evaporators. In this study, an alternate strategy for the concentration of fruit juice was proposed based on stripping of water from fruit juice by an unsaturated gaseous stream in contactors operating under a high gravitational field created by rotating the contactors. Two such contactors were studied – a packed bed rotating about a vertical axis and the other a rotating baffled contactor wherein the phases zigzag across concentric circular baffles fitted in the inner surface of the disks. The following conclusions were made

- ❖ Simultaneous heat and mass transfer experiments performed with an air-water system indicated that the evaporation rate was higher in the baffled rotating contactor compared to rotating packed bed contactor.
- ❖ The volumetric mass transfer in the baffled rotating contactor varied between 7 kg/m³s and 20 kg/m³s for the range of various conditions (rotational speed: 200rpm - 1000 rpm; airflow: 200 L/min - 400 L/min; liquid flow rate: 0.5 L/min - 1.5 L/min; temperature: 45 - 60 °C)
- ❖ The evaporation rate of water achieved in the baffled contactor is nearly 30 times higher than with the direct contact evaporation technique proposed by Ribeiro et al. by bubbling hot air through the solution. The evaporation rate achieved in this study is 38 g/min at a superficial gas velocity of 53 cm/s for pure water at 50 °C.

- ❖ The equipment volume for the same evaporation rate was theoretically calculated to be lower as compared to conventional thin-film evaporators.

The experimental studies for concentration of fruit juices was carried out for two hours in the two rotating contactors by continuously recirculating a fixed volume of fruit juice through the contactor. The results were compared with wiped film evaporator.

- ❖ The performance of rotating baffled contactor (RC-1) for concentration of fruit juice was significantly better than rotating packed bed contactor (RC-2). For the range of operating conditions studied

- Maximum concentration achieved in orange juice in RC-1 was 32.8 °Brix and 24.6 °Brix in RC-2 (from an initial 10 °Brix).
- Maximum concentration of tomato and watermelon fruit juice (Lycopene rich fruits) attained in RC-1 were 15.7 °Brix and 27.5 °Brix from the initial 4.2 °Brix and 5.9 °Brix respectively. The values for concentration in both juices achieved in RC-2 was 10.9 °Brix and 15.9 °Brix.
- Maximum concentration achieved in black grapes and pomegranate juices (antioxidant-rich fruit juices) were 45.8 °Brix and 59.4 °Brix in RC-1. The corresponding concentration values achieved in RC-2 were 35.8 °Brix and 47 °Brix respectively.
- Maximum concentration achieved in sugar-rich grapes juice was 45.6 °Brix and in sugarcane juice was 29.3 °Brix in the rotating baffled contactor. The total soluble solids in RC-2 were 36.3 °Brix and 21.5 °Brix respectively.

- ❖ Both the rotating contactors were more efficient than wiped film evaporator.

- ❖ Response surface methodology was used to study the individual contribution of various operating parameters and a quadratic model was developed for all seven fruit juices. The coefficient of determination (R^2 value) for orange, black grapes, grapes, pomegranate, tomato, watermelon, and sugarcane was 0.9766, 0.9779, 0.9699, 0.9806, 0.9646, 0.9745 and 0.9775 respectively which indicates good agreement between the predicted values and the experimental ones. The ANOVA results also predicted the statistical significance of the study.
- ❖ The physiochemical analysis reported in this study suggests that there is no drastic change in the pH, total acid content, and color content of the feed juice and the concentrated juice.

8.2 Future scope

The results suggested the possibility of improving the efficiency of evaporators for the concentration of solution that would help to reduce energy requirement and volume of the contactor. The benefits to society will be

- Lower cost of the product as the cost of production is reduced.
- The results suggest that the equipment size can be drastically decreased. The small-sized equipment can be more easily transported to hilly terrain helping in the development of industry in these regions.

Some of the future scopes of work based on this study are

- ❖ Carry out the process using vacuum instead of air from removing vapor from the rotating baffled contactor.
- ❖ The results indicate that there is a significant enhancement in concentration rate as one shift from the conventional contactors to those based on high gravity. Even

among high-gravity equipment, the more recently proposed baffled contactor gave better mass transfer performance than the traditional rotating packed bed. The significantly better performance of the baffled contactor suggests a detailed study of flow hydrodynamics and micro-mixing which are not available in the literature needs to be done to identify the reason for the better performance in order to develop more efficient contactors.

- ❖ Recent studies for liquid-liquid extraction have shown that spiral rotating contactor is more efficient than a baffled contactor. This contactor needs to be investigated for gas-liquid system involved in concentration of fruit juice using this process.
- ❖ One of the main failings of traditional film evaporators operating under terrestrial gravity is the fouling of the heating transfer surface due to accumulation of precipitates at higher temperature. This decreases the evaporation rate due to additional heat transfer resistance. Spinning disk contactor wherein liquid flows as a thin film under centrifugal acceleration which is hundred times the terrestrial gravity could be exploited to carry out the precipitates and free the heating surface of any accumulation.

List of Figures

Fig. 1.1: Process layout for production of fruit juice concentrate

Fig. 2.1: Schematic diagram of a horizontal tube evaporator

Fig. 2.2: Schematic diagram of a short-tube calandria evaporator

Fig. 2.3: Schematic diagram of a long-tube rising film evaporator

Fig. 2.4: Schematic diagram of a forced circulation evaporator

Fig. 2.5: Schematic diagram of a falling film evaporator

Fig. 2.6: Schematic diagram of a wiped film evaporator

Fig. 2.7: Schematic diagram of a multiple-effect evaporator

Fig. 2.8: Schematic diagram of a spray dryer unit

Fig. 2.9: Schematic diagram of a freeze concentration unit

Fig. 2.10: Pictorial representation of concentration polarization

Fig. 2.11: Schematic diagram of a direct contact evaporator unit

Fig. 2.12: Schematic diagram of a Rotating Packed bed

Fig. 3.1: Schematic diagram of conventional gas liquid contactors (a. Spray column, b. packed column, c. tray column)

Fig. 3.2: **a.** Schematic diagram of split packed Rotating Packed bed, **b.** Schematic diagram of waveform disc.

Fig. 3.3: Schematic diagram of Rotor Stator Spinning Disk Contactor

Fig. 3.4: Schematic diagram of Rotating Spiral Bed

Fig. 3.5: Schematic diagram of Rotating zigzag bed

Fig. 4.1: The internal schematic diagram (side view) of the two rotors

Fig. 4.2: Pictorial representation of the Rotating baffled contactor (RC-1)

Fig. 4.3: Front view of the Rotating baffled contactor (RC-1)

Fig. 4.4: Pictorial representation of the Rotating packed bed contactor (RC-2)

Fig 4.5: Schematic diagram of Experimental setup for air-water system (a. rotating baffled contactor, b. casing, c. motor, d. air compressor, e. liquid pump, f. solution tank, g. stirrer h. Liquid rotameter, i. air rotameter, j. liquid distributor)

Fig. 4.6: Schematic diagram of Experimental setup for fruit juice concentration (a. rotating baffled contactor, b. casing, c. motor, d. air compressor, e. liquid pump, f. solution tank, g. stirrer h. Liquid rotameter, i. air rotameter, j. liquid distributor)

Fig. 4.7: Pictorial representation of Experimental setup for fruit juice concentration

Fig. 4.8: Schematic diagram of Wiped film evaporator setup

Fig. 4.9: Gallic acid standard curve

Fig. 4.10: Catechin standard curve

Fig. 4.11: Ascorbic acid standard curve

Fig. 4.12: Trolox standard curve

Fig 5.1: The influence of rotor speed on the evaporation rate of two rotating contactors

Fig 5.2: The influence of air flow rate on the evaporation rate of two rotating contactors

Fig 5.3: The influence of water flow rate on the evaporation rate of two rotating contactors

Fig 5.4: The influence of temperature on the evaporation rate of two rotating contactors

Fig 5.5: The influence of rotor speed on the volumetric mass transfer coefficient of two rotating contactors

Fig 5.6: The influence of air flow rate on the volumetric mass transfer coefficient of two rotating contactors

Fig 5.7: The influence of water flow rate on the volumetric mass transfer coefficient

Fig 5.8: Volumetric mass transfer predicted vs. experimental

Fig 5.9: Variation of theoretical plate numbers with Rotational speed in RC-1

Fig 5.10: Relation between temperature difference, ΔT [eq. (5.6)] and calculated volume of the agitated film evaporator

Fig 6.1: Comparative study in concentration of orange juice in Wiped film evaporator and Rotating packed bed RC-2

Fig 6.2: Influence of rotational speed on orange juice concentration in RC-1 and RC-2

Fig 6.3: Effect of orange juice flow rate on the concentration in RC-1 and RC-2

Fig 6.4: Influence of air flow rate on orange juice concentration in RC-1 and RC-2

Fig 6.5: Influence of temperature on orange juice concentration in RC-1 and RC-2.

Fig 6.6: Predicted value vs actual value of concentration of orange juice

Fig. 6.7: Interactive effect of air flow rate (Litre/min) and liquid flow rate (Litre/min) on the concentration of juice

Fig. 6.8: Interactive effect of air flow rate (Litre/min) and rotor speed (rev/min) on the concentration of orange juice

Fig. 6.9: Interactive effect of liquid flow rate (Litre/min) and rotor speed (rev/min) on the concentration of juice

Fig. 6.10: Interactive effect of rotor speed (rev/min) and temperature ($^{\circ}\text{C}$) on the concentration of orange juice

Fig. 6.11: Interactive effect of rotor speed (rev/min) and temperature ($^{\circ}\text{C}$) on the concentration of orange juice

Fig. 6.12: Interactive effect of temperature ($^{\circ}\text{C}$) and liquid flow rate (Litre/min) on the concentration of orange juice

Fig 7a.1: Influence of rotational speed on red fruit juice concentration in RC-1 and RC-2

Fig 7a.2: Influence of air flow rate on red fruit juice concentration in RC-1 and RC-2

Fig 7a.3: Influence of juice flow rate on red fruit juice concentration in RC-1 and RC-2

Fig 7a.4: Influence of temperature on red fruit juice concentration in RC-1 and RC-2

Fig. 7a.5: Comparative study of the concentration of tomato juice in three different contactors

Fig. 7a.6: Comparative study of the concentration of watermelon juice in three different contactors

Fig. 7a.7: Predicted value vs actual value of concentration of tomato juice

Fig 7a.8: Predicted value vs actual value of concentration of watermelon juice

Fig. 7a.9: Interactive effect of air flow rate (Litre/min) and liquid flow rate (Litre/min) on the concentration of tomato juice (a) and watermelon juice (b)

Fig. 7a.10: Interactive effect of air flow rate (Litre/min) and rotor speed (rev/min) on the concentration of tomato juice (a) and watermelon juice (b)

Fig. 7a.11: Interactive effect of air flow rate (Litre/min) and temperature ($^{\circ}\text{C}$) on the concentration of tomato juice (a) and watermelon juice (b)

Fig. 7a.12: Interactive effect of rotor speed (rev/min) and liquid flow rate (Litre/min) on the concentration of tomato juice (a) and watermelon juice (b)

Fig. 7a.13: Interactive effect of temperature ($^{\circ}\text{C}$) and liquid flow rate (Litre/min) on the concentration of tomato juice (a) and watermelon juice (b)

Fig. 7a.14: Interactive effect of rotor speed (rev/min) and temperature ($^{\circ}\text{C}$) on the concentration of tomato juice (a) and watermelon juice (b)

Fig 7b.1a: Influence of rotational speed on black grapes and pomegranate fruit juices concentration in RC-1

Fig 7b.1b: Influence of rotational speed on black grapes and pomegranate fruit juices concentration in RC-2

Fig 7b.2a: Influence of air flow rate on black grapes and pomegranate fruit juices concentration in RC-1

Fig 7b.2b: Influence of air flow rate on black grapes and pomegranate fruit juices concentration in RC-2

Fig 7b.3a: Influence of liquid flow rate on black grapes and pomegranate fruit juices concentration in RC-1

Fig 7b.3b: Influence of liquid flow rate on black grapes and pomegranate fruit juices concentration in RC-2

Fig 7b.4a: Influence of temperature on black grapes and pomegranate fruit juices concentration in RC-1

Fig 7b.4b: Influence of temperature on black grapes and pomegranate fruit juices concentration in RC-2

Fig. 7b.5a: Comparative study of the concentration of black grapes juice in three different contactors

Fig. 7b.5b: Comparative study of the concentration of pomegranate juice in three different contactors

Fig 7b.6: Predicted value vs actual value of concentration of pomegranate juice

Fig 7b.7. Predicted value vs actual value of concentration of Black grapes juice

Fig. 7b.8: Interactive effect of air flow rate (litre/min) and liquid flow rate (litre/min) on the concentration of pomegranate juice (a) and black grapes juice (b)

Fig. 7b.9: Interactive effect of air flow rate (litre/min) and rotor speed (rev/min) on the concentration of pomegranate juice (a) and black grapes juice (b)

Fig. 7b.10: Interactive effect of air flow rate (litre/min) and temperature ($^{\circ}\text{C}$) on the concentration of pomegranate juice (a) and black grapes juice (b)

Fig. 7b.11: Interactive effect of rotor speed (rev/min) and liquid flow rate (litre/min) on the concentration of pomegranate juice (a) and black grapes juice (b)

Fig. 7b.12: Interactive effect of temperature ($^{\circ}\text{C}$) and liquid flow rate (litre/min) on the concentration of pomegranate juice (a) and black grapes juice (b)

Fig. 7b.13: Interactive effect of rotor speed (rev/min) and temperature ($^{\circ}\text{C}$) on the concentration of pomegranate juice (a) and black grapes juice (b)

Fig 7c.1: Influence of rotational speed on sugar containing fruit juice concentration in RC-1 and RC-2

Fig 7c.2: Influence of air flow rate on sugar containing fruit juice concentration in RC-1 and RC-2

Fig 7c.3: Influence of juice flow rate on sugar containing juice concentration in RC-1 and RC-2

Fig 7c.4: Influence of temperature on sugar containing juice concentration in RC-1 and RC-2

Fig. 7c.5a: Comparative study of the concentration of grapes juice in three different contactors

Fig. 7c.5b: Comparative study of the concentration of sugarcane juice in three different contactors

Fig. 7c.6: Predicted value vs actual value of concentration of Grapes juice

Fig. 7c.7: Predicted value vs actual value of concentration of sugarcane juice

Fig. 7c.8: Interactive effect of air flow rate (litre/min) and liquid flow rate (litre/min) on the concentration of grapes juice (a) and sugarcane juice (b)

Fig. 7c.9: Interactive effect of air flow rate (litre/min) and rotor speed (rev/min) on the concentration of grapes juice (a) and sugarcane juice (b)

Fig. 7c.10: Interactive effect of air flow rate (litre/min) and temperature ($^{\circ}\text{C}$) on the concentration of grapes juice (a) and sugarcane juice (b)

Fig. 7c.11: Interactive effect of rotor speed (rev/min) and liquid flow rate (litre/min) on the concentration of grapes juice (a) and sugarcane juice (b)

Fig. 7c.12: Interactive effect of temperature ($^{\circ}\text{C}$) and liquid flow rate (litre/min) on the concentration of grapes juice (a) and sugarcane juice (b)

Fig. 7c.13: Interactive effect of rotor speed (rev/min) and temperature ($^{\circ}\text{C}$) on the concentration of grapes juice (a) and sugarcane juice (b)

List of Tables

Table 1.1: Daily recommendation of various nutrient and their fruit sources

Table 1.2: Different Membrane separation techniques and their applications

Table 2.1: Literature of various juices concentrated in different membrane techniques

Table 3.1: Mass transfer coefficient in different gas-liquid contactors

Table 3.2: Mass transfer coefficient of different gas-liquid operations in rotating packed bed

Table 6.1: Experimental range and various levels of independent variables

Table 6.2: Statistics used in evaluation of the goodness-of-fit of the response to the models in orange juice.

Table 6.3: Analysis of variance for the response surface quadratic model in orange juice.

Table 6.4: Physicochemical data of the feed, clarified juice and the concentrate of orange juice.

Table 6.5: Total Phenolics, Flavonoids, and Antioxidant capacity of the feed, clarified juice, and the concentrate.

Table 7a.1: Statistics used in evaluation of the goodness-of-fit of the responses to the models in red fruit juices.

Table 7a.2: Analysis of variance for the response surface quadratic model (Tomato juice).

Table 7a.3: Analysis of variance for the response surface quadratic model (Watermelon juice).

Table 7a.4: Physicochemical test results for red feed juice and their respective concentrates

Table 7b.1: Statistics used in evaluation of the goodness-of-fit of the responses to the models in antioxidant-rich fruit juices.

Table 7b.2: Analysis of variance for the response surface quadratic model (Pomegranate juice).

Table 7b.3: Analysis of variance for the response surface quadratic model (Black grapes juice).

Table 7b.4: Physicochemical analysis of the feed and concentrated pomegranate and black grapes juices.

Table 7c.1: Statistics used in evaluation of the goodness-of-fit of the responses to the models for grapes and sugarcane juice.

Table 7c.2: Analysis of variance for the response surface quadratic model (Grapes juice).

Table 7c.3: Analysis of variance for the response surface quadratic model (Sugarcane juice).

Table 7c.4: Physicochemical analysis of the feed and concentrated grapes and sugarcane juice.